

## Durham E-Theses

---

### *Aspects of gauge/string theory duality: BMN correspondence and MHV rules*

George Georgiou

#### How to cite:

---

Georgiou, George (2007) Aspects of gauge/string theory duality: BMN correspondence and MHV rules. Doctoral thesis, Durham University.

#### Use policy

---

The full-text may be used and/or reproduced, and given to third parties in any format or medium, without prior permission or charge, for personal research or study, educational, or not-for-profit purposes provided that:

- a full bibliographic reference is made to the original source
- a <https://etheses.durham.ac.uk/id/eprint/2626/> is made to the metadata record in Durham E-Theses
- the full-text is not changed in any way

The full-text must not be sold in any format or medium without the formal permission of the copyright holders.

Please consult the [full Durham E-Theses policy](#) for further details.

# Aspects of gauge/string theory duality: BMN correspondence and MHV rules

George Georgiou

The copyright of this thesis rests with the author or the university to which it was submitted. No quotation from it, or information derived from it may be published without the prior written consent of the author or university, and any information derived from it should be acknowledged.

A Thesis presented for the degree of  
Doctor of Philosophy



Centre for Particle Theory  
Department of Physics  
University of Durham  
England

May 2005



16 APR 2007

## **Dedicated to my parents and to Konstantina, for being always there**

Galileo: During my free hours, of which I have many, I have gone over my case and have considered how the world of science, in which no longer I count myself, will judge it. Even a wool-merchant, apart from buying cheaply and selling dear, must also be concerned that the trade in wool can be carried on unhindered. In this respect the pursuit of science seems to me to require particular courage. It is concerned with knowledge, achieved through doubt. Making knowledge about everything available for everybody, science strives to make sceptics of them all. Now the great part of the population is kept permanently by their princes, landlords and priests in a nacreous haze of superstition and outmoded words which obscure the machinations of such characters. The misery of the multitude is as old as the hills, and from pulpit and desk is proclaimed as immutable as the hills. Our new device of doubt delighted the great public, which snatched the telescope from our hands and turned it on its tormentors. These selfish and violent men, who greedily exploited the fruits of science to their own use, simultaneously felt the cold eye of science turned on a thousand-year-old, but artificial misery which clearly could be eliminated by eliminating them. They drenched us with their threats and bribes, irresistible to weak souls. But could we deny ourselves to the crowd and still remain scientists? The movements of the stars have become clearer; but to the mass of the people the movements of their masters are still incalculable. The fight of the measurability of the heavens has been won through doubt; but the fight of the Roman housewife for milk is ever and again lost through faith. Science, Sarti, is concerned with both battle-fronts. A humanity which stumbles in this age-old nacreous haze of superstition and outmoded words, too ignorant to develop fully its own powers, will not be capable of developing the powers of nature which you reveal. What are you working for? I maintain that the only purpose of science is to ease the hardship of human existence. If scientists, intimidated by self-seeking people in power, are content to amass knowledge for the sake of

---

knowledge, then science can become crippled, and your new machines will represent nothing but new means of oppression. With time you may discover all that is to be discovered, and your progress will only be a progression away from mankind. The gulf between you and them can one day become so great that your cry of jubilation over some new achievement may be answered by a universal cry of horror. I, as a scientist, had a unique opportunity. In my days astronomy reached the market-places. In these quite exceptional circumstances, the steadfastness of one man could have shaken the world. If only I had resisted, if only the natural scientists had been able to evolve something like the Hippocratic oath of the doctors, the vow to devote their knowledge wholly to the benefit of mankind! As things now stand, the best one can hope for is for a race of inventive dwarfs who can be hired for anything. Moreover, I am now convinced, Sarti, that I never was in real danger. For a few years I was as strong as the authorities. And I surrendered my knowledge to those in power, to use, or not to use, or to misuse, just as suited their purposes. I have betrayed my profession. A man who does what I have done can not be tolerated in the ranks of science.

"The life of Galileo", Bertolt Brecht

**Science is the belief in the ignorance of the experts.**

R. P. Feynman

# Aspects of gauge/string theory duality: BMN correspondence and MHV rules

George Georgiou

Submitted for the degree of Doctor of Philosophy

May 2005

## Abstract

One of the most striking examples of duality correspondence between gauge theories and string theories is the AdS/CFT duality. It relates the type IIB superstring theory on  $AdS_5 \times S^5$  to 4-dimensional  $N = 4$  Yangs Mills in its superconformal phase. However, the quantisation of string theory on curved backgrounds appears to be notoriously difficult rendering direct tests of the conjecture elusive. One way to circumvent this problem is by taking the Penrose limit of the  $AdS_5 \times S^5$  geometry to obtain the pp-wave background where string theory is soluble. The corresponding limit in gauge theory is to restrict to particular class of "long" operators called BMN operators. It is this correspondence we study in the first part of this thesis. In particular, we provide with a number of rigorous tests of the BMN correspondence beyond the supergravity limit, that probe the truly quantum realm of string theory. By exploring the correspondence, we learn how the correspondence is realised and how the 3-string amplitudes can be obtained purely from perturbative gauge theory calculations for almost all species of string excitations. We also clarify the role of the  $\mathbb{Z}_2$  symmetry the pp-wave background possesses and discuss the consequences this symmetry has on the choice of the 3-string vertex.

There is another type of duality which relates the same  $N = 4$  SYM to a different string theory. This is a weak-to-weak coupling duality recently proposed by Witten. It states that tree level amplitudes of  $N = 4$  SYM can be reproduced by integrating over the moduli space of certain D-instantons in open topological B-model in super-twistor space. This duality has inspired a novel diagrammatic method for calculating

all gluon tree level scattering amplitudes in  $N = 4$  SYM. The second part of this thesis is devoted to the generalisation of this approach to tree amplitudes with fermions and scalars and to theories with less or no supersymmetry at all. We also argue that the method works for a finite number of colours as well and that there is a simple way to directly write down all tree level amplitudes without encountering unphysical singularities.

# Declaration

The work in this thesis is based on research carried out at the Center for Particle Theory, Department of Physics, University of Durham, England. No part of this thesis has been submitted elsewhere for any other degree or qualification and it is all my own work unless referenced to the contrary in the text. Chapters 2, 3, 4, 5, and 6 are based on joined research with my supervisor Professor Valentin V. Khoze, Dr. Gabriele Travaglini, and Professor E. W. N. Glover published in [1–5]. References to other people’s work are given as appropriate throughout the text.

**Copyright © 2005 by George Georgiou.**

“The copyright of this thesis rests with the author. No quotations from it should be published without the author’s prior written consent and information derived from it should be acknowledged”.

# Acknowledgements

I would like to thank all the people who have helped me in one way or another all these years and have contributed to the completion of this work.

First of all, I am deeply indebted to my supervisor V. V. Khoze for his mentorship, encouragement and support through the years. Next I would like to thank Gabriele Travaglini. He has been not only an ideal collaborator but also an invaluable friend. Prof. Nigel Glover was the first person to meet in the physics department and since then his guidance and encouragement has remained undiminished. I would also like to thank the people of the physics department of Queen Mary University of London, and specially Bill Spence, Andreas Brandhuber and Sanjaye Ramgoolam, for their kindness and hospitality whenever I visited their department.

My deepest thanks go to the people who have been my teachers throughout the years. I'd like to thank Kostas Adamos who lit the fire in me, Georgios Tiktopoulos from whom I've learned quantum field theory, Nicolas Tracas, Kostas Farakos, Dennis Bonatsos, Georgios Koutsoumbas, Sofronis Papadopoulos and many others.

During the years I was studying in Durham I was really lucky to have the support and faithful friendship of Apostolos Dimitriadis, Georgios Kampalios and Konstantinos Kyritsis. It was a great pleasure to discuss with them, sometimes for hours, about physics and philosophy.

My studies have been funded by the States Scholarship Foundation of Greece (I.K.Y.).

This work is dedicated to my parents and to Konstantina Mara, those who loved me beyond any doubt.

# Contents

<b>Abstract</b>	<b>iv</b>
<b>Declaration</b>	<b>vi</b>
<b>Acknowledgements</b>	<b>vii</b>
<b>1 Introduction</b>	<b>1</b>
1.1 Motivation and outline . . . . .	1
1.2 1/N Expansion Of Gauge Theories . . . . .	9
1.3 Type IIB supergravity . . . . .	13
1.4 The AdS/CFT correspondence . . . . .	19
1.5 Penrose limit of the AdS geometry . . . . .	24
1.6 Light cone string field theory . . . . .	26
1.6.1 Bosonic Part Of The Free String Action . . . . .	26
1.6.2 Fermionic Part Of The Free String Action . . . . .	29
1.6.3 General Structure Of Light Cone String Field Theory . . . . .	33
1.6.4 String Interactions In The Plane Wave . . . . .	36
1.7 The Plane Wave/SYM Duality . . . . .	43
<b>2 Vertex-Correlator Correspondence In The pp-wave</b>	<b>49</b>
2.1 The vertex-correlator duality . . . . .	52
2.2 Two-point correlators . . . . .	54
2.3 Three-point functions . . . . .	59
2.3.1 One string and two supergravity states . . . . .	60
2.3.2 Three-point functions with two string states . . . . .	68

2.4	Tests of the correspondence . . . . .	72
2.4.1	$1_{-(n'_2+n'_3)}2_{n'_2}3_{n'_3} + vac \rightarrow 1_{-(n_2+n_3)}2_{n_2}3_{n_3}$ . . . . .	72
2.4.2	$1_{n'_2}2_{-(n'_2+n'_3)}3_{n'_3} + vac \rightarrow 1_{-(n_2+n_3)}2_{n_2}3_{n_3}$ . . . . .	74
2.4.3	$1_{-n'_2}2_{n'_2} + 3_0 \rightarrow 1_{-(n_2+n_3)}2_{n_2}3_{n_3}$ . . . . .	75
2.4.4	$1_{n'_2}2_{-n'_2} + 3_0 \rightarrow 1_{-(n_2+n_3)}2_{n_2}3_{n_3}$ . . . . .	75
<b>3</b>	<b>Tests of the Extended BMN Correspondence and the role of <math>\mathbb{Z}_2</math> Symmetry</b>	<b>76</b>
3.1	The dilatation operator in SYM and the natural string basis . . . . .	80
3.2	Tests of the correspondence in the two-impurity sector: scalar, mixed, and vector states . . . . .	84
3.2.1	Matrix elements with scalar BMN states . . . . .	90
3.2.2	Matrix elements with mixed BMN states . . . . .	91
3.2.3	Matrix elements with vector BMN states . . . . .	91
3.2.4	Generalisation to all representations for two-impurity BMN states	92
3.3	A technical aside: three-point function with mixed impurities . . . . .	94
3.3.1	Diagrams originating from the “pure” BMN parts . . . . .	95
3.3.2	Diagrams from compensating terms . . . . .	97
3.3.3	Summary: the result for mixed impurities . . . . .	100
3.4	The correspondence for an arbitrary number of scalar impurities . . . . .	101
3.4.1	The results in field theory . . . . .	101
3.4.2	The results in string field theory . . . . .	106
3.5	A technical aside: calculation of general scalar BMN three-point functions . . . . .	108
<b>4</b>	<b>The BMN correspondence in the fermionic sector</b>	<b>114</b>
4.1	Fermion BMN operators . . . . .	116
4.2	Conjugation of scalar and fermion operators . . . . .	120
4.3	Matrix elements of $H_{\text{string}}$ in string field theory . . . . .	121
4.4	Matrix elements of $\Delta$ in $\mathcal{N} = 4$ Yang-Mills . . . . .	124
4.4.1	The three-point function of fermion BMN operators . . . . .	126
4.5	Testing the BMN correspondence in the fermion sector . . . . .	133

<b>5</b>	<b>Tree Amplitudes in Gauge Theory as Scalar MHV Diagrams</b>	<b>139</b>
5.1	Tree Amplitudes . . . . .	143
5.1.1	Colour decomposition . . . . .	143
5.1.2	Helicity amplitudes . . . . .	145
5.2	Calculating Amplitudes Using Scalar Graphs . . . . .	148
5.2.1	Calculating $---++\dots++$ amplitudes with 2 fermions .	149
5.2.2	Tests of the amplitude (5.27)–(5.30) . . . . .	152
5.2.3	Calculating $---++\dots++$ amplitudes with 4 fermions .	153
<b>6</b>	<b>Non-MHV tree amplitudes in gauge theory</b>	<b>159</b>
6.1	Amplitudes in the spinor helicity formalism . . . . .	160
6.2	Gluonic NMHV amplitudes and the CSW method . . . . .	161
6.3	NMHV $(---)$ Amplitudes with Two Fermions . . . . .	164
6.4	NMHV $(---)$ Amplitudes with Four Fermions . . . . .	170
6.5	Iterations of the Analytic Supervertex . . . . .	173
6.5.1	Analytic Supervertex . . . . .	173
6.5.2	Scalar graphs with analytic vertices . . . . .	175
6.5.3	Two analytic supervertices . . . . .	175
<b>7</b>	<b>Conclusions</b>	<b>178</b>
<b>A</b>	<b>Expressions for Neumann matrices</b>	<b>188</b>
<b>B</b>	<b>The bosonic part of the three-string vertex</b>	<b>192</b>
<b>C</b>	<b>Notation and conventions in gauge theory</b>	<b>194</b>
<b>D</b>	<b>The three-string vertex</b>	<b>196</b>
<b>E</b>	<b>Summing over the BMN phase factors</b>	<b>198</b>
<b>F</b>	<b>The functions <math>X</math>, <math>Y</math> and <math>H</math></b>	<b>199</b>

<b>G More detailed calculations for the evaluation of the Feynman diagrams</b>	<b>201</b>
<b>H Note on Spinor Conventions</b>	<b>204</b>

# List of Figures

1.1	Three string interaction vertex in the light cone gauge. According to the prescription stated below (1.99) $\alpha_1, \alpha_2 > 0$ whereas $\alpha_3 < 0$ . Note also that, due to closed string boundary conditions, $\sigma = 0, \sigma = 2\pi\alpha_1$ and $\sigma = 2\pi(\alpha_1 + \alpha_2)$ are identified and $I$ is the interaction point. . . . .	36
2.1	Interacting diagrams for the 2-point function where $\phi_1$ interacts with $Z$ . These diagrams give rise to $P_1$ . . . . .	57
2.2	Interacting diagrams for the 2-point function with $\phi_2$ interactions. These diagrams give rise to $P_2$ . . . . .	57
2.3	Interacting diagrams for the 2-point function with $\phi_3$ interactions. These diagrams give rise to $P_3$ . . . . .	58
2.4	Interacting diagrams for the two-point function. These diagrams give rise to $P_4 = 0$ . There are six additional diagrams with $\phi_2$ and $\phi_3$ exchanged. Their sum is also zero. . . . .	58
2.5	A typical free diagram for $G_3$ . This diagram gives rise to $X_{123}$ . There are five additional diagrams with $\phi_1, \phi_2$ and $\phi_3$ interchanged. $a, b$ and $c$ are the positions of the impurities in the trace. For this particular diagram, $a = 2, b = 4, c = 6$ . . . . .	61
2.6	Interacting diagrams for $G_3$ . These diagrams give rise to $Y_{123}$ . There are four additional diagrams with $\phi_2$ and $\phi_3$ exchanged. . . . .	62
2.7	Interacting diagrams for $G_3$ . These diagrams give rise to $Y_{231}$ . There are four additional diagrams with $\phi_1$ and $\phi_3$ exchanged. . . . .	63
2.8	Interacting diagrams for $G_3$ , contributing to $Y_{312}$ . There are four additional diagrams with $\phi_1$ and $\phi_2$ exchanged. . . . .	64

2.9	Interacting diagrams for $G_3$ . Diagrams 2.9a, 2.9c, 2.9e and 2.9g have an opposite sign with respect to 2.9b, 2.9d, 2.9f and 2.9h, so they cancel pairwise. There are additional diagrams where $\phi_2$ and $\phi_3$ are exchanged which also add up zero. Additional diagrams where $\phi_2$ or $\phi_3$ (rather than $\phi_1$ interact with $Z$ also cancel in the same way. . . . .	64
2.10	Free diagrams for $G_3$ . This diagram gives rise to $P$ . . . . .	66
2.11	Interacting diagrams for $G'_3$ contributing to $Q_1$ . The $\phi_1$ line is in the $a^{th}$ position in the $\bar{O}_{n_2, n_3}^J(0)$ trace and $\phi_3$ is in the $b^{th}$ position. . . . .	67
2.12	Interacting diagrams for $G'_3$ contributing to $Q_2$ . . . . .	67
2.13	Interacting diagrams for $G'_3$ contributing to $Q_3$ . There are also diagrams with $\phi_1$ and $\phi_2$ exchanged. . . . .	68
3.1	Diagrams with scalar impurity interacting. Diagrams 3.1a and 3.1d have positive signs, all the others have negative signs. . . . .	96
3.2	Diagrams with vector impurity interacting associated to $P_I$ . . . . .	97
3.3	Diagrams with vector impurity interacting associated to $P_{II}$ . . . . .	98
3.4	Diagrams originating from the compensating term in the ‘internal’ operator (at $x_1$ ). In these diagrams no gluons are emitted or exchanged. . . . .	99
3.5	Gluon emission diagrams originating from the compensating term in the internal operator. . . . .	100
3.6	Gluon interaction diagrams, from the compensating term in the internal operator. . . . .	101
3.7	Feynman diagrams where a scalar impurity from $\mathcal{O}_1$ interacts with a $Z$ field. The dots stand for impurities which have free contractions. These diagrams are also accompanied by their mirror images, where the interaction occurs in the bottom part of the diagram. . . . .	110
3.8	In Figure 3.8a we take the pure BMN part in the external operator, whereas in 3.8b we take the compensating term. In both cases we take the compensating term in $\mathcal{O}_1$ and the pure BMN part in $\mathcal{O}_2$ . Here $i$ and $j$ label the position of the corresponding $\phi$ in the barred BMN operator. . . . .	111

3.9	In Figure 3.9a we take the BMN part in the external operator, whereas in 3.9b we take the compensating term. . . . .	113
4.1	Feynman diagrams from the pure BMN parts: of type I (in 4.1a and 4.1d) and type II (4.1b and 4.1e). Diagrams 4.1d, 4.1e, are the mirrors of 4.1a, 4.1b. Diagrams 4.1d and 4.1e have phase factors which are the complex conjugate of those of 4.1a and 4.1b. The gluon interaction diagrams in 4.1c and 4.1f have the same BMN factor and cancel each other. . . . .	127
4.2	Gluon emission diagrams originating from the compensating term in the internal operator. The gluon is absorbed by the fermion field. There are also mirror diagrams, not drawn in this figure. . . . .	130
4.3	Gluon emission diagrams originating from the compensating term in the internal operator. The gluon is absorbed by the $Z$ field. . . . .	131
5.1	Tree diagrams with MHV vertices contributing to the $---++++\dots++$ amplitude with 2 fermions and $n - 2$ gluons in Eq. (5.24). Fermions are represented by dashed lines and gluons – by solid lines. . . . .	150
5.2	Diagrams contributing to the 4-fermion $n$ -point amplitude (5.40) . . . . .	155
6.1	Tree diagrams with MHV vertices contributing to the amplitude $A_n(\Lambda_{m_1}^-, g_{m_2}^-, g_{m_3}^-, \Lambda_k^+)$ . Fermions, $\Lambda^+$ and $\Lambda^-$ , are represented by dashed lines and negative helicity gluons, $g^-$ , by solid lines. Positive helicity gluons $g^+$ emitted from each vertex are indicated by dotted semicircles with labels showing the bounding $g^+$ lines in each MHV vertex. . . . .	166
6.2	Tree diagrams with MHV vertices contributing to the amplitude $A_n(\Lambda_{m_1}^-, g_{m_2}^-, \Lambda_k^+, g_{m_3}^-)$ . . . . .	168
6.3	Tree diagrams with MHV vertices contributing to the amplitude $A_n(\Lambda_{m_1}^-, \Lambda_k^+, g_{m_2}^-, g_{m_3}^-)$ . . . . .	170
6.4	Tree diagrams with MHV vertices contributing to the four fermion amplitude $A_n(g_1^-, \Lambda_{m_2}^-, \Lambda_{m_3}^-, \Lambda_{m_p}^+, \Lambda_{m_q}^+)$ . . . . .	171
6.5	Tree diagrams with MHV vertices contributing to the four fermion amplitude $A_n(g_1^-, \Lambda_{m_2}^-, \Lambda_{m_p}^+, \Lambda_{m_3}^-, \Lambda_{m_q}^+)$ . . . . .	172

---

6.6	Tree diagrams with MHV vertices contributing to the first amplitude of Eq. (6.34b). . . . .	176
-----	---	-----

# Chapter 1

## Introduction

### 1.1 Motivation and outline

To the best of our knowledge, there are four fundamental interactions in Nature, the electromagnetic, the weak nuclear, the strong nuclear, and the gravitational. The framework currently used to describe the first three is based on quantum field theory<sup>1</sup> with certain gauge symmetries. In this model, called the Standard Model, both the fundamental particles that feel the forces and the fundamental particles that carry the forces, called gauge bosons, are considered to be point-like. This means that the interaction between these particles occur at one space-time point. This fact leads to divergences that arise when two or more vertices get arbitrarily close. The success of quantum field theory rests on the fact that these divergences may be removed in a consistent and physically meaningful way by using the renormalisation programme. Although not completely satisfactory from the mathematical point of view, this method was used to calculate observables which were found to agree with experiment to a very high accuracy.

Despite its agreement with all experimental data from accelerators, the Standard Model is theoretically unsatisfactory and leaves many open questions and space for physics beyond the Standard Model. Even if we forget about gravity for a moment,

---

<sup>1</sup>Reconciling special relativity with quantum mechanics and demanding local interactions leads necessarily to quantum field theory.



the Standard Model contains at least 19 arbitrary parameters that we would like to be able to calculate. Moreover, the Higgs mechanism, which is believed to be the origin of the particle masses does not occur naturally but must be put by hand. Is the Higgs boson the true origin of the particle masses? Why are there so many different types of quarks and leptons and why do their weak interactions mix in the peculiar way observed? In addition, the gauge groups used in the Standard Model are dictated by experiment and within the Standard Model there are no indications at all as to their origin. Is there a simple group framework for unifying all the particle interactions, a so-called Grand Unified Theory?

But the most severe obstacle for considering the Standard Model as a complete description of Nature is that it does not include gravity. The most familiar force has eluded quantisation for a long time. This failure is intimately connected with the divergences that appear when quantum field theory is applied to point particles. In technical terms, gravity is a non-renormalisable theory since its coupling constant has dimensions  $[\text{mass}]^{-2}$ .

For some time, it was hoped that locally supersymmetric theories, that is supergravity theories, could be finite. By now we know that even these theories diverge at the three loop level. Is a consistent quantum field theory of gravity and thus a theory of everything doomed for ever? Not if we are willing to depart from the notion of the elementary particles being point-like. It now appears that gravity may be consistently quantized if we let the force be carried by a one dimensional object. The quantum theory in which the fundamental constituents are one dimensional extended objects is called string theory. Here the basic idea is, that all matter is made of very tiny strings, open or closed, so that while a particle looks like a point at distances of the order of  $10^{-13}$  cm, if we magnify it to scales of the order of  $10^{-33}$  cm, then we'll see that it is extended like a string of infinitesimal width. The different types of particles we observe are just different excitations of the same string. So instead of having many different particles as the building blocks of Nature, one has only two, an open string and a closed string. Furthermore, a particular excitation of the closed string corresponds to a massless, spin 2 state, that can be identified as the graviton. Thus, string theory necessarily contains quantum gravity.

As mentioned above, consistent string theories seem to avoid the severe difficulties that plague the point particle theories. In particular, string perturbation theory is finite at one loop and it is a common belief that this holds at higher loop order. There are one or two intuitive arguments as to why strings yield improved ultraviolet behaviour compared to the one point particle theories exhibit. In point particle theories the interaction occurs at one and the same for all observers in relative motion space-time point. The coordinates of this point for two observers are related by a Lorentz transformation. Contrary, in string theory there is no well defined notion of when and where the interaction happened as the space-time point of interaction appears to be different to two observers in different frames. Since the divergences in point particle theories occur when two or more vertices coincide and since this is impossible in string theory it seems plausible that string loop diagrams do not suffer from infinities. This has been checked by explicit calculations only at one loop level. Another hint for improved ultraviolet behaviour in a quantum theory is provided by symmetry. Even in the simple case of quantum electrodynamics the gauge symmetry the theory possesses improves the ultraviolet behaviour of the vacuum polarisation diagram. The diagram is logarithmically divergent instead of quadratically divergent as one superficially should expect. The same happens for the photon-photon scattering diagram, which is superficially logarithmically divergent, but turns out to be finite. Another example is given by supersymmetry. Supersymmetric theories exhibit better ultraviolet behaviour than the non-supersymmetric ones. To conclude, the more symmetry the theory possesses the better its ultraviolet behaviour is. String theory has a rich symmetry content, so ultraviolet convergence should not be something completely unexpected.

As mentioned above, strings can be either open or closed. In addition, they may be oriented or un oriented. Consistent open string theories necessarily include closed strings, because the interactions allow a single open string to self-interact and join its free ends to form a closed string. On the contrary, closed string theories need not include open strings.

As is well-known, point particles can live in any space-time dimension. This is not the case for strings since conformal invariance of the theory restricts the number

of the space-time dimensions to a specific value, the critical dimension. The critical dimension is closely related to the number of string world-sheet supersymmetries. Conformally invariant actions can be constructed when there are  $N = 0, 1, 2, 4$  local two-dimensional supersymmetries. The corresponding critical dimensions are  $D = 26, 10, 4, -2$ . The last case is obviously ruled out and the same is true for  $N = 2$  since in this case two of the four dimensions must be time-like. Therefore we are left with  $N = 0, 1$ . But the non-supersymmetric case  $N = 0$  can also be discarded since the lowest lying state is a tachyon.

Let us, now, briefly comment on the consistent  $N = 1$  theories. The open superstring theory with  $N = 1$  world-sheet supersymmetry is known as type I superstring theory. One can show that this theory exhibits  $N = 1$  space-time supersymmetry. One can also attach group charges at the ends of the strings, thereby enriching the theory with gauge interactions. Any group choice is consistent at the tree level. However, at the quantum level the demand that the theory does not have chiral anomalies requires the group to be  $SO(32)$ . As discussed above, open string theories necessarily contain closed strings. Since the latter have no free ends, they are singlets under the Yang-Mills group.

Closed string theories with both the left and the right movers possessing  $N = 1$  local world-sheet supersymmetry are called type II. The theory has two space-time supersymmetries. In the type IIA theory, these space-time supersymmetries are of opposite chirality, while in the type IIB theory are of the same chirality. Type IIB theories have no room for a Yang-Mills group, at least when all 10 dimensions are uncompactified.

When the right movers, let's say, are world-sheet supersymmetric, but the left mover are not, one ends up with the heterotic string. In order to obtain a 10 dimensional theory 16 of the 26 bosonic degrees of freedom of the left movers should be compactified resulting in the introduction of a gauge interaction. Consistency of the theory demands that the compactification is done in such a way that the gauge group is  $E_8 \times E_8$ ,  $spin(32)/Z_2$   $SO(16) \times SO(16)$ . The first two choices give theories with spacetime supersymmetry, while the latter does not.

If we wish to construct more realistic models we have to get down to four di-

mensions by considering string theory on  $R^4 \times M_6$  where  $M_6$  is some six-dimensional compact manifold. It is the geometry of this manifold which determines the low energy physics of the theory. Should we insist that there be an unbroken  $N = 1$  supersymmetry on the four non-compact dimensions, then  $M_6$  must be a Calabi-Yau manifold or a 6-dimensional orbifold. The way the compactification is being done can lead to many different gauge symmetries. It is even possible to cleverly compactify the to get gauge groups as  $SU(3) \times SU(2) \times U(1)$ . To conclude, there are consistent perturbative expansions of string theory around a classical background metric that give reasonable phenomenology. Despite having the potential to describe Nature in a consistent way, string theory leave some unanswered questions ( such as, choice of the vacuum, explanation of why the cosmological constant is so small) and more work has to be done before it makes a decent contact to phenomenology.

In the course of trying to describe quark confinement and to construct a quantum field theory of gravity an intriguing possibility appeared. Namely that there may exist certain dualities between string theories and gauge theories or, even more generally, between gravitational and non-gravitational theories. These dualities are remarkable because they claim an equivalence between two seemingly different physical systems, one that describes gravity on one hand, and one without gravity at all on the other. There are several arguments supporting the expectation of a duality between string theory and gauge theory. One of them has been provided by 't Hooft at 1974.

't Hooft noticed that the Feynman diagram expansion of the large  $N$ -limit of  $U(N)$  gauge theories can be arranged according to the genus  $h$  of the Riemann surface on which the diagram can be drawn and that any correlation function accepts a double expansion, in powers of the effective coupling constant  $\lambda = g_{YM}^2 N$  as well as  $1/N^{2h}$ . This genus expansion of gauge theory reminds the perturbative series of a string theory, where each diagram of genus  $h$  is suppressed by a factor of  $g_s^{2h}$ . Thus, it seems natural to conjecture a duality between gauge theory and string theory with coupling  $g_s \sim 1/N$ . Another hint comes from the study of black holes. Consider, for example, the Bekenstein-Hawking relation for the entropy of an isolated black hole  $S_{bh} = A/4G$ . Since the entropy of the black hole is proportional to the area  $A$  of its horizon and not the volume enclosed by this area, as would be the case for statistical mechanics and

quantum field theory, one may conjecture that there exists a holographic description of the black hole's degrees of freedom in terms of some quantum field theory living on the horizon, so that  $S_{bh} = S_{QFT} \sim A$ . The above argument points to the conjecture that Nature obeys a holographic principle, which states that the number of the degrees of freedom of quantum gravity on some manifold scales as the area of its boundary, suggesting that a field theory on the boundary can be used to describe the physics of gravity in the bulk. One of the most concrete and interesting realisations of the string/gauge theory dualities came from the study of the near horizon geometry of D-3 branes by Maldacena. Maldacena conjectured that type IIB string theory on the  $AdS_5 \times S^5$  background is dual to superconformal  $N = 4$ ,  $D = 4$  Yang-Mills that lives on the boundary of  $AdS_5$ . However, as will be discussed later in this chapter, this is a duality between a strongly coupled theory and a weakly coupled theory. Ideally, one would like to have a weak to weak duality, because in such a case perturbative calculations can be made on both sides of the duality. Such a duality is realised by taking the Penrose limit of the  $AdS_5 \times S^5$  geometry. In particular one focuses on the neighbourhood of the geodesic of a massless particle sitting in the centre of  $AdS_5$  and rotating around an equator of the  $S^5$ . In this limit, only a particular subsector of  $N = 4$  SYM, known as the BMN sector, survives. The interesting feature of this weak to weak duality is that it provides an example where the string/gauge correspondence can be studied beyond the supergravity approximation. It is the study of this duality the first four chapters of this thesis are devoted to.

Recently, Witten proposed that tree level amplitudes of  $N = 4$  SYM can be reproduced by integrating over the moduli space of certain D-instantons in the open string topological B-model whose target space is the supertwistor space  $CP^{3|4}$ . This gives rise to a new duality between weakly coupled  $N = 4$  SYM and a weakly coupled, topological string theory in twistor space. Inspired by this duality, a novel diagrammatic method for calculating all gluon scattering amplitudes at tree level was proposed by Cachazo, Svrcek, and Witten. This method was based on the fact that after Fourier transforming these amplitudes from the helicity basis to twistor space they acquire a surprisingly simple geometric structure, namely the amplitudes are supported on certain configurations of curves in twistor space. This method uses

maximally helicity violating (MHV) amplitudes as effective vertices continued off-shell in a particular fashion and connected by scalar propagators. Chapters 5 and 6 are devoted to the generalisation of this approach to tree amplitudes with gluinos and scalars in the external lines. We also argue that the method applies to theories with less or no supersymmetry at all and a finite number of colours.

This thesis is organised as follows: in the rest of chapter 1 we examine the large- $N$  expansion of gauge theories providing thus evidence for the gauge/string theory dualities. Then, after giving some details about type IIB supergravity theory we briefly describe how the AdS/CFT correspondence arises. Subsequently, we examine the Penrose limit of the AdS geometry and show that free string theory on the resulting plane wave background can be exactly quantised in the light-cone gauge. After that, we develop string field theory which is the appropriate framework to describe string interactions in the presence of a non-zero five-form flux. Finally, at the end of chapter 1, we discuss the plane wave/SYM correspondence as was first proposed in [41] and refined later in [44, 45].

In chapter 2 we calculate 2-point and 3-point correlation functions of  $\Delta$ -BMN operators with three scalar impurities involving up to two string states, and up to order  $g_2\lambda'$ . Conformal invariance of the gauge theory restricts the form of the 2-point and 3-point correlators of conformal primary operators. By using this form and a simple trick, we show how to uniquely determine the 3-point function coefficient directly from the single trace expressions without having to take into account the mixing between single and double trace operators. We, then, use the expressions obtained to provide evidence for a vertex-correlator duality in the pp-wave background.

In chapter 3, after describing the correspondence between the natural string basis and the isomorphic to it gauge theory basis, we explore and verify the pp-wave/SYM correspondence in all directions of the two  $SO(4)$  groups. To achieve this we compare matrix elements of the dilatation operator of  $N = 4$  SYM with the corresponding string amplitudes. This is done for operators involving two scalar, mixed, and vector impurities. We find perfect agreement. In this way, we also clarify the role of the  $\mathbb{Z}_2$  symmetry of the pp-wave background and reproduce the string amplitudes involving two scalar, mixed, and vector states from field theory. Furthermore, we calculate

the matrix elements of  $\Delta - J$  and  $H_{string}$  for states with an arbitrary number of scalar impurities to find, again, perfect agreement. In all cases, in order to extract the desired matrix elements on the field theory side, we first compute the 3-point function coefficient of the appropriate states and from this we easily determine the matrix elements of the dilatation operator.

In chapter 4, we study the BMN correspondence in the fermionic sector. In the beginning we discuss the BMN operators with two fermionic impurities of the same chirality. We then examine how the notion of conjugation as Hermitian conjugation followed by an inversion is applied to the case of a fermionic impurity. This notion of conjugation is crucial if we want the two point function of fermion  $\Delta$ -BMN operator to take the simple canonical form of (4.25) signifying, thus, the orthonormality of the BMN states. Next we calculate the matrix elements of the string Hamiltonian in string field theory and the corresponding matrix elements of the dilatation operator in  $N = 4$  SYM to find agreement for all the representations of two impurity BMN operators. We close this chapter with a brief comment about the action of the  $\mathbb{Z}_2$  on the string amplitudes involving fermionic impurities.

The aim of chapter 5 is to generalise the novel diagrammatic approach of Cachazo, Svrcek, and Witten for calculating gluon tree amplitudes of gauge theories to tree amplitudes which involve fermion fields as well. In the first section of this chapter we briefly recall well-known results about the decomposition of the full amplitudes into a colour factor and a purely kinematic factor and about the helicity amplitudes formalism. We then proceed to apply this method in order to derive expressions for the next to MHV amplitudes involving two and four fermion fields. For simplicity the negative helicity particles are considered to be consecutive. Furthermore, we successfully check the formulae obtained against some previously known results for amplitudes with 4 and 5 external legs.

Chapter 6 starts with a brief review of the spinor helicity formalism. Next we use supersymmetric Ward Identities to express the next to MHV purely gluonic amplitudes in terms of next to MHV amplitudes with gluons and two fermions. In sections 3 and 4 we derive expressions for the NMHV amplitudes with three negative helicities involving gluons and fermions by using the CSW scalar graph method. Section 5 of

this chapter considers the scalar graph method with the single analytic supervertex of Nair [120]. We provide a single formula which gives rise to all tree-level next to MHV amplitudes with three negative helicities in  $0 \leq \mathcal{N} \leq 4$  supersymmetric gauge theories, involving all possible configurations of gauge fields, fermions and scalars. In principle there is no obstacle to continue with further iterations of the analytic supervertex and derive formal expressions for tree amplitudes with an arbitrary number of negative helicities.

## 1.2 1/N Expansion Of Gauge Theories

In a classic paper [6], at 1974, 't Hooft made the remarkable observation that in addition to the expansion in powers of the effective coupling constant  $\lambda = g_{YM}^2 N$ , one may also classify the Feynman diagrams of an  $U(N)$  Yang-Mills gauge theory in powers of  $1/N^2$ . Thus any correlation function has a double expansion, in powers of  $\lambda$  as well as  $1/N^2$ . For large enough  $N$ , the leading term in the  $1/N^2$  expansion comes from the planar diagrams. Any graph that can be drawn on a surface of genus  $h$  is suppressed by a factor of  $1/N^{2h}$ . This genus expansion of Feynman graphs in gauge theory resembles a similar situation in string theory, where the loop diagrams whose world-sheet has genus  $h$  are suppressed by  $g_s^{2h}$  ( $g_s$  is the string coupling). Thus, there is a certain similarity between perturbative gauge and string theories. This can sometimes be made quantitative and lead to a duality correspondence between a gauge and a string theory.

To see these aspects in some detail, let us consider an  $SU(N)$  Yang-Mills gauge theory where the bosons transform in the adjoint representation while the fermions belong either to the adjoint ( $\psi^i$ ) or the fundamental ( $\zeta$ ) representation of  $SU(N)$ . In order to simplify the argument let us supplement the  $SU(N)$  generators  $T^a$ ,  $a = 1, \dots, N^2 - 1$  by adding the  $N \times N$  matrix  $T^0 = I/\sqrt{N}$ . This amounts to extending the gauge group from  $SU(N)$  to  $U(N)$ . We shall also choose the  $U(N)$  generators to satisfy the normalisation condition  $Tr(T^a T^b) = \delta^{ab}$ . The Lagrangian of such a theory

is written as

$$\begin{aligned} \mathcal{L} = & -\frac{1}{4}Tr(F^{\mu\nu}F_{\mu\nu}) + iTr(\bar{\psi}^i\gamma^\mu D_\mu\psi^i) + i\bar{\zeta}^i\gamma^\mu\hat{D}_\mu\zeta_i + \mathcal{L}_{g.f.} + \mathcal{L}_{ghost} \\ & [-g_{YM}^2Tr(\phi^i\phi^j\phi^k\phi^l)C_{ijkl} - g_{YM}Tr(\bar{\psi}^i\psi^j\phi^k)\tilde{C}_{ijk} + g_J(x)G_J(x) + \text{h. c.}], \end{aligned} \quad (1.1)$$

where we have also allowed for some internal R-symmetry group under which the Lagrangian is a singlet.  $\mathcal{L}_{g.f.}$ ,  $\mathcal{L}_{ghost}$  correspond to the gauge fixing and ghost part of the Lagrangian which we do not write explicitly. Finally, (1.1) also contains terms like  $g_J G_J$  since we are interested in calculating correlation functions of single trace gauge invariant operators  $G_J$  of the form  $G_J^{(n)}(x) = Tr(\Phi^1(x)\Phi^2(x)\dots\Phi^n(x))$ . Here  $g_J$  is the source to which  $G_J$  is coupled and  $\Phi^i$  is any of the adjoint fields appearing in (1.1).

The correlator of  $k$  of the composite single trace operators  $\langle \prod_{J=1}^k G_J^{(n_J)}(x_J) \rangle$  can be calculated diagrammatically. One can see from (1.1) that any three-point vertex comes with a factor of  $g_{YM}$  while any four-point vertex with a factor of  $g_{YM}^2$ . One can also consider the insertion of each operator  $G_J^{(n)}$  as an  $n$ -point vertex.

Let us now concentrate on the case where the number of the colours is much greater than one, i.e.  $N \gg 1$ . Then the correlator in question is proportional to  $l = g_{YM}^{\tilde{V}_3+2\tilde{V}_4} N^I$ , where  $\tilde{V}_3$  and  $\tilde{V}_4$  are the numbers of the 3 and 4 point vertices that appear in the Lagrangian (1.1) and are not coupled to the external sources  $g_J$ . In addition, let us denote by  $V_n$  the total number of the  $n$ -point vertices and by  $I$  the number of closed colour loops. Furthermore,  $V'_n$  is the number of the  $n$ -point single trace gauge invariant operators coupled to external sources. It is obvious that  $V_n = V'_n$  for  $n \neq 3, 4$  whereas  $V_n = \tilde{V}_n + V'_n$  for  $n = 3, 4$ . Each closed loop gives a factor of  $N$  since  $\sum_{i=1}^N \delta_i^i = N$ , thus and the factor of  $N^I$  in the expression for  $l$ . Next we consider the number of propagators which is  $P = \frac{1}{2} \sum_n n V_n$  since each propagator is connecting two vertices. The number of faces of the diagram is given by  $F = L + I$ , where  $L$  is how many closed fermion loops with fermions in the fundamental representation are there. Furthermore, let us denote by  $V = \sum_n V_n$  the total number of vertices.

Using Euler's theorem, which states that  $F - P + V = 2 - 2h$  one can write  $l$  as:

$$\begin{aligned}
l &= (g_{YM}^2)^{\tilde{V}_3/2+\tilde{V}_4} N^{\tilde{V}_3/2+\tilde{V}_4} N^{-\tilde{V}_3/2-\tilde{V}_4} N^{F-L} \\
&= (g_{YM}^2 N)^{\tilde{V}_3/2+\tilde{V}_4} N^{-\tilde{V}_3/2-\tilde{V}_4} N^{F-P+V-L} N^{P-V} \\
&= \lambda^{\tilde{V}_3/2+\tilde{V}_4} N^{2-2h-L} N^{-\tilde{V}_3/2-\tilde{V}_4} N^{\frac{3\tilde{V}_3+4\tilde{V}_4+\sum_n nV'_n}{2}-\tilde{V}_3-\tilde{V}_4-\sum_n V'_n} \\
&= \lambda^{\tilde{V}_3/2+\tilde{V}_4} N^{2-2h-L} N^{\sum_n -V'_n} N^{\sum_n n/2V'_n}.
\end{aligned} \tag{1.2}$$

The  $N^{\sum_{n>4} n/2V'_n}$  factor in the above equation is not relevant since it cancels out if we normalise the single trace operators  $G_J^{(n)} = \frac{1}{N^{n/2}} Tr(\Phi^1 \dots \Phi^n)$  in such a way that their free planar 2-point function is one. At the end, what we are left with is:

$$l = \lambda^{\tilde{V}_3/2+\tilde{V}_4} N^{2-2h-L-\sum_n V'_n}. \tag{1.3}$$

From (1.3), we see that the Yang-Mills coupling constant appears only in the combination  $g_{YM}^2 N = \lambda$ . Thus, it seems natural to keep  $\lambda$  fixed as  $N \rightarrow \infty$ . The fact that  $\lambda$  is the correct effective coupling constant for large-N theories can also be seen if we consider the running of the coupling constant  $g$  for QCD with gauge group  $SU(N)$  and quarks with  $N_f$  different flavours. The  $\beta$ -function of this theory is given by [8]

$$\beta = \mu \frac{dg}{d\mu} = -\left(\frac{11}{3}N - \frac{2N_f}{3}\right) \frac{g^3}{16\pi^2} + O(g^5). \tag{1.4}$$

If we keep  $N_f$  fixed, as  $N \rightarrow \infty$ , (1.4) becomes

$$\mu \frac{dg}{d\mu} = -\frac{11}{3}N \frac{g^3}{16\pi^2} + O(g^5). \tag{1.5}$$

The last equation has a well-defined large-N limit if we scale the coupling  $g$  in such a way that  $\lambda = g^2 N$  is fixed. Then (1.5) results to

$$\mu \frac{d\lambda}{d\mu} = -\frac{11}{3} \frac{\lambda^2}{8\pi^2}. \tag{1.6}$$

In this way, the scale parameter of the strong interactions  $\Lambda_{QCD}$  is held fixed as  $N \rightarrow \infty$  since  $N$  drops out of (1.6).

From (1.3), one can see that any correlator has a double expansion of the form  $\sum_{h=0}^{\infty} N^{2-2h-L-\sum_n V'_n} \sum_{n=0}^{\infty} c_{hn} \lambda^n$ . Thus, in addition to the usual coupling constant expansion one also has an expansion in powers of  $\frac{1}{N}$ . This fact strongly reminds the situation in string theory where each world-sheet of genus  $h$  is weighted by a factor

$g_s^{-(2-2h-b)}$ , where  $b$  is the number of boundaries of the world-sheet. Thus, it appears natural to conjecture a duality correspondence between large- $N$  gauge theory and a string theory. In this duality, the genus of the world-sheet in string theory corresponds to the genus of the surface where the Feynman diagrams, of a particular kind, are drawn. Furthermore, each gauge invariant operator participating in the correlator contributes a factor of  $\frac{1}{N} \sim g_s$  corresponding to a vertex operator inserted on the string world-sheet.

If we ignore fermions in the fundamental representation of the  $SU(N)$  subgroup of  $U(N)$  the corresponding string theory is an oriented closed string theory. The inclusion of matter fields in the fundamental representation would result to the inclusion of propagators with a single line giving rise to boundaries of the corresponding surfaces (this can also happen when we calculate correlators of gauge invariant operators  $G_j$  that involve fields in the fundamental representation). As a result, the open string sector should also be taken into account in the dual string model. Finally, the fact that each line on the gauge diagram has a direction means that one can define an orientation of the surface on which the diagram is drawn, that is the dual string theory is a theory of oriented strings.

If the gauge group is  $SO(N)$  or  $USP(N)$  then the adjoint representation is the product of two fundamental representations, instead of one fundamental and one anti-fundamental, and since the fundamental representation is real no arrows can be drawn on the propagators of the diagram. As a result, the surface on which the diagram is drawn may be non-orientable resulting to non-orientable dual string theories.

The arguments given above indicate that large- $N$  gauge theories may be dual to string theories with a coupling proportional to  $\frac{1}{N}$ , but it gives no indication as to precisely which string theory is dual to a particular gauge theory. To construct the dual string theory is a highly non-trivial task, and since 't Hooft's original observation many attempts have been made to construct such dualities explicitly. Such attempts led to dualities between two-dimensional gauge theories and string theories [9, 10]. However, the situation for four-dimensional gauge gauge theories is much less tractable, partly because the planar diagram expansion -which corresponds to

free string theory- of such theories is very complicated<sup>2</sup>.

The seminal breakthrough of Maldacena [7] occurred almost a quarter of a century after 't Hooft's paper. Maldacena conjectured that type-IIB string theory on the  $AdS_5 \times S^5$  background is dual to the superconformal  $N = 4$ ,  $D = 4$  Yang-Mills ( $N = 4$  SYM) that lives on the boundary of  $AdS_5$ .

### 1.3 Type IIB supergravity

Before proceeding to state the Maldacena conjecture more precisely, let us review some facts related to type IIB supergravity (type IIB sugra). Type IIB sugra describes the low energy behaviour of the classical effective action of type IIB string theory. Its field content is the massless spectrum of type IIB strings which is given in terms of the transverse  $SO(8)$  representations as [11, 12]

<u>field</u>	<u><math>SO(8)</math> rep.</u>	<u>degrees of freedom</u>	
$G_{\mu\nu}$ metric – graviton	$35_v$	35 bosonic	
$C + i\Phi$ axion – dilaton	$1 \oplus 1$	2 bosonic	
$B_{\mu\nu} + iA_{2\mu\nu}$ rank 2 antisymmetric	$28 \oplus 28$	56 bosonic	(1.7)
$A_{4\mu\nu\rho\sigma}^+$ antisymmetric rank 4	$35_c$	35 bosonic	
$\psi_{\mu\alpha}^I$ $I = 1, 2$ Majorana – Weyl gravitinos	$56_s \oplus 56_s$	112 fermionic	
$\lambda_{\alpha}^I$ $I = 1, 2$ Majorana – Weyl dilatinos	$8_s \oplus 8_s$	16 fermionic.	

Type IIB sugra is chiral, which means that the two gravitinos have the same chirality, while the two dilatinos have the same chirality but opposite to that of

---

<sup>2</sup>For large- $N$  four-dimensional QCD this difficulty is also associated to the fact that QCD is neither supersymmetric nor conformally invariant.

the gravitinos. The gravitinos are traceless, namely  $\Gamma^{\mu\alpha\beta}\psi_{\mu\beta}^I = 0$ . The fact that the theory is chiral is related to the fact that in the GS formulation of the type IIB superstrings one assigns the same chirality to the Majorana-Weyl spinors  $S^{1a}$ ,  $S^{2a}$  of the right and left movers respectively. That is :  $(8_v + 8_c) \otimes (8_v + 8_c) = (1 \oplus 1 \oplus 28 \oplus 35_v \oplus 28 \oplus 35_c)_B \oplus (8_s \oplus 8 \oplus_c \oplus 56_s \oplus 56_s)_F$ , where the first (second)  $8_v + 8_c$  corresponds to the right movers (left movers). It should be noted that type IIB sugra can not be obtained by dimensional reduction of a higher dimensional theory. Furthermore, there is no completely satisfactory covariant action for type IIB sugra since the usual term  $\int d^{10}\sqrt{|G|} |F_5|^2$  describes both the self-dual and the antiself-dual part of  $F_5$ . As a consequence, one has to impose the self-duality of  $F_5$  as a supplementary condition. However, the theory has covariant equations of motion (e.o.m.) which can be obtained as follows: First, one writes down the local supersymmetry transformations of the fields including all possible terms compatible with the symmetries of the theory- general coordinate invariance, local Lorentz invariance, gauge invariance for the 2-form fields, local  $U(1)$  symmetry and global  $SU(1,1)$  symmetry- with unknown, to be determined, coefficients. Then by applying the commutator of two SUSY transformations to the fields  $[\delta_1, \delta_2]\Phi$  and by demanding closure of the algebra one determines the unknown coefficients, as well as the e.o.m.. This is possible because we are dealing with an on-shell formulation (no auxiliary fields are there to close the algebra) so the algebra closes only if one uses the e.o.m.. It happens that the above method completely determines both the SUSY transformations and the e.o.m.. For more details see [13] and references therein. The covariant e.o.m. derived in this way can be deduced from the action [11]

$$S_{IIB} = +\frac{1}{4\kappa_B^2} \int \sqrt{|G|} e^{-2\Phi} (2R_G + 8\partial_\mu\Phi\partial^\mu\Phi - |H_3|^2) \quad (1.8)$$

$$-\frac{1}{4\kappa_B^2} \int \left[ \sqrt{|G|} (|F_1|^2 + |\tilde{F}_3|^2 + \frac{1}{2}|\tilde{F}_5|^2) + A_4^+ \wedge H_3 \wedge F_3 \right] + \text{fermions}$$

where the field strengths are defined by

$$F_1 = dC, \quad H_3 = dB, \quad F_3 = dA_2, \quad F_5 = dA_4^+$$

$$\tilde{F}_3 = F_3 - CH_3, \quad \tilde{F}_5 = F_5 - \frac{1}{2}A_2 \wedge H_3 + \frac{1}{2}B \wedge F_3 \quad (1.9)$$

with the additional condition  $*F_5 = F_5$  for the self-duality of the five form field  $F_5$ . The p+1-form fields that appear in (1.7) naturally couple to surfaces of dimension

p+1 through the diffeomorphic invariant action

$$S_{p+1} = T_{p+1} \int_{\Sigma_{p+1}} A_{p+1} = T_{p+1} \int d^{p+1}x A_{12\dots p+1}, \quad (1.10)$$

where the p+1-form field is

$$A_{p+1} = \frac{1}{(p+1)!} A_{\mu_1 \dots \mu_{p+1}} dx^{\mu_1} \wedge \dots \wedge dx^{\mu_{p+1}}. \quad (1.11)$$

This is, actually, the generalisation of the coupling of the electromagnetic potential  $A_\mu$  to the world-line of a particle of charge  $q$ ,  $S_{int} = -q \int A_\mu dx^\mu$ . (1.10) is invariant under gauge transformations of the form

$$A_{p+1} \longrightarrow A'_{p+1} = A_{p+1} + d\rho_p, \quad (1.12)$$

where  $\rho_p$  is an arbitrary p-form and  $d$  is the exterior derivative. The gauge invariant field strength  $F_{p+2}$  is defined through  $F_{p+2} = dA_{p+1}$  (this is gauge invariant since  $d^2\rho_p = 0$ ). One can also define a charge associated with the potential  $A_{p+1}$  as

$$Q = \int_{S_{8-p}} *F_{p+2}. \quad (1.13)$$

Solutions to the sugra e.o.m. that have non-zero  $A_{p+1}$  charges are known as p-branes. Each p-brane has a magnetic dual D-4-p brane (D is the space-time dimension, D=10 for type IIB theories) which couples to the magnetic dual potential  $A_{D-3-p}^m$  defined by

$$F_{D-2-p}^m = *F_{p+2} \iff dA_{D-3-p}^m = *dA_{p+1}. \quad (1.14)$$

From (1.7) one can easily specify the possible branes of type IIB sugra. These are: the  $F1$  brane (the fundamental string) which couples to the 2-form  $B_{2\mu\nu}$  and its magnetic dual  $NS5$  brane, the  $D1$  string which couples to  $A_{2\mu\nu}$  and its dual  $D5$  brane, the  $D3$  brane which couples to the self-dual  $A_{4\mu\nu\rho\sigma}$  and its dual  $D3$  brane, and finally the  $D(-1)$  instanton  $A_0 = C + e^{-i\phi}$  and its dual  $D7$  brane. For a complete classification of branes in sugra theories see [11]. One can visualise a p-brane as a p+1 dimensional flat surface and look for solutions with maximal rotational symmetry  $SO(D-p-1)$  in the transverse D-p-1 dimensional space. The above restrictions lead to ansatz for the metric of the form

$$ds^2 = A(\vec{y})dx^\mu dx_\mu + B(\vec{y})dy^i dy_i, \quad \mu = 0, \dots, p, \quad i = 1, \dots, D-p-1. \quad (1.15)$$

When the above ansatz is substituted in the sugra field equations one gets

$$ds^2 = H(\vec{y})^{1/2} dx^\mu dx_\mu + H(\vec{y})^{1/2} dy^i dy_i, \quad e^\phi = H^{3-\frac{p}{4}} \quad (1.16)$$

for Dp branes and

$$ds^2 = dx^\mu dx_\mu + H(\vec{y}) dy^i dy_i, \quad e^{2\phi} = H \quad (1.17)$$

for the NS5 brane. The function H satisfies

$$\square_y H(\vec{y}) = 0. \quad (1.18)$$

The most general solution to (1.18) with the boundary condition that the metric becomes the flat space metric when  $y \rightarrow \infty$  is

$$H(\vec{y}) = 1 + \sum_I \frac{c_I}{|\vec{y} - \vec{y}_I|^{D-3-p}} \quad (1.19)$$

with  $c_I = N_I \rho_p$  where  $\rho_p = g_s (4\pi)^{5-\frac{p}{2}} \Gamma(\frac{7-p}{2}) \alpha'^{\frac{D-3-p}{2}}$  for the case of Dp branes. The above solution corresponds to a configuration of  $N_1$  branes situated at point  $y_1$ ,  $N_2$  branes situated at  $y_2$ , etc.. Although being a solution it is not  $SO(D-p-1)$  symmetric in the transverse space. If one insists to a symmetric solution then all the branes have to coincide and the solution becomes

$$H(\vec{y}) = 1 + \frac{N \rho_p}{y^{D-3-p}}, \quad (1.20)$$

where  $N = \sum_I N_I$ . Actually, this solution is the solution for an extremal black p brane with charge

$$N = Q = \int_{S_{8-p}} *F_{p+2}. \quad (1.21)$$

This solution preserves half of the supersymmetries, so it is a 1/2 BPS object (see [14]).

One final comment is in order. By inspection of the equation of motion for the metric

$$\begin{aligned} R_{\mu\nu} &= \frac{1}{4} H_{\mu\rho\sigma} H_\nu{}^{\rho\sigma} + e^{2\Phi} \left( F_{1\mu} F_{1\nu} + \frac{1}{4} \tilde{F}_{3\mu\sigma\rho} \tilde{F}_{3\nu}{}^{\rho\sigma} + \frac{1}{24} \tilde{F}_{5\mu\rho\sigma\tau\nu}^+ \tilde{F}_{5\nu}^{+\rho\sigma\tau\nu} \right) \\ &+ \text{(terms involving derivatives of } \phi \text{ and C)} \end{aligned} \quad (1.22)$$

one sees that the  $F1$  and  $NS5$  solutions have vanishing R-R fields  $F_i$  and non-vanishing NS-NS fields. This means that the solution one obtains does not depend on the string coupling  $g_s = e^\phi$ ,  $\phi = \langle \Phi \rangle$ . On the other hand, D-branes carry a R-R charge, i.e. one of the  $F_i$  in (1.22) is non-zero, so the solution will involve  $g_s$  (see the second term of (1.22)). In fact for these solutions  $\rho_p \sim g_s$ . In the weak string coupling limit  $g_s \rightarrow 0$  the metric becomes flat everywhere except on the plane  $\vec{y} = 0$ . This means that the closed strings move freely in flat space-time, except when they reach the D-brane at  $\vec{y} = 0$ . When they touch the D-brane, they can open and stay attached to it. Their open ends are restricted to move on the brane while the string can oscillate in 10 dimensions. Thus, the correct boundary conditions turn out to be, Dirichlet boundary conditions in the directions perpendicular to the brane, and Neumann boundary conditions in the directions parallel to the brane.

D-branes were first introduced in [15] where it was shown that the stack of  $N$  D $p$ -branes on top of each other carries a  $p+1$ -form charge of magnitude

$$N = Q = \int_{S_{8-p}} *F_{p+2}. \quad (1.23)$$

It was also shown that when  $p$  is odd exactly one half of the space-time supercharges of type IIB theory are broken by the configuration of the D-branes. So, the D-brane is a half BPS object in string theory carrying a R-R charge. One, thus, is led to believe that the extremal black  $p$ -brane solution of supergravity and the D $p$ -brane describe the same object. Of particular interest is the case of D3-branes whose complete solution is given by

$$\begin{aligned} g_s &= e^\phi, \phi = \text{const.}, C = \text{const.}, B_{\mu\nu} = A_{2\mu\nu} = 0 \\ ds^2 &= H(\vec{y})^{-\frac{1}{2}} dx^\mu dx_\mu + H(\vec{y})^{\frac{1}{2}} (dr^2 + r^2 d\Omega_5^2) \\ F_5 &= (1 + *) dt \wedge dx^1 \wedge dx^2 \wedge dx^3 \wedge dH^{-1}, \end{aligned} \quad (1.24)$$

where

$$H = 1 + \frac{R^4}{r^4}, R^4 = 4\pi g_s \alpha'^2 N. \quad (1.25)$$

The above sugra solution is self-dual, it has a constant axion and dilaton field, its world-volume is Poincare invariant and despite the form of the metric is regular at

$\vec{y} = 0$  (this can be checked by evaluating the curvature tensor and verifying that it is finite at  $\vec{y} = 0$ ).

Let us, now, take the low energy limit  $\alpha' \rightarrow 0$  while keeping the energies of the objects in string units fixed, namely

$$\frac{E_p}{l_s} = E_p \sqrt{\alpha'} = \text{fixed}. \quad (1.26)$$

$E_p$  is the energy of an object as measured by an observer situated at position  $r$ , while by  $E$  we denote the energy of the same object as measured by an observer at infinity.

These two are related by

$$E = H^{-\frac{1}{4}} E_p \quad (1.27)$$

due to the redshift (from (1.24)  $g_{tt} = -H^{-\frac{1}{2}}$ ). For objects near the brane, that is near  $\vec{y} = 0$  (1.27) becomes

$$E \simeq \frac{r}{\sqrt{\alpha'}} E_p \frac{1}{(4\pi g_s N)^{\frac{1}{4}}} \simeq E_p \sqrt{\alpha'} \frac{1}{(4\pi g_s N)^{\frac{1}{4}}} \frac{r}{\alpha'}. \quad (1.28)$$

Since we send  $\alpha' \rightarrow 0$  keeping  $E_p \sqrt{\alpha'}$  fixed the last equation implies that we should also keep  $\frac{r}{\alpha'}$  fixed. At this limit the sugra solution (1.24) becomes

$$\begin{aligned} g_s &= e^\phi, \quad \phi = \text{const.}, \quad C = \text{const.}, \quad B_{\mu\nu} = A_{2\mu\nu} = 0 \\ ds^2 &= \frac{r^2}{R^2} dx^\mu dx_\mu + R^2 \frac{dr^2}{r^2} + R^2 d\Omega_5^2 \\ F_5 &= \frac{1 + *}{g_s} dt \wedge dx^1 \wedge dx^2 \wedge dx^3 \wedge d\frac{r^4}{R^4} = (1 + *)(-16\pi\alpha'^2 N d\Omega_5), \end{aligned} \quad (1.29)$$

where  $d\Omega_5$  is the volume element of a unit 5-sphere. Thus, the geometry of the background given in (1.29) is that of an  $AdS_5 \times S^5$  space with constant five form flux through the 5-sphere  $S^5$ . From the point of view of an observer at infinity there are two kinds of low energy excitations: a) massless particles with large wavelengths that propagate in the bulk,

b) excitations of any energy  $E_p$  that live closer and closer to the brane ( $r = 0$ ).

These two low energy sectors of the theory are decoupled from each other since as we approach  $r = 0$  the redshift becomes infinite and the excitations can not climb the gravitational potential and escape in the asymptotic region. As a result the throat geometry (the geometry near  $r = 0$ ) is decoupled from the asymptotic regime, in the low energy limit. Thus, we have ended with two decoupled sectors, the near horizon region of the geometry and free bulk supergravity.

## 1.4 The AdS/CFT correspondence

Another description of the same system is to consider type IIB string theory in flat space with  $N$  coincident D3-branes. As discussed above string theory on this background accommodates both closed and open strings. For energies much less than  $1/l_s$  only the massless spectrum can be excited and the theory can be described by an effective Lagrangian consisted of three parts:

- a) type IIB sugra + higher order terms. This part is the effective Lagrangian describing the closed string massless states.
- b)  $N = 4$  SYM Lagrangian define on the brane world-volume+ higher order corrections. This part comes from the massless open string spectrum.
- c) An effective part describing the interactions between the brane modes and the sugra bulk modes.

Taking the low energy limit  $\alpha' \rightarrow 0$  the interaction part as well as the higher order corrections vanish resulting to two decoupled systems [14]. Free bulk supergravity, on one hand, and the maximally supersymmetric  $N = 4$  four-dimensional SYM on the other. Comparing now this description to the alternative one given in terms of the sugra solution (1.29) we see that in both cases we have two decoupled theories in the low energy limit. Since in both cases one of the theories is bulk sugra, it seems justified to conjecture the equivalence of the second decoupled system appearing in both descriptions. This is the Maldacena conjecture which states that:

**Type IIB superstring theory on  $AdS_5 \times S^5$  is dual to  $N = 4$  4-dimensional SYM with gauge group  $SU(N)$  in its superconformal phase.**

It should be noted that both the  $AdS_5$  and the  $S^5$  have the same radius given by  $R^4 = 4\pi g_s \alpha'^2 N$  and that the five-form  $F_5$  has integer flux  $N$  through the 5-sphere  $S^5$ . Furthermore,  $4\pi g_s = g_{YM}^2$  and  $\langle C \rangle = \theta_I$ , that is the axion expectation value is the instanton angle in gauge theory.

The conjecture stated above is the strong version of the ADS/CFT correspondence. It is believed to hold for any values of  $N$  and of  $g_s$ . This form of the conjecture is, however, very difficult to be checked mainly because the quantization of

string theory on  $AdS_5 \times S^5$  appears to be notoriously difficult.

A weaker form of the conjecture is to assume the equivalence of the two theories but only in the large- $N$  limit. That is when we keep  $\lambda = g_{YM}^2 N$  fixed and finite and we send  $N \rightarrow \infty$ . This means that the string coupling is

$$g_s = \frac{\lambda}{N} \rightarrow 0. \quad (1.30)$$

As discussed in section 1.1 the loop expansion in string theory corresponds to the  $\frac{1}{N}$  expansion in field theory. But since the conjecture holds for  $N \rightarrow \infty$ , that is  $g_s \rightarrow 0$ , one gets a correspondence between classical string theory (no loops) and the large- $N$  limit of  $N = 4$  SYM.

A still weaker form says that the conjecture is valid only for large  $\lambda = g_s N$ . Actually, this is the condition that the sugra solution for D3-branes is a good approximation to the full string theory solution. This is so because one can trust the sugra only when the radius  $R$  of the solution is much greater than the string length  $l_s = \sqrt{\alpha'}$ , that is only when

$$(4\pi g_s N)^{1/4} l_s \gg l_s \iff \lambda = g_s N \gg 1. \quad (1.31)$$

But in the limit  $\lambda \gg 1$  the gauge theory is strongly coupled so one ends up with a duality between classical type IIB supergravity and the large  $\lambda$  limit of  $N = 4$  SYM. In this case only sugra and not the full string theory on  $AdS_5$  agrees with field theory.

Let us first concentrate on the strongest form of AdS/CFT. Since one identifies two apparently different theories one should also be able to show that the symmetries of the two theories are identical. This is indeed the case, since the maximal bosonic subgroup  $SU(2, 2) \otimes SU(4)_R$  of the superconformal group  $SU(2, 2 | 4)$  of  $N = 4$  SYM is identical to the isometry group of the  $AdS_5 \times S^5$  background which is  $SO(2, 4) \otimes SO(6)$  since  $SU(2, 2) \sim SO(2, 4)$  and  $SU(4)_R \sim SO(6)$ . In the above,  $SO(2, 4)$  is the conformal group in 4-dimensions and  $SU(4)_R$  is the internal R-symmetry of  $N = 4$  SYM.

As was mentioned in section 1.2 only one half of the supersymmetries are preserved by the stack of  $N$  coincident D3-branes. However, in the near horizon limit the 16 SUSY's which are broken in the full D3-brane solution are restored resulting to the  $SU(2, 2 | 4)$  symmetry group of the maximally supersymmetric  $AdS_5 \times S^5$

Type IIB string theory	$\mathcal{N} = 4$ conformal super-Yang-Mills
Supergravity Excitations 1/2 BPS, spin $\leq 2$	Chiral primary + descendants $\mathcal{O}_2 = \text{tr} X^{\{i} X^{j\}} + \text{desc.}$
Supergravity Kaluza-Klein 1/2 BPS, spin $\leq 2$	Chiral primary + Descendants $\mathcal{O}_\Delta = \text{tr} X^{\{i_1 \dots X^{i_\Delta\}} + \text{desc.}$
Type IIB massive string modes non-chiral, long multiplets	Non-Chiral operators, dimensions $\sim \lambda^{1/4}$ e.g. Konishi $\text{tr} X^i X^i$
Multiparticle states	products of operators at distinct points $\mathcal{O}_{\Delta_1}(x_1) \dots \mathcal{O}_{\Delta_n}(x_n)$
Bound states	product of operators at same point $\mathcal{O}_{\Delta_1}(x) \dots \mathcal{O}_{\Delta_n}(x)$

Table 1.1: Mapping of String and SUGRA states onto SYM Operators

solution. Finally, the Montonen-Olive symmetry of  $N = 4$  SYM with group  $SL(2, Z)$  is identified to the global discrete symmetry of type IIB string theory which mixes the axion and dilaton expectation values according to

$$\tau \longrightarrow \tau' = \frac{a\tau + b}{c\tau + d}, \quad a, b, c, d, \in Z, \quad \tau = \langle C \rangle + ie^{-\phi}. \quad (1.32)$$

One can actually do even better and show that the representations of the supergroup  $SU(2, 2 | 4)$  coincide on both sides of the duality. In fact, one is able to map string and sugra states of the *AdS* side onto SYM gauge invariant operators. In particular, single particle states (or canonical fields) correspond to single trace operators, while multi-particle states correspond to products of single trace operators at different points. Finally, products of single trace operators at the same point correspond to bound states on the *AdS* side. The complete correspondence between the representations of  $SU(2, 2 | 4)$  as taken from [11] is given in Table 1. The first two lines of Table 1 show the correspondence between the short 1/2 BPS multiplets of single trace gauge invariant operators and the supergravity multiplet. The canonical fields in the sugra multiplet arise from the dimensional reduction of the 10-dimensional type IIB sugra multiplet. Since these fields have helicities between -2 and 2 they belong to short multiplets of the superconformal algebra in agreement with the field

theory side. Although no-one has been able to compute the full spectrum of type IIB string theory on  $AdS_5 \times S^5$  one can, however, estimate that the mass of the massive string states will be of the order  $m \sim \frac{1}{l_s}$ . Using the mass/dimension relation, this estimation gives a prediction for the dimension of the non-chiral, unprotected operators that correspond to these massive states. For a scalar operator, for instance, one has

$$m^2 R^2 = \Delta(\Delta - 4) \implies \Delta \sim mR \implies \Delta \sim \frac{1}{l_s} (4\pi l_s^4 g_s N)^{1/4} = (4\pi g_s N)^{1/4} \implies \Delta \sim \lambda^{1/4} \quad (1.33)$$

for large  $g_s N$ . The exact correspondence between the fields of D=10 sugra multiplet and the SYM operators can be found in [11].

Having established the operator/state correspondence one can go further and map the correlation functions on both sides of the correspondence. The way to achieve this was first proposed in [35, 36]. Consider, for example, a scalar bulk field  $\varphi_\Delta(z)$  defined on Euclidean  $AdS_5$  with metric

$$ds^2 = \frac{1}{z_0^2} (dz_0^2 + d\vec{z}). \quad (1.34)$$

The boundary of  $AdS_5$  is the hypersurface  $z_0^2$  so  $\partial AdS_5 = R^4$ . Assuming that the fields become asymptotically free as we approach the boundary, that is they satisfy

$$(\square + m_\delta)\varphi_\Delta^0 = 0, \quad (1.35)$$

where

$$\square = -\frac{1}{\sqrt{g}} \partial_\mu \sqrt{g} g^{\mu\nu} \partial_\nu = -z_0^2 \partial_0^2 + (d-1)z_0 \partial_0 - z_0^2 \partial_i^2, \quad (1.36)$$

we can determine their asymptotical behaviour which reads

$$\varphi_\Delta^0 = z_0^\Delta \tilde{\varphi}(\vec{z}) \text{ or } \varphi_\Delta^0 = z_0^{4-\Delta} \tilde{\varphi}(\vec{z}). \quad (1.37)$$

Solutions with the former asymptotical behaviour correspond to normalised bulk excitations and as argued in [16] determine the vacuum expectation values of operators of associated dimensions and quantum numbers. On the other hand, solutions with the latter asymptotical behaviour do not correspond to bulk excitations, but describe

the coupling of external sources to string theory. The relation put forward in [35,36] states that the generating function of the correlators in field theory is equal to the string partition function where the field  $\varphi_\Delta(z_0, \vec{z})$  obeys the asymptotics

$$\varphi_\Delta(z_0, \vec{z}) \Big|_{z_0 \rightarrow 0} = z_0^{4-\Delta} \varphi_\Delta^{(0)}(\vec{z}), \quad (1.38)$$

namely that

$$\langle e^{\int d^4z \varphi_\Delta^{(0)}(\vec{z}) \mathcal{O}_\Delta(\vec{z})} \rangle_{SYM} = Z_{st}[\varphi_\Delta(z_0, \vec{z}) \Big|_{z_0 \rightarrow 0} = z_0^{4-\Delta} \varphi_\Delta^{(0)}(\vec{z})]. \quad (1.39)$$

Here  $\mathcal{O}(\vec{z})$  is the SYM operator which corresponds to the bulk field  $\varphi_\Delta(z_0, \vec{z})$  and  $\varphi_\Delta^{(0)}(\vec{z})$  is an arbitrary function which acts as a source for  $\mathcal{O}(\vec{z})$  on the CFT side.

In the supergravity approximation  $\alpha' \rightarrow 0$ ,  $g_s N \gg 1$  one can approximate the string partition function by

$$Z_{st} \simeq e^{-S_{SUGRA}[\varphi_\Delta]}, \quad (1.40)$$

where  $S_{SUGRA}[\varphi_\Delta]$  is the extremum of the sugra action when all the fields  $\varphi_\Delta$  satisfy the asymptotic behaviour of (1.38). The last equation implies that the generating functional  $W$  of connected Green functions on the SYM side defined by

$$\langle e^{\int d^4z \varphi_\Delta^{(0)}(\vec{z}) \mathcal{O}_\Delta(\vec{z})} \rangle_{SYM} = e^{-W} \quad (1.41)$$

is equal to the classical sugra action.

We close this section by considering the three point functions of chiral (1/2 BPS) primary operators  $\mathcal{O}_\Delta$ . These can be calculated perturbatively on the SYM side when  $\lambda \ll 1$ . On the AdS side one is able to calculate these functions at the classical sugra limit, that is when  $N \gg 1$ ,  $\lambda \gg 1$ . Thus the two results are not directly comparable since they are valid for different values of the coupling constant. Nevertheless, if one insists to make the comparison he sees that

$$\lim_{N, \lambda = g_s N \rightarrow \infty} c_{\Delta_1, \Delta_2, \Delta_3}(g_s, N) \Big|_{AdS} = \lim_{N \rightarrow \infty} c_{\Delta_1, \Delta_2, \Delta_3}(0, N) \Big|_{SYM}. \quad (1.42)$$

One can interpret this result as non-renormalisation of the three-point functions of 1/2 BPS operators. One, thus, is led to conjecture that

$$\lim_{N \rightarrow \infty} c_{\Delta_1, \Delta_2, \Delta_3}(g_s, N) \Big|_{AdS} = \lim_{N \rightarrow \infty} c_{\Delta_1, \Delta_2, \Delta_3}(g_{YM}^2, N) \Big|_{SYM}, \quad (1.43)$$

where the large- $N$  limit of the three-point function is independent of the coupling constant  $g_s = g_{YM}^2$ . Consequently, one can make the final step and conjecture that the coefficient as calculated from the *AdS* side is equal to the coefficient as calculated from the SYM side for all values of  $g_{YM}$  and  $N$ , that is

$$c_{\Delta_1, \Delta_2, \Delta_3}(g_s, N) \Big|_{AdS} = c_{\Delta_1, \Delta_2, \Delta_3}(g_{YM}^2, N) \Big|_{SYM}. \quad (1.44)$$

The conjecture that the three-point functions do not receive radiative corrections was checked to order  $g_{YM}^2$  in [17]. These non-renormalisation effects were also studied in [18–21, 23, 24] for 1/2 BPS operators and in [22] for 1/4 BPS operators. We shall see later how this correspondence between the three-point function coefficient and the bulk sugra coupling is realised in the BMN limit of the AdS/CFT duality. For higher point correlators and their connection to sugra bulk couplings see [11] and references therein.

## 1.5 Penrose limit of the AdS geometry

In this section, we describe how the Penrose limit of the  $AdS_5 \times S^5$  geometry is taken to obtain the pp-wave geometry.

Let us start with  $AdS_5 \times S^5$  metric using coordinates that can globally cover the hyperboloid  $AdS_5$ . In these coordinates the metric and five-form field become [14]:

$$\begin{aligned} ds^2 &= R^2(-\cosh^2 \rho dt^2 + d\rho^2 + \sinh^2 \rho d\Omega_3^2) + R^2(\cos^2 \theta d\phi^2 + d\theta^2 + \sin^2 \theta d\Omega_3^2) \\ F_{S^5} &= 4Nd\Omega_5, \quad F_{AdS_5} = *F_{S^5}. \end{aligned} \quad (1.45)$$

Here  $R$  is the common radius of  $AdS_5$  and  $S^5$ , and  $d\Omega_3^2$  is the metric on a unit 3-sphere. Imagine, now, an observer who boosts up to the speed of light along the null geodesic defined by

$$\rho = \theta = 0, \quad \tau - \phi = \text{const.}, \quad (1.46)$$

that is along the equator of  $S^5$  at  $\rho = 0$ . The geometry this observer sees is the geometry of the vicinity of the null geodesic and can be determined if we let  $R \rightarrow \infty$

and then scale the coordinates according to

$$x^- = R^2(\tau - \phi), \quad x^+ = \frac{1}{2}(\tau + \phi), \quad \rho = \frac{x}{R}, \quad \theta = \frac{y}{R}, \quad (1.47)$$

keeping  $x^+$ ,  $x^-$ ,  $x$ ,  $y$  and all the other coordinates fixed. Rewriting the metric in terms of the new coordinates and taking the limit  $R \rightarrow \infty$  one obtains:

$$ds^2 = -2dx^+dx^- - (x^2 + y^2)(dx^+)^2 + dx^i dx^i + dy^i dy^i, \quad (1.48)$$

where  $i = 1, \dots, 4$ . The Penrose limit of the self-dual five-form is

$$F_5 = \frac{4}{g_s} dx^+ \wedge (dx^1 \wedge \dots \wedge dx^4 + dy^1 \wedge \dots \wedge dy^4). \quad (1.49)$$

Finally, one can rescale  $x^+$  and  $x^-$ ,  $x^+ \rightarrow \mu x^+$ ,  $x^- \rightarrow \frac{x^-}{\mu}$  to get the plane wave solution

$$ds^2 = -2dx^+dx^- - \mu^2(x^2 + y^2)(dx^+)^2 + dx^i dx^i + dy^i dy^i$$

$$F_5 = \frac{4\mu}{g_s} dx^+ (dx^1 \wedge \dots \wedge dx^4 + dy^1 \wedge \dots \wedge dy^4). \quad (1.50)$$

From (1.50) it is immediate to see that the plane wave solution is symmetric under the group  $SO(4)_x \otimes SO(4)_y \otimes \mathbb{Z}_2$ , where the first  $SO(4)_x$  group rotates the four  $x$ 's among themselves while the second  $SO(4)_y$  rotates the four  $y$ 's among themselves. Furthermore, there is also a discrete  $\mathbb{Z}_2$  symmetry which exchanges the  $x$  coordinates with the  $y$  coordinates, i.e.  $\mathbb{Z}_2 : x^i \longleftrightarrow y^i$ .

The plane wave solution considered in (1.50) is a special case of a most general class of backgrounds called pp-waves. The latter are defined as those backgrounds which have a covariantly constant null Killing vector  $u^\mu$ , i.e.

$$\nabla_\mu u_\nu = 0, \quad u^\mu u_\mu = 0 \quad (1.51)$$

(in the special case of (1.50) this null Killing vector is  $\frac{\partial}{\partial x^-}$ ). The most general form of the metric can be found in [25]. As discussed in [26, 27] the existence of a covariantly null Killing vector ensures that the pp-wave solutions are  $\alpha'$  exact solutions of supergravity. As mentioned in [25], taking the Penrose limit of a specific geometry results to a geometry that preserves at least as many supersymmetries as the

initial geometry was preserving. In our case, since the  $AdS_5 \times S^5$  background preserves all 32 SUSY's we expect that the plane wave solution of (1.50) is also maximally supersymmetric. In order to verify this one should find 32 linearly independent Killing spinors  $\epsilon^\alpha$  for which the dilatino and gravitino variations vanish, i.e.

$$\delta_\epsilon \lambda^\alpha = (\tilde{D})^\alpha_\beta \epsilon^\alpha = 0, \quad \delta_\epsilon \psi_\mu^\alpha = (\hat{D}_\mu)^\alpha_\beta \epsilon^\alpha = 0, \quad \alpha, \beta = 1, 2. \quad (1.52)$$

The  $\epsilon^\alpha$  are two -since type IIB theory is a  $\mathcal{N} = 2$  theory- 32-component Weyl-Majorana spinors of the same chirality-since type IIB theory is chiral-. The expressions for the supercovariant derivatives  $(\tilde{D})^\alpha_\beta$ ,  $(\hat{D}_\mu)^\alpha_\beta$  can be found in [25, 28]. For the special case of the plane wave background of (1.50),  $(\tilde{D})^\alpha_\beta$  becomes identically zero and  $(\hat{D}_\mu)^\alpha_\beta$  takes the form

$$(\hat{D}_\mu)^\alpha_\beta = \delta^\alpha_\beta \left( \partial_\mu + \frac{1}{4} \omega_\mu^{ab} \Gamma_{ab} \right) + \frac{ig_s}{16 \cdot 5!} (\sigma^2)^\alpha_\beta \Gamma^{\nu\rho\lambda\sigma\delta} F_{\nu\rho\lambda\sigma\delta}, \quad (1.53)$$

where  $\omega_\mu^{ab}$  is the spin connection. The 32 Killing spinors that satisfy  $(\hat{D}_\mu)^\alpha_\beta \epsilon^\alpha = 0$ , as well as the isometries of the plane wave background and the supersymmetry algebra in the light cone gauge can be found in [25].

## 1.6 Light cone string field theory

### 1.6.1 Bosonic Part Of The Free String Action

In this section, we briefly review light cone string field theory on the pp-wave background. We start by writing down the bosonic part of the free Green-Schwarz (GS) superstring. This is [29]:

$$S_B = \frac{1}{4\pi\alpha'} \int d^2\sigma \sqrt{-g} g^{ab} G_{\mu\nu} \partial_a X^\mu \partial_b X^\nu, \quad (1.54)$$

where as usual  $G_{\mu\nu}$  is the pp-wave spacetime metric and  $g^{ab}$  the world-sheet metric. One can immediately see that the five form field  $F_5$  does not enter the bosonic part of the action resulting to an  $SO(8)$  invariant action. Plugging the metric in (1.54) we get:

$$S_B = \frac{1}{4\pi\alpha'} \int d^2\sigma g^{ab} \left( -2\partial_a X^+ \partial_b X^- + \partial_a X^I \partial_b X^I - \mu^2 X_I^2 \partial_a X^+ \partial_b X^+ \right). \quad (1.55)$$

Using the fact that the above action is diffeomorphic invariant, as well as Weyl invariant, one can set  $g^{ab} = \eta^{ab}$ . Even after this choice there is still some residual gauge symmetry, namely any change of variables of the form  $\sigma_+ = \tau + \sigma = f_+(\sigma_+)$ ,  $\sigma_- = \tau - \sigma = f_-(\sigma_-)$  together with a Weyl rescaling of the metric leaves the action invariant. One can completely fix the gauge if in addition to  $g^{ab} = \eta^{ab}$  one imposes the condition

$$X^+ = x^+ + \alpha' p^+ \tau. \quad (1.56)$$

This is the light cone gauge. In this gauge only the physical degrees of freedom  $X^I$ ,  $I = 1, \dots, 8$  are dynamical variables.  $X^-$  is determined by setting

$$T_{ab} = \frac{1}{\sqrt{-g}} \frac{\delta S}{\delta g^{ab}} = 0. \quad (1.57)$$

More precisely,

$$\frac{\delta S}{\delta g_{\tau\sigma}} = 0 \Rightarrow \partial_\sigma X^- = \frac{1}{\alpha' p^+} \partial_\sigma X^I \partial_\tau X^I, \quad (1.58)$$

and

$$\begin{aligned} \frac{\delta S}{\delta g_{\tau\tau}} = \frac{\delta \mathcal{L}}{\delta g_{\sigma\sigma}} = 0 \Rightarrow \\ \partial_\tau X^- = \frac{1}{2\alpha' p^+} \left( \partial_\tau X^I \partial_\tau X^I + \partial_\sigma X^I \partial_\sigma X^I - (\mu\alpha' p^+)^2 X^I X^I \right). \end{aligned} \quad (1.59)$$

The advantage of working in the light cone gauge is that all the degrees of freedom after the gauge fixing are dynamical and thus no negative norm states appear in the spectrum.

The equations of motion (e.o.m.) for the  $X^I$  as derived from (1.55) are:

$$(\partial_\tau^2 - \partial_\sigma^2 - \mu^2) X^I = 0. \quad (1.60)$$

These e.o.m. can also be derived from the light cone action:

$$\begin{aligned} S_B^{l.c.} &= \frac{1}{4\pi\alpha'} \int d\tau \int_0^{2\pi} d\sigma \left[ \partial_\tau X^I \partial_\tau X^I - \partial_\sigma X^I \partial_\sigma X^I - (\mu\alpha' p^+)^2 X_I^2 \right] \\ &= \frac{1}{4\pi\alpha'} \int d\tau \int_0^{2\pi\alpha' p^+} d\sigma \left[ \partial_\tau X^I \partial_\tau X^I - \partial_\sigma X^I \partial_\sigma X^I \right]. \end{aligned} \quad (1.61)$$

$$S_B^{l.c.} = \frac{1}{4\pi\alpha'} \int d\tau \int_0^{2\pi\alpha' p^+} d\sigma \left[ \partial_\tau X^I \partial_\tau X^I - \partial_\sigma X^I \partial_\sigma X^I - \mu^2 X_I^2 \right]. \quad (1.62)$$

This action is quadratic in  $X^I$ 's and hence it is solvable. The equations of motion for  $X^I$ ,

$$(\partial_\tau^2 - \partial_\sigma^2 - \mu^2) X^I = 0, \quad (1.63)$$

should be solved together with the closed string boundary conditions

$$X^I(\sigma + 2\pi\alpha'p^+) = X^I(\sigma). \quad (1.64)$$

Using these boundary conditions one obtains

$$X^I = x_0^I \cos \mu\tau + \frac{p_0^I}{\mu p^+} \sin \mu\tau + \sqrt{\frac{\alpha'}{2}} \sum_{n=1}^{\infty} \frac{1}{\sqrt{\omega_n}} \left[ \alpha_n^I e^{\frac{-i}{\alpha'p^+}(\omega_n\tau+n\sigma)} + \tilde{\alpha}_n^I e^{\frac{-i}{\alpha'p^+}(\omega_n\tau-n\sigma)} + \alpha_n^{I\dagger} e^{\frac{+i}{\alpha'p^+}(\omega_n\tau+n\sigma)} + \tilde{\alpha}_n^{I\dagger} e^{\frac{+i}{\alpha'p^+}(\omega_n\tau-n\sigma)} \right], \quad (1.65)$$

where

$$\omega_n = \sqrt{n^2 + (\alpha'\mu p^+)^2}, \quad n \geq 0, \quad (1.66)$$

and  $\alpha$  and  $\tilde{\alpha}$  correspond to the right and left moving modes.

Defining the canonical momentum conjugate to  $X^I$  as usual

$$P^I = \frac{\partial L}{\partial \partial_\tau X^I} = \frac{\delta S}{\delta \partial_\tau X^I} = \frac{1}{2\pi\alpha'} \partial_\tau X^I \quad (1.67)$$

one can easily obtain the light-cone Hamiltonian

$$H_B^{l.c.} = \frac{1}{4\pi\alpha'} \int_0^{2\pi\alpha'p^+} d\sigma \left[ (2\pi\alpha')^2 P_I^2 + (\partial_\sigma X^I)^2 + \mu^2 X_I^2 \right]. \quad (1.68)$$

Since this Hamiltonian is quadratic in  $X^I$  and  $P^I$  it can be diagonalised<sup>3</sup>. Substituting for the mode expansion in (1.68) one gets

$$H_B^{l.c.} = \frac{1}{\alpha'p^+} \left[ \alpha' \mu p^+ \alpha_0^{I\dagger} \alpha_0^I + \sum_{n=1}^{\infty} \omega_n (\alpha_n^{I\dagger} \alpha_n^I + \tilde{\alpha}_n^{I\dagger} \tilde{\alpha}_n^I) \right] + \frac{8}{\alpha'p^+} \left( \frac{1}{2} \alpha' \mu p^+ + \sum_{n=1}^{\infty} \omega_n \right), \quad (1.69)$$

where we have defined

$$\tilde{\alpha}_0^I \equiv \alpha_0^I = \frac{1}{\sqrt{2\mu p^+}} p_0^I - i \sqrt{\frac{\mu p^+}{2}} x_0^I. \quad (1.70)$$

<sup>3</sup>In order for the theory to be quantised one has to impose the usual equal time quantisation conditions, namely  $[X^I(\sigma, \tau), P^J(\sigma', \tau)] = i\delta^{IJ}\delta(\sigma - \sigma')$ . When the expressions for  $X^I$  and  $P^I$  in terms of the creation and destruction operators are substituted in the last equation it leads to  $[x_0^I, p_0^J] = i\delta^{IJ}$ ,  $[\alpha_n^I, \alpha_m^{J\dagger}] = [\tilde{\alpha}_n^I, \tilde{\alpha}_m^{J\dagger}] = \delta^{IJ}\delta_{mn}$ .

The last infinite term in (1.69) comes from normal ordering the operators  $\alpha$  and  $\alpha^\dagger$  and it cancels against a similar term that appears in the fermionic part of the Hamiltonian. This zero point cancellation is something we should expect since the theory is supersymmetric (no spontaneous SUSY breaking occurs) and thus the energy of the vacuum  $|v, p^+\rangle$  should be zero.

Two comments are in order. First, the zero mode excitations  $\alpha_0^{I\dagger} |v, p^+\rangle$  have non-zero energy in contrast to the flat case. This is basically due to the  $(\mu X^I)^2$  term that appears in (1.68). Second, as one should expect the light-cone Hamiltonian is the conjugate momentum to the light-cone time  $X^+$ , given by  $P^- = \frac{2}{\alpha' p^+} (\partial_\tau X^- + (\mu X^I)^2)$  as one can see using (1.55).

### 1.6.2 Fermionic Part Of The Free String Action

We now proceed to the fermionic part of the type IIB superstring action in the light-cone gauge. As argued in [96] the fermionic part can be obtained from the quadratic fermionic term of the flat space GS action if one substitutes the usual derivative  $\partial_b$  with the supercovariant derivative

$$(\hat{D}_b)^\gamma{}_\beta = \delta^\gamma{}_\beta \partial_b + \partial_b X^\mu (\Omega_\mu)^\gamma{}_\beta, \quad (1.71)$$

where

$$(\Omega_\mu)^\gamma{}_\beta = \delta^\gamma{}_\beta \frac{1}{4} \omega_\mu^{ab} \Gamma_{ab} + \frac{i g_s}{16 \cdot 5!} (\sigma^2)^\gamma{}_\beta \Gamma^{\nu\rho\lambda\sigma\delta} F_{\nu\rho\lambda\sigma\delta}. \quad (1.72)$$

For the plane wave background of (1.50) it is straightforward to show that

$$\begin{aligned} \Omega_- &= 0, \quad (\Omega_I)^\alpha{}_\beta = \frac{i\mu}{4} \Gamma^+(\Pi + \Pi') \Gamma^I (\sigma^2)^\alpha{}_\beta, \\ (\Omega_+)^\alpha{}_\beta &= -\frac{1}{2} \mu^2 x^I \Gamma^{+I} \delta^\alpha{}_\beta + \frac{i\mu}{4} (\Pi + \Pi') \Gamma^+ \Gamma_+ (\sigma^2)^\alpha{}_\beta. \end{aligned} \quad (1.73)$$

The fermionic part of the action then reads

$$S_F = \frac{i}{4\pi\alpha'} \int d^2\sigma (\theta^\alpha)^\top (\beta^{ab})_{\alpha\rho} \partial_a X^\mu \Gamma_\mu (\hat{D}_b)^\rho{}_\beta \theta^\beta, \quad (1.74)$$

where

$$(\beta^{ab})_{\alpha\rho} = \sqrt{-g} g^{ab} \delta_{\alpha\rho} - \epsilon^{ab} (\sigma^3)_{\alpha\rho}. \quad (1.75)$$

In the above equation  $\theta^\alpha$ ,  $\alpha = 1, 2$  are the two 32-component Majorana-Weyl 10-dimensional spinors of the same chirality. The conventions for the gamma matrices

are the same as in [25]. The gauge fixing in the fermionic sector can be achieved by choosing

$$\Gamma^+ \theta^\alpha = 0, \quad (1.76)$$

as in the flat space case. Condition (1.76) implies that

$$\bar{\theta}^\alpha \Gamma^I \theta^\beta = 0, \quad \forall \alpha, \beta \quad (1.77)$$

and

$$(\Omega_I)^\alpha{}_\beta \theta^\beta = 0 \quad (1.78)$$

since the  $\Gamma^+$  of  $\Omega_I$  can be commuted to the right, to act directly at  $\theta^\beta$ , to give zero. Taking (1.76), (1.77), and (1.78) into account the fermionic part of the action reduces to

$$S_F^{l.c.} = \frac{i}{4\pi\alpha'} \int d\tau \int_0^{2\pi\alpha'p^+} d\sigma [(\theta^\alpha)^\top (\beta^{ab})_{\alpha\rho} (\partial_a X^+ \Gamma_+) (\delta^\rho{}_\beta \partial_b + \partial_b X^+ (\Omega_+)^\rho{}_\beta) \theta^\beta]. \quad (1.79)$$

The next step involves plugging the expression for  $\Omega_+$  as well as  $X^+$  in (1.79) to obtain

$$S_F^{l.c.} = \frac{-i}{4\pi\alpha'} \int d\tau \int_0^{2\pi\alpha'p^+} d\sigma [\theta^\dagger \partial_\tau \theta + \theta \partial_\tau \theta^\dagger + \theta \partial_\sigma \theta + \theta^\dagger \partial_\sigma \theta^\dagger - 2i\mu \theta^\dagger \Pi \theta]. \quad (1.80)$$

In (1.80)  $\theta^1$  and  $\theta^2$  have been combined to give a complex 16-dimensional  $SO(8)$  spinor  $\theta = (\theta^1 + i\theta^2)/\sqrt{2}$  and its complex conjugate  $\theta^\dagger = (\theta^1 - i\theta^2)/\sqrt{2}$  (one should not forget that due to the Majorana condition and the fact that the we have chosen the 10-dimensional matrices to be purely imaginary,  $\theta^1$  and  $\theta^2$  are real). Note, also, that the last fermion mass term in (1.80) breaks the transverse  $SO(8)$  symmetry of the metric to  $SO(4) \otimes SO(4)$  since  $\Pi = \gamma^1 \gamma^2 \gamma^3 \gamma^4$  involves only the first four  $SO(8)$   $\gamma^I$ 's.

One can now decompose the complex spinor  $\theta$  belonging to the  $8_s$  representation of  $SO(8)$  to spinors belonging to the  $((2, 1), (2, 1)) \oplus ((1, 2), (1, 2))$  representations of  $SO(4) \otimes SO(4)$ .

Doing so, the action becomes

$$S_F^{l.c.} = \frac{-i}{4\pi\alpha'} \int d\tau \int_0^{2\pi\alpha'p^+} d\sigma \left[ \theta_{\alpha\beta}^\dagger \partial_\tau \theta^{\alpha\beta} + \theta^{\alpha\beta} \partial_\tau \theta_{\alpha\beta}^\dagger + \theta_{\alpha\beta} \partial_\sigma \theta^{\alpha\beta} + \theta^{\alpha\beta} \partial_\sigma \theta_{\alpha\beta}^\dagger - \right.$$

$$2i\mu\theta_{\alpha\beta}^\dagger\theta^{\alpha\beta} + \theta_{\dot{\alpha}\dot{\beta}}^\dagger\partial_\tau\theta^{\dot{\alpha}\dot{\beta}} + \theta^{\dot{\alpha}\dot{\beta}}\partial_\tau\theta_{\dot{\alpha}\dot{\beta}}^\dagger + \theta_{\alpha\beta}^\dagger\partial_\sigma\theta^{\alpha\beta} + \theta^{\dot{\alpha}\dot{\beta}}\partial_\sigma\theta_{\dot{\alpha}\dot{\beta}}^\dagger + 2i\mu\theta_{\dot{\alpha}\dot{\beta}}^\dagger\theta^{\dot{\alpha}\dot{\beta}} \Big]. \quad (1.81)$$

In order to get (1.81) we have chosen a representation of the  $SO(8)$   $\gamma^I$ 's such that  $\Pi$  takes the diagonal form  $\Pi = \begin{pmatrix} \mathbf{1}_4 & \mathbf{0}_4 \\ \mathbf{0}_4 & -\mathbf{1}_4 \end{pmatrix}$ . The relative minus sign between the mass terms of the dotted and the undotted  $\theta$ 's is due to the fact that  $\Pi$  is essentially the  $\gamma^5$  matrix of the first  $SO(4)$ . It will, thus, act on the first index of the spinor to give  $\Pi\theta^{\alpha\beta} = \theta^{\alpha\beta}$  and  $\Pi\theta^{\dot{\alpha}\dot{\beta}} = -\theta^{\dot{\alpha}\dot{\beta}}$ . The e.o.m. derived from (1.81) are

$$\begin{aligned} (\partial_\tau + \partial_\sigma)(\theta_{\alpha\beta} + \theta_{\alpha\beta}^\dagger) - i\mu(\theta_{\alpha\beta} - \theta_{\alpha\beta}^\dagger) &= 0, \\ (\partial_\tau - \partial_\sigma)(\theta_{\alpha\beta} - \theta_{\alpha\beta}^\dagger) - i\mu(\theta_{\alpha\beta} + \theta_{\alpha\beta}^\dagger) &= 0, \end{aligned} \quad (1.82)$$

with similar equations for the dotted spinors. The solution to (1.82) is easily obtained and is given by

$$\begin{aligned} \theta_{\alpha\beta} &= \frac{1}{\sqrt{p^+}}\beta_{0\ \alpha\beta} e^{i\mu\tau} + \frac{1}{\sqrt{2p^+}} \sum_{n=1}^{\infty} c_{-n} \left[ (1 - \rho_{-n})\beta_{n\ \alpha\beta} e^{\frac{-i}{\alpha'p^+}(\omega_n\tau+n\sigma)} \right. \\ &+ (1 + \rho_{-n})\beta_n^\dagger{}_{\ \alpha\beta} e^{\frac{+i}{\alpha'p^+}(\omega_n\tau+n\sigma)} \Big] + c_n \left[ (1 - \rho_n)\tilde{\beta}_{n\ \alpha\beta} e^{\frac{-i}{\alpha'p^+}(\omega_n\tau-n\sigma)} \right. \\ &+ (1 + \rho_n)\tilde{\beta}_n^\dagger{}_{\ \alpha\beta} e^{\frac{+i}{\alpha'p^+}(\omega_n\tau-n\sigma)} \Big] \end{aligned} \quad (1.83)$$

where  $\omega_n$  is defined in (1.66) and

$$\rho_{\pm n} = \frac{\omega_n \mp n}{\alpha'\mu p^+}, \quad c_{\pm n} = \frac{1}{\sqrt{1 + \rho_{\pm n}^2}}. \quad (1.84)$$

The canonical momentum conjugate to  $\theta^{\alpha\beta}$  is  $P_{\alpha\beta} = \frac{\delta S}{\delta\partial_\tau\theta^{\alpha\beta}} = \frac{i}{2\pi\alpha'}\theta_{\alpha\beta}^\dagger$ . Quantization of the theory is achieved by imposing the equal time anticommutation relations appropriate for fermions

$$\{\theta^{\alpha\beta}(\sigma, \tau), \theta_{\rho\lambda}^\dagger(\sigma', \tau)\} = 2\pi\alpha'\delta_\rho^\alpha\delta_\lambda^\beta\delta(\sigma - \sigma'). \quad (1.85)$$

The coefficients  $c_{-n}$  and  $c_n$  in (1.83) are chosen in such a way that (1.85) leads to

$$\{\beta_0^{\alpha\beta}, \beta_0^\dagger{}_{\ \gamma\delta}\} = \delta_\gamma^\alpha\delta_\delta^\beta, \quad \{\beta_n^{\alpha\beta}, \beta_m^\dagger{}_{\ \gamma\delta}\} = \{\tilde{\beta}_n^{\alpha\beta}, \tilde{\beta}_m^\dagger{}_{\ \gamma\delta}\} = \delta_{mn}\delta_\gamma^\alpha\delta_\delta^\beta, \quad (1.86)$$

with similar relations for the dotted spinors. Finally, the anticommutator of a dotted and an undotted spinor is always zero.

Using the mode expansion given in (1.83) and the anticommutation relations of (1.86) it is straightforward to derive the light-cone (l.c.) Hamiltonian

$$H_{l.c.}^{fer.} = \frac{1}{\alpha' p^+} \left[ \alpha' \mu p^+ \beta_{0\alpha\beta}^\dagger \beta_0^{\alpha\beta} + \sum_{n=1}^{\infty} \omega_n (\beta_{n\alpha\beta}^\dagger \beta_n^{\alpha\beta} + \beta_{n\dot{\alpha}\dot{\beta}}^\dagger \beta_n^{\dot{\alpha}\dot{\beta}} + \tilde{\beta}_{n\alpha\beta}^\dagger \tilde{\beta}_n^{\alpha\beta} + \tilde{\beta}_{n\dot{\alpha}\dot{\beta}}^\dagger \tilde{\beta}_n^{\dot{\alpha}\dot{\beta}}) \right] - \frac{8}{\alpha' p^+} \left( \frac{1}{2} \alpha' \mu p^+ + \sum_{n=1}^{\infty} \omega_n \right). \quad (1.87)$$

The total free l.c. Hamiltonian is the sum of the bosonic and fermionic part. The zero point energy of the bosonic part cancels the zero point energy of the fermionic part, as advertised previously. The eigenvalues of the total Hamiltonian are always non-negative, as they should be.

We close this section by deriving the level matching condition which puts constraints on the physical spectrum of the theory. Starting from

$$\begin{aligned} \frac{\delta(S_B + S_F)}{\delta g^{\tau\sigma}(\sigma)} = 0 &\Rightarrow \partial_\sigma X^- = \partial_\tau X^I \partial_\sigma X^I - \frac{i}{2} \bar{\theta}^\alpha \Gamma^+ \partial_\sigma \theta_\alpha \Rightarrow \\ X^-(2\pi\alpha' p^+) - X^-(0) &= \int_0^{2\pi\alpha' p^+} d\sigma (\partial_\tau X^I \partial_\sigma X^I - \frac{i}{2} \bar{\theta}^\alpha \Gamma^+ \partial_\sigma \theta_\alpha) = \\ \sum_{n=1}^{\infty} n (\alpha_n^{I\dagger} \alpha_n^I + \beta_{n\alpha\beta}^\dagger \beta_n^{\alpha\beta} + \beta_{n\dot{\alpha}\dot{\beta}}^\dagger \beta_n^{\dot{\alpha}\dot{\beta}} - \tilde{\alpha}_n^{I\dagger} \tilde{\alpha}_n^I - \tilde{\beta}_{n\alpha\beta}^\dagger \tilde{\beta}_n^{\alpha\beta} - \tilde{\beta}_{n\dot{\alpha}\dot{\beta}}^\dagger \tilde{\beta}_n^{\dot{\alpha}\dot{\beta}}). \end{aligned} \quad (1.88)$$

Since we have closed string boundary conditions  $X^-(2\pi\alpha' p^+) = X^-(0)$  (1.88) implies that the physical states are those which satisfy

$$\sum_{n=1}^{\infty} n (\alpha_n^{I\dagger} \alpha_n^I + \beta_{n\alpha\beta}^\dagger \beta_n^{\alpha\beta} + \beta_{n\dot{\alpha}\dot{\beta}}^\dagger \beta_n^{\dot{\alpha}\dot{\beta}} - \tilde{\alpha}_n^{I\dagger} \tilde{\alpha}_n^I - \tilde{\beta}_{n\alpha\beta}^\dagger \tilde{\beta}_n^{\alpha\beta} - \tilde{\beta}_{n\dot{\alpha}\dot{\beta}}^\dagger \tilde{\beta}_n^{\dot{\alpha}\dot{\beta}}) | \Psi \rangle = 0. \quad (1.89)$$

The vacuum of the theory is defined as this state which is annihilated by all destruction operators, namely

$$\begin{aligned} \alpha_n^I | v, p^+ \rangle = \tilde{\alpha}_n^I | v, p^+ \rangle = 0 \\ \beta_n^{\alpha\beta} | v, p^+ \rangle = \beta_n^{\dot{\alpha}\dot{\beta}} | v, p^+ \rangle = \tilde{\beta}_n^{\alpha\beta} | v, p^+ \rangle = \tilde{\beta}_n^{\dot{\alpha}\dot{\beta}} | v, p^+ \rangle = 0. \end{aligned} \quad (1.90)$$

Obviously  $H^{l.c.} | v, p^+ \rangle = 0$ .

To summarise, we have seen that the free<sup>4</sup> type IIB string theory on the pp-wave background is solvable if one works in the light -cone gauge. The next step would be

<sup>4</sup>By free we mean that we set the string coupling  $g_s = 0$ .

to study the interacting theory. Usually, this is done by using first quantised string theory, that is a two-dimensional  $\sigma$ -model plus vertex operators. However, in the case of the pp-wave background this approach becomes cumbersome, principally due to the presence of the non-zero five form field  $F_5$ . An alternative way to proceed is to employ string field theory. String field theory (SFT) in the light cone gauge was first introduced in [30, 31, 89] for the bosonic string in flat space-time and then was generalised to the supersymmetric strings in [90–92].

### 1.6.3 General Structure Of Light Cone String Field Theory

In order to formulate SFT one can mimic the procedure followed to write down the second quantized theory for the point particle. Let us, therefore, postulate the existence of an object  $\Phi[X^+, x^-, X^I(\sigma), \theta_{\alpha\beta}(\sigma), \theta_{\dot{\alpha}\dot{\beta}}(\sigma)]$  that plays the role of the string "wave function".  $\Phi$  is a functional of the string coordinates  $X^I(\sigma), \theta_{\alpha\beta}(\sigma), \theta_{\dot{\alpha}\dot{\beta}}(\sigma)$ , and depends also on the light-cone time  $X^+$  and the zero mode of  $X^-$ , i.e.  $x^-$ ,

$$\Phi : (X^I(\sigma), \theta_{\alpha\beta}(\sigma), \theta_{\dot{\alpha}\dot{\beta}}(\sigma), X^+, x^-) \longrightarrow \mathbb{R}. \quad (1.91)$$

One can Fourier transform with respect to one or more of the coordinates  $X^I(\sigma), \theta_{\alpha\beta}(\sigma), \theta_{\dot{\alpha}\dot{\beta}}(\sigma), x^-$ . For the moment, let us Fourier transform only with respect to  $x^-$ .

Then the wavefunction becomes a function of  $\Phi = \Phi[X^+, p^+, X^I(\sigma), \theta_{\alpha\beta}(\sigma), \theta_{\dot{\alpha}\dot{\beta}}(\sigma)]$ . As usual, the wavefunction  $\Phi$  is promoted to an operator upon quantization. This operator will create and/or destroy complete strings and not a quantum of a particular string mode, as is done by  $\alpha_n^I, \alpha_n^{I\dagger}$ , the first quantized annihilation and creation operators.

The light-cone dynamics of  $\Phi$  is governed by the non-relativistic Schrodinger equation,

$$i \frac{\partial \Phi}{\partial X^+} = H_{SFT} \Phi, \quad (1.92)$$

where  $H_{SFT}$  is the light-cone string field theory Hamiltonian. To a first approximation, that is at the free string theory limit, it is equal to the sum of (1.68) and (1.87). Our principal aim, however, is to include interactions. In such a case, the

Hamiltonian is corrected to get the form  $H_{SFT} = H_2^{l.c.} + g_s H_3 + g_s^2 H_4 + \dots$ ,  $H_2^{l.c.}$  is the Hamiltonian of the string theory  $\sigma$ -model, while the interaction terms  $H_i$  describe the splitting and joining of strings. The way to specify the interaction terms is to use all the symmetries of the theory in order to restrict the form of such terms. In the case of flat space the symmetries are enough to completely fix the form of the interaction terms. In the case of the plane wave the symmetries are less than flat space and additional input is required in order to uniquely specify these terms. This is the reason for the two different three string vertices appearing in the literature. The first was derived by Spradlin and Volovich in [52] and elaborated by Pankiewicz and Stefanski [54, 55, 65] while the second was derived in [40, 58, 68]. In fact, any linear combination of these vertices satisfies the restrictions put by supersymmetry and can be thought as an acceptable vertex. This observation was put in good use in [32] where it is argued that holography should be the guiding principle to specify the correct combination. The authors of [32] have shown that the pp-wave/SYM duality is not exhausted to comparisons between two point functions but that there is also a direct correspondence between the coefficients of the three point functions in SYM theory and the three string amplitude on the pp-wave background. This correspondence, already existing in AdS/CFT, remains valid when the BMN limit is taken. It was first put forward in [37, 47], and [1, 101] where the bosonic part of the string vertex -whose complete version was derived in [32]- was obtained using field theoretical arguments. We will further discuss these aspects later.

(1.92) can be derived from the second quantized Hamiltonian <sup>5</sup>

$$\mathcal{H} = \int dp^+ D^8 X(\sigma) D^8 \theta(\sigma) p^+ \Phi^\dagger H_{SFT} \Phi \quad (1.93)$$

as the Heisenberg e.o.m. for the string field  $\Phi$ , namely

$$i \frac{\partial \Phi}{\partial X^+} = [\Phi, \mathcal{H}], \quad (1.94)$$

---

<sup>5</sup>In fact, this is how to take any symmetry generator  $g$  on the world sheet -such as  $H_2^{l.c.}$  which generates time translations or rotation generators  $j^{ij}$  or supercharges  $q$  which generate the SUSY transformations- and construct a free field realisation of the corresponding space-time operator  $\mathcal{H}_2, \mathcal{J}^{ij}, \mathcal{Q}$  through the formula  $G_2 = \int dp^+ p^+ D^8 X D^8 \theta \Phi^\dagger g \Phi$ .

using the equal time commutator

$$\left[ \Phi[X^+, p_1^+, X_1^I(\sigma), \theta_1^{\alpha\beta}(\sigma), \theta_1^{\dot{\alpha}\dot{\beta}}(\sigma)], \Phi[X^+, p_2^+, X_2^I(\sigma), \theta_2^{\alpha\beta}(\sigma), \theta_2^{\dot{\alpha}\dot{\beta}}(\sigma)] \right] = \frac{1}{p_1^+} \delta(p_1^+ + p_2^+) \Delta^8(X_1^I(\sigma) - X_2^I(\sigma)) \Delta^4(\theta_1^{\alpha\beta}(\sigma) - \theta_2^{\alpha\beta}(\sigma)) \Delta^4(\theta_1^{\dot{\alpha}\dot{\beta}}(\sigma) - \theta_2^{\dot{\alpha}\dot{\beta}}(\sigma)). \quad (1.95)$$

Before we sketch the way to derive the interaction term  $H_3$  let us solve the free Schrodinger equation for the string field. For simplicity we shall restrict ourselves to the bosonic part of the Hamiltonian. The manipulations of the fermionic part are quite similar and will not be needed in what follows. As a first step, we define new creation and annihilation operators by

$$a_n = \frac{1}{\sqrt{2i}}(\alpha_n + \tilde{\alpha}_n), \quad a_{-n} = \frac{1}{\sqrt{2}}(\tilde{\alpha}_n - \alpha_n), \quad n > 0, \quad (1.96)$$

and  $a_0 = \alpha_0$ . Then the bosonic part of the Hamiltonian becomes

$$H_{2B}^{l.c.} = \frac{1}{\alpha} \sum_{n \in \mathbb{Z}} \omega_n a_n^\dagger a_n. \quad (1.97)$$

Next one can define position and momentum operators in terms of the  $a$  and  $a^\dagger$  as is done in the case of a single harmonic oscillator to obtain

$$H_2^{l.c.} = \frac{1}{\alpha} \sum_{n=-\infty}^{+\infty} \left[ p_n^2 + \frac{1}{4} \omega_n^2 x_n^2 \right] = \frac{1}{\alpha} \sum_{n=-\infty}^{+\infty} \left[ p_n^2 - \frac{1}{4} \omega_n^2 \left( \frac{\delta}{\delta p_n^I} \right)^2 \right], \quad (1.98)$$

where  $\alpha = \alpha' p^+$ . From (1.97) it is clear that the total Hamiltonian is the sum of an infinite number of noninteracting harmonic oscillators, and thus the eigenfunctions of the Schrodinger equation are products of momentum eigenfunctions, one for each oscillator. That is the most general solution is of the form

$$\Phi = e^{-ip^- X^+} \sum_{\{N_n\}} A(\{N_n\}, p^+) \prod_{n=-\infty}^{+\infty} \psi_{N_n}(p_n), \quad (1.99)$$

where  $\psi(p_n)$  is the eigenfunction of the  $n$ -th mode in momentum space. Furthermore, if  $p^+ > 0$  then  $A(\{N_n\}, p^+)$  is the annihilation operator for a whole string with  $N_n$  quanta in the  $n$ -th mode while if  $p^+ < 0$ ,  $A(\{N_n\}, p^+) = A^\dagger(\{N_n\}, -p^+)$  is the creation operator for whole string with the same excitations.

### 1.6.4 String Interactions In The Plane Wave

In this subsection we briefly describe how the three-string interaction term is obtained in the case of the plane wave background. The situation is very similar to the flat case, although some new features arise.

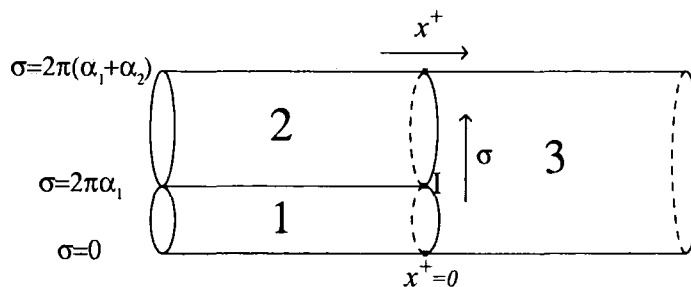


Figure 1.1: Three string interaction vertex in the light cone gauge. According to the prescription stated below (1.99)  $\alpha_1, \alpha_2 > 0$  whereas  $\alpha_3 < 0$ . Note also that, due to closed string boundary conditions,  $\sigma = 0, \sigma = 2\pi\alpha_1$  and  $\sigma = 2\pi(\alpha_1 + \alpha_2)$  are identified and  $I$  is the interaction point.

The process we intend to describe is depicted in Figure 1.1. Two strings, string 1 and string 2, propagate freely until the interaction takes place at light cone time zero to give a longer string, string 3.

The main idea is to try to exploit the (super)symmetries of the theory. Before doing so, let us summarise these symmetries. They can be divided in two groups [25,52]: i) the kinematical generators,  $\mathcal{P}^+, \mathcal{K}^I, \mathcal{L}^I, \mathcal{J}_{ij}, \mathcal{J}_{ab}, \mathcal{Q}_{\alpha\beta}, \mathcal{Q}_{\dot{\alpha}\dot{\beta}}$ . Here  $\mathcal{K}^I, \mathcal{L}^I$  is a linear combination of  $\mathcal{P}^I$  and  $\mathcal{J}^{+I}$ , and  $\mathcal{J}_{ij}, \mathcal{J}_{ab}$  are the generators of the  $SO(4) \otimes SO(4)$  group. These generators are not corrected by the interactions and their form does not depend on  $g_s$  [52].

ii) The dynamical generators,  $\mathcal{Q}_{\alpha\beta}^{(0)}, \mathcal{Q}_{\dot{\alpha}\dot{\beta}}^{(0)}, \mathcal{H}_2$ , which are quadratic in the string worldsheet fields. These generators can, and indeed, receive  $g_s$  corrections [54,55,91].

First we make use of the commutation relations of the string field theory Hamiltonian with the kinematical generators. From the relations

$$[\mathcal{H}, \mathcal{L}^I] = i\mu\mathcal{K}^I, \quad [\mathcal{H}, \mathcal{K}^I] = -i\mu\mathcal{L}^I \quad (1.100)$$

and taking into account the expressions for  $\mathcal{K}^I$  and  $\mathcal{L}^I$

$$\mathcal{K}^I = \sin \mu X^+ \mathcal{P}^I + \mu \mathcal{X}^I \cos \mu X^+ \mathcal{P}^+, \quad \mathcal{L}^I = \sin \mu X^+ \mathcal{P}^I - \mu \mathcal{X}^I \cos \mu X^+ \mathcal{P}^+ \quad (1.101)$$

one immediately sees that (1.100) hold up to order  $g_s$  if

$$[\mathcal{H}_3, \mathcal{P}^I] = [\mathcal{H}_3, e(\alpha) \mathcal{X}^I] = 0, \quad (1.102)$$

where  $e(\alpha) = \text{sign}(\alpha)$  and  $\alpha = \alpha' p^+$ . Furthermore, in a similar way, the requirement that the commutation relations of the Hamiltonian with the kinematical supercharges  $\mathcal{Q}_{\alpha\beta}$ ,  $\mathcal{Q}_{\dot{\alpha}\dot{\beta}}$  hold up to order  $g_s$  implies

$$[\mathcal{H}_3, \Lambda_{\alpha\beta}] = [\mathcal{H}_3, e(\alpha) \Theta_{\alpha\beta}] = 0, \quad [\mathcal{H}_3, \Lambda_{\dot{\alpha}\dot{\beta}}] = [\mathcal{H}_3, e(\alpha) \Theta_{\dot{\alpha}\dot{\beta}}] = 0. \quad (1.103)$$

$\Lambda$  and  $\Theta$  denote the second quantised versions of  $\lambda$  and  $\theta$  respectively,

i.e.  $\Lambda = \int dp^+ p^+ D^8 P D^8 \Phi^\dagger \lambda \Phi$ . Finally since  $\mathcal{P}^+$  commutes with all generators we obtain

$$[\mathcal{P}^+, \mathcal{H}_3] = 0. \quad (1.104)$$

The above relations actually hold for all the  $g_s^{n-2}$  corrections of the Hamiltonian, namely

$$[\mathcal{H}_n, \mathcal{P}^I] = [\mathcal{H}_n, e(\alpha) \mathcal{X}^I] = 0, \quad (1.105)$$

and similarly for the commutators with the supercharges.

(1.102) and (1.103) can be interpreted as momentum conservation of the bosonic and fermionic fields (equations involving  $\mathcal{P}$  and  $\Lambda$ ) and continuity of the string world-sheet as string one and string two merge to give string three (equations involving  $e(\alpha) \mathcal{X}$  and  $e(\alpha) \Theta$ ). (1.102), (1.103), and (1.104) are guaranteed if we include a factor of

$$\Delta^8 \left[ \sum_{r=1}^3 P_{(r)}^I(\sigma) \right] \Delta^4 \left[ \sum_{r=1}^3 \lambda_{(r)}^{\alpha\beta}(\sigma) \right] \Delta^4 \left[ \sum_{r=1}^3 \lambda_{(r)}^{\dot{\alpha}\dot{\beta}}(\sigma) \right] \delta \left( \sum_{r=1}^3 \alpha_{(r)} \right) \quad (1.106)$$

in the three-string vertex <sup>6</sup>.  $\Delta$ -functionals are products of an infinite number of  $\delta$ -functions of the corresponding argument at different values of  $\sigma$ . Thus the three-string Hamiltonian can be written as

$$\mathcal{H}_3 = \int d\mu_3 h_3 \Phi(1) \Phi(2) \Phi(3), \quad (1.107)$$

<sup>6</sup>That this is the case can be easily seen if one takes the commutator of the second quan-

where  $\Phi(r)$  is the string field of the  $r^{\text{th}}$  string,  $h_3 = h_3(\alpha_{(r)}, P_{(r)}, X_{(r)}, \theta_{(r)}, \lambda_{(r)})$  is to be determined later using the dynamical part of the superalgebra and

$$d\mu_3 = \left( \prod_{r=1}^3 d\alpha_{(r)} D^8 P_{(r)}(\sigma) D^8 \lambda_{(r)}(\sigma) \right) \Delta^8 \left[ \sum_{r=1}^3 P_{(r)}^l(\sigma) \right] \Delta^4 \left[ \sum_{r=1}^3 \lambda_{(r)}^{\alpha\beta}(\sigma) \right] \Delta^4 \left[ \sum_{r=1}^3 \lambda_{(r)}^{\dot{\alpha}\dot{\beta}}(\sigma) \right] \delta \left( \sum_{r=1}^3 \alpha_{(r)} \right). \quad (1.108)$$

For a moment let us forget about  $h_3$  and plug the expressions for  $\Phi(r)$  in (1.107) to obtain

$$\mathcal{H}_3 = \int d\mu_3 \sum_{\{N^1\}, \{N^2\}, \{N^3\}} c(\{N^1\}, \alpha_1; \{N^2\}, \alpha_2; \{N^3\}, \alpha_3) A(\{N^1\}, \alpha_1) A(\{N^2\}, \alpha_2) A(\{N^3\}, \alpha_3). \quad (1.109)$$

It is now convenient to identify the operator  $\mathcal{H}_3$  with a state in the three particle Hilbert space  $|V_3\rangle$  such that

$$\langle \{N^1\}, \alpha_1 | \langle \{N^2\}, \alpha_2 | \langle \{N^3\}, -\alpha_3 | V_3 \rangle = c(\{N^1\}, \alpha_1; \{N^2\}, \alpha_2; \{N^3\}, \alpha_3). \quad (1.110)$$

Then, the state  $|V_3\rangle$  can be written as

$$|V_3\rangle = \sum_{\{N^1\}, \{N^2\}, \{N^3\}} c(\{N^1\}, \alpha_1; \{N^2\}, \alpha_2; \{N^3\}, \alpha_3) | \{N^1\}, \alpha_1 \rangle | \{N^2\}, \alpha_2 \rangle | \{N^3\}, -\alpha_3 \rangle, \quad (1.111)$$

where

$$c(\{N^1\}, \alpha_1; \{N^2\}, \alpha_2; \{N^3\}, \alpha_3) = \int d\mu_3 \prod_{r=1}^3 \prod_{n=-\infty}^{\infty} \psi_{N_n^r}(p_{n(r)}). \quad (1.112)$$

In the equations above we have concentrated on the bosonic degrees of freedom and have suppressed the fermionic ones which can be handled in a similar way.

Now we have to express the delta functionals in a form that allows the integrations appearing in the measure  $d\mu_3$  to be done explicitly. First of all  $\prod_{r=1}^3 D^8 P_{(r)} =$

---

tized Hamiltonian in the form of (1.107) with the second quantized expressions for  $\mathcal{P}$  and  $\Lambda$ . The result is proportional to  $\sum_r p_{(r)}(\sigma) \Delta[\sum_r p_{(r)}(\sigma)] = 0$  and similarly for  $\Lambda$ . The rest equations describing the worldsheet continuity also hold since the corresponding commutators of  $\mathcal{H}_3$  with  $e(\alpha)\mathcal{X}(\sigma)$  and  $e(\alpha)\Theta(\sigma)$  result to expressions proportional to  $\sum_r e(\alpha_r) \frac{\delta}{\delta p_r(\sigma)} \Delta[\sum_r p_{(r)}(\sigma)] = 0$  and  $\sum_r e(\alpha_r) \frac{\delta}{\delta \lambda_{(r)}(\sigma)} \Delta[\sum_r \lambda_{(r)}(\sigma)] = 0$ .

$\prod_{r=1}^3 \prod_{k=-\infty}^{\infty} dp_{k(r)}$ . Second, we recall that the the delta functional can be written as a product of delta functions for each Fourier mode of its argument, that is  $\Delta [\sum_{r=1}^3 P_{(r)}(\sigma)] = \prod_{k=-\infty}^{\infty} \delta(\int_0^{2\pi|\alpha_3|} d\sigma e^{ik\sigma/|\alpha_3|} \sum_{r=1}^3 P_{(r)})$ . Keeping in mind that  $\sum_{r=1}^3 P_{(r)} = P_3 + \theta(2\pi\alpha_1 - \sigma)P_1 + \theta(2\pi\alpha_1\sigma - 2\pi\alpha_1)P_2$  one obtains

$$\Delta[P_{(r)}(\sigma)] = \prod_{m=-\infty}^{\infty} \delta\left(\sum_{r,n} X_{mn}^r p_{n(r)}\right) \quad (1.113)$$

where  $X_{mn}^3 = \delta_{mn}$  and

$$X_{mn}^1(\beta) = \frac{2(-1)^{m+n+1}}{\pi} \frac{m\beta \sin \pi m\beta}{n^2 - m^2 \beta^2}, \quad X_{m,0}^1(\beta) = \frac{\sqrt{2}(-1)^m \sin \pi m\beta}{\pi m\beta} \quad (1.114)$$

$$X_{-m,-n}^1(\beta) = \frac{2(-1)^{m+n+1}}{\pi} \frac{n \sin \pi m\beta}{n^2 - m^2 \beta^2}, \quad X_{0,0}^1 = 1, \quad X_{m,n}^1 = 0 \text{ otherwise,}$$

$\beta = \frac{\alpha_1}{\alpha_3}$  and in (1.114)  $m, n > 0$ . Then,  $X_{m,n}^2$  can be written in terms of  $X^1$  as  $X_{m,n}^2(\beta) = (-1)^n X_{m,n}^1(\beta + 1)$  for any  $m, n \in \mathbb{Z}$ . In what follows we will also need the following identity for the momentum eigenstate

$$|p_n\rangle = \left(\frac{2}{\pi\omega_n}\right)^{1/4} \exp\left[-\frac{1}{\omega_n} p_n^2 + \frac{2}{\sqrt{\omega_n}} p_n a_n^\dagger - \frac{1}{2} a_n^\dagger a_n^\dagger\right] |v\rangle. \quad (1.115)$$

Multiplying both sides by the identity  $I = \sum_{N_n=0}^{\infty} |N_n\rangle\langle N_n|$  results to

$$\sum_{N_n=0}^{\infty} |N_n\rangle \psi_{N_n}(p_n) = \left(\frac{2}{\pi\omega_n}\right)^{1/4} \exp\left[-\frac{1}{\omega_n} p_n^2 + \frac{2}{\sqrt{\omega_n}} p_n a_n^\dagger - \frac{1}{2} a_n^\dagger a_n^\dagger\right] |v\rangle. \quad (1.116)$$

Using (1.116), (1.111), and (1.112) and restricting ourselves to the bosonic part of the vertex, we arrive finally at

$$|E_a\rangle = \int d\mu_{3B} \exp\left[\sum_{n=-\infty}^{\infty} \sum_{r=1}^3 \left(-\frac{1}{\omega_{n(r)}} p_{n(r)}^2 + \frac{2}{\sqrt{\omega_{n(r)}}} p_{n(r)} a_{n(r)}^\dagger - \frac{1}{2} a_{n(r)}^\dagger a_{n(r)}^\dagger\right)\right] |v\rangle_3, \quad (1.117)$$

where  $d\mu_{3B}$  is the bosonic part of the measure, given by

$$d\mu_{3B} = \prod_{m=-\infty}^{\infty} \delta\left(\sum_{r,n} X_{mn}^r p_{n(r)}\right) \prod_{r=1}^3 \prod_{k=-\infty}^{\infty} dp_{k(r)}. \quad (1.118)$$

The delta functions in  $d\mu_{3B}$  allow us to replace the modes of string 3 in terms of the modes of strings 1 and 2. Then we are in position to perform the Gaussian integrals of (1.117) in the infinite many variables  $x_{k(1)}$  and  $x_{k(2)}$  with the result [52]

$$|E_a\rangle = \exp\left[\frac{1}{2} \sum_{r,s=1}^3 \sum_{m,n \in \mathbb{Z}} \delta^{IJ} a_{m(r)}^{I\dagger} \bar{N}_{mn}^{(rs)} a_{n(s)}^{J\dagger}\right] |v\rangle_3 \quad (1.119)$$

where the Neumann matrices  $\overline{N}_{mn}^{(rs)}$  are given by

$$\overline{N}_{mn}^{(rs)} = \delta^{rs} \delta_{mn} - 2\sqrt{\omega_{m(r)}\omega_{n(s)}}(X^{(r)}\Gamma_a^{-1}X^{(s)})_{mn} , \quad (1.120)$$

in which

$$(\Gamma_a^{-1})_{mn} = \sum_{r=1}^3 \sum_{p \in \mathbb{Z}} \omega_{p(r)} X_{mp}^{(r)} X_{pn}^{(r)} \quad (1.121)$$

and  $\omega_{n(r)} = \sqrt{n^2 + \mu^2 \alpha_r^2}$ . Similarly one can work out the fermionic integrals with fermionic Neumann functions  $\overline{Q}_{mn}^{(rs)}$  [65]

$$|E_b\rangle = \exp \left[ \frac{1}{2} \sum_{r,s=1}^3 \sum_{m,n \geq 0} (b_{-m(r)}^{\dagger\alpha\beta} b_{n(s)\alpha\beta}^{\dagger} + b_{m(r)}^{\dagger\dot{\alpha}\dot{\beta}} b_{-n(s)\dot{\alpha}\dot{\beta}}^{\dagger}) \overline{Q}_{mn}^{(rs)} \right] |v\rangle_3 \quad (1.122)$$

(Explicit formulas for  $\overline{Q}_{mn}^{(rs)}$  and  $\overline{N}_{mn}^{(rs)}$  can be found in [65, 98].)

Let us, now, assemble all the pieces and write the three string vertex as

$$|\hat{H}_3\rangle = H_3 |V_3\rangle, \quad (1.123)$$

with a similar expression for the dynamical supercharges

$$|\hat{Q}_3\rangle = Q_3 |V_3\rangle, \quad (1.124)$$

where  $|V_3\rangle$  has been determined previously

$$|V_3\rangle = |E_a\rangle \otimes |E_b\rangle \delta\left(\sum_r \alpha_r\right). \quad (1.125)$$

We now move on to sketch how the prefactors  $H_3$  and  $Q_3$  are determined <sup>7</sup> The relations we need are the (anti-)commutation relations between the dynamical generators at first order in  $g_s$ . These read

$$[\mathcal{H}_3, \mathcal{Q}_{\alpha\dot{\beta}}^{(0)}] + [\mathcal{H}_2, \mathcal{Q}_{\alpha\dot{\beta}}^{(3)}] = 0 , \quad (1.126a)$$

$$\{\mathcal{Q}_{\alpha\dot{\beta}}^{(3)}, (\mathcal{Q}^{(0)})_{\dot{\rho}\lambda}^{\dagger}\} + \{\mathcal{Q}_{\alpha\dot{\beta}}^{(0)}, (\mathcal{Q}^{(3)})_{\dot{\rho}\lambda}^{\dagger}\} = 0 , \quad (1.126b)$$

$$\{\mathcal{Q}_{\dot{\alpha}\beta}^{(3)}, (\mathcal{Q}^{(0)})_{\rho\lambda}^{\dagger}\} + \{\mathcal{Q}_{\dot{\alpha}\beta}^{(0)}, (\mathcal{Q}^{(3)})_{\rho\lambda}^{\dagger}\} = 2\epsilon_{\dot{\alpha}\rho}\epsilon_{\beta\lambda}\mathcal{H}_3 , \quad (1.126c)$$

$$\{\mathcal{Q}_{\alpha\dot{\beta}}^{(3)}, (\mathcal{Q}^{(0)})_{\rho\lambda}^{\dagger}\} + \{\mathcal{Q}_{\alpha\dot{\beta}}^{(0)}, (\mathcal{Q}^{(3)})_{\rho\lambda}^{\dagger}\} = 2\epsilon_{\alpha\rho}\epsilon_{\dot{\beta}\lambda}\mathcal{H}_3. \quad (1.126d)$$

<sup>7</sup>The necessity of the prefactors may be seen in exactly the same way as in the flat case [13].

To work out  $H_3$  and  $Q_3$  we have to solve (1.126). These equations written in terms of the state representation become

$$\sum_{r=1}^3 \left( \mathcal{H}_{2(r)}(Q_3)_{\alpha\dot{\beta}} - Q_{\alpha\dot{\beta}(r)}^{(0)} H_3 \right) |V_3\rangle = 0, \quad (1.127a)$$

$$\sum_{r=1}^3 \left( Q_{\alpha\dot{\beta}(r)}^{(0)} (Q_3)_{\dot{\rho}\lambda}^\dagger + Q_{\dot{\rho}\lambda(r)}^{(0)\dagger} (Q_3)_{\alpha\dot{\beta}} \right) |V_3\rangle = 0, \quad (1.127b)$$

$$\sum_{r=1}^3 \left( Q_{\dot{\alpha}\beta(r)}^{(0)} (Q_3)_{\dot{\rho}\lambda}^\dagger + Q_{\dot{\rho}\lambda(r)}^{(0)\dagger} (Q_3)_{\dot{\alpha}\beta} \right) |V_3\rangle = 2\epsilon_{\dot{\alpha}\rho}\epsilon_{\beta\lambda} H_3 |V_3\rangle, \quad (1.127c)$$

$$\sum_{r=1}^3 \left( Q_{\alpha\dot{\beta}(r)}^{(0)} (Q_3)_{\rho\dot{\lambda}}^\dagger + Q_{\rho\dot{\lambda}(r)}^{(0)\dagger} (Q_3)_{\alpha\dot{\beta}} \right) |V_3\rangle = 2\epsilon_{\alpha\rho}\epsilon_{\dot{\beta}\dot{\lambda}} H_3 |V_3\rangle. \quad (1.127d)$$

These equations, being linear in  $Q_3$  and  $H_3$ , only allow us to determine  $\mathcal{H}_3$  and  $Q_3$  up to an overall  $\mu$  (or more precisely  $\alpha'\mu p^+$ ) dependent factor. This should be contrasted with the flat space case, where besides the above there is an extra condition coming from the boost in the light cone directions generated by  $J^{+-}$  [90]. In the plane wave background, however, this boost symmetry is absent and this overall factor should be fixed in some other way, e.g. by comparing the SFT results by their gauge theory correspondents (which are valid for  $\alpha'\mu p^+ \gg 1$ ) or by the results of sugra on the plane wave background (which are trustworthy for  $\alpha'\mu p^+ \ll 1$ ).

First we note that, in order not to spoil the momentum conservation and the world sheet continuity conditions (1.102) and (1.103), the prefactors should (anti)commute with the kinematical constraints. One can show that there exist linear combinations of the bosonic and fermionic creation operators which satisfy these continuity conditions:

$$\mathcal{K}^I = \sum_{r=1}^3 \sum_{n \in \mathbb{Z}} K_{n(r)} a_{n(r)}^{I\dagger}, \quad \tilde{\mathcal{K}}^I = \sum_{r=1}^3 \sum_{n \in \mathbb{Z}} \tilde{K}_{n(r)} a_{n(r)}^{I\dagger}, \quad \tilde{K}_{n(r)} = K_{n(r)}^* \quad (1.128a)$$

$$Y^{\alpha\beta} = \sum_{r=1}^3 \sum_{n \geq 0} \bar{G}_{n(r)} b_{n(r)}^{\dagger\alpha\beta}, \quad Z^{\dot{\alpha}\dot{\beta}} = \sum_{r=1}^3 \sum_{n \geq 0} \bar{G}_{n(r)} b_{-n(r)}^{\dagger\dot{\alpha}\dot{\beta}}, \quad \bar{G}_{n(r)} = \bar{G}_{n(r)}^*. \quad (1.128b)$$

$K_{n(r)}$ ,  $\tilde{K}_{n(r)}$ ,  $\bar{G}_{n(r)}$  have complicated expressions and are functions of  $\mu$  and  $p^+$ . Their explicit formulas can be found in [52, 65, 68, 98]. Any function of  $\mathcal{K}^I$ ,  $\tilde{\mathcal{K}}^I$ ,  $Y^{\alpha\beta}$  and  $Z^{\dot{\alpha}\dot{\beta}}$  would guarantee the continuity conditions.

Therefore, making an ansatz for  $H_3$ ,  $Q_3$  and being equipped with (1.128) we can solve (1.127). To obtain the results one should work out a number of relations and

identities among  $K$ 's,  $Y$ 's and  $Z$ 's. The detailed calculations, which are lengthy, can be found in [65]. The expressions obtained therein are:

$$(Q_3)_{\alpha\beta} = e^{i\pi/4} |\alpha_3|^{3/2} \sqrt{-\beta(\beta+1)} \left( S_{\dot{\rho}\dot{\beta}}^+(Z) T_{\alpha\lambda}^+(Y^2) \tilde{\mathcal{K}}_1^{\dot{\rho}\lambda} + i S_{\alpha\lambda}^+(Y) T_{\dot{\rho}\dot{\beta}}^-(\tilde{Z}^2) \tilde{\mathcal{K}}_2^{\dot{\rho}\lambda} \right) f(\mu) \quad (1.129)$$

$$(Q_3)_{\dot{\alpha}\dot{\beta}} = -e^{-i\pi/4} |\alpha_3|^{3/2} \sqrt{-\beta(\beta+1)} \left( S_{\lambda\dot{\beta}}^-(Y) T_{\dot{\alpha}\dot{\rho}}^-(Z^2) \tilde{\mathcal{K}}_1^{\lambda\dot{\rho}} + i S_{\dot{\alpha}\dot{\rho}}^-(Z) T_{\lambda\dot{\beta}}^+(\tilde{Y}^2) \tilde{\mathcal{K}}_2^{\lambda\dot{\rho}} \right) f(\mu) \quad (1.130)$$

$$\begin{aligned} H_3 = & \left[ \left( \mathcal{K}^i \tilde{\mathcal{K}}^j + \frac{\mu\beta(\beta+1)}{2} \alpha_3^3 \delta^{ij} \right) V_{ij} - \left( \mathcal{K}^a \tilde{\mathcal{K}}^b + \frac{\mu\beta(\beta+1)}{2} \alpha_3^3 \delta^{ab} \right) V_{ab} \right. \\ & \left. - \mathcal{K}_1^{\dot{\alpha}\rho} \tilde{\mathcal{K}}_2^{\dot{\beta}\lambda} S_{\rho\lambda}^+(Y) S_{\dot{\alpha}\dot{\beta}}^-(Z) - \tilde{\mathcal{K}}_1^{\dot{\alpha}\rho} \mathcal{K}_2^{\dot{\beta}\lambda} S_{\rho\lambda}^-(Y) S_{\dot{\alpha}\dot{\beta}}^+(Z) \right] f(\mu) \end{aligned} \quad (1.131)$$

where  $\beta = \frac{\alpha_1}{\alpha_3}$ ,  $|\alpha_3| = \alpha' p^+$  (note that in our conventions  $\alpha_3 < 0$  and  $-1 \leq \beta < 0$ ) and

$$\tilde{\mathcal{K}}_1^{\dot{\alpha}\rho} \equiv \tilde{\mathcal{K}}^i(\sigma_i)^{\dot{\alpha}\rho}, \quad \mathcal{K}_1^{\dot{\alpha}\rho} \equiv \mathcal{K}^i(\sigma_i)^{\dot{\alpha}\rho}, \quad \tilde{\mathcal{K}}_2^{\dot{\alpha}\rho} \equiv \tilde{\mathcal{K}}^a(\sigma_a)^{\dot{\alpha}\rho}, \quad \mathcal{K}_2^{\dot{\alpha}\rho} \equiv \mathcal{K}^a(\sigma_a)^{\dot{\alpha}\rho}, \quad (1.132)$$

$$S^\pm(Y) = Y \pm \frac{i}{3} Y^3, \quad T^\pm(Z^2) = \epsilon \pm i Z^2 - \frac{1}{6} Z^4, \quad (1.133)$$

$$\begin{aligned} V_{ij} = & \delta_{ij} \left[ 1 + \frac{1}{12} (Y^4 + Z^4) + \frac{1}{144} Y^4 Z^4 \right] - \frac{i}{2} \left[ Y_{ij}^2 (1 + Z^4) - Z_{ij}^2 (1 + \frac{1}{12} Y^4) \right] \\ & + \frac{1}{4} (Y^2 Z^2)_{ij} \end{aligned} \quad (1.134)$$

$$\begin{aligned} V_{ab} = & \delta_{ab} \left[ 1 - \frac{1}{12} (Y^4 + Z^4) + \frac{1}{144} Y^4 Z^4 \right] - \frac{i}{2} \left[ Y_{ab}^2 (1 - Z^4) - Z_{ab}^2 (1 - \frac{1}{12} Y^4) \right] \\ & + \frac{1}{4} (Y^2 Z^2)_{ab} \end{aligned} \quad (1.135)$$

In the above,

$$\begin{aligned} Y_{\alpha\beta}^2 & \equiv Y_{\alpha\rho} Y_{\beta}^{\rho}, \quad \tilde{Y}_{\alpha\beta}^2 \equiv Y_{\rho\alpha} Y_{\beta}^{\rho}, \quad Y_{\alpha\beta}^4 \equiv Y_{\alpha\rho}^2 (Y^2)_{\beta}^{\rho} = \frac{-1}{2} \epsilon_{\alpha\beta} Y^4, \quad \tilde{Y}_{\alpha\beta}^4 \equiv \tilde{Y}_{\alpha\rho}^2 \\ & (\tilde{Y}^2)_{\beta}^{\rho} = \frac{1}{2} \epsilon_{\alpha\beta} Y^4, \quad Y_{\alpha\beta}^3 \equiv Y_{\alpha\rho} Y^{\lambda\rho} Y_{\lambda\beta}, \quad Y_{ij}^2 = (\sigma_{ij})^{\alpha\beta} Y_{\alpha\beta}^2, \\ & Z_{ij}^2 = (\sigma_{ij})^{\dot{\alpha}\dot{\beta}} Z_{\dot{\alpha}\dot{\beta}}^2, \quad (Y^2 Z^2)_{ij} = Y_{k(i}^2 Z_{j)k}^2, \end{aligned}$$

where  $Y^4 \equiv Y_{\alpha\beta}^2 (Y^2)^{\dot{\alpha}\dot{\beta}} = -\tilde{Y}_{\alpha\beta}^2 (\tilde{Y}^2)^{\dot{\alpha}\dot{\beta}}$ . Note that  $Y^2$ ,  $\tilde{Y}^2$  (and similarly  $Z_{\dot{\alpha}\dot{\beta}}^2$ ,  $\tilde{Z}_{\dot{\alpha}\dot{\beta}}^2$ ) are symmetric *matrices*, i.e. both of their indices belong to only one of  $SO(4)$ 's;

in fact  $Y^2$  and  $Z^2$  are matrices in the first  $SO(4)$  and  $\tilde{Y}^2$  and  $\tilde{Z}^2$  in the second one, moreover  $V_{ij}$  and  $V_{ab}$  are Hermitian,  $V_{ij}^* = V_{ji}$  and  $V_{ab}^* = V_{ba}$ . The function  $f(\mu)$  (or more precisely  $f(\alpha'\mu p^+)$ ) is an overall factor which is not fixed through the superalgebra requirements.

One should note an important feature of the three string vertex constructed above, namely as  $\mu \rightarrow 0$ , and the pp-wave metric becomes the flat space metric, the vertex goes smoothly to the flat case string theory vertex. Another important feature it has is that it is  $\mathbb{Z}_2$  invariant (in fact it respects the full  $SO(4) \otimes SO(4) \otimes \mathbb{Z}_2$  of the plane wave background).

An important point to be emphasized is that there is no way to derive the prefactor from first principles. As soon as the kinematical part of the vertex is determined one makes an ansatz for the prefactor and then checks that the complete vertex obeys the pp-wave algebra up to the desired order in  $g_s$ . A different way to realise the supersymmetry algebra [68] is to act on the kinematical vertex with the free part of the Hamiltonian and the dynamical supercharges,

$$| \hat{H}_3 \rangle = \sum_{r=1}^3 H_{2(r)} | V_3 \rangle, \quad | Q_{3\dot{\alpha}} \rangle = \sum_{r=1}^3 Q_{\dot{\alpha}(r)}^{(0)} | V_3 \rangle, \quad | \tilde{Q}_{3\dot{\alpha}} \rangle = \sum_{r=1}^3 \tilde{Q}_{\dot{\alpha}(r)}^{(0)} | V_3 \rangle. \quad (1.136)$$

With this ansatz the relations (1.127) are a direct consequence of the free theory (anti)commutation relations between the dynamical generators. Furthermore, it can be shown [68] that the full ansatz (1.136) satisfies also the kinematical constraints.

A last comment to be made is that since Eqs. (1.127) are linear with respect to  $H_3$  and  $Q_3$  any linear combination of the two different proposals for the three-string vertex satisfies both the kinematical and dynamical constraints.

## 1.7 The Plane Wave/SYM Duality

In this section, we briefly describe the plane wave/SYM duality, as it was originally proposed by Berenstein, Maldacena and Nastase (BMN) and extended later in [44,45].

In [41], BMN proposed an intriguing correspondence between type IIB superstring theory on a pp-wave background geometry and a sector of  $\mathcal{N} = 4$  Super Yang-Mills (SYM). BMN compared the exact expression [42] for the mass spectrum of the string

states in free string theory,  $g_{\text{st}} = 0$ , to the planar anomalous dimension of certain field theory operators - since then called the BMN operators - to the first order in the 't Hooft coupling of the theory  $\lambda'$ , finding remarkable agreement. Shortly after it was shown in [43] that, thanks to the superconformal invariance of the  $\mathcal{N} = 4$  theory, it was actually possible to reproduce from field theory the full (all orders in  $\lambda'$ ) expression for the masses of string states at  $g_{\text{st}} = 0$ . An important step forward was subsequently taken in [44, 45], where the correspondence was expressed as [45]

$$\frac{1}{\mu} H_{\text{string}} = \Delta - J, \quad (1.137)$$

where  $H_{\text{string}}$  is the *interacting* string Hamiltonian,  $\mu$  is the scale parameter of the pp-wave metric, and  $\Delta - J$  is the difference between the gauge theory dilatation operator  $\Delta$  and the R-charge  $J$ . The relation (1.137) is conjectured to hold in the double-scaling limit  $N \sim J^2 \rightarrow \infty$  to all orders in the two parameters of the theory,  $g_2$  and  $\lambda'$ , where

$$\lambda' = \frac{g_{\text{YM}}^2 N}{J^2} = \frac{1}{(\mu p^+ \alpha')^2}, \quad (1.138)$$

$$g_2 = \frac{J^2}{N} = 4\pi g_{\text{st}} (\mu p^+ \alpha')^2. \quad (1.139)$$

Here  $\lambda'$  is the effective 't Hooft coupling of the BMN sector [41], and  $g_2$  is the genus counting parameter of Feynman diagrams [41, 46, 47]. The right hand sides of (1.138), (1.139) express  $\lambda'$  and  $g_2$  in terms of the parameters in pp-wave string theory, so that  $1/\lambda' \propto \mu$  measures the deviation from flat space  $\mu \rightarrow 0$  and, importantly, the Yang-Mills genus counting parameter  $g_2$  is proportional to the string coupling  $g_{\text{st}}$ .

Let us see, in some detail, how the correspondence arises. As discussed above, the full symmetry of the pp-wave background is  $SO(4) \otimes SO(4) \otimes \mathbb{Z}_2$ . The first  $SO(4)$  is a remnant of the  $SO(2, 4)$  isometry group of  $AdS_5$  while the second  $SO(4)$  is a remnant of the  $SO(6)$  isometry group of  $S^5$ . As mentioned in section 1.5 the plane wave geometry is obtained if one focuses on the neighbourhood of the null trajectory travelling around an equator of the  $S^5$ . An obvious question to be asked is the following: what is the effect of taking this Penrose limit of the  $AdS$  geometry on the gauge theory side of the  $AdS/CFT$  correspondence? First of all, focusing

around an equator of the five sphere means that we break its  $SO(6)$  isometry group down to  $SO(4) \otimes SO(2)$ . On the gauge theory side, this means that we should single out two -let's say  $\phi_5$  and  $\phi_6$ - of the six  $\phi$  fields which transform under the  $SO(6)$  R-symmetry of the field theory Langrangian. From now on, when we refer to the R-charge of a state we mean the charge associated to this  $U(1) \sim SO(2)$  subgroup of  $SO(6)$ . Second, let us recall that the *AdS/CFT* correspondence relates the energy  $E = i\partial_\tau$  of a string state in  $AdS_5 \times S^5$  to the energy of a state in  $N = 4$  living on  $R \times S^3$ , which is the conformal boundary of  $AdS_5 \times S^5$  in global coordinates. By the operator-state map, the energy of a state on  $R \times S^3$ , where  $S^3$  has unit radius, becomes the conformal dimension  $\Delta$  of an operator in  $R^4$ . Likewise, the angular momentum around the equator of  $S^5$   $J = -i\partial_\phi$  becomes the R-charge under the  $U(1)$  subgroup of the full  $SO(6)$  R-symmetry of  $N = 4$  SYM. As a result, we have the following relations

$$\begin{aligned} p^- &= -p^+ = i\partial_{x^+} = i\mu(\partial_\tau + \partial_\phi) = \mu(\Delta - J) \\ p^+ &= -p^- = i\partial_{x^-} = \frac{i}{2\mu R^2}(\partial_\tau - \partial_\phi) = \frac{\Delta + J}{2\mu R^2}. \end{aligned} \quad (1.140)$$

Since in the Penrose limit  $R \rightarrow \infty$  (1.140) suggests that we should restrict ourselves to those operators that have finite  $\Delta - J$  and their  $\Delta + J$  should go as  $\Delta + J \sim R^2 \sim \sqrt{N}$ . We have, thus, seen that the Penrose limit induces the following double scaling limit in the  $\mathcal{N} = 4$   $SU(N)$  SYM,

$$N \rightarrow \infty, \quad J \rightarrow \infty \quad \text{with} \quad \frac{J^2}{N} = \text{fixed} \quad \text{and} \quad g_{\text{YM}} = \text{fixed}. \quad (1.141)$$

Two important remarks are in order. First, since the BMN limit of (1.141) is a large- $N$  limit one should expect that only the planar diagrams would survive as it happens in any large- $N$  gauge theory (see discussion in the introduction). However, this is not the case for the BMN limit, mainly because the operators under consideration does not remain fixed but their "length"  $J \rightarrow \infty$  goes to infinity as  $\sqrt{N}$ . The result is that each non-planar diagram of genus  $h$  comes with a combinatorial factor of  $J^{4h}$  which when combined with the usual large- $N$  suppression of  $1/N^{2h}$  gives a finite contribution, namely  $J^{4h}/N^{2h} = g_2^{2h}$ . Consequently, we see that in the BMN limit the effective genus counting number is  $g_2$  and not  $1/N^{2h}$ . Second, because of

the fact that  $g_{YM}$  is kept fixed the 't Hooft coupling constant  $\lambda = g_{YM}^2 N \rightarrow \infty$ . Then, one would naively expect that the conformal dimension of any operator, that does not belong to a short multiplet and thus is not protected, would diverge in the limit of large 't Hooft coupling (see discussion around (1.33)). This means that the corresponding string state would have infinite mass and therefore decouple from the theory. Again this is not the case for there exists a special class of (almost BPS) operators called BMN operators whose conformal dimension is finite [41], [43] and depends on the effective coupling constant  $\lambda'$ . These operators we describe below.

One important point, to keep in mind, is that the PP-wave/SYM duality appears to be a weak/weak coupling duality, despite the fact that the 't Hooft coupling is infinite. This is so, because a new effective coupling  $\lambda'$  appears. As a result, both the string coupling and the gauge theory coupling can be kept small at the same time. This means that perturbative calculations can be done on both sides of the duality. A second important point, that will be clear in a while, is that in the context of this duality, it is the first time that checking the correspondence goes beyond the sugra states.

To begin with, let us consider the ground state of the string  $|v, p^+\rangle$ . This has zero energy and (1.140) implies that the corresponding gauge operator should have  $\Delta - J = 0$ . Furthermore, let's restrict ourselves to single trace operators and  $g_2 = 0$  (actually  $g_2$  controls the mixing between single and multi trace operators). These restrictions will be removed later. There is a unique operator satisfying the above requirements. This is

$$\mathcal{O}_{vac} = \frac{1}{\sqrt{JN^J}} \text{Tr} Z^J \longleftrightarrow |v, p^+\rangle. \quad (1.142)$$

Here  $Z = 1/\sqrt{2}(\phi_5 + \phi_6)$  (the  $U(1) \sim SO(2)$  group generates rotations in the  $\phi_5 - \phi_6$  plane). The first excited states are the supergravity states and their corresponding single trace operators

$$\mathcal{O}_i = \frac{1}{\sqrt{N^{J+1}}} \text{Tr}(\phi_i Z^J) \longleftrightarrow \alpha_0^{i\dagger} |v, p^+\rangle. \quad (1.143)$$

These operators can be generated if one acts with the broken rotations of  $SO(6)$  upon the the vacuum operator [49]. Then the Z fields are rotated to the corresponding  $\phi_i$

field. Acting more than once with the same rotation will either change another  $Z$  field to  $\phi_i$  or change the  $\phi_i$  to a  $\bar{Z}$ . Acting with a different rotation will give the higher excited sugra state

$$\mathcal{O}_{ij} = \frac{1}{\sqrt{JN^{J+2}}} \sum_{l=0}^J \text{Tr}(\phi_i Z^l \phi_j Z^{J-l}) \longleftrightarrow \alpha_0^{i\dagger} \alpha_0^{j\dagger} |v, p^+\rangle. \quad (1.144)$$

In the above, string excitations belong to the first  $SO(4)$ . Acting to the vacuum with the broken superconformal symmetries will give rise to insertions of the second  $SO(4)$ , namely  $D_i Z$ ,  $i = 1, \dots, 4$ . This way all the higher excited sugra states can be obtained. All the operators above are 1/2 BPS and thus their anomalous dimension does not receive corrections.

One can, however, consider the following non-BPS operators where each impurity is accompanied by a phase. These operators correspond to "massive" string states<sup>8</sup>. The first such operator is

$$\mathcal{O}_{i,n} \sim \sum_{l=0}^J e^{2\pi i n l / J} \text{Tr}(Z^l \phi_i Z^{J-l}) \longleftrightarrow \alpha_n^{i\dagger} |v, p^+\rangle. \quad (1.145)$$

Due to the cyclicity of the trace the sum in the above equation gives zero except when  $n = 0$ . So we have "reinvented" the sugra state. It should be noted that the string state corresponding to (1.145) for  $n \neq 0$  simply do not exist because they do not satisfy the level matching condition. The first meaningful non-sugra state is written as

$$\mathcal{O}_{ij,m}^J = \mathcal{C} \left[ \sum_{l=0}^J e^{\frac{2\pi i m l}{J}} \text{Tr}(\phi_i Z^l \phi_j Z^{J-l}) - \delta_{ij} \text{Tr}(\bar{Z} Z^{J+1}) \right] \longleftrightarrow \alpha_n^{i\dagger} \alpha_{-n}^{j\dagger} |v, p^+\rangle. \quad (1.146)$$

To obtain (1.146) we have used the cyclicity of the trace to bring  $\phi_i$  first in the trace and the fact that  $n_1 + n_2 = 0$ . The way the correspondence works should be clear by now. Each insertion of an impurity is accompanied by a phase depending on the worldsheet momentum. Those operators for which the momenta do not sum to zero vanish due to cyclicity of the trace implementing this way the level matching condition. The dictionary between impurity insertions and string creation operators

<sup>8</sup>To be accurate even the supergravity states on the pp-wave are massive. What we precisely mean is excitations with  $n \neq 0$

is thus as follows

$$\begin{aligned}
 \alpha^{i\dagger} &\longleftrightarrow \phi_i, \quad i = 1, \dots, 4, \\
 \alpha^{i\dagger} &\longleftrightarrow D_{i-4}Z, \quad i = 5, \dots, 8 \\
 \beta_{\alpha\beta}^\dagger &\longleftrightarrow \lambda_{r-1\beta}, \quad r = 3, 4, \quad \alpha, \beta = 1, 2, \\
 \beta_{\dot{\alpha}\dot{\beta}}^\dagger &\longleftrightarrow \bar{\lambda}_{\dot{r}\dot{\beta}}, \quad \dot{r} = 1, 2, \quad \dot{\alpha}, \dot{\beta} = 1, 2.
 \end{aligned} \tag{1.147}$$

The last two lines of (1.147) give the correspondence between the the fermionic string oscillators and the BMN fermions of  $N = 4$  SYM whose Euclidean Lagrangian is given in the Appendix C. We'll have more to say about the correspondence in the fermionic sector in Chapter 4.

In the next chapter we turn to a systematic study of correlation functions of BMN operators [47, 73–76, 101] in the light of the pp-wave/SYM correspondence [41].

## Chapter 2

# Vertex-Correlator Correspondence In The pp-wave

As discussed in the previous chapter the pp-wave/SYM correspondence of Berenstein, Maldacena and Nastase (BMN) [41] represents all massive modes of type IIB superstring in the plane wave background in terms of composite BMN operators of  $\mathcal{N} = 4$  Yang-Mills theory in 4D. In its minimal form, this correspondence emphasizes a duality relation between the masses of string states and the anomalous dimensions of the corresponding BMN operators in gauge theory in the large  $N$  double scaling limit. This relation has been verified in the planar limit of SYM perturbation theory in [34, 41, 43]. Calculations in the BMN sector of gauge theory at the nonplanar level were performed in [46, 47, 73, 76] also taking into account mixing effects of planar BMN operators. The minimal mass-dimension type duality relation was extended in [44, 45] to all orders in the effective genus expansion parameter  $g_2$  and expressed in the form  $H_{\text{string}} = H_{\text{SYM}} - J$ . Here  $H_{\text{string}}$  is the full string field theory Hamiltonian, and  $H_{\text{SYM}} - J = \Delta - J$  is the gauge theory Hamiltonian (the conformal dimension) minus the R-charge. Work in this direction includes [48, 49, 67].

In this chapter, instead, we address a more ambitious duality relation [101] of a *vertex-correlator* type, summarized in the next Section. This type of correspondence for pp-waves was first discussed in [47] and relates the coefficients of 3-point correlators of BMN operators in gauge theory to 3-string vertices in lightcone string field theory in the pp-wave background. It is well-known and discussed in chapter 1

to some extent, that in the AdS/CFT scenario, in addition to the relation between the masses of supergravity states and the dimensions of the dual gauge theory operators, one can also compare directly the correlation functions in gauge theory with supergravity interactions in the bulk [35,36]. Since the pp-wave/CFT correspondence can be viewed as a particular limit of the AdS/CFT correspondence, it is natural to expect that a version of vertex–correlator type duality will hold in the pp-wave/SYM correspondence.

Building on previous work [37,47,73,74], the authors of [101] were able to represent all known gauge theory results for 3-point functions of BMN operators with 2 scalar impurities in terms of a single concise expression involving the 3-string vertex in light-cone string field theory in the pp-wave background. The goal of the present chapter is to test this relation at the level of BMN operators with 3 scalar impurities.

In conformal theory, the two- and three-point functions of conformal primary operators are completely determined by conformal invariance of the theory. One can always choose a basis of scalar conformal primary operators such that the two-point functions take the canonical form:

$$\langle \mathcal{O}_{\Delta_\alpha}^\dagger(x) \mathcal{O}_{\Delta_\beta}(0) \rangle = \frac{\delta_{\alpha\beta}}{(x^2)^{\Delta_\alpha}}, \quad (2.1)$$

$$\langle \mathcal{O}_{\Delta_1}(x_1) \mathcal{O}_{\Delta_2}(x_2) \mathcal{O}_{\Delta_3}^\dagger(x_3) \rangle = \frac{C_{123}}{(x_{12}^2)^{\frac{\Delta_1+\Delta_2-\Delta_3}{2}} (x_{13}^2)^{\frac{\Delta_1+\Delta_3-\Delta_2}{2}} (x_{23}^2)^{\frac{\Delta_2+\Delta_3-\Delta_1}{2}}}. \quad (2.2)$$

where  $x_{12}^2 := (x_1 - x_2)^2$ . Since the form of the  $x$ -dependence of conformal 3-point functions is universal, it is natural to expect that  $C_{123}$  is related to the interaction of the corresponding three string states in the pp-wave background. Note, that in order to be able to use the coefficients  $C_{123}$ , it is essential to work on the SYM side with  $\Delta$ -BMN operators. These operators are defined in such a way that they do not mix with each other (i.e. have definite scaling dimensions  $\Delta$ ) and which are conformal primary operators. Conformal invariance of the  $\mathcal{N} = 4$  theory then implies that the 2-point correlators of scalar  $\Delta$ -BMN operators are canonically normalized, and the 3-point functions take the simple form (2.2). Defined in this way, the basis of  $\Delta$ -BMN operators is unique and distinct from other BMN bases considered in the literature. For 2 scalar impurities, this  $\Delta$ -BMN basis was constructed in [73].

In this chapter we will work with scalar<sup>1</sup>  $\Delta$ -BMN operators  $\mathcal{O}_{n_1 n_2 n_3}$  with 3 impurities which correspond to the string bra-state  $\langle 0 | \alpha_{n_1}^1 \alpha_{n_2}^2 \alpha_{n_3}^3$ . In string theory  $n_i$  are the labels of string oscillators  $\alpha_{n_i}^i$ , and the level matching constraint is  $n_1 + n_2 + n_3 = 0$ . Bare single-trace BMN operators with 3 different real scalar impurities [45, 47] are given by

$$\mathcal{O}_{n_1 n_2 n_3} \equiv \mathcal{O}_{n_1 n_2 n_3}^{123} + \mathcal{O}_{n_1 n_2 n_3}^{132} = \frac{1}{J\sqrt{N^{J+3}}} \sum_{0 \leq l, k}^{l+k \leq J} [q_2^l q_3^{l+k} \text{tr}(\phi_1 Z^l \phi_2 Z^k \phi_3 Z^{J-l-k}) + q_3^l q_2^{l+k} \text{tr}(\phi_1 Z^l \phi_3 Z^k \phi_2 Z^{J-l-k})] \quad (2.3)$$

where  $q_2 = e^{2\pi i n_2 / J}$  and  $q_3 = e^{2\pi i n_3 / J}$ , and from now on, we always set  $n_1 = -n_2 - n_3$ . There are two terms on the right hand side of (2.3) since there are two inequivalent orderings of  $\phi_1$ ,  $\phi_2$  and  $\phi_3$  inside the trace<sup>2</sup>.

Operators (2.3) are the starting point for building the  $\Delta$ -BMN operators. In interacting field theory, bare operators have to be UV-renormalized and the effects of operator mixing have to be taken into account. It is well-known by now [38, 39, 73, 76] that the single-trace BMN operators mix with the multi-trace operators even in free theory at non-planar level, i.e. starting from order  $g_2(\lambda')^0$ . Hence, in order to calculate the leading-order contribution to the 3-point coefficient  $C_{123} \propto g_2$  in (2.2), one has to work with the order  $g_2$   $\Delta$ -BMN operators which involve the single-trace expressions (2.3) plus a linear combination of double-trace operators with coefficients of order  $g_2(\lambda')^0$ . For the simpler case of 2 scalar impurities, the single-double trace mixing effects have been calculated in [73], and the corresponding conformal 3-point function coefficients  $C_{123}$  were determined. One of the main technical results of the present chapter will be a determination of the coefficients  $C_{123}$  for  $\Delta$ -BMN operators with 3 scalar impurities (and general oscillator labels  $n_2, n_3 \in \mathbb{Z}$ ).

The chapter is organized as follows. In Section 2.1 we summarize the vertex-correlator duality proposal of [101] and write down the relevant equations. In Section 2.2 we calculate 2-point correlators of operators  $\mathcal{O}_{n_1 n_2 n_3}$  to order  $\lambda'$  in planar pertur-

<sup>1</sup>Vector operators, i.e.  $\Delta$ -BMN operators with vector impurities, discussed in [71, 72, 94], will be considered in the next chapter.

<sup>2</sup>Note that in both terms  $\phi_2$  in the  $Z$ -position  $l$  is accompanied by  $q_2^l$ , similarly for  $\phi_3$ . Hence, each of the two terms contributes to the same string state.

bation theory in the BMN limit. This is necessary in order to canonically normalize the UV-renormalized operators to order  $\lambda'$ . Section 2.3 contains our main technical results on the field theory side. There we calculate 3-point functions involving operators  $\mathcal{O}_{n_1 n_2 n_3}$ . We first derive the conformal expression (2.2) and extract the coefficient  $C_{123}$  for 3-point functions containing 1 general and 2 chiral operators (i.e. 1 string and 2 supergravity states in dual string theory). We then generalize this calculation of  $C_{123}$  to the case of two string states. In the final Section we demonstrate that the results of Section 2.3 are in complete agreement with the vertex–correlator duality prediction [101] of Section 2.1.

## 2.1 The vertex–correlator duality

Here we give a brief summary of the duality relation. For more detail, we refer the reader to [101].

For the bosonic external string states  $\langle\Phi_i|$  the proposed correspondence relation is

$$\mu(\Delta_1 + \Delta_2 - \Delta_3) C_{123} = \langle\Phi_1|\langle\Phi_2|\langle\Phi_3| \mathbf{P} \exp\left(\frac{1}{2} \sum_{r,s=1}^3 \sum_{m,n=-\infty}^{\infty} \sum_{I=1}^8 \alpha_m^{rI\dagger} \hat{N}_{mn}^{rs} \alpha_n^{sI}\right) |0\rangle_{123}. \quad (2.4)$$

This relation, is conjectured to be valid to all orders in  $\lambda'$  and to the leading order in  $g_2$  in the double scaling limit. Equation (2.4), originally proposed in [47], is the first key element of the vertex-correlator duality.  $\hat{N}_{mn}$  are the Neumann matrices in the  $\alpha$ -basis of string oscillators. These matrices were recently calculated in [98] as an expansion in inverse powers of  $\mu$  at  $\mu \rightarrow \infty$ . Results of [98] for  $\hat{N}_{mn}$  constitute the second element of the proposed duality. The relevant for us leading order expressions of  $\hat{N}_{mn}$  directly in the  $\alpha$ -oscillator basis can be found in the Appendix A.

The third and final element of the vertex–correlator duality is the expression [101] for the bosonic part of the string field theory prefactor,  $\mathbf{P}$ , which appears on the right hand side of (2.4),

$$\mathbf{P} = (-1)^p C_{\text{norm}} (\mathbf{P}_I + \mathbf{P}_{II}), \quad (2.5)$$

where<sup>3</sup>

$$P_I = \sum_{r=1}^3 \sum_{m=-\infty}^{+\infty} \frac{\omega_{rm}}{\alpha_r} \alpha_m^{rI\dagger} \alpha_m^{rI}, \quad (2.6)$$

$$P_{II} = \frac{1}{2} \sum_{r,s=1}^3 \sum_{m,n>0} \frac{\omega_{rm}}{\alpha_r} (\hat{N}_{m-n}^{rs} - \hat{N}_{mn}^{rs}) (\alpha_m^{rI\dagger} \alpha_n^{sI\dagger} + \alpha_{-m}^{rI\dagger} \alpha_{-n}^{sI\dagger} - \alpha_m^{rI\dagger} \alpha_{-n}^{sI\dagger} - \alpha_{-m}^{rI\dagger} \alpha_n^{sI\dagger}) \quad (2.7)$$

and

$$C_{\text{norm}} = g_2 \frac{\sqrt{y(1-y)}}{\sqrt{J}} = C_{123}^{\text{vac}}. \quad (2.8)$$

The only new ingredient here compared to [101] is the overall sign  $(-1)^p$  in (2.5), where  $p \equiv \frac{1}{2} \sum_{r=1}^3 \sum_{m=-\infty}^{+\infty} \alpha_m^{rI\dagger} \alpha_m^{rI}$  counts the number of impurities. For all the cases involving BMN operators with 2 impurities considered in [101], it turns out that  $(-1)^p = (-1)^2 = 1$ , and hence is irrelevant. In the present chapter, all the cases involving 3 impurities will lead to an overall minus sign,  $(-1)^p = (-1)^3 = -1$ .

In terms of the original SFT  $a$ -oscillator basis the full prefactor takes a remarkably simple form

$$P = (-1)^p C_{\text{norm}} \sum_{r=1}^3 \left( \sum_{m>0} \frac{\omega_{rm}}{\alpha_r} a_m^{rI\dagger} a_m^{rI} + \mu \text{sign}(\alpha_r) a_0^{rI\dagger} a_0^{rI} \right), \quad (2.9)$$

however, as in [101], we will continue using the prefactor in the BMN  $\alpha$ -oscillator basis, (2.6) and (2.7), where the comparison with the gauge theory BMN correlators is most direct.

This prefactor, and in particular the second term  $P_{II}$ , was constructed in [101] to reproduce a particular class of field theory results for the 3-point functions<sup>4</sup>. It was then successfully tested in [101] against all the available field theory results involving BMN operators with 2 scalar impurities and also the simplest cases involving BMN operators with 3 impurities. In Section 2.4 we will verify that the duality relation (2.4) with the prefactor (2.5) holds at the 3-impurity level.

We emphasize that the matching to field theory results is highly non-trivial even though the choice [101] of the prefactor in (2.5) is “phenomenological”. In the next two Sections we will assemble a detailed SYM calculation of the 3-point coefficients

<sup>3</sup>We are using standard definitions for the SFT quantities in the pp-wave background such as  $\omega_{rm}$ ,  $\alpha_r$  and  $\mu$ , which are summarized in the Appendix A.

<sup>4</sup>We note that (2.5) is different from the earlier proposals for the prefactor in [53, 54, 98].

for BMN correlators with 3 impurities, (2.26), (2.27). We should emphasize that a *coincidental* agreement of our SYM results and the string vertex with the prefactor (2.5) (which a priori knows nothing about 3-impurity operators) is very unlikely.

## 2.2 Two-point correlators

As explained earlier, on the SYM side of our proposed correspondence we must use the  $\Delta$ -BMN operators  $\mathcal{O}$ . For BMN operators with 2 scalar impurities this basis was constructed in [73] to order  $g_2(\lambda')^0$  and  $g_2^2(\lambda')^0$  and involves a linear combination of the original single-trace BMN operator and the double-trace (in general multi-trace) BMN operators.

There are two important cases where simplifications occur such that at the leading non-vanishing order in  $g_2$ , only the single-trace operators (2.3) need to be taken into account. The first case involves 2-point functions  $\langle \mathcal{O}\bar{\mathcal{O}} \rangle$ , and will be considered in this Section. The second case involves 3-point functions  $\langle \mathcal{O}_1\mathcal{O}_2\bar{\mathcal{O}}_3 \rangle$ , where  $\mathcal{O}_1$  and  $\mathcal{O}_2$  are chiral BMN operators, and  $\mathcal{O}_3$  is a general one, i.e. two supergravity and one string state in dual string theory. This case will be considered in the first part of the next Section. It is easy to check (see e.g. [73]) that in both cases the contributions from double- and higher trace operators to  $\mathcal{O}$ 's give vanishing contributions to the correlators at the leading order in  $g_2$  and in the double-scaling limit.

Before we continue we make a final general comment. One can split scalar interactions of the  $\mathcal{N} = 4$  SYM Lagrangian into D-terms, F-terms and K-terms as is done in [47, 73] and show that at one loop level the D-terms cancel against the gluon exchanges and scalar self-energies. So one is left only with F-terms and K-terms. However the K-terms have vanishing contribution in the cases we are going to consider since K-terms couple only to  $SO(6)$  traces. Thus, there is only an F-term interaction to consider which has a factor of  $g_{YM}^2$  for every vertex where a  $\phi^i$  line crosses a  $Z = \frac{\phi^5 + i\phi^6}{\sqrt{2}}$  line, and a factor of  $-g_{YM}^2$  when the lines do not cross.

In this Section we calculate 2-point correlators  $\langle \mathcal{O}\bar{\mathcal{O}} \rangle$  of renormalized operators (2.3) in planar perturbation theory to order  $\lambda'$ . This is needed to normalize the operators correctly, such that (2.1) holds at order  $\lambda'$ . In this and the next Section we

will be calculating Feynman diagrams in dimensional reduction to  $4 - 2\epsilon$  dimensions, and in coordinate space. Our calculations follow and generalize the approach of [74].

We note that bare operators in (2.3) were normalized in such a way that their free 2-point planar correlator is

$$\langle \bar{\mathcal{O}}_{n_1 n_2 n_3}(0) \mathcal{O}_{\bar{n}_1 \bar{n}_2 \bar{n}_3}(x) \rangle = \delta_{n_2, \bar{n}_2} \delta_{n_3, \bar{n}_3} \Delta(x)^{J+3} \quad (2.10)$$

in the BMN limit. Here  $\Delta(x)$  is the scalar propagator,

$$\Delta(x) = \frac{\Gamma(1 - \epsilon)}{(4\pi^{2-\epsilon})(x^2)^{1-\epsilon}} \quad (2.11)$$

There are four contributions to consider,  $\langle \bar{\mathcal{O}}^{123}(0) \mathcal{O}^{123}(x) \rangle$ ,  $\langle \bar{\mathcal{O}}^{132}(0) \mathcal{O}^{132}(x) \rangle$ ,  $\langle \bar{\mathcal{O}}^{123}(0) \mathcal{O}^{132}(x) \rangle$  and  $\langle \bar{\mathcal{O}}^{132}(0) \mathcal{O}^{123}(x) \rangle$ . The last two correlators vanish in free theory (since the 3  $\phi$ 's are different), and will be shown to vanish also at order  $\lambda'$  at the planar level.

We first calculate the interacting part of  $\langle \bar{\mathcal{O}}^{123}(0) \mathcal{O}^{123}(x) \rangle$ ,

$$\langle \bar{\mathcal{O}}^{123}(0) \mathcal{O}^{123}(x) \rangle = \frac{\Delta(x)^{J+3}}{J^2} (-g_{YM}^2 N) I(x) (P_1 + P_2 + P_3) \quad (2.12)$$

where  $I(x)$  is the interaction integral with  $\Delta(x)^2$  removed:

$$\begin{aligned} I(x) &= \left( \frac{\Gamma(1 - \epsilon)}{4\pi^{2-\epsilon}} \right)^2 (x^2)^{2-2\epsilon} \int \frac{d^{4-2\epsilon} y}{(y^2)^{2-2\epsilon} (y-x)^{2(2-2\epsilon)}} \\ &= \frac{1}{8\pi^2} \left( \frac{1}{\epsilon} + \gamma + 1 + \log \pi + \log x^2 + \mathcal{O}(\epsilon) \right). \end{aligned} \quad (2.13)$$

We will use a subtraction scheme which subtracts the  $1/\epsilon$  pole together with (an arbitrary) finite part  $s$

$$\frac{1}{\epsilon} + s. \quad (2.14)$$

$P_1$ ,  $P_2$  and  $P_3$  on the right hand side of (2.12) are the total contributions of the phase factors for the diagrams of Figure 2.1, Figure 2.2 and Figure 2.3 respectively. Denoting by  $q_2, q_3$  the BMN phases of the  $\mathcal{O}_{\bar{n}_1 \bar{n}_2 \bar{n}_3}(x)$  operator, and by  $\bar{r}_2, \bar{r}_3$  the BMN

phases of the  $\bar{\mathcal{O}}_{n_1 n_2 n_3}(0)$  operator, we obtain

$$\begin{aligned}
P_1 &= \sum_{1 \leq l, 0 \leq k}^{l+k \leq J} [q_2^l q_3^{l+k} \bar{r}_2^l \bar{r}_3^{l+k} - q_2^l q_3^{l+k} \bar{r}_2^{l-1} \bar{r}_3^{l+k-1}] \\
&\quad + \sum_{0 \leq l, 0 \leq k}^{l+k \leq J-1} [q_2^l q_3^{l+k} \bar{r}_2^l \bar{r}_3^{l+k} - q_2^l q_3^{l+k} \bar{r}_2^{l+1} \bar{r}_3^{l+k+1}] \\
&= \sum_{0 \leq l, 0 \leq k}^{l+k \leq J-1} [q_2^{l+1} q_3^{l+k+1} \bar{r}_2^{l+1} \bar{r}_3^{l+k+1} - q_2^{l+1} q_3^{l+k+1} \bar{r}_2^l \bar{r}_3^{l+k}] \\
&\quad + \sum_{0 \leq l, 0 \leq k}^{l+k \leq J-1} [q_2^l q_3^{l+k} \bar{r}_2^l \bar{r}_3^{l+k} - q_2^l q_3^{l+k} \bar{r}_2^{l+1} \bar{r}_3^{l+k+1}] \\
&= \sum_{0 \leq l, 0 \leq k}^{l+k \leq J-1} q_2^l q_3^{l+k} \bar{r}_2^l \bar{r}_3^{l+k} (1 + q_2 q_3 \bar{r}_2 \bar{r}_3 - q_2 q_3 - \bar{r}_2 \bar{r}_3) \\
&= \sum_{0 \leq l, 0 \leq k}^{l+k \leq J-1} (q_2 \bar{r}_2)^l (q_3 \bar{r}_3)^{l+k} [(1 - q_2 q_3)(1 - \bar{r}_2 \bar{r}_3)] \tag{2.15}
\end{aligned}$$

To derive (2.15) we have added the contributions of four diagrams in Figure 2.1 and noted that contributions of diagrams where a  $Z$  line crosses a  $\phi$  line in the  $Z$ - $\phi$  interaction (the second and the fourth diagrams in Figure 2.1) have a relative minus sign compared to the  $Z$ - $\phi$  interaction without crossing (the first and the third diagrams in Figure 2.1).

Similarly from four diagrams of Figure 2.2 and from four diagrams of Figure 2.3 we get

$$P_2 = \sum_{0 \leq l, 0 \leq k}^{l+k \leq J-1} (q_2 \bar{r}_2)^l (q_3 \bar{r}_3)^{l+k} [(1 - q_2)(1 - \bar{r}_2)] q_3 \bar{r}_3 \tag{2.16}$$

$$P_3 = \sum_{0 \leq l, 0 \leq k}^{l+k \leq J-1} (q_2 \bar{r}_2)^l (q_3 \bar{r}_3)^{l+k} [(1 - q_3)(1 - \bar{r}_3)] \tag{2.17}$$

We now evaluate the double sum:

$$\begin{aligned}
\sum_{0 \leq l, 0 \leq k}^{l+k \leq J-1} (q_2 \bar{r}_2)^l (q_3 \bar{r}_3)^{l+k} &= \sum_{l=0}^{J-1} (q_2 \bar{r}_2 q_3 \bar{r}_3)^l \sum_{k=0}^{J-1-l} (q_3 \bar{r}_3)^k \\
&= \begin{cases} 0 & \text{when } q_2 \bar{r}_2 \neq 1 \text{ and } q_3 \bar{r}_3 \neq 1 \\ J(J+1)/2 & \text{when } q_2 \bar{r}_2 = 1 = q_3 \bar{r}_3 \\ -\frac{J}{q_2 \bar{r}_2 - 1} & \text{when } q_2 \bar{r}_2 \neq 1 \text{ and } q_3 \bar{r}_3 = 1 \\ \frac{J}{q_3 \bar{r}_3 - 1} & \text{when } q_2 \bar{r}_2 = 1 \text{ and } q_3 \bar{r}_3 \neq 1 \end{cases} \tag{2.18}
\end{aligned}$$

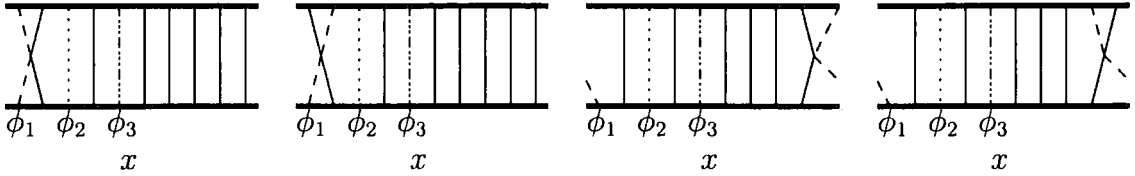


Figure 2.1: Interacting diagrams for the 2-point function where  $\phi_1$  interacts with  $Z$ . These diagrams give rise to  $P_1$ .

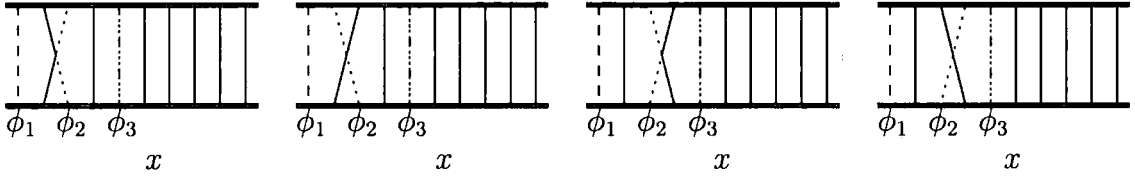


Figure 2.2: Interacting diagrams for the 2-point function with  $\phi_2$  interactions. These diagrams give rise to  $P_2$ .

It is clear that, in the BMN limit, the correlator is non-zero only when  $q_2\bar{\Gamma}_2 = 1 = q_3\bar{\Gamma}_2$ , that is, when the operators in the correlator are the same.

The result for the second correlator,  $\langle \bar{\mathcal{O}}^{132}(0)\mathcal{O}^{132}(x) \rangle$ , is obtained from the first one by interchanging labels 2 and 3. The sum of the two contributions,  $\langle \bar{\mathcal{O}}^{123}(0)\mathcal{O}^{123}(x) \rangle + \langle \bar{\mathcal{O}}^{132}(0)\mathcal{O}^{132}(x) \rangle$ , will have the second term on the right hand side of (2.18) doubled up, and the third and fourth terms cancelled.

We now show that the other two correlators  $\langle \bar{\mathcal{O}}^{123}(0)\mathcal{O}^{132}(x) \rangle$  and  $\langle \bar{\mathcal{O}}^{132}(0)\mathcal{O}^{123}(x) \rangle$ , vanish in our case. There are 12 diagrams to consider, the first 6 are shown in Figure 2.4.

The combined phase factor with these six diagrams is:

$$\begin{aligned}
 P_4 &= \sum_{k=0}^J (q_2^0 q_3^k \bar{\Gamma}_2^{-0-k} \bar{\Gamma}_3^k - q_2^0 q_3^k \bar{\Gamma}_2^{-J-k} \bar{\Gamma}_3^k) \\
 &+ \sum_{l=0}^J (q_2^l q_3^l \bar{\Gamma}_2^{-l} \bar{\Gamma}_3^l) - q_2^l q_3^l \bar{\Gamma}_2^{-l} \bar{\Gamma}_3^l + \sum_{l=0}^J (q_2^l q_3^J \bar{\Gamma}_2^{-l} \bar{\Gamma}_3^J - q_2^l q_3^0 \bar{\Gamma}_2^{-l} \bar{\Gamma}_3^J) = 0. \quad (2.19)
 \end{aligned}$$

The remaining six diagrams are obtained from the ones in Figure 2.4 by exchanging  $\phi_2$  and  $\phi_3$ . They also sum to zero. Thus, the non-diagonal terms do not contribute to the correlator at the planar level.

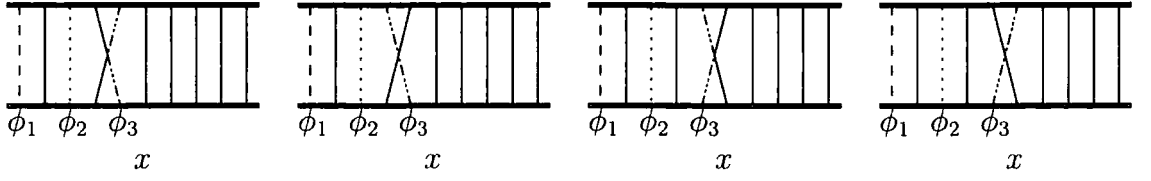


Figure 2.3: Interacting diagrams for the 2-point function with  $\phi_3$  interactions. These diagrams give rise to  $P_3$ .

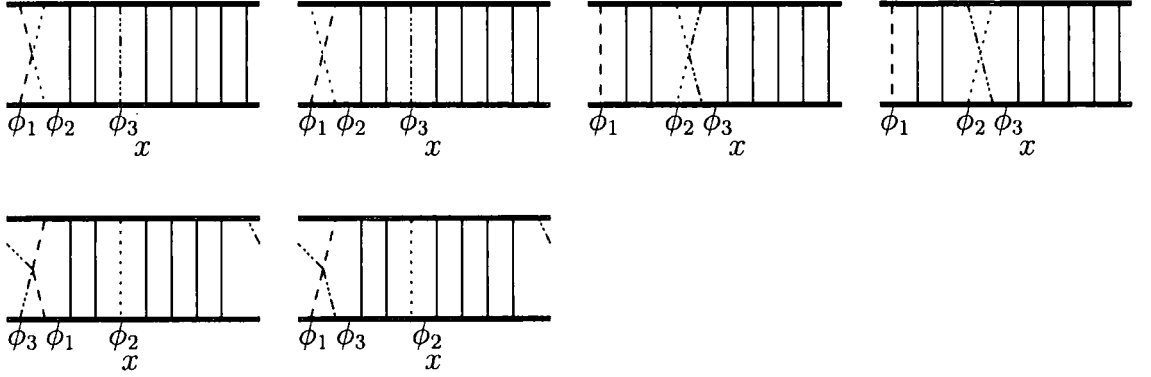


Figure 2.4: Interacting diagrams for the two-point function. These diagrams give rise to  $P_4 = 0$ . There are six additional diagrams with  $\phi_2$  and  $\phi_3$  exchanged. Their sum is also zero.

Finally, combining with the free result we obtain

$$\begin{aligned} \langle \bar{\mathcal{O}}_{n_1 n_2 n_3}(0) \mathcal{O}_{\bar{n}_1 \bar{n}_2 \bar{n}_3}(x) \rangle &= \delta_{n_2 \bar{n}_2} \delta_{n_3 \bar{n}_3} \Delta(x)^{J+3} I(x) \\ &\times \{1 - g_{YM}^2 N [(1 - q_2 q_3)(1 - \bar{q}_2 \bar{q}_3) + (1 - q_2)(1 - \bar{q}_2) + (1 - \bar{q}_3)(1 - q_3)]\}, \end{aligned} \quad (2.20)$$

where the four terms in curly brackets correspond respectively to the free contribution,  $P_1$ ,  $P_2$  and  $P_3$ . Now, substituting (2.13) for  $I(x)$  with a subtraction (2.14), and using an expansion

$$\Delta(x)^\alpha \simeq 1 + \alpha \log \Delta(x) = 1 + \alpha(-\log 4\pi^2 - \log x^2) + O(\epsilon) \quad (2.21)$$

we derive the final expression for the 2-point function,

$$\langle \bar{\mathcal{O}}_{n_1 n_2 n_3}(0) \mathcal{O}_{\bar{n}_1 \bar{n}_2 \bar{n}_3}(x) \rangle = \delta_{n_2 \bar{n}_2} \delta_{n_3 \bar{n}_3} \Delta(x)^{J+3+\alpha} [1 - \alpha(\gamma + 1 - \log 4\pi - s)] \quad (2.22)$$

where  $\alpha$  denotes

$$\alpha = \frac{\lambda'}{2} [(n_2 + n_3)^2 + n_2^2 + n_3^2], \quad (2.23)$$

and, from the right hand side of (2.22), it has to be identified with the anomalous dimension of  $\mathcal{O}_{n_1 n_2 n_3}$ ,

$$\Delta - J = 3 + \alpha = 3 + \frac{\lambda'}{2} [(n_2 + n_3)^2 + n_2^2 + n_3^2], \quad (2.24)$$

in agreement with dual string theory prediction.

The normalized operator is given by

$$\mathcal{O}_{n_1 n_2 n_3} = \frac{1 + \alpha/2(\gamma + 1 - \log 4\pi - s)}{J\sqrt{N^{J+3}}} \sum_{0 \leq l, k}^{l+k \leq J} [q_2^l q_3^{l+k} \text{tr}(\phi_1 Z^l \phi_2 Z^k \phi_3 Z^{J-l-k}) + q_3^l q_2^{l+k} \text{tr}(\phi_1 Z^l \phi_3 Z^k \phi_2 Z^{J-l-k})] \quad (2.25)$$

## 2.3 Three-point functions

Here our goal is evaluate 3-point functions involving BMN operators with 3 scalar impurities in planar perturbation theory to order  $\lambda'$ . We will consider two such 3-point functions,

$$G_3(x_1, x_2) = \langle \bar{\mathcal{O}}_{n_1 n_2 n_3}^J(0) \mathcal{O}_{n'_1 n'_2 n'_3}^{J_1}(x_1) \mathcal{O}_{\text{vac}}^{J_2}(x_2) \rangle \quad (2.26)$$

and

$$G'_3(x_1, x_2) = \langle \bar{\mathcal{O}}_{n_1 n_2 n_3}^J(0) \mathcal{O}_{n'_2 - n'_2}^{J_1}(x_1) \mathcal{O}_0^{J_2}(x_2) \rangle \quad (2.27)$$

Here  $\mathcal{O}_{n_1 n_2 n_3}^J$  with  $n_1 = -n_2 - n_3$ , is a  $\Delta$ -BMN operator with 3 scalar impurities, it is given by (2.25) plus multi-trace expressions<sup>5</sup> at higher orders in  $g_2$ . The operator  $\mathcal{O}_{n'_2 - n'_2}^{J_1}$  is a  $\Delta$ -BMN operator with 2 scalar impurities, at the classical single-trace level it is given by

$$\mathcal{O}_{n'_2 - n'_2}^{J_1} = \frac{1}{\sqrt{J N^{J_1+2}}} \sum_{l=0}^{J_1} r_2^l \text{tr}(\phi_1 Z^l \phi_2 Z^{J_1-l}), \quad (2.28)$$

and the remaining operators are chiral and are protected against quantum corrections,

$$\mathcal{O}_0^{J_2} = \frac{1}{\sqrt{N^{J_2+1}}} \text{tr}(\phi_3 Z^{J_2}), \quad \mathcal{O}_{\text{vac}}^{J_2} = \frac{1}{\sqrt{J_2 N^{J_2}}} \text{tr}(Z^{J_2}). \quad (2.29)$$

---

<sup>5</sup>In fact, it follows from the analysis of [73] that at the relevant to us first order in  $g_2$ , only the double-trace corrections and only to the barred operators in (2.26) and (2.27) give non-vanishing contributions.

We also note that the R-charge conservation implies that

$$J_2 = J - J_1 \quad (2.30)$$

In the first subsection we will derive conformal expressions (2.2) and determine the 3-point coefficients  $C_{123}$  for both of these Green functions in the settings where the barred operator is general, and the two unbarred operators are chiral, i.e. correspond to two supergravity states. As mentioned earlier, in this case, only the single-trace contributions to the operators are relevant at the leading non-vanishing order in  $g_2$ , thus simplifying our analysis significantly.

In the second subsection we will calculate the 3-point coefficients of (2.26) and (2.27) in the general case of two non-chiral operators. Here the double-trace corrections are important, in order to derive the conformal expression (2.2). However, using a simple trick we will show how to uniquely determine the coefficients  $C_{123}$  directly from the single-trace expressions for the operators, thus obtaining the main results of this Section, Eqs. (2.73), (2.74) and (2.82), (2.81).

### 2.3.1 One string and two supergravity states

As explained above, in this subsection only, we set  $n'_1 = n'_2 = n'_3 = 0$  and consider

$$G_3(x_1, x_2) = \langle \bar{\mathcal{O}}_{n_1 n_2 n_3}^J(0) \mathcal{O}_{000}^{J_1}(x_1) \mathcal{O}_{\text{vac}}^{J_2}(x_2) \rangle \quad (2.31)$$

and

$$G'_3(x_1, x_2) = \langle \bar{\mathcal{O}}_{n_1 n_2 n_3}^J(0) \mathcal{O}_{00}^{J_1}(x_1) \mathcal{O}_0^{J_2}(x_2) \rangle \quad (2.32)$$

At first we consider the 3-point function  $G_3(x_1, x_2)$  and express it as follows:

$$G_3(x_1, x_2) = \frac{1 + \frac{\alpha}{2}(\gamma + 1 - \log 4\pi - s)}{J\sqrt{N^{J+3}}} \frac{N^{J+2} J_2}{J_1 \sqrt{J_2 N^{J_1+3} N^{J_2}}} \frac{1}{\Delta(x_1)^{J_1+3} \Delta(x_2)^{J_2} (X - \lambda Y K(x_1, x_2))} \quad (2.33)$$

where  $\lambda = g_{YM}^2 N$  and  $X$  and  $Y$  are the combined phase-factors at the free and interacting level respectively.  $K(x_1, x_2)$  is the interaction integral for the diagrams depicted on Figures 2.6–2.9 (as in [74]):

$$\begin{aligned} K(x_1, x_2) &= \left( \frac{\Gamma(1-\epsilon)}{4\pi^{2-\epsilon}} \right)^2 (x_1^2)^{1-\epsilon} (x_2^2)^{1-\epsilon} \int \frac{d^{4-2\epsilon} y}{(y^2)^{2-2\epsilon} (y-x_1)^{2(1-\epsilon)} (y-x_2)^{2(1-\epsilon)}} \\ &= \frac{1}{16\pi^2} \left( \frac{1}{\epsilon} + \gamma + 2 + \log \pi + \log \frac{x_1^2 x_2^2}{x_{12}^2} + O(\epsilon) \right) \end{aligned} \quad (2.34)$$

The first fraction on the right hand side of (2.33) arises from the normalization of  $\bar{\mathcal{O}}_{n_1 n_2 n_3}^J$ . The denominator of the second fraction arises from the normalizations of the other two operators, while the summation over the  $J + 2$  loops gives a factor of  $N^{J+2}$ . The remaining factor of  $J_2$  comes from the Wick contractions with  $\mathcal{O}_{\text{vac}}^{J_2}$ .

Free diagrams are shown in Figure 2.5. There are six diagrams because of the six different ways of arranging three  $\phi$ 's in a trace. We denote with  $X_{123}$  the combined phase factor of a free diagram where  $\phi_1$  comes first,  $\phi_2$  is second and  $\phi_3$  is third.

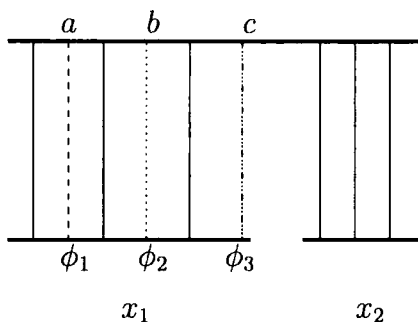


Figure 2.5: A typical free diagram for  $G_3$ . This diagram gives rise to  $X_{123}$ . There are five additional diagrams with  $\phi_1$ ,  $\phi_2$  and  $\phi_3$  interchanged.  $a$ ,  $b$  and  $c$  are the positions of the impurities in the trace. For this particular diagram,  $a = 2$ ,  $b = 4$ ,  $c = 6$ .

We have:

$$X_{123} = \sum_{a=1}^{J_1+1} \sum_{b=a+1}^{J_1+2} \sum_{c=b+1}^{J_1+3} \bar{q}_2^{b-a-1} \bar{q}_3^{c-a-2} \xrightarrow{J \rightarrow \infty} J^3 \int_0^{J_1/J} da \int_a^{J_1/J} db \int_b^{J_1/J} dc e^{-2\pi i n_2 (b-a)} e^{-2\pi i n_3 (c-a)} \quad (2.35)$$

$$X_{231} = \sum_{a=1}^{J_1+1} \sum_{b=a+1}^{J_1+2} \sum_{c=b+1}^{J_1+3} \bar{q}_2^{J-(c-a-2)} \bar{q}_3^{J-(c-b-1)} \xrightarrow{J \rightarrow \infty} J^3 \int_0^{J_1/J} da \int_a^{J_1/J} db \int_c^{J_1/J} dc e^{-2\pi i n_2 (-1)(c-a)} e^{-2\pi i n_3 (-1)(c-b)} \quad (2.36)$$

$$X_{312} = \sum_{a=1}^{J_1+1} \sum_{b=a+1}^{J_1+2} \sum_{c=b+1}^{J_1+3} \bar{q}_2^{c-b-1} \bar{q}_3^{J-(b-a-1)} \xrightarrow{J \rightarrow \infty} J^3 \int_0^{J_1/J} da \int_a^{J_1/J} db \int_b^{J_1/J} dc e^{-2\pi i n_2 (c-b)} e^{-2\pi i n_3 (-1)(b-a)} \quad (2.37)$$

$$(2.38)$$

where  $a, b, c$  are the positions of the first, second and third impurities in the trace. Also it is easy to see that  $X_{132}$  is equal to  $X_{123}$  with  $\bar{q}_2$  and  $\bar{q}_3$  exchanged,  $X_{213}$  is  $X_{312}$  with  $\bar{q}_2$  and  $\bar{q}_3$  exchanged and,  $X_{321}$  is  $X_{231}$  with  $\bar{q}_2$  and  $\bar{q}_3$  exchanged.

The sum of the six  $X$ 's is:

$$X = J^3 \int_0^{J_1/J} da \int_0^{J_1/J} db \int_0^{J_1/J} dc e^{-2\pi n_2(b-a)} e^{-2\pi n_3(c-a)} \quad (2.39)$$

For example the part of the above sum with  $c > b > a$  is  $X_{123}$ , the part with  $c > a > b$  is  $X_{213}$  and so on. Evaluating the integral we get

$$X = J^3 2^3 \frac{\sin(\pi n_2 J_1/J) \sin(\pi n_3 J_1/J) \sin(\pi(n_2 + n_3) J_1/J)}{(2\pi)^3 (n_2 + n_3) n_2 n_3} \quad (2.40)$$

We now calculate the phase factors coming from interacting planar diagrams. In the case where  $\phi_1$  interacts with  $Z$  we have eight diagrams with the first four shown in Figure 2.6 and the remaining four obtained by interchanging  $\phi_2$  and  $\phi_3$ . We do not need to consider diagrams where  $\phi_i$  interacts with  $\phi_j$  since they will be suppressed in the BMN limit relative to  $\phi$ - $Z$  interactions of Figure 2.6.

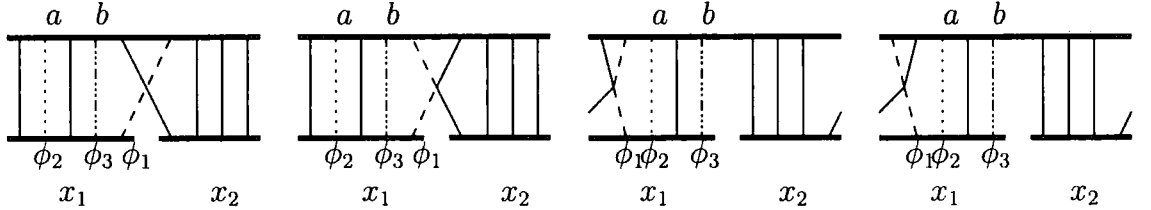


Figure 2.6: Interacting diagrams for  $G_3$ . These diagrams give rise to  $Y_{123}$ . There are four additional diagrams with  $\phi_2$  and  $\phi_3$  exchanged.

The phase combined factor of the four diagrams in Figure 2.6 is:

$$\begin{aligned} Y_{123} &= \sum_{a=1}^{J_1+1} \sum_{b=a+1}^{J_1+2} \left[ -\bar{q}_2^{J-(J_1+3-a-1)} \bar{q}_3^{J-(J_1+3-b)} + \bar{q}_2^{J-(J_1+3-a-2)} \bar{q}_3^{J-(J_1+3-b-1)} \right] \\ &\quad + \sum_{a=3}^{J_1+2} \sum_{b=a+1}^{J_1+3} \left[ \bar{q}_2^{a-3} \bar{q}_3^{b-4} - \bar{q}_2^{a-2} \bar{q}_3^{b-3} \right] \\ &= \sum_{a=1}^{J_1+1} \sum_{b=a+1}^{J_1+2} \bar{q}_2^{-(J_1-a+1)} \bar{q}_3^{-(J_1-b+2)} (1 - \bar{q}_2^{-1} \bar{q}_3^{-1}) + \sum_{a=3}^{J_1+2} \sum_{b=a+1}^{J_1+3} \bar{q}_2^{a-3} \bar{q}_3^{b-4} (1 - \bar{q}_2 \bar{q}_3) \\ &\rightarrow \frac{2\pi i (n_2 + n_3)}{J} \left[ \sum_{a=3}^{J_1+2} \sum_{b=a+1}^{J_1+3} \bar{q}_2^{a-3} \bar{q}_3^{b-4} - \sum_{a=1}^{J_1+1} \sum_{b=a+1}^{J_1+2} \bar{q}_2^{a-1} \bar{q}_3^{b-2} \bar{q}_2^{-J_1} \bar{q}_3^{-J_1} \right] \end{aligned} \quad (2.41)$$

In deriving the last line above, we have used that  $1 - \bar{q}_2 \bar{q}_3 \rightarrow \frac{2\pi i(n_2 + n_3)}{J}$  in the BMN limit. Converting the sum into an integral we get

$$\begin{aligned} Y_{123} &= 2\pi i(n_2 + n_3)J \int_0^{J_1/J} da \int_a^{J_1/J} db e^{-2\pi i n_2 a} e^{-2\pi i n_3 b} [1 - e^{-2\pi i(n_3 + n_2)(-J_1/J)}] \\ &= -J[1 - e^{-(A_2 + A_3)J_1/J}] \frac{e^{(A_3 + A_2)J_1/J} A_3 - e^{A_3 J_1/J} (A_2 + A_3) + A_2}{A_3 A_2} \end{aligned} \quad (2.42)$$

where  $A_2 = -2\pi i n_2$  and  $A_3 = -2\pi i n_3$ . We must add 4 more diagrams with  $\phi_2$  and  $\phi_3$  exchanged. This gives the expression above with  $n_2$  and  $n_3$  exchanged. If we sum the two contributions we get:

$$Y_{123} + Y_{132} = \frac{4(n_3 + n_2)^2 J \sin(\pi n_2 J_1/J) \sin(\pi n_3 J_1/J) \sin(\pi(n_3 + n_2)J_1/J)}{\pi(n_3 + n_2)n_2 n_3} \quad (2.43)$$

In the case where  $\phi_2$  interacts we have again eight diagrams, see Figure 2.7.

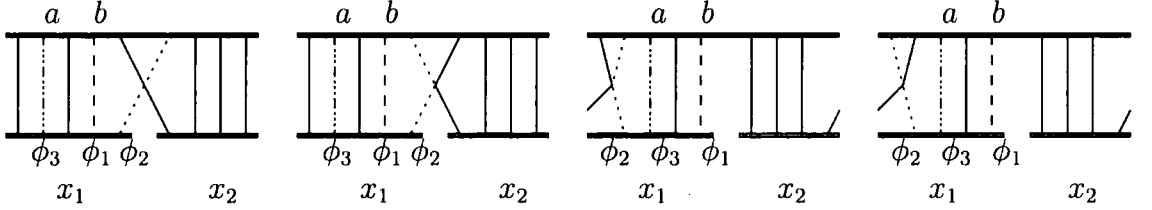


Figure 2.7: Interacting diagrams for  $G_3$ . These diagrams give rise to  $Y_{231}$ . There are four additional diagrams with  $\phi_1$  and  $\phi_3$  exchanged.

The combined phase factor of four diagrams in Figure 2.7 is easily obtained by substituting  $n_2 \rightarrow n_3$  and  $n_3 \rightarrow -(n_2 + n_3)$  into (2.42), as follows from comparing diagrams in Figures 2.6 and 2.7 and remembering that  $n_1 := -(n_2 + n_3)$ . In the BMN limit we have,

$$Y_{231} = J[1 - e^{A_2 J_1/J}] \frac{-e^{-A_2 J_1/J} (A_2 + A_3) + e^{-(A_3 + A_2)J_1/J} A_2 + A_3}{A_3(A_2 + A_3)} \quad (2.44)$$

Now we consider the above diagrams with  $\phi_1$  and  $\phi_3$  exchanged, i.e.  $-(n_2 + n_3) \leftrightarrow n_3$  and  $n_2$  unchanged in (2.44),

$$Y_{213} = J[1 - e^{A_2 J_1/J}] \frac{e^{-A_2 J_1/J} A_3 + e^{A_3 J_1/J} A_2 - A_2 - A_3}{A_3(A_2 + A_3)} \quad (2.45)$$

Summing the above contributions we arrive at

$$Y_{231} + Y_{213} = \frac{4n_2^2 J \sin(\pi n_2 J_1/J) \sin(\pi n_3 J_1/J) \sin(\pi(n_3 + n_2)J_1/J)}{\pi(n_3 + n_2)n_2 n_3} \quad (2.46)$$

Similarly, for diagrams in Figure 2.8 and their four partners, we find:

$$Y_{312} + Y_{321} = \frac{4n_3^2 J \sin(\pi n_2 J_1/J) \sin(\pi n_3 J_1/J) \sin(\pi(n_3 + n_2)J_1/J)}{\pi(n_3 + n_2)n_2 n_3} \quad (2.47)$$

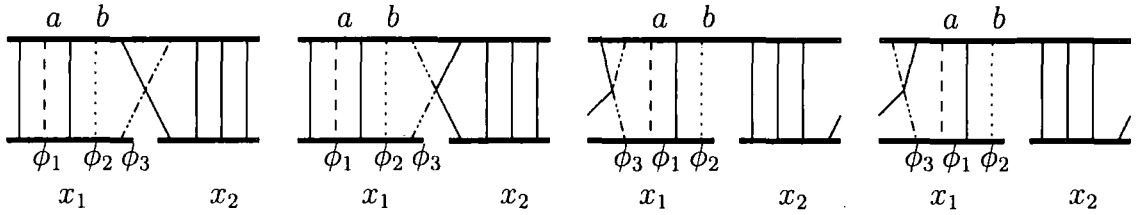


Figure 2.8: Interacting diagrams for  $G_3$ , contributing to  $Y_{312}$ . There are four additional diagrams with  $\phi_1$  and  $\phi_2$  exchanged.

For completeness, we note that diagrams without  $x_1$ -to- $x_2$  connection, depicted in Figure 2.9, sum to zero.

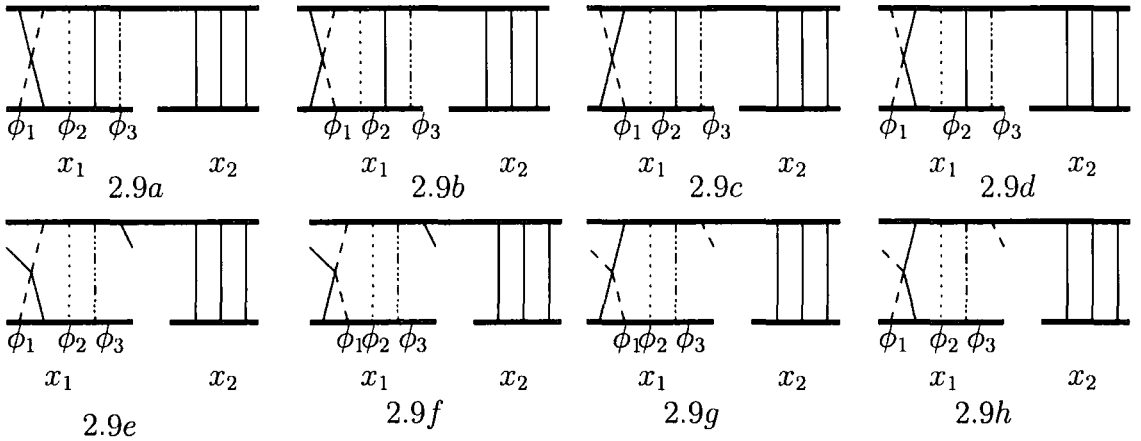


Figure 2.9: Interacting diagrams for  $G_3$ . Diagrams 2.9a, 2.9c, 2.9e and 2.9g have an opposite sign with respect to 2.9b, 2.9d, 2.9f and 2.9h, so they cancel pairwise. There are additional diagrams where  $\phi_2$  and  $\phi_3$  are exchanged which also add up zero. Additional diagrams where  $\phi_2$  or  $\phi_3$  (rather than  $\phi_1$ ) interact with  $Z$  also cancel in the same way.

Putting together all the expressions above, we get for  $G_3$

$$G_3(x_1, x_2) = \frac{1 + \alpha/2(\gamma + 1 - \log 4\pi - s)}{J\sqrt{N^{J+3}}} \frac{N^{J+2} J_2}{J_1 \sqrt{J_2 N^{J_1+3} N^{J_2}}} \Delta(x_1)^{J_1+3} \Delta(x_2)^{J_2} \\ \times \frac{J^3 \sin(\pi n_2 J_1/J) \sin(\pi n_3 J_1/J) \sin(\pi(n_3 + n_2) J_1/J)}{\pi^3 (n_3 + n_2) n_2 n_3} \\ \times \left[ 1 - \frac{\lambda'}{4} ((n_3 + n_2)^2 + n_2^2 + n_3^2) \left( \frac{1}{\epsilon} + \gamma + 2 + \log \pi + \log \frac{x_1^2 x_2^2}{x_{12}^2} \right) \right] \quad (2.48)$$

Subtracting  $1/\epsilon + s$  we obtain the result

$$G_3(x_1, x_2) = C_{123} \Delta(x_1)^{J_1+3+\alpha/2} \Delta(x_2)^{J_2+\alpha/2} \Delta(x_{12})^{-\alpha/2} \quad (2.49)$$

with

$$C_{123} = \frac{J^2 \sqrt{J_2}}{J_1 N \pi^3} \frac{\sin(\pi n_2 J_1/J) \sin(\pi n_3 J_1/J) \sin(\pi(n_3 + n_2) J_1/J)}{(n_3 + n_2) n_2 n_3} \left( 1 - \frac{\alpha}{2} \right) \quad (2.50)$$

A few comments are in order. First, we note that we have proved that to order in  $\lambda'$  and  $g_2$  we are working here,  $G_3$  takes the conformal form of (2.2). This is so since (2.49) is nothing other than the conformal expression (2.2) for  $G_3$ . Second, we have derived the expression for the coefficient  $C_{123}$  given by (2.50). This expression does not depend on  $s$  and, hence, is the subtraction scheme independent, as expected. In what follows, and in parallel with [73, 101], we will use only the leading order in  $\lambda'$  part of  $C_{123}$ , i.e. will set  $\alpha = 0$  in (2.50). This is because the, yet unaccounted, mixing effects at order  $\lambda'$  can change *constant* order  $\lambda'$  contributions to  $C_{123}$  (but not the logarithms in (2.49), which cannot appear in the  $x$ -independent mixing matrices).

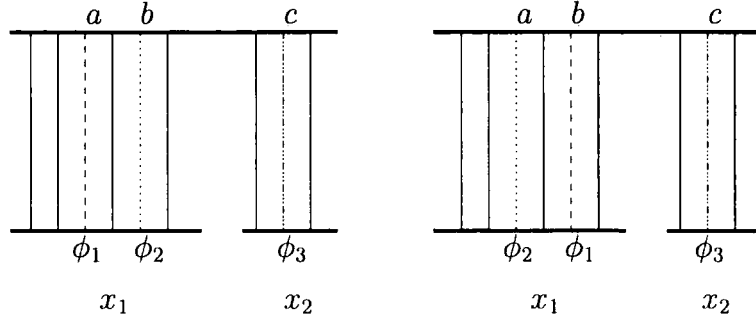
*Three-point correlator  $G'_3(x_1, x_2)$*

We now consider the second 3-point function,  $G'_3(x_1, x_2)$ , of Eq. (2.32). Its structure is much the same as for  $G_3(x_1, x_2)$  leading to the following expression

$$G'_3(x_1, x_2) = \frac{1 + \alpha/2(\gamma + 1 - \log 4\pi - s)}{J\sqrt{N^{J+3}}} \frac{N^{J+2}}{\sqrt{J_1 N^{J_1+2} N^{J_2+1}}} \\ \times \Delta(x_1)^{J_1+2} \Delta(x_2)^{J_2+1} (P - \lambda Q K(x_1, x_2)) \quad (2.51)$$

where  $P$  and  $Q$  are the phase factors to be determined shortly.

$P$  is the phase factor which we get by summing the contributions from the two free diagrams depicted in Figure 2.10.

Figure 2.10: Free diagrams for  $G_3$ . This diagram gives rise to  $P$ .

$$P = \sum_{a=1}^{J_1+1} \sum_{b=a+1}^{J_1+2} \sum_{c=J_1+3}^{J_1+3} \bar{q}_2^{b-a-1} \bar{q}_3^{c-a-2} + \sum_{a=1}^{J_1+1} \sum_{b=a+1}^{J_1+2} \sum_{c=J_1+3}^{J_1+3} \bar{q}_2^{J-(b-a-1)} \bar{q}_3^{c-b-1} \quad (2.52)$$

Converting the above sum into an integral one finds

$$\begin{aligned} P &= J^3 \int_0^{J_1/J} da \int_a^{J_1/J} db \int_{J_1/J}^1 dc e^{-2\pi i n_2(b-a)} e^{-2\pi i n_3(c-a)} \\ &+ J^3 \int_0^{J_1/J} da \int_a^{J_1/J} db \int_{J_1/J}^1 dc e^{-2\pi i n_2(-1)(b-a)} e^{-2\pi i n_3(c-b)} \\ &= J^3 \int_0^{J_1/J} da \int_0^{J_1/J} db \int_{J_1/J}^1 dc e^{-2\pi i n_2(b-a)} e^{-2\pi i n_3(c-a)} \end{aligned} \quad (2.53)$$

Evaluating the integral we finally arrive at

$$P = -J^3 \frac{\sin(\pi n_2 J_1/J) \sin(\pi n_3 J_1/J) \sin(\pi(n_3 + n_2) J_1/J)}{\pi^3 (n_3 + n_2) n_2 n_3}. \quad (2.54)$$

Now we have to account for the interacting diagrams. In the case where  $\phi_1$  takes part in the interaction we have four diagrams which are shown in Figure 2.11. The corresponding phase factor is

$$\begin{aligned} Q_1 &= \sum_{a=1}^{J_1+1} \sum_{b=J_1+4}^{J_1+3} -\bar{q}_2^{J-(J_1+3-a)} \bar{q}_3^{b-(J_1+3)} + \bar{q}_2^{J-(J_1+2-a)} \bar{q}_3^{b-(J_1+2)} \\ &+ \sum_{a=3}^{J_1+2} \sum_{b=J_1+3}^{J_1+2} \bar{q}_2^{a-3} \bar{q}_3^{b-4} - \bar{q}_2^{a-2} \bar{q}_3^{b-3}, \end{aligned} \quad (2.55)$$

which in the BMN limit is

$$\begin{aligned} Q_1 &= 2\pi i (n_2 + n_3) J (1 - e^{-2\pi i (n_3 + n_2)(-1) J_1/J}) \int_0^{J_1/J} da \int_{J_1/J}^1 db e^{-2\pi i n_2 a} e^{-2\pi i n_3 b} \\ &= -\frac{4}{\pi} J (n_3 + n_2)^2 \frac{\sin(\pi n_2 J_1/J) \sin(\pi n_3 J_1/J) \sin(\pi(n_3 + n_2) J_1/J)}{(n_3 + n_2) n_2 n_3} \end{aligned} \quad (2.56)$$

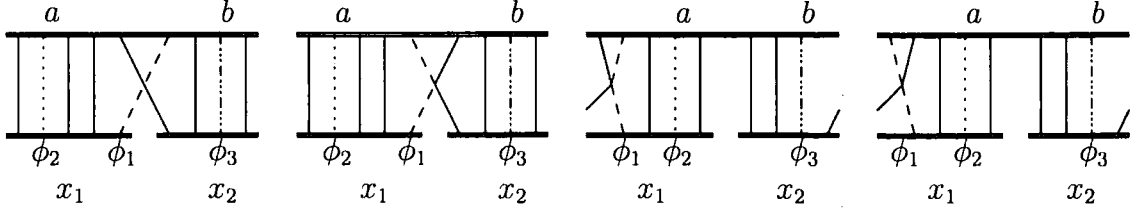


Figure 2.11: Interacting diagrams for  $G'_3$  contributing to  $Q_1$ . The  $\phi_1$  line is in the  $a^{\text{th}}$  position in the  $\bar{O}_{n_2, n_3}^J(0)$  trace and  $\phi_3$  is in the  $b^{\text{th}}$  position.

In the case where  $\phi_2$  takes part in the interaction we have again four diagrams which are shown in Figure 2.12. The corresponding phase factor is

$$\begin{aligned}
 Q_2 = & \sum_{a=1}^{J_1+1} \sum_{b=J_1+4}^{J+3} -\bar{q}_2^{J_1+2-a} \bar{q}_3^{b-a-2} + \bar{q}_2^{J_1+a} \bar{q}_3^{b-a-2} \\
 & + \sum_{a=3}^{J_1+2} \sum_{b=J_1+3}^{J+2} \bar{q}_2^{-(a-3)} \bar{q}_3^{b-a-1} - \bar{q}_2^{-(a-2)} \bar{q}_3^{b-a-1} , \quad (2.57)
 \end{aligned}$$

which in the BMN limit becomes

$$\begin{aligned}
 Q_2 = & -J^2 \frac{2\pi i n_2}{J} (1 - e^{-2\pi i n_2 J_1/J}) \int_0^{J_1/J} da \int_{J_1/J}^1 db e^{-2\pi i n_2(-a)} e^{-2\pi i n_3(b-a)} \\
 = & -\frac{4}{\pi} J n_2 \frac{\sin(\pi n_2 J_1/J) \sin(\pi n_3 J_1/J) \sin(\pi(n_3 + n_2) J_1/J)}{(n_3 + n_2) n_2 n_3} \quad (2.58)
 \end{aligned}$$

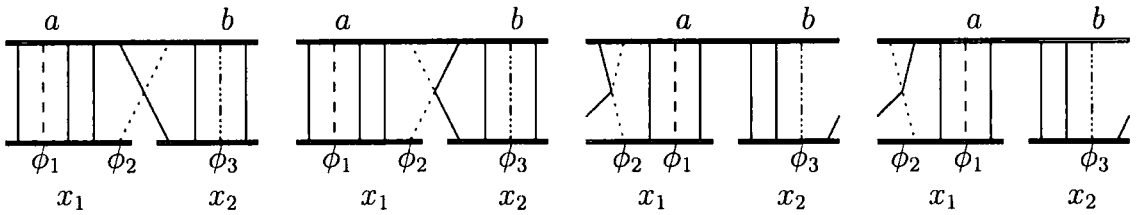


Figure 2.12: Interacting diagrams for  $G'_3$  contributing to  $Q_2$ .

For interacting  $\phi_3$  there are eight diagrams. The first four are depicted in Figure 2.13, and the other four are obtained by exchanging  $\phi_1$  with  $\phi_2$ . The phase factor associated with the four diagrams of Figure 2.13 in the BMN limit is

$$Q_3^{(1)} = J^2 \frac{2\pi i n_3}{J} (1 - e^{-2\pi i n_3 J_1/J}) \int_0^{J_1/J} da \int_a^{J_1/J} db e^{-2\pi i n_2(b-a)} e^{-2\pi i n_3(-a)} \quad (2.59)$$

The phase factor  $Q_3^{(2)}$  for the remaining four diagrams is obtained by exchanging  $n_1 \leftrightarrow n_2$  in  $Q_3^{(1)}$ . Adding the two we obtain

$$\begin{aligned} Q_3 &= Q_3^{(1)} + Q_3^{(2)} = 2\pi i n_3 J (1 - e^{-2\pi i n_3 J_1/J}) \int_0^{J_1/J} da \int_0^{J_1/J} db e^{-2\pi i n_2 (b-a)} e^{-2\pi i n_3 (-a)} \\ &= -\frac{4}{\pi} J n_3^2 \frac{\sin(\pi n_2 J_1/J) \sin(\pi n_3 J_1/J) \sin(\pi (n_3 + n_2) J_1/J)}{(n_3 + n_2) n_2 n_3} \quad (2.60) \end{aligned}$$

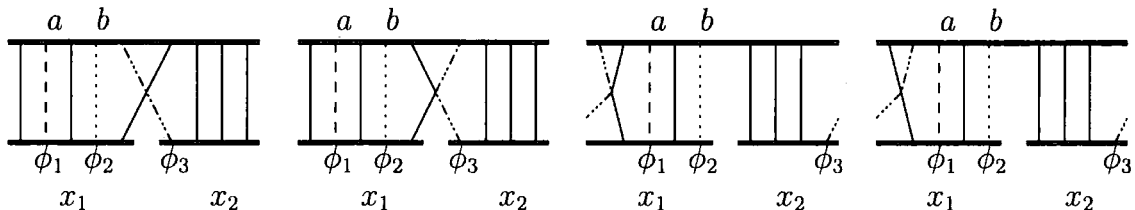


Figure 2.13: Interacting diagrams for  $G'_3$  contributing to  $Q_3$ . There are also diagrams with  $\phi_1$  and  $\phi_2$  exchanged.

Taking everything into account, our final expression for  $G'_3$  takes the conformal form

$$G'_3(x_1, x_2) = C'_{123} \Delta(x_1)^{J_1+2+\alpha/2} \Delta(x_2)^{J_2+1+\alpha/2} \Delta(x_{12})^{-\alpha/2} \quad (2.61)$$

with the 3-point coefficient

$$C'_{123} = -\frac{J^2}{\sqrt{J_1} N \pi^3} \frac{\sin(\pi n_2 J_1/J) \sin(\pi n_3 J_1/J) \sin(\pi (n_3 + n_2) J_1/J)}{(n_3 + n_2) n_2 n_3} (1 - \alpha/2) \quad (2.62)$$

This expression is again subtraction scheme independent. As in the case of  $G_3$  discussed earlier, we will set  $\alpha = 0$  on the right hand side of (2.62) to be safe from unknown mixing effects at order  $\lambda'$ .

### 2.3.2 Three-point functions with two string states

We are now ready to finally address the general case and calculate the 3-point coefficients of (2.26) and (2.27) for two non-chiral operators. Here the mixing of the known single-trace BMN operators with double-trace corrections is important as it does contribute to the conformal expression (2.2). However, our goal is not to derive

the conformal expression on the right hand side of (2.2) (which must be correct anyway, as far as the mixing effects are such that we are dealing with scalar conformal primary operators). Our goal is to calculate the coefficient  $C_{123}$ . At leading order, the only mixing effect which contributes to the right hand side of (2.2) is the mixing with the double-traces of the barred operator  $\bar{\mathcal{O}}_{n_1 n_2 n_3}^J(0)$  in (2.26) and (2.27). These mixing effects will affect the free-theory contribution  $C_{123}^{\text{free}}$  and also the logarithmic terms  $\lambda' \log|x_1|$  and  $\lambda' \log|x_2|$  due to interactions of the double-trace in  $\bar{\mathcal{O}}_{n_1 n_2 n_3}^J(0)$  with the BMN operators at  $x_1$  and  $x_2$ . But, these mixing effects cannot affect the third logarithm,  $\lambda' \log|x_1 - x_2|$ . Hence our programme is to assume the conformal form, and by carefully evaluating the terms proportional to  $\lambda' \log|x_1 - x_2|$ , to determine  $C_{123}$ . In doing so we can neglect the double-trace corrections and work with the original single-trace expressions.

We start with

$$G_3(x_1, x_2) = \langle \bar{\mathcal{O}}_{n_1 n_2 n_3}^J(0) \mathcal{O}_{n'_1 n'_2 n'_3}^{J_1}(x_1) \mathcal{O}_{\text{vac}}^{J_2}(x_2) \rangle . \quad (2.63)$$

The calculation is done as in the previous subsection, except that now we have additional phase factors coming from non-zero  $n'_2$  and  $n'_3$ . The result for phase factor  $X$  coming from the free diagrams of Figure 2.5 is obtained from (2.39) by substituting  $n_2 - n'_2/y$  for  $n_2$  and  $n_3 - n'_3/y$  for  $n_3$  where  $y = J_1/J$ . The final result is

$$X = J^3 2^3 \frac{\sin(\pi n_2 y) \sin(\pi n_3 y) \sin(\pi(n_2 + n_3)y)}{(2\pi)^3 (n_2 + n_3 - \frac{n'_3 + n'_2}{y})(n_2 - \frac{n'_2}{y})(n_3 - \frac{n'_3}{y})} . \quad (2.64)$$

To simplify notation somewhat, we will define

$$\Pi := \frac{\sin(\pi n_2 y) \sin(\pi n_3 y) \sin(\pi(n_2 + n_3)y)}{(n_2 + n_3 - \frac{n'_3 + n'_2}{y})(n_2 - \frac{n'_2}{y})(n_3 - \frac{n'_3}{y})} . \quad (2.65)$$

Next we evaluate the interacting diagrams of Figure 2.6,

$$\begin{aligned}
Y_{123} &= \sum_{a=1}^{J_1+1} \sum_{b=a+1}^{J_1+2} [-\bar{q}_2^{J-(J_1+3-a-1)} \bar{q}_3^{J-(J_1+3-b)} + \bar{q}_2^{J-(J_1+3-a-2)} \bar{q}_3^{J-(J_1+3-b-1)}] r_2^{a-1} r_3^{b-2} \\
&\quad + \sum_{a=3}^{J_1+2} \sum_{b=a+1}^{J_1+3} [\bar{q}_2^{a-3} \bar{q}_3^{b-4} - \bar{q}_2^{a-2} \bar{q}_3^{b-3}] r_2^{a-3} r_3^{b-4} = \\
&\quad \sum_{a=1}^{J_1+1} \sum_{b=a+1}^{J_1+2} \bar{q}_2^{-(J_1-a+1)} \bar{q}_3^{-(J_1-b+2)} r_2^{a-1} r_3^{b-2} (1 - \bar{q}_2^{-1} \bar{q}_3^{-1}) \\
&\quad + \sum_{a=3}^{J_1+2} \sum_{b=a+1}^{J_1+3} \bar{q}_2^{a-3} \bar{q}_3^{b-4} r_2^{a-3} r_3^{b-4} (1 - \bar{q}_2 \bar{q}_3) \\
&\rightarrow \frac{2\pi i(n_2 + n_3)}{J} \left[ \sum_{a=3}^{J_1+2} \sum_{b=a+1}^{J_1+3} (\bar{q}_2 r_2)^{a-3} (\bar{q}_3 r_3)^{b-4} - \sum_{a=1}^{J_1+1} \sum_{b=a+1}^{J_1+2} (\bar{q}_2 r_2)^{a-1} (\bar{q}_3 r_3)^{b-2} \bar{q}_2^{-J_1} \bar{q}_3^{-J_1} \right] \quad (2.66)
\end{aligned}$$

Converting the last sum into an integral we obtain,

$$\begin{aligned}
Y_{123} &= 2\pi i(n_2 + n_3) J \int_0^y da \int_a^y db e^{-2\pi i(n_2 - \frac{n'_2}{y})a} e^{-2\pi i(n_3 - \frac{n'_3}{y})b} [1 - e^{2\pi i(n_3 + n_2)y}] \\
&= 2\pi i J(n_2 + n_3) [1 - e^{2\pi i(n_3 + n_2)y}] \frac{e^{(A_3 + A_2)y} A_3 - e^{A_3 y} A_2 - e^{A_3 y} A_3 + A_2}{(A_3 + A_2) A_3 A_2}
\end{aligned}$$

where  $A_2 = -2\pi i(n_2 - \frac{n'_2}{y})$ ,  $A_3 = -2\pi i(n_3 - \frac{n'_3}{y})$ ,  $r_2 = e^{2\pi i n'_2 / J_1}$  and  $r_3 = e^{2\pi i n'_3 / J_1}$ .

Expression for  $Y_{132}$  is obtained by interchanging  $A_2$  and  $A_3$  in  $Y_{123}$ . After some algebra we get

$$Y_{123} + Y_{132} = \frac{4(n_3 + n_2)(n_3 + n_2 - \frac{n'_2 + n'_3}{y}) J}{\pi} \Pi \quad (2.67)$$

Similarly, for diagrams of Figure 2.7 we obtain (in the BMN limit)

$$\begin{aligned}
Y_{231} &= 2\pi i n_2 J \int_0^y da \int_0^y db e^{2\pi i(n_2 - \frac{n'_2}{y})b} e^{2\pi i(n_3 - \frac{n'_3}{y})(b-a)} [1 - e^{-2\pi i n_2 y}] \\
&= 2\pi i n_2 J [1 - e^{-2\pi i n_2 y}] \frac{e^{-A_2 y} A_2 + e^{-A_2 y} A_3 - e^{-(A_3 + A_2)y} A_2 - A_3}{(A_3 + A_2) A_3 A_2} \quad (2.68)
\end{aligned}$$

Now consider the above diagrams with  $\phi_1$  and  $\phi_3$  exchanged. In the BMN limit we find

$$\begin{aligned}
Y_{213} &= -2\pi i n_2 J \int_0^y da \int_0^y db e^{-2\pi i(n_2 - \frac{n'_2}{y})(-a)} e^{-2\pi i(n_3 - \frac{n'_3}{y})(b-a)} [1 - e^{-2\pi i n_2 y}] \\
&= -2\pi i n_2 J [1 - e^{-2\pi i n_2 y}] \frac{e^{-A_2 y} A_3 + e^{A_3 y} A_2 - A_2 - A_3}{(A_3 + A_2) A_3 A_2} \quad (2.69)
\end{aligned}$$

Summing the two we arrive at

$$Y_{231} + Y_{213} = \frac{4n_2(n_2 - \frac{n'_2}{y})J}{\pi} \Pi . \quad (2.70)$$

Similarly for the diagrams of Figure 2.8 we get:

$$Y_{312} + Y_{321} = \frac{4n_3(n_3 - \frac{n'_3}{y})J}{\pi} \Pi . \quad (2.71)$$

Using the above phase factors and concentrating on the logarithmic terms of the 3-point function we have

$$G_3(x_1, x_2) = C_{123}^{(0)} \Delta(x_1)^{J_1+3} \Delta(x_2)^{J_2} [1 - \frac{\lambda'}{4}(n_2(n_2 - \frac{n'_2}{y}) + n_3(n_3 - \frac{n'_3}{y}) + (n_3 + n_2)(n_3 + n_2 - \frac{n'_2 + n'_3}{y})) \log \frac{x_1^2 x_2^2}{x_{12}^2} + C' \log x_1^2 + \dots] \quad (2.72)$$

The last term in the equation above comes from the diagrams of Figure 2.9 which no longer sum to zero as in the case with two supergravity states. However we do not need to know the coefficient of this term since the  $\log x_1^2$  receives corrections from the double-trace operators. From the equation above one can easily read the coefficient  $C_{123}$  at order  $g_2$

$$C_{123} = C_{123}^{(0)} \frac{n_2(n_2 - \frac{n'_2}{y}) + n_3(n_3 - \frac{n'_3}{y}) + (n_3 + n_2)(n_3 + n_2 - \frac{n'_2 + n'_3}{y})}{n_2^2 + n_3^2 + (n_2 + n_3)^2 - \frac{n_2'^2 + n_3'^2 + (n_2' + n_3')^2}{y^2}} \quad (2.73)$$

where

$$C_{123}^{(0)} = \frac{J\sqrt{J}\sqrt{1-y} \sin(\pi n_2 y) \sin(\pi n_3 y) \sin(\pi(n_2 + n_3)y)}{Ny\pi^3 (n_2 + n_3 - \frac{n'_2 + n'_3}{y})(n_2 - \frac{n'_2}{y})(n_3 - \frac{n'_3}{y})} \quad (2.74)$$

*Three-point correlator  $G'_3(x_1, x_2)$*

Finally we consider the  $G'_3$  function with two string states

$$G'_3(x_1, x_2) = \langle \bar{\mathcal{O}}_{n_1 n_2 n_3}^J(0) \mathcal{O}_{n'_2 - n'_2}^{J_1}(x_1) \mathcal{O}_0^{J_2}(x_2) \rangle \quad (2.75)$$

Similarly to the earlier analysis, we determine  $P$  from free diagrams in Figure 2.10,

$$P = -\frac{J^3 \sin(\pi n_2 y) \sin(\pi n_3 y) \sin(\pi(n_3 + n_2)y)}{\pi^3 (n_3 + n_2 - \frac{n'_2}{y})(n_2 - \frac{n'_2}{y})n_3} \quad (2.76)$$

The diagrams of Figure 2.11, Figure 2.12 and Figure 2.13 lead to the expressions for  $Q_1$ ,  $Q_2$  and  $Q_3$  respectively

$$Q_1 = -\frac{4}{\pi} J(n_3 + n_2)(n_3 + n_2 - \frac{n'_2}{y}) \frac{\sin(\pi n_2 y) \sin(\pi n_3 y) \sin(\pi(n_3 + n_2)y)}{(n_3 + n_2 - \frac{n'_2}{y})(n_2 - \frac{n'_2}{y})n_3} \quad (2.77)$$

$$Q_2 = -\frac{4}{\pi} J n_2 \left( n_2 - \frac{n'_2}{y} \right) \frac{\sin(\pi n_2 y) \sin(\pi n_3 y) \sin(\pi(n_3 + n_2)y)}{(n_3 + n_2 - \frac{n'_2}{y})(n_2 - \frac{n'_2}{y})n_3} \quad (2.78)$$

$$Q_3 = -\frac{4}{\pi} J n_3^2 \frac{\sin(\pi n_2 y) \sin(\pi n_3 y) \sin(\pi(n_3 + n_2)y)}{(n_3 + n_2 - \frac{n'_2}{y})(n_2 - \frac{n'_2}{y})n_3} \quad (2.79)$$

Using the above results the three-point function reads

$$G'_3(x_1, x_2) = \tilde{C}_{123}^{(0)} \Delta(x_1)^{J_1+2} \Delta(x_2)^{J_2+1} \left[ 1 - \frac{\lambda'}{4} (n_3^2 + n_2(n_2 - \frac{n'_2}{y})) \right. \\ \left. + (n_3 + n_2)(n_3 + n_2 - \frac{n'_2}{y}) \log \frac{x_1^2 x_2^2}{x_{12}^2} + C' \log x_1^2 + C'' \log x_2^2 + \dots \right] \quad (2.80)$$

where

$$\tilde{C}_{123}^{(0)} = -\frac{J\sqrt{J}}{\sqrt{y}N\pi^3} \frac{\sin(\pi n_2 y) \sin(\pi n_3 y) \sin(\pi(n_3 + n_2)y)}{(n_3 + n_2 - \frac{n'_2}{y})(n_2 - \frac{n'_2}{y})n_3} \quad (2.81)$$

And our final expression for  $\tilde{C}_{123}$  is

$$\tilde{C}_{123} = \tilde{C}_{123}^{(0)} \frac{n_3^2 + n_2(n_2 - \frac{n'_2}{y}) + (n_3 + n_2)(n_3 + n_2 - \frac{n'_2}{y})}{n_2^2 + n_3^2 + (n_2 + n_3)^2 - \frac{2n_2^2}{x^2}} \quad (2.82)$$

## 2.4 Tests of the correspondence

In this section we test the correspondence proposed in [101] and outlined in Section 2.1 against the gauge theory results of Section 2.3.

### 2.4.1 $1_{-(n'_2+n'_3)} 2_{n'_2} 3_{n'_3} + vac \rightarrow 1_{-(n_2+n_3)} 2_{n_2} 3_{n_3}$

In this case the external string state is

$$\langle \Phi | = \langle 0 | \alpha_{-(n_2+n_3)}^{3i_1} \alpha_{n_2}^{3i_2} \alpha_{n_3}^{3i_3} \alpha_{-(n'_2+n'_3)}^{1i_1} \alpha_{n'_2}^{1i_2} \alpha_{n'_3}^{1i_3} \quad (2.83)$$

In the expression above, 1 and 3 denote the first and the third string in the vertex. In order to avoid confusion, and distinguish from the indices corresponding to scalar impurities,  $\phi_1, \phi_2, \phi_3$ , we label the latter with  $i_1, i_2, i_3$ . Since all three SYM impurities are different, we note that  $i_1 \neq i_2 \neq i_3$  and the repeated indices in the external states are not summed over.

The contribution of the first part of the prefactor  $P_I$  is

$$\langle \Phi | P_I | V_B \rangle = \frac{1}{2\mu} \left[ \frac{n_2'^2 + n_3'^2 + (n_2' + n_3')^2}{y^2} - n_2^2 - n_3^2 - (n_2 + n_3)^2 \right] \\ \times \hat{N}_{n_2, n'_2}^{31} \hat{N}_{n_3, n'_3}^{31} \hat{N}_{n_2+n_3, n'_2+n'_3}^{31} \quad (2.84)$$

which, using the expression for the Neumann matrices (see Appendix A ),

$$\hat{N}_{mn}^{31} = \hat{N}_{-m-n}^{31} = \frac{(-1)^{m+n+1}}{\pi} \frac{\sin(\pi my)}{\sqrt{y}(m-n/y)} + \mathcal{O}\left(\frac{1}{\mu^2}\right), \quad (2.85)$$

becomes

$$\langle \Phi | P_I | V_B \rangle = -\frac{1}{2\mu y^{3/2} \pi^3} \left[ \frac{n_2'^2 + n_3'^2 + (n_2' + n_3')^2}{y^2} - n_2^2 - n_3^2 - (n_2 + n_3)^2 \right] \Pi \quad (2.86)$$

Now consider  $P_{II}$ . The contributing terms in  $P_{II}$  for the state under consideration are

$$\begin{aligned} P_{II} = & \frac{1}{2} \left[ \left( \frac{\omega_{3n_2}}{\alpha_3} + \frac{\omega_{1n_2'}}{\alpha_1} \right) (\hat{N}_{n_2, -n_2'}^{31} - \hat{N}_{n_2, n_2'}^{31}) \alpha_{n_2}^{3i_2 \dagger} \alpha_{n_2'}^{1i_2 \dagger} \right. \\ & + \left( \frac{\omega_{3n_3}}{\alpha_3} + \frac{\omega_{1n_3'}}{\alpha_1} \right) (\hat{N}_{n_3, -n_3'}^{31} - \hat{N}_{n_3, n_3'}^{31}) \alpha_{n_3}^{3i_3 \dagger} \alpha_{n_3'}^{1i_3 \dagger} \\ & \left. + \left( \frac{\omega_{3n_1}}{\alpha_3} + \frac{\omega_{1n_1'}}{\alpha_1} \right) (\hat{N}_{-n_1, n_1'}^{31} - \hat{N}_{-n_1, -n_1'}^{31}) \alpha_{n_1}^{3i_1 \dagger} \alpha_{n_1'}^{1i_1 \dagger} \right] \end{aligned} \quad (2.87)$$

Using this we find

$$\begin{aligned} \langle \Phi | P_{II} | V_B \rangle = & -\frac{1}{4\mu} \left[ \left( n_2^2 - \frac{n_2'^2}{y^2} \right) N_{-n_2, -n_2'}^{31} \hat{N}_{n_3, n_3'}^{31} \hat{N}_{-n_1, -n_1'}^{31} \right. \\ & + \left( n_3^2 - \frac{n_3'^2}{y^2} \right) N_{-n_3, -n_3'}^{31} \hat{N}_{n_2, n_2'}^{31} \hat{N}_{-n_1, -n_1'}^{31} \\ & \left. + \left( n_1^2 - \frac{n_1'^2}{y^2} \right) N_{n_1, n_1'}^{31} \hat{N}_{n_3, n_3'}^{31} \hat{N}_{n_2, n_2'}^{31} \right] \end{aligned} \quad (2.88)$$

Recalling that  $n_1 = -(n_2 + n_3)$  and  $n_1' = -(n_2' + n_3')$  and substituting into the above result the expressions (2.85) for the Neumann matrices  $\hat{N}$  and expressions for the Neumann matrices  $N_{-, -}$  (see Appendix A)

$$N_{-m-n}^{31} = \frac{2(-1)^{m+n}}{\pi} \frac{n \sin(\pi my)}{y^{3/2}(m^2 - n^2/y^2)} + \mathcal{O}\left(\frac{1}{\mu^2}\right), \quad (2.89)$$

we obtain

$$\langle \Phi | P_{II} \hat{V} | 0 \rangle = -\frac{1}{2\mu \pi^3 y^{5/2}} \left[ n_2'(n_2 - \frac{n_2'}{y}) + n_3'(n_3 - \frac{n_3'}{y}) + n_1'(n_1 - \frac{n_1'}{y}) \right] \Pi \quad (2.90)$$

Adding these results for  $P_I$  and  $P_{II}$  and multiplying by  $(-1)^p C_{norm} = -g_2 \frac{\sqrt{y(1-y)}}{\sqrt{J}}$

we get the string theory answer

$$-\frac{g_2 \sqrt{1-y}}{2\mu \pi^3 \sqrt{J} y} \left[ n_2(n_2 - \frac{n_2'}{y}) + n_3(n_3 - \frac{n_3'}{y}) + (n_3 + n_2)(n_3 + n_2 - \frac{n_2' + n_3'}{y}) \right] \Pi \quad (2.91)$$

which is *exactly the SYM result*,  $\mu(\Delta_1 + \Delta_2 - \Delta_3)C_{123}$ , since

$$\mu(\Delta_1 + \Delta_2 - \Delta_3) = \frac{1}{2\mu} \left[ \frac{n_2'^2 + n_3'^2 + (n_2' + n_3')^2}{y^2} - n_2^2 - n_3^2 - (n_2 + n_3)^2 \right] \quad (2.92)$$

and  $C_{123}$ , given by (2.73), (2.74), reads

$$C_{123} = \frac{J\sqrt{J}\sqrt{1-y}}{Ny\pi^3} \frac{n_2(n_2 - \frac{n_2'}{y}) + n_3(n_3 - \frac{n_3'}{y}) + (n_3 + n_2)(n_3 + n_2 - \frac{n_2' + n_3'}{y})}{n_2^2 + n_3^2 + (n_2 + n_3)^2 - \frac{n_2'^2 + n_3'^2 + (n_2' + n_3')^2}{y^2}} \Pi. \quad (2.93)$$

### 2.4.2 $1_{n_2'} 2_{-(n_2' + n_3')} 3_{n_3'} + vac \rightarrow 1_{-(n_2 + n_3)} 2_{n_2} 3_{n_3}$

In this case the external string state is

$$\langle \Phi | = \langle 0 | \alpha_{-(n_2 + n_3)}^{3i_1} \alpha_{n_2}^{3i_2} \alpha_{n_3}^{3i_3} \alpha_{n_2'}^{1i_1} \alpha_{-(n_2' + n_3')}^{1i_2} \alpha_{n_3'}^{1i_3} \quad (2.94)$$

and the operator  $\mathcal{O}_1(x_1)$  is

$$\mathcal{O}_1(x_1) = \frac{1}{J\sqrt{N^{J+3}}} \sum_{0 \leq a, b}^{a+b \leq J} [r_2^a r_3^{a+b} \text{tr}(\phi_2 Z^a \phi_1 Z^b \phi_3 Z^{J-a-b}) + r_3^a r_2^{a+b} \text{tr}(\phi_2 Z^a \phi_3 Z^b \phi_1 Z^{J-a-b})] \quad (2.95)$$

Using the cyclic property of the trace,  $\mathcal{O}_1(x_1)$  can also be written as

$$\mathcal{O}_1(x_1) = \frac{1}{J\sqrt{N^{J+3}}} \sum_{0 \leq a, b}^{a+b \leq J} [\tilde{r}_2^a \tilde{r}_3^{a+b} \text{tr}(\phi_1 Z^a \phi_2 Z^b \phi_3 Z^{J-a-b}) + \tilde{r}_3^a \tilde{r}_2^{a+b} \text{tr}(\phi_1 Z^a \phi_3 Z^b \phi_2 Z^{J-a-b})] \quad (2.96)$$

where  $\tilde{r}_2 = (r_2 r_3)^{-1}$  and  $\tilde{r}_3 = r_3$ . Hence, we find the 3-point function for this process by substituting  $n_2' \rightarrow -(n_2' + n_3')$ ,  $n_3' \rightarrow n_3'$  and  $-(n_2' + n_3') = n_1 \rightarrow n_2'$  into the SYM expression (2.93) and also to (2.92).

Thus, the result on the gauge theory side for this process is

$$\begin{aligned} \mu(\Delta_1 + \Delta_2 - \Delta_3)C_{123} = & -\frac{g_2}{2\mu} \frac{\sqrt{1-y} \sin(\pi n_2 y) \sin(\pi n_3 y) \sin(\pi(n_2 + n_3)y)}{\pi^3 \sqrt{J} y (n_2 + \frac{n_2' + n_3'}{y})(n_3 - \frac{n_3'}{y})(n_2 + n_3 + \frac{n_2'}{y})} \\ & \times \left[ n_2(n_2 + \frac{n_2' + n_3'}{y}) + n_3(n_3 - \frac{n_3'}{y}) + (n_2 + n_3)(n_2 + n_3 + \frac{n_2'}{y}) \right] \quad (2.97) \end{aligned}$$

On the string theory side of the correspondence the calculation follows the same lines as in 2.4.1, and the result is in precise agreement with the SYM formula (2.97).

This is also true for the remaining four cases involving different permutations of the three  $\phi$ 's in the trace of the shortest BMN operator.

### 2.4.3 $1_{-n'_2}2_{n'_2} + 3_0 \rightarrow 1_{-(n_2+n_3)}2_{n_2}3_{n_3}$

Here we consider the case which corresponds to  $G'_3$ , i.e. where instead of the vacuum state for the string 2, we have a supergravity state. The external string state now is

$$\langle \Phi | = \langle 0 | \alpha_{-(n_2+n_3)}^{3i_1} \alpha_{n_2}^{3i_2} \alpha_{n_3}^{3i_3} \alpha_{-n'_2}^{1i_1} \alpha_{+n'_2}^{1i_2} \alpha_0^{2i_3} \quad (2.98)$$

The result in the SYM side can be obtained from (2.82) and (2.81) and is

$$\begin{aligned} \mu(\Delta_1 + \Delta_2 - \Delta_3) \tilde{C}_{123} = & \frac{1}{2\mu} \frac{J\sqrt{J}}{\sqrt{y}N\pi^3} \frac{\sin(\pi n_2 y) \sin(\pi n_3 y) \sin(\pi(n_3 + n_2)y)}{(n_3 + n_2 - \frac{n'_2}{y})(n_2 - \frac{n'_2}{y})n_3} \\ & (n_3^2 + n_2(n_2 - \frac{n'_2}{y}) + (n_3 + n_2)(n_3 + n_2 - \frac{n'_2}{y})). \quad (2.99) \end{aligned}$$

This expression is again, as it is easy to check using the Neumann matrices from the Appendix A, in precise agreement with the expression on the string theory side of the duality relation (2.4).

### 2.4.4 $1_{n'_2}2_{-n'_2} + 3_0 \rightarrow 1_{-(n_2+n_3)}2_{n_2}3_{n_3}$

As a final example we consider the case where the external string state is

$$\langle \Phi | = \langle 0 | \alpha_{-(n_2+n_3)}^{3i_1} \alpha_{n_2}^{3i_2} \alpha_{n_3}^{3i_3} \alpha_{n'_2}^{1i_1} \alpha_{-n'_2}^{1i_2} \alpha_0^{2i_3} \quad (2.100)$$

The result on the SYM side is given by

$$\begin{aligned} \mu(\Delta_1 + \Delta_2 - \Delta_3) \tilde{C}_{123} = & \frac{1}{2\mu} \frac{J\sqrt{J}}{\sqrt{y}N\pi^3} \frac{\sin(\pi n_2 y) \sin(\pi n_3 y) \sin(\pi(n_3 + n_2)y)}{(n_3 + n_2 + \frac{n'_2}{y})(n_2 + \frac{n'_2}{y})n_3} \\ & (n_3^2 + n_2(n_2 + \frac{n'_2}{y}) + (n_3 + n_2)(n_3 + n_2 + \frac{n'_2}{y})) \quad (2.101) \end{aligned}$$

which is in precise agreement with the string vertex–correlator duality prediction (2.4).

In this chapter, we have found compelling agreement between the three string amplitudes on the pp-wave background and the corresponding three-point function coefficients calculated in field theory. Although the prefactor (2.9) of the string vertex is in a sense "phenomenological" a coincidental agreement between field theory and string theory is highly unlikely. We will comment on the relation of this string field theory vertex with the holographic one obtained by Dobashi and Yoneya in the concluding chapter of this thesis.

# Chapter 3

## Tests of the Extended BMN

### Correspondence and the role of $\mathbb{Z}_2$

### Symmetry

In this chapter, we examine the BMN correspondence as extended in [44, 45] by studying BMN operators with scalar, vector and mixed impurities. We also clarify the role of the  $\mathbb{Z}_2$  symmetry of the pp-wave background and its realisation on the gauge theory side.

The correspondence is now expressed in the form of equation (1.137). Since the two Hamiltonians,  $H_{\text{string}}$  and  $\Delta$ , act on the states of two different theories, the duality relation (1.137) requires an isomorphism between the Hilbert spaces of the light-cone gauge pp-wave string field theory and of the BMN sector of the  $\mathcal{N} = 4$  gauge theory. More specifically, we need to establish a one-to-one correspondence between the bases of two theories,  $\{|s_\alpha\rangle^{\text{string}}\}$  and  $\{|s_\alpha\rangle^{\text{SYM}}\}$ ,

$$|s_\alpha\rangle^{\text{string}} \leftrightarrow |s_\alpha\rangle^{\text{SYM}} , \quad (3.1)$$

which preserves the scalar product,

$$\text{string}\langle s_\alpha | s_\beta \rangle^{\text{string}} = \text{SYM}\langle s_\alpha | s_\beta \rangle^{\text{SYM}} . \quad (3.2)$$

Then the correspondence (1.137) holds at the matrix elements level,

$$\text{string}\langle s_\alpha | \mu^{-1} H_{\text{string}} | s_\beta \rangle^{\text{string}} = \text{SYM}\langle s_\alpha | \Delta - J | s_\beta \rangle^{\text{SYM}} . \quad (3.3)$$

The string field theory Hilbert space is equipped with a natural basis of multi-string states,

$$\{|s_\alpha\rangle^{\text{string}}\} = |\text{string}_a\rangle, |\text{string}_b\rangle \otimes |\text{string}_c\rangle, |\text{string}_d\rangle \otimes |\text{string}_e\rangle \otimes |\text{string}_f\rangle, \dots \quad (3.4)$$

which diagonalises the free string Hamiltonian and is automatically orthonormal. Here  $a, b, \dots$  are the labels of single-string states. This basis does not diagonalise the full string Hamiltonian,  $H_{\text{string}}$ , since free string states in (3.4) can interact (split and join). The splitting and joining of a single string state is described by the three-string interaction, and the corresponding matrix element on the left hand side of (3.3) is

$$\langle \text{string}_a | H_{\text{string}}^{\text{int}} | \text{string}_b \rangle \otimes | \text{string}_c \rangle \equiv \langle \text{string}_a | \langle \text{string}_b | \langle \text{string}_c | H_3 \rangle . \quad (3.5)$$

Here  $|H_3\rangle$  is the three-string interaction vertex in the light-cone string field theory in the pp-wave background. It was originally obtained by Spradlin and Volovich [52, 53]. Its expression is recalled in Appendix B.<sup>1</sup> However, there is a puzzle related to the three-string amplitudes (3.5) built on the Spradlin-Volovich vertex which we would like to clarify in this chapter, among other things. As discussed in chapter 1, the presence of a non-trivial R–R field in the pp-wave background breaks the light-cone Lorentz symmetry  $SO(8)$  down to  $SO(4) \times SO(4) \times \mathbb{Z}_2$ . Apparently, the  $\mathbb{Z}_2$  part of the bosonic symmetry of the pp-wave background is not respected by the Spradlin-Volovich three-string interactions [53, 56–59]: there is a relative minus sign in the string amplitude involving states with two oscillators along the first  $SO(4)$  compared to that with two oscillators along the second  $SO(4)$ . An unbroken  $\mathbb{Z}_2$ -invariance would not allow this to happen. We will argue now that this minus sign implies a spontaneous breaking of the  $\mathbb{Z}_2$  symmetry of the string field theory in the pp-wave background.

The ket-vertex  $|H_3\rangle$  (B.1), (B.2) of [52, 53] is built on the string state  $|0\rangle$  which is the ground state of the theory in flat background, but not in the pp-wave background. At the same time, the external string bra-states in (3.5) are built on the true pp-wave ground state  $|v\rangle$ . It was explained in [58] that these two states,  $|0\rangle$  and  $|v\rangle$ ,

---

<sup>1</sup>For notational simplicity and in order to distinguish this vertex from other proposals, we will sometimes refer to the vertex of [52–55] simply as the Spradlin-Volovich vertex.

have an opposite  $\mathbb{Z}_2$  parity, i.e. cannot be both invariant under  $\mathbb{Z}_2$ . Hence, it follows immediately [53, 58] that the amplitude (3.5) is not invariant under the action of  $\mathbb{Z}_2$ , but changes sign. In the recent paper [65], the result of [52, 53], which utilised the vacuum  $|0\rangle$ , was compared with an alternative formalism of constructing  $|H_3\rangle$  starting directly from the true ground-state  $|v\rangle$ . The two formalisms were found to be identical [66]. Following [52, 53, 65] we choose the  $\mathbb{Z}_2$ -parity prescription

$$\mathbb{Z}_2 : |0\rangle \rightarrow |0\rangle , \quad \mathbb{Z}_2 : |v\rangle \rightarrow -|v\rangle . \quad (3.6)$$

This means that the vertex  $|H_3\rangle$  built on  $|0\rangle$  is invariant under  $\mathbb{Z}_2$ , but the pp-wave string ground-state  $\langle v|$  and, hence, the external states  $\langle \text{string}_a | \langle \text{string}_b | \langle \text{string}_c |$  in (3.5), acquire a minus sign. This implies a spontaneous breaking of the  $\mathbb{Z}_2$  symmetry of the string field theory in the pp-wave background, which is the physical reason for the minus sign of the matrix element discussed above.

One of the objectives of this chapter is to verify with an independent gauge theory calculation this important minus sign (and hence the spontaneous breaking of  $\mathbb{Z}_2$ ), as well as the related fact that the three-string amplitude (3.5) vanishes for string states with one direction along the first, and one one direction along the second  $SO(4)$ , i.e. one vector and one scalar impurity in the gauge theory language.

As already mentioned, and following [45, 48, 61], in order to compare (3.5) with matrix elements of the dilatation operator in gauge theory via (3.3), it is important to identify a basis in gauge theory which is isomorphic to the natural string basis (3.4). We discuss this issue in section 3.1. States in the isomorphic to string basis,  $\{|s_\alpha\rangle^{\text{SYM}}\}$ , are obtained from linear combinations of the original multi-trace BMN [41] operators  $\mathcal{O}_\alpha(x)$ ,

$$|s_\alpha\rangle^{\text{SYM}} = U_{\alpha\beta} \mathcal{O}_\beta(x=0)|0\rangle , \quad (3.7)$$

where  $U_{\alpha\beta}$  is an  $x$ -independent matrix. This matrix was determined in [45, 48] by requiring that (3.3) holds, i.e. that the known three-string interaction vertex of the pp-wave light-cone string field theory [52, 53] is reproduced from gauge theory matrix elements of the dilatation operator involving BMN states (operators) with two scalar impurities.

In this chapter we will take  $U_{\alpha\beta}$  determined in [48], and use it to construct the

gauge theory basis (3.7) for an arbitrary number of scalar impurities. With this in hand we can compute generic gauge theory matrix elements on the right hand side of (3.3). The contributions on the left hand side of (3.3) are then computed using (3.5). We will verify (3.3) and hence the Spradlin-Volovich expression for  $|H_3\rangle$  for *generic* bosonic impurities. First successful steps in this direction have been already taken in [48, 49] at the level of arbitrary number of identical scalar impurities.<sup>2</sup> However, the inclusion of vector impurities is essential in order to address in the gauge theory the two important properties of the three-string interaction discussed earlier:

- (1) the vanishing of the three-string amplitude for string states with one vector and one scalar impurity; and
- (2) the relative minus sign in the string amplitude involving states with two vector impurities compared to that with two scalar impurities.

In section 3.1 we describe the isomorphism between the BMN basis in SYM and the natural string basis in the dual string theory. In section 3.2 we will verify (1) and (2) working at the two-impurity level, and will consider all representations of BMN operators with two vector or scalar impurities, i.e. symmetric traceless, antisymmetric and singlet. By considering BMN operators with vector, scalar and mixed (scalar+vector) impurities we explore and verify the correspondence (3.3) for string states in all the directions of the two  $SO(4)$  groups.

In section 3.4, we will calculate the gauge theory matrix elements of  $\Delta - J$  for states with an arbitrary number of scalar impurities. Next we compute the corresponding three-string amplitudes derived from the three-string vertex and compare them to the field theory result, finding perfect agreement.

Finally, sections 3.3 and 3.5 are dedicated to computations of three-point correlators of BMN operators. These results are used earlier in sections 3.2 and 3.4 for the calculation of matrix elements. More specifically, in section 3.3 we compute the coefficient of the conformal three-point function of BMN operators with mixed (one scalar and one vector) impurities. In section 3.5 we generalise this analysis to the case of BMN operators with an arbitrary number of scalar impurities.

---

<sup>2</sup>For further tests of the correspondence in the open-closed string sector, see [67].

### 3.1 The dilatation operator in SYM and the natural string basis

As mentioned earlier, the BMN basis in SYM which is isomorphic to the natural string basis in dual string field theory, is a certain linear combination (3.7) of the original BMN operators  $\mathcal{O}_\alpha(x)$  proposed in [41]. The states in the natural string basis are not identically equal to the original BMN operators since the former are automatically orthonormal, while the latter are not, and their overlaps depend on the string coupling  $g_2$ . In other words, the matrix  $U$  in (3.7) is not simply the identity matrix.

Apart from the original BMN basis, there is another distinguished basis of the conformal primary BMN operators  $\mathcal{O}_{\Delta_\alpha}(x)$  which are the eigenstates of the dilatation operator  $\Delta$  in gauge theory. This  $\Delta$ -BMN basis is again a linear combination of the states from the original BMN basis  $\mathcal{O}_\alpha(x)$  with a different  $x$ -independent matrix  $U$ . For BMN operators with scalar impurities, this basis was constructed in [73] and extended to include vector and mixed impurities in [62]. The  $\Delta$ -BMN basis is particularly convenient since the two- and three-point correlation functions of  $\Delta$ -BMN operators can be written in the simple canonical form with a universal  $x$ -dependence, guaranteed by conformal invariance of the theory. For conformal primary operators with scalar impurities these canonical correlators are particularly simple and are given by (2.1), (2.2). Canonical expression for the correlators involving conformal primary operators with vector impurities appear to be much less illuminating and harder to interpret, however it was noted in [62] that this difficulty is avoided and the correlators for all types of impurities can be expressed in the same form, similar to (2.1) and (2.2), if on the left hand sides of (2.1) and (2.2) we use a different notion of conjugation  $\bar{\mathcal{O}}$  instead of  $\mathcal{O}^\dagger$  [62]. This different notion of operator conjugation is defined as *hermitian conjugation* followed by an *inversion* of the operator argument  $x'_\mu = x_\mu/x^2$ . Under inversion a scalar operator  $\mathcal{O}_\Delta(x)$  of conformal dimension  $\Delta$  transforms as

$$\mathcal{O}_\Delta^\dagger(x) \rightarrow \mathcal{O}'_\Delta(x') = x^{2\Delta} \mathcal{O}_\Delta^\dagger(x) \quad , \quad x_\mu \rightarrow x'_\mu = \frac{x_\mu}{x^2} \quad , \quad (3.8)$$

while a vector or tensor operator (i.e. operator with vector impurities) contains a

factor  $J_{\mu\nu}(x) = \delta_{\mu\nu} - 2x_\mu x_\nu / x^2$  on the right hand side for each vector index of the operator.  $J_{\mu\nu}(x)$  is the usual inversion tensor, in terms of which the Jacobian of the inversion is expressed  $\partial x'_\mu / \partial x_\nu = J_{\mu\nu}(x) / x^2$ . This prescription is essential in order to make vector  $\Delta$ -BMN operators orthonormalisable, see section 2 of [62] for more details.

With this prescription, the two-point function (2.1) for vector and for scalar  $\Delta$ -BMN operators takes the same simple form:

$$\langle \bar{\mathcal{O}}_{\Delta_\alpha}(x) \mathcal{O}_{\Delta_\beta}(0) \rangle = \delta_{\alpha\beta} , \quad (3.9)$$

which does not depend on  $x$  and hence has the meaning of overlap of the corresponding states in the gauge theory Hilbert space.

Note, however, that these  $\Delta$ -BMN states are the eigenstates of  $\Delta$ , i.e. the eigenstates of the full interacting string Hamiltonian, so they cannot be identically equal to the states from the natural string basis. The relation between the two bases is again a linear combination

$$|s_\alpha\rangle^{\text{SYM}} = U_{\alpha\beta} \mathcal{O}_{\Delta_\beta}(x=0)|0\rangle , \quad (3.10)$$

with another constant matrix  $U_{\alpha\beta}$ . In general, for any basis of operators  $\tilde{\mathcal{O}}_\alpha$  such that

$$\tilde{\mathcal{O}}_\alpha = U_{\alpha\beta} \mathcal{O}_{\Delta_\beta} , \quad (3.11)$$

the overlap is given by

$$\langle \bar{\tilde{\mathcal{O}}}_\alpha(x) \tilde{\mathcal{O}}_\beta(0) \rangle = U_{\beta\gamma} U_{\gamma\alpha}^\dagger \equiv S_{\beta\alpha} . \quad (3.12)$$

The operators  $\tilde{\mathcal{O}}_\alpha$  do not anymore have definite scaling dimensions  $\Delta$ , but since they are expressed as a linear superposition of conformal primary operators which do, there is no problem in performing the inversion required to define  $\bar{\tilde{\mathcal{O}}}_\alpha(x)$ , and the right hand side of (3.12) follows.

Now we describe a practical way of how to calculate simultaneously the overlaps and the matrix elements of the anomalous dimension operator  $\delta = \Delta - \Delta_{\text{cl}}$ , where  $\Delta_{\text{cl}}$  is the engineering dimension. Let us define the barred-operator  $\bar{\tilde{\mathcal{O}}}(x)$  as the

Hermitian conjugation of  $\tilde{\mathcal{O}}(x)$  followed by an inversion of the resulting operator, defined as if it was free, i.e. instead of the factor  $x^{2\Delta}$  in (3.8) we put  $x^{2\Delta_{\text{cl}}}$ , such that,

$$\bar{\mathcal{O}}_{\Delta}(x) \equiv x^{2\Delta_{\text{cl}}} J \cdot \mathcal{O}_{\Delta}^{\dagger}(x) , \quad (3.13)$$

where  $J_{\mu\nu}(x)$  is the usual inversion tensor for each vector index (each vector impurity) of the operator. Then the two-point function takes the form:

$$\langle \bar{\mathcal{O}}_{\alpha}(x) \tilde{\mathcal{O}}_{\beta}(0) \rangle = U_{\beta\gamma} e^{\delta_{\gamma} \log x^{-2}} U_{\gamma\alpha}^{\dagger} = S_{\beta\alpha} + T_{\beta\alpha} \log x^{-2} + \mathcal{O}((\log x^{-2})^2) . \quad (3.14)$$

Here we have expanded the full result in powers of  $\log x^{-2}$ . The overlap of the two states is defined as the zeroth-order term in the expansion,  $S_{\beta\alpha} = U_{\beta\gamma} U_{\gamma\alpha}^{\dagger}$ , and the matrix of anomalous dimensions in this basis is the first order term,

$$T_{\beta\alpha} = U_{\beta\gamma} \delta_{\gamma} U_{\gamma\alpha}^{\dagger} . \quad (3.15)$$

We note that (3.14), and hence the definitions of the overlap and the anomalous dimension matrix, are valid to all orders in the gauge coupling, and so can be in principle computed to all orders in  $\lambda'$  and  $g_2$  for any basis  $\tilde{\mathcal{O}}_{\alpha}$ .

By initially relating this basis to the  $\Delta$ -BMN basis we avoided all the problems of removing the ‘non-universal’  $x$ -dependence on the right hand side of the correlator. Now we can forget about the  $\Delta$ -BMN basis and follow the simple prescription discussed above: for an arbitrary basis, the overlap matrix  $S_{\beta\alpha}$  and the anomalous dimensions matrix  $T_{\beta\alpha}$  are the zeroth and the first term in the expansion of (3.14) in powers of  $\log x^{-2}$ .

We now consider the original BMN basis, for which we have

$$\langle \bar{\mathcal{O}}_{\alpha}(x) \mathcal{O}_{\beta} \rangle = S_{\beta\alpha} + T_{\beta\alpha} \log x^{-2} + \dots , \quad (3.16)$$

and relate this basis to the isomorphic to string basis via (3.7),

$$\mathcal{O}_{\beta}^{\text{string}} = U_{\beta\gamma} \mathcal{O}_{\gamma} , \quad \bar{\mathcal{O}}_{\alpha}^{\text{string}} = \bar{\mathcal{O}}_{\delta} U_{\delta\alpha}^{\dagger} . \quad (3.17)$$

In the isomorphic to string basis (which is automatically orthonormal, as explained earlier) we get

$$S^{\text{string}} = \mathbb{1} = USU^{\dagger} , \quad T^{\text{string}} = UTU^{\dagger} . \quad (3.18)$$

We note that  $S$  is a Hermitian, positive matrix (it is a matrix of norms), therefore the matrix  $S^{-1/2}$  is well-defined.<sup>3</sup>  $S$  is then diagonalised by the matrix  $U := S^{-1/2} \cdot V$ , where  $V^\dagger V = \mathbb{1}$ :

$$S \longrightarrow USU^\dagger = \mathbb{1} \quad , \quad (3.19)$$

$$T \longrightarrow UTU^\dagger = V^\dagger(S^{-\frac{1}{2}}TS^{-\frac{1}{2}})V \quad . \quad (3.20)$$

The arbitrariness contained in  $V$ , which is still left at this stage was fixed in [45, 48] by requiring that (3.3) holds and that the known three-string interaction vertex of the pp-wave light-cone string field theory [52, 53] is reproduced from gauge theory matrix elements involving BMN states (operators) with two scalar impurities. This condition implies  $V = \mathbb{1}$ . Hence, the matrix of anomalous dimensions in the string basis is given by

$$\Gamma := T^{\text{string}} = S^{-\frac{1}{2}} T S^{-\frac{1}{2}} \quad . \quad (3.21)$$

In the following sections we will show that, with the same choice of  $V = \mathbb{1}$ , the matrix elements of  $\Gamma$  between BMN operators with

- two vector impurities,
- one vector and one scalar impurity and, finally,
- an arbitrary number of scalar impurities,

precisely agree with the corresponding matrix elements of the interacting string Hamiltonian. We will consider all representations of BMN operators with vector or scalar impurities, i.e. symmetric traceless, antisymmetric and singlet. The inclusion of vector, mixed (scalar-vector) and scalar BMN operators allows us to study the correspondence for string states in all of the pp-wave light-cone directions.

Other studies of the dilatation operator in gauge theory and its interpretation in quantum mechanical models, which we do not pursue here, can be found in the recent papers [79, 81–83].

---

<sup>3</sup>We would like to point out that this matrix  $S^{-\frac{1}{2}}$  appears also in [61] and [82].

## 3.2 Tests of the correspondence in the two-impurity sector: scalar, mixed, and vector states

In this and the following sections we will need the expressions for the single-trace original BMN operators:

$$\mathcal{O}_{\text{vac}}^J = \frac{1}{\sqrt{JN_0^J}} \text{Tr} Z^J, \quad (3.22)$$

$$\mathcal{O}_{ij,m}^J = c \left( \sum_{l=0}^J e^{\frac{2\pi i m l}{J}} \text{Tr} (\phi_i Z^l \phi_j Z^{J-l}) \right), \quad (3.23)$$

$$\mathcal{O}_{\mu\nu,m}^J = \frac{c}{2} \left( \sum_{l=0}^J e^{\frac{2\pi i m l}{J}} \text{Tr} [(D_\mu Z) Z^l (D_\nu Z) Z^{J-l}] + \text{Tr} [(D_\mu D_\nu Z) Z^{J+1}] \right) \quad (3.24)$$

$$\mathcal{O}_{i\mu,m}^J = \frac{c}{\sqrt{2}} \left( \sum_{l=0}^J e^{\frac{2\pi i m l}{J}} \text{Tr} [\phi_i Z^l (D_\mu Z) Z^{J-l}] + \text{Tr} [(D_\mu \phi_i) Z^{J+1}] \right), \quad (3.25)$$

where  $i, j = 1, \dots, 4$ ,  $\mu, \nu = 1, \dots, 4$  label the scalar and the vector impurities. Note that in writing  $\mathcal{O}_{ij,m}^J$  and  $\mathcal{O}_{\mu\nu,m}^J$  we have taken  $i \neq j$  and  $\mu \neq \nu$ , where the above expressions take the simple form (3.23) and (3.24). We also defined

$$c := \frac{1}{\sqrt{JN_0^{J+2}}}, \quad N_0 := \frac{g^2}{2} \frac{N}{4\pi^2}. \quad (3.26)$$

The normalisation of the operators is such that their two-point functions take the canonical form in the planar limit. We also note that expressions for  $\mathcal{O}_{\mu\nu,n}^J$  and  $\mathcal{O}_{i\mu,m}^J$  contain appropriate compensating terms [71, 72]. These terms are required in order for the corresponding operator to be conformal primaries in the BMN limit.

The operators in (3.23)–(3.25) are the original BMN operators. They are related to each other by supersymmetry transformations [72]. In order to test the correspondence, we need to use a different basis of operators which is isomorphic to string states, as discussed earlier. Importantly, the isomorphic to string operators  $\tilde{\mathcal{O}}_{i\mu,m}^J$ ,  $\tilde{\mathcal{O}}_{\mu\nu,m}^J$  are related to the  $\tilde{\mathcal{O}}_{ij,m}^J$  in exactly the same way as the original BMN operators are. This is because the matrix  $U$  in (3.11) is a numerical matrix, i.e. it does not contain any fields and does not transform under supersymmetry. Hence,  $U$  is the same for scalar, vector and mixed impurity BMN operators.

We will also need the expressions for the double-trace operators

$$\mathcal{T}_{ij,m}^{J,y} = : \mathcal{O}_{ij,m}^{y \cdot J} : : O_{\text{vac}}^{(1-y) \cdot J} : , \quad (3.27)$$

$$\mathcal{T}_{\mu\nu,m}^{J,y} = : \mathcal{O}_{\mu\nu,m}^{y \cdot J} : : O_{\text{vac}}^{(1-y) \cdot J} : , \quad (3.28)$$

$$\mathcal{T}_{i\mu,m}^{J,y} = : \mathcal{O}_{i\mu,m}^{y \cdot J} : : O_{\text{vac}}^{(1-y) \cdot J} : , \quad (3.29)$$

where  $y \in (0, 1)$ .

From the three-string vertex of [52, 53] one extracts the following matrix elements of the string Hamiltonian in the large- $\mu$  limit:

$$\frac{1}{\mu} \langle \mathcal{O}_{ij,m}^J | H_{\text{string}} | \mathcal{T}_{ij,n}^{J,y} \rangle = -C_{\text{norm}} \frac{\lambda'}{\pi^2 y} \sin^2(\pi m y) , \quad (3.30)$$

$$\frac{1}{\mu} \langle \mathcal{O}_{i\mu,m}^J | H_{\text{string}} | \mathcal{T}_{i\mu,n}^{J,y} \rangle = 0 , \quad (3.31)$$

$$\frac{1}{\mu} \langle \mathcal{O}_{\mu\nu,m}^J | H_{\text{string}} | \mathcal{T}_{\mu\nu,n}^{J,y} \rangle = C_{\text{norm}} \frac{\lambda'}{\pi^2 y} \sin^2(\pi m y) , \quad (3.32)$$

for  $\mu \neq \nu$  and  $i \neq j$ . The overall normalisation  $C_{\text{norm}}$  is left undetermined in string field theory. In order to get agreement with the field theory result we will set here<sup>4</sup>

$$C_{\text{norm}} = -\frac{g_2}{2} \frac{\sqrt{y(1-y)}}{\sqrt{J}} . \quad (3.33)$$

Using this normalisation, (3.30) and (3.32) become

$$\frac{1}{\mu} \langle \mathcal{O}_{ij,m}^J | H_{\text{string}} | \mathcal{T}_{ij,n}^{J,y} \rangle = -\frac{1}{\mu} \langle \mathcal{O}_{\mu\nu,m}^J | H_{\text{string}} | \mathcal{T}_{\mu\nu,n}^{J,y} \rangle = \lambda' \frac{g_2}{\sqrt{J}} \frac{\sqrt{(1-y)/y} \sin^2(\pi m y)}{2\pi^2} . \quad (3.34)$$

As mentioned earlier, the agreement of (3.30) with the corresponding gauge theory matrix elements was found in [48]. We will show that agreement with gauge theory holds also for (3.31) and (3.32).

We now need the explicit form of the matrices  $S$  and  $T$  in the original BMN basis. Both  $S$  and  $T$  have an expansion in powers of  $g_2$ , but in our analysis we will need

<sup>4</sup> $C_{\text{norm}}$  is further discussed in section 3.4.2, where we consider the case of arbitrary many impurities, see (3.115).

their expressions only up to and including  $\mathcal{O}(g_2)$  terms. We will also work at one loop in the Yang-Mills effective coupling  $\lambda'$ , where the matrix  $T$  is of  $\mathcal{O}(\lambda')$ , whereas  $S$  is of  $\mathcal{O}(1)$ . In this case, (3.14) is simply

$$\langle \mathcal{O}_\alpha(0) \bar{\mathcal{O}}_\beta(x) \rangle = S_{\alpha\beta} + T_{\alpha\beta} \log(x\Lambda)^{-2}. \quad (3.35)$$

The pleasant fact is that expressions for  $S$  and  $T$  are closely related and can be obtained from the coefficients of the three-point functions, which were derived in [62, 73] for BMN operators with two scalar and two vector impurities, respectively. We also need to know  $S$  and  $T$  in the case of mixed (i.e. one scalar and one vector) impurities. The three-point functions of such BMN operators were not considered previously, and they will be calculated in section 3.3.

The diagonal elements of  $S$  and  $T$  can be immediately obtained from

$$\langle \mathcal{O}_{AB,m}^J(0) \bar{\mathcal{O}}_{AB,n}^J(x) \rangle = \delta_{mn} (1 + \lambda' m^2 \log(\Lambda x)^{-2}), \quad (3.36)$$

$$\langle \mathcal{T}_{AB,m}^{J,y}(0) \bar{\mathcal{T}}_{AB,n}^{J,z}(x) \rangle = \delta_{mn} \delta_{yz} (1 + \lambda' (m^2/y^2) \log(\Lambda x)^{-2}). \quad (3.37)$$

The previous expressions are valid up to  $\mathcal{O}(\lambda')$  and  $\mathcal{O}(g_2)$ , and were derived originally in [47, 73] for the scalar case, and in [71, 93, 94] for the mixed and vector case.

To determine the off-diagonal elements, we need to compute the two-point correlators  $\langle \mathcal{T}_{AB,m}^{J,y}(0) \bar{\mathcal{O}}_{AB,n}^J(x) \rangle$ . To this end, let us momentarily focus on the following class of *three-point* correlators,

$$G(x_1, x_2, x_3) = \langle \mathcal{O}_{AB,n}^{y,J}(x_1) \mathcal{O}_{\text{vac}}^{(1-y),J}(x_2) \bar{\mathcal{O}}_{AB,m}^J(x_3) \rangle, \quad (3.38)$$

where  $A = (i, \mu)$  and  $A \neq B$ . On general grounds, these three-point function have the form [47, 73, 74, 76]

$$G(x_1, x_2, x_3) = g_2 C_{m,ny} [1 - \lambda' (a_{m,ny} \log(x_{31}\Lambda)^2 + b_{m,ny} \log(x_{32}x_{31}\Lambda/x_{12}))], \quad (3.39)$$

where  $g_2 C_{m,ny}$  is the tree-level contribution, with

$$C_{m,ny} := \frac{\sqrt{(1-y)/y} \sin^2(\pi m y)}{\sqrt{J} \pi^2 (m - n/y)^2}, \quad (3.40)$$

and the coefficients  $a_{m,ny}$  and  $b_{m,ny}$  must be calculated in perturbation theory at  $\mathcal{O}(\lambda')$ . The *two*-point function  $\langle \mathcal{T}_{AB,n}^{J,y}(0) \bar{\mathcal{O}}_{AB,m}^J(x) \rangle$  can easily be deduced from (3.38) by setting  $x_{13} = x_{23} = x$  and  $x_{12} = \Lambda^{-1}$  [76],

$$\langle \mathcal{T}_{AB,n}^{J,y}(0) \bar{\mathcal{O}}_{AB,m}^J(x) \rangle = g_2 C_{m,ny} [1 + \lambda' (a_{m,ny} + b_{m,ny}) \log(x\Lambda)^{-2}] . \quad (3.41)$$

The matrices  $S$  and  $T$  are then given, up to  $\mathcal{O}(g_2)$ , by

$$S = \begin{pmatrix} \delta_{mn} & g_2 C_{m,qz} \\ g_2 C_{py,n} & \delta_{pq} \end{pmatrix} + \mathcal{O}(g_2^2) = \mathbf{1} + g_2 s + \mathcal{O}(g_2^2) , \quad (3.42)$$

$$(3.43)$$

$$T = \lambda' \begin{pmatrix} m^2 \delta_{mn} & g_2 C_{m,ny} (a + b)_{m,qz} \\ g_2 C_{py,n} (a + b)_{py,n} & (p^2/y^2) \delta_{pq} \delta_{yz} \end{pmatrix} + \mathcal{O}(g_2^2) \quad (3.44)$$

$$\equiv d + g_2 t + \mathcal{O}(g_2^2) ,$$

with

$$d = \lambda' \begin{pmatrix} m^2 \delta_{mn} & 0 \\ 0 & (p^2/y^2) \delta_{pq} \delta_{yz} \end{pmatrix} , \quad (3.45)$$

$$t = \lambda' \begin{pmatrix} 0 & C_{m,ny} (a + b)_{m,qz} \\ C_{py,n} (a + b)_{py,n} & 0 \end{pmatrix} . \quad (3.46)$$

It then follows that

$$S^{-1/2} = \mathbf{1} - g_2 (s/2) + \mathcal{O}(g_2^2) \quad (3.47)$$

diagonalises  $S$  at  $\mathcal{O}(g_2)$ .

We now need to compute the explicit expressions for  $a_{mn}^y$  and  $b_{mn}^y$ , in the scalar case, mixed (scalar-vector) case, and finally in the vector case.

It is easy to compute at  $\mathcal{O}(\lambda')$  the coefficient  $a_{mn}^y$  in planar perturbation theory, which turns out to be

$$a_{m,ny} = \frac{n^2}{y^2} , \quad (3.48)$$

independently of the type of impurity considered. Notice that this is exactly the  $\mathcal{O}(\lambda')$  anomalous dimension<sup>5</sup> of the “small” BMN operator at  $x_1$ .

We will now explain how  $b_{m,ny}$  is determined from the coefficients of the conformal three-point function. First we note that the correlator (3.38) does not take the conformal form (2.2) since the original BMN operators in (3.39) are not conformal primaries for  $g_2 \neq 0$  due to operator mixing [73, 95]. However, at leading order in  $g_2$ , the only mixing effect which contributes to (2.2) is the presence of the double-trace corrections in the expression for the conjugate  $\Delta$ -BMN operator.<sup>6</sup> Importantly, [1, 62], these mixing effects cannot affect the remaining logarithm,  $\lambda' \log x_{12}^2$ , which can then be computed without taking into account mixing altogether. Hence, we can use the right hand side of the conformal expression (2.2) in order to compute the coefficient  $b_{m,ny}$  in (3.39). Expanding the right-hand side of (2.2) to  $\mathcal{O}(\lambda')$ , and equating the coefficient of the  $\log x_{12}^2$  to the corresponding term in (3.38), we obtain

$$g_2 C_{m,ny} b_{m,ny} = (m^2 - n^2/y^2) C(C_{nD-n}, \text{vac} | A_m B_{-m}), \quad (3.49)$$

where  $C(C_{nD-n}, \text{vac} | A_m B_{-m})$  is the coefficient  $C_{123}$  of the conformal three-point function  $\langle \mathcal{O}_{CD,n}^{J_1}(x_1) \mathcal{O}_{\text{vac}}^{J_2}(x_2) \bar{\mathcal{O}}_{AB,m}^J(x_3) \rangle$ . We used  $\Delta_1 = J_1 + 2 + \lambda' n^2/y^2$ ,  $\Delta_2 = J$ , and  $\Delta_3 = J + 2 + \lambda' m^2$ .

Equation (3.49) determines  $b_{m,ny}$  in terms of the coefficients  $C(C_{nD-n}, \text{vac} | A_m B_{-m})$  of the three-point function. These coefficients for BMN operators with two scalar impurities, one scalar and one vector impurity, and two vector impurities are given

---

<sup>5</sup>It is immediate to convince oneself that the Feynman diagrams contributing to the  $\log x_{31}^2$  part of  $\langle \mathcal{O}_{AB,n}^{y \cdot J}(x_1) \mathcal{O}_{\text{vac}}^{(1-y) \cdot J}(x_2) \bar{\mathcal{O}}_{AB,m}^J(x_3) \rangle$  are those where the operator  $\mathcal{O}_{\text{vac}}^{(1-y) \cdot J}(x_2)$  does not participate in the interaction, i.e. they are precisely the Feynman diagrams contributing to the anomalous dimension of  $\mathcal{O}_{AB,n}^{y \cdot J}(x_1)$  - embedded in a three-point function.

<sup>6</sup>This is because the double-trace corrections to the single-trace expression for an original BMN operator is of  $\mathcal{O}(g_2)$ , i.e. suppressed with  $1/N$ . This can be compensated by factorising the three-point function into a product of two two-point functions, which is possible only for the double-trace mixing in the operator  $\bar{\mathcal{O}}$ .

by:

$$C(k_n l_{-n}, \text{vac} | i_m j_{-m}) = C_{123}^{\text{vac}} \frac{2 \sin^2(\pi m y)}{y \pi^2 (m^2 - \frac{n^2}{y^2})^2} \times \left( \delta_{i(k} \delta_{l)j} m^2 + \delta_{i[k} \delta_{l]j} \frac{mn}{y} + \frac{1}{4} \delta_{ij} \delta_{kl} \frac{n^2}{y^2} \right) \quad (3.50)$$

$$C(j_n \nu_{-n}, \text{vac} | i_m \mu_{-m}) = C_{123}^{\text{vac}} \frac{2 \sin^2(\pi m y)}{y \pi^2 (m^2 - \frac{n^2}{y^2})^2} \delta_{ij} \delta_{\mu\nu} \frac{1}{4} \left( m + \frac{n}{y} \right)^2, \quad (3.51)$$

$$C(\rho_n \sigma_{-n}, \text{vac} | \mu_m \nu_{-m}) = C_{123}^{\text{vac}} \frac{2 \sin^2(\pi m y)}{y \pi^2 (m^2 - \frac{n^2}{y^2})^2} \times \left( \delta_{\mu(\rho} \delta_{\sigma)\nu} \frac{n^2}{y^2} + \delta_{\mu[\rho} \delta_{\sigma]\nu} \frac{mn}{y} + \frac{1}{4} \delta_{\mu\nu} \delta_{\rho\sigma} m^2 \right), \quad (3.52)$$

where  $C_{123}^{\text{vac}} = \sqrt{J_1 J_2} / N = (g_2 / \sqrt{J}) \sqrt{y(1-y)}$ , and the symmetric traceless and antisymmetric traceless combinations of two Kronecker deltas are defined as

$$\delta_{i(k} \delta_{l)j} = \frac{1}{2} (\delta_{ik} \delta_{lj} + \delta_{il} \delta_{kj}) - \frac{1}{4} \delta_{ij} \delta_{kl}, \quad \delta_{i[k} \delta_{l]j} = \frac{1}{2} (\delta_{ik} \delta_{lj} - \delta_{il} \delta_{kj}). \quad (3.53)$$

The three-point function coefficient for scalars (3.50) was derived in [73] (the simple case  $n = 0$  was first obtained in [74]), whereas that for the vectors, (3.52), was recently obtained in [62]. The three-point function coefficient (3.51) for the case of mixed scalar-vector impurities is a new result, and its derivation is presented in section 3.3 of this chapter.

From (3.50)–(3.52) and (3.49), it is then immediate to derive the coefficients  $b_{m,ny}$  which correspond to considering scalar, mixed, or vector BMN operators in (3.38):

$$[b_{m,ny}]_{\text{scalar}} = m^2 - \frac{mn}{y}, \quad (3.54)$$

$$[b_{m,ny}]_{\text{scalar-vector}} = \frac{1}{2} \left( m^2 - \frac{n^2}{y^2} \right), \quad (3.55)$$

$$[b_{m,ny}]_{\text{vector}} = -\frac{n^2}{y^2} + \frac{mn}{y}. \quad (3.56)$$

In conclusion, using (4.43) we get, up to  $\mathcal{O}(g_2)$ ,

$$\langle T_{ij,n}^{J,y}(0) \bar{\mathcal{O}}_{ij,m}^J(x) \rangle = g_2 C_{m,ny} \left[ 1 + \lambda' \left( m^2 - \frac{mn}{y} + \frac{n^2}{y^2} \right) \log(x\Lambda)^{-2} \right], \quad (3.57)$$

$$\langle T_{j\nu,n}^{J,y}(0) \bar{\mathcal{O}}_{i\mu,m}^J(x) \rangle = g_2 C_{m,ny} \left[ 1 + \frac{\lambda'}{2} \left( m^2 + \frac{n^2}{y^2} \right) \log(x\Lambda)^{-2} \right] \delta_{ij} \delta_{\mu\nu}, \quad (3.58)$$

$$\langle \mathcal{T}_{\mu\nu,n}^{J,y}(0) \bar{\mathcal{O}}_{\mu\nu,m}^J(x) \rangle = g_2 C_{m,ny} \left[ 1 + \lambda' \left( \frac{mn}{y} \right) \log(x\Lambda)^{-2} \right]. \quad (3.59)$$

We will now make use of the expressions for these three correlators to construct the matrix  $T$ , and therefore the matrix  $\Gamma$  dual to  $H_{\text{string}}^{\text{int}}$ , in the three cases of BMN states with (i) two scalar, (ii) one scalar and one vector, and finally (iii) two vector impurities. These three cases are addressed separately below.

### 3.2.1 Matrix elements with scalar BMN states

This case was first analysed in [48], and we review it here for completeness.

Substituting (3.48) and (3.54) in (3.44), we find that the matrix  $T_{\text{scalar}}$  is given, at  $\mathcal{O}(g_2)$ , by<sup>7</sup>

$$\begin{aligned} T_{\text{scalar}} &= \lambda' \begin{pmatrix} m^2 & g_2 C_{m,ny} (m^2 - mn/y + n^2/y^2) \\ g_2 C_{ny,m} (m^2 - mn/y + n^2/y^2) & n^2/y^2 \end{pmatrix} \\ &\equiv d + g_2 t_{\text{scalar}}. \end{aligned} \quad (3.60)$$

Multiplying it on the left and on the right by  $S^{-1/2} = \mathbb{1} - g_2(s/2) + \mathcal{O}(g_2^2)$  we get the expression for the matrix  $\Gamma$  introduced in (3.21) at  $\mathcal{O}(g_2)$ :

$$\Gamma_{\text{scalar}} = d + g_2 [t_{\text{scalar}} - (1/2)\{s, d\}] \quad (3.61)$$

$$= \lambda' \begin{pmatrix} m^2 & (g_2 C_{m,ny}/2) (m - n/y)^2 \\ (g_2 C_{ny,m}/2) (m - n/y)^2 & n^2/y^2 \end{pmatrix},$$

from which it follows, using the definition (3.40) of  $C_{m,ny}$ ,

$$\langle \mathcal{O}_{ij,m}^J | \Gamma_{\text{scalar}} | \mathcal{T}_{ij,n}^{J,y} \rangle = \lambda' \frac{g_2}{\sqrt{J}} \frac{\sqrt{(1-y)/y} \sin^2(\pi my)}{2\pi^2}. \quad (3.62)$$

This result was first found in [48]. (3.62) agrees with (3.30) after choosing the normalisation (3.33) for the string result.

<sup>7</sup>We use a somewhat simplified, but correct, notation for the indices of the matrices  $S$  and  $T$ .

### 3.2.2 Matrix elements with mixed BMN states

In this case, using (3.48) and (3.55) we can determine the matrix  $T_{\text{mixed}}$  in (3.44) for the case of mixed impurities. It is given, at  $\mathcal{O}(g_2)$ , by the following expression:

$$T_{\text{mixed}} = \lambda' \begin{pmatrix} m^2 & g_2 C_{m,ny} (m^2 + n^2/y^2)/2 \\ g_2 C_{ny,m} (m^2 + n^2/y^2)/2 & n^2/y^2 \end{pmatrix} \quad (3.63)$$

$$\equiv d + g_2 t_{\text{mixed}} ,$$

where we used  $a_{m,ny} + b_{m,ny}^{\text{mixed}} = (m^2 + n^2/y^2)/2$ . It then follows that

$$\Gamma_{\text{mixed}} = d + g_2 [t_{\text{mixed}} - (1/2)\{s, d\}] = \lambda' \begin{pmatrix} m^2 & 0 \\ 0 & n^2/y^2 \end{pmatrix} , \quad (3.64)$$

and hence

$$\langle \mathcal{O}_{i\mu,m}^J | \Gamma_{\text{mixed}} | \mathcal{T}_{i\mu,n}^{J,y} \rangle = 0 . \quad (3.65)$$

This verifies in gauge theory the vanishing of the three-string amplitude (3.31) between states with one scalar and one vector impurity, which was predicted in [53].

### 3.2.3 Matrix elements with vector BMN states

Finally, we study the case of vector BMN impurities. Using (3.48) and (3.56) we obtain the matrix  $T_{\text{vector}}$  in (3.44) for the case of vector impurities. At  $\mathcal{O}(g_2)$ , it is given by:

$$T_{\text{vector}} = \lambda' \begin{pmatrix} m^2 & g_2 C_{m,ny} (mn/y) \\ g_2 C_{ny,m} (mn/y) & n^2/y^2 \end{pmatrix} \quad (3.66)$$

$$\equiv d + g_2 t_{\text{vector}} ,$$

where we used  $a_{m,ny} + b_{m,ny}^{\text{vector}} = mn/y$ . It then follows that

$$\Gamma_{\text{vector}} = d + g_2 [t_{\text{vector}} - (1/2)\{s, d\}] \quad (3.67)$$

$$= \lambda' \begin{pmatrix} m^2 & -(g_2 C_{m,ny}/2) (m - n/y)^2 \\ -(g_2 C_{m,ny}/2) (m - n/y)^2 & n^2/y^2 \end{pmatrix},$$

from which we get

$$\begin{aligned} \langle \mathcal{O}_{\mu\nu,m}^J | \Gamma_{\text{vector}} | \mathcal{T}_{\mu\nu,n}^{J,y} \rangle &= -\lambda' \frac{g_2}{\sqrt{J}} \frac{\sqrt{(1-y)/y} \sin^2(\pi m y)}{2\pi^2} \quad (3.68) \\ &= -\langle \mathcal{O}_{ij,m}^J | \Gamma_{\text{scalar}} | \mathcal{T}_{ij,n}^{J,y} \rangle. \end{aligned}$$

As advertised earlier, the off-diagonal elements  $\langle \mathcal{O}_{\mu\nu,m}^J | \Gamma_{\text{vector}} | \mathcal{T}_{\mu\nu,n}^{J,y} \rangle$  of  $\Gamma_{\text{vector}}$  are precisely the opposite of the corresponding elements  $\langle \mathcal{O}_{ij,m}^J | \Gamma_{\text{scalar}} | \mathcal{T}_{ij,n}^{J,y} \rangle$  of  $\Gamma_{\text{scalar}}$ . This again had been predicted in string field theory in [53]. As explained in the introduction, this signals the spontaneous breaking of  $\mathbb{Z}_2$  symmetry in pp-wave string theory.

### 3.2.4 Generalisation to all representations for two-impurity BMN states

Finally, we extend our previous computations to include all representations of scalar and vector BMN operators with two impurities.

We recall here the results from the previous sections:

$$\begin{aligned} \langle \mathcal{O}_{ij,m}^J | \Gamma_{\text{scalar}} | \mathcal{T}_{ij,n}^{J,y} \rangle &= -\langle \mathcal{O}_{\mu\nu,m}^J | \Gamma_{\text{vector}} | \mathcal{T}_{\mu\nu,n}^{J,y} \rangle = \lambda' \frac{g_2}{\sqrt{J}} \frac{\sqrt{(1-y)/y} \sin^2(\pi m y)}{2\pi^2}, \\ \langle \mathcal{O}_{k\mu,m}^J | \Gamma_{\text{mixed}} | \mathcal{T}_{l\nu,n}^{J,y} \rangle &= 0, \quad (3.69) \end{aligned}$$

( $i \neq j$ ,  $\mu \neq \nu$ ) which correspond to the string field theory amplitude (3.30), (3.31) and (3.32). From these results it is immediate to obtain

$$\langle \mathcal{O}_{\nu\mu,m}^J | \Gamma_{\text{vector}} | \mathcal{T}_{\mu\nu,n}^{J,y} \rangle = \langle \mathcal{O}_{\mu\nu,m}^J | \Gamma_{\text{vector}} | \mathcal{T}_{\mu\nu,n}^{J,y} \rangle, \quad (3.70)$$

since this amounts to complex conjugate the BMN phase factor contained in  $\mathcal{O}_{\mu\nu,m}^J$ , i.e. to exchange  $m \rightarrow -m$  (same considerations apply for the scalar amplitude). Equation (3.70) follows since the first expression in (3.69) is even in  $m$ . Therefore

we can at once obtain the result for the symmetric-traceless and antisymmetric representations for vectors:

$$\langle \mathcal{O}_{(\mu\nu),m}^J | \Gamma_{\text{vector}} | \mathcal{T}_{(\rho\sigma),n}^{J,y} \rangle = -\lambda' \frac{g_2}{\sqrt{J}} \frac{\sqrt{(1-y)/y} \sin^2(\pi m y)}{\pi^2} \delta_{\mu(\rho} \delta_{\sigma)\nu} , \quad (3.71)$$

$$\langle \mathcal{O}_{[\mu\nu],m}^J | \Gamma_{\text{vector}} | \mathcal{T}_{[\rho\sigma],n}^{J,y} \rangle = 0 , \quad (3.72)$$

whereas for scalars,

$$\langle \mathcal{O}_{(ij),m}^J | \Gamma_{\text{scalar}} | \mathcal{T}_{(kl),n}^{J,y} \rangle = \lambda' \frac{g_2}{\sqrt{J}} \frac{\sqrt{(1-y)/y} \sin^2(\pi m y)}{\pi^2} \delta_{i(k} \delta_{l)j} , \quad (3.73)$$

$$\langle \mathcal{O}_{[ij],m}^J | \Gamma_{\text{scalar}} | \mathcal{T}_{[kl],n}^{J,y} \rangle = 0 . \quad (3.74)$$

Here we have defined

$$\mathcal{O}_{(\mu\nu)} = \frac{1}{2}(\mathcal{O}_{\mu\nu} + \mathcal{O}_{\nu\mu}) - \frac{\delta_{\mu\nu}}{4} \sum_{\rho} \mathcal{O}_{\rho\rho} , \quad \mathcal{O}_{[\mu\nu]} = \frac{1}{2}(\mathcal{O}_{\mu\nu} - \mathcal{O}_{\nu\mu}) . \quad (3.75)$$

The vector singlet case can be treated instantly by noticing that the three-point function coefficient for vector singlets is actually the same as the three-point function coefficient for the symmetric-traceless scalars, as it can be seen by comparing (3.50) to (3.52). This, together with (3.73), immediately implies that<sup>8</sup>

$$\begin{aligned} \langle \mathcal{O}_{\text{vector } 1,m}^J | \Gamma_{\text{vector}} | \mathcal{T}_{\text{vector } 1,n}^{J,y} \rangle &= \lambda' \frac{g_2}{\sqrt{J}} \frac{\sqrt{(1-y)/y} \sin^2(\pi m y)}{\pi^2} \\ &= -\langle \mathcal{O}_{\text{scalar } 1,m}^J | \Gamma_{\text{scalar}} | \mathcal{T}_{\text{scalar } 1,n}^{J,y} \rangle , \end{aligned} \quad (3.76)$$

where  $\mathcal{O}_1 = (1/2) \sum_{\mu} \mathcal{O}_{\mu\mu}$ . We notice that the result for the scalar singlet amplitude  $\langle \mathcal{O}_{\text{scalar } 1,m}^J | \Gamma_{\text{scalar}} | \mathcal{T}_{\text{scalar } 1,n}^{J,y} \rangle$  agrees with the result found in [49]. The opposite sign in (3.76) for the vector singlet compared to the scalar singlet case is again a manifestation of the (spontaneously broken)  $\mathbb{Z}_2$  symmetry in pp-wave string theory.

<sup>8</sup>The reader willing to derive explicitly the result (3.76) for vector singlets should be aware that, for singlets, (4.43) should be modified to  $\langle \mathcal{T}_{1,n}^{J,y}(0) \bar{\mathcal{O}}_{1,m}^J(x) \rangle = g_2 C_{m,ny} [1 + \lambda' (a_{m,ny} + b_{m,ny}) \log(x\Lambda)^{-2}] + g_2 C_{-m,ny} [1 + \lambda' (a_{-m,ny} + b_{-m,ny}) \log(x\Lambda)^{-2}]$ , and that, from the result (3.52) derived in [62], it follows that  $[b_{m,ny}]_{\text{vector},1} = m^2 - mn/y$ .

### 3.3 A technical aside: three-point function with mixed impurities

In this section we derive the expression (3.51).

Here we would like to compute the coefficient of the three-point function of one vacuum operator (3.22) and two conformal primary  $\Delta$ -BMN operators with one scalar and one vector impurity,

$$\tilde{\mathcal{O}}_{i\mu,m}^J = \mathcal{O}_{i\mu,m}^J + \dots, \quad (3.77)$$

where  $\mathcal{O}_{i\mu,m}^J$  is defined in (3.25). The operator  $\tilde{\mathcal{O}}_{i\mu,m}^J$  has a definite scaling dimension,  $\Delta_n = \Delta_{\text{cl}} + \delta_n$ , which implies that the single-trace expression  $\mathcal{O}_{i\mu,m}^J$  on the right hand side of (3.77) must be accompanied by multi-trace corrections (and other mixing effects) at higher orders in  $g_2$  [73,95]. The dots on the right hand side of (3.77) stand for these corrections.

Nevertheless, our strategy is to study the three-point correlator of the *original* BMN operators  $\mathcal{O}_{i\mu,m}^J$ ,

$$\langle \mathcal{O}_{j\nu,n}^{y\cdot J}(x_1) \mathcal{O}_{\text{vac}}^{(1-y)\cdot J}(x_2) \bar{\mathcal{O}}_{i\mu,m}^J(x_3) \rangle = \quad (3.78)$$

$$g_2 C_{m,ny} \left[ 1 - \lambda' \left( a_{m,ny} \log(x_{31}\Lambda)^2 + b_{m,ny}^{\text{mixed}} \log \left| \frac{x_{32}x_{31}\Lambda}{x_{12}} \right| \right) \right] \delta_{\mu\nu} \delta_{ij},$$

and to focus on the computation of the coefficient  $b_{m,ny}^{\text{mixed}}$  of the  $\log x_{12}$ . This is because, for reasons explained in the paragraph below (3.48), this coefficient can be computed without taking into account mixing altogether, and is directly related to the coefficient of the three-point function of conformal primary BMN operators with mixed impurities through (3.49). Therefore, from now on we will work with the original BMN operator (3.25).

The mixed BMN operator in (3.25) contains two terms: a “pure” BMN part and a compensating term, first and second term on the right hand side of (3.25), respectively. The Feynman diagrams contributing to the Green’s function in (3.78) can be divided into two classes: those obtained by taking only the pure BMN part of  $\mathcal{O}_{j\nu,n}^{y\cdot J}(x_1)$  and  $\bar{\mathcal{O}}_{i\mu,m}^J(x_3)$  and those where the compensating part is taken (in one or both operators). As already explained, we will focus only on diagrams which

can produce a  $\log x_{12}$  dependence, and both classes of diagrams contribute to the coefficient  $b_{m,ny}^{\text{mixed}}$  in (3.78). For the sake of clarity, we quote here the results from these two classes of diagrams:

$$[b_{m,ny}^{\text{mixed}}]_{\text{BMN}} = m \left( m - \frac{n}{y} \right), \quad (3.79)$$

$$[b_{m,ny}^{\text{mixed}}]_{\text{comp}} = -\frac{1}{2} \left( m - \frac{n}{y} \right)^2. \quad (3.80)$$

The total result

$$[b_{m,ny}]_{\text{scalar-vector}} = [b_{m,ny}^{\text{mixed}}]_{\text{BMN}} + [b_{m,ny}^{\text{mixed}}]_{\text{comp}} = \frac{1}{2} \left( m^2 - \frac{n^2}{y^2} \right), \quad (3.81)$$

was anticipated in (3.55). We now compute separately these two classes of diagrams. Our notation and conventions are summarised in Appendix G.

### 3.3.1 Diagrams originating from the “pure” BMN parts

We consider first the diagrams where the scalar impurity interacts. These are represented in Figure 3.1. The result for these diagrams is:

$$\left( \frac{2}{g^2} \right) \left( \frac{g^2}{2} \right)^4 \cdot 2(P_I - P_{II} + \bar{P}_I - \bar{P}_{II}) \cdot (2\delta_{\mu\nu})\delta_{ij} \cdot X. \quad (3.82)$$

The first term on the right hand side of (3.82) comes from the diagram 3.1a (the coefficient of 2 is easily seen from  $-V_F$  in (C.5)), the second term is the sum of diagrams 3.1b and 3.1c. The relative sign is also immediately seen from the commutators in  $-V_F$ . We have taken into account the fact that diagrams 3.1b and 3.1c give the same contribution.<sup>9</sup>

The third and fourth term in (3.82) come from the mirror diagrams 3.1d, 3.1e and 3.1f, where the  $\phi$  interaction is now at the bottom. The factor  $2\delta_{\mu\nu}$  comes from the free contraction<sup>10</sup> of the  $\overline{D_\mu Z}$  impurity with the  $D_\nu Z$  impurity. The coefficients

<sup>9</sup>This is a simple corollary of the cancellation of D-terms against gluon interactions and self-energies in three-point functions of BMN operators at  $\mathcal{O}(\lambda')$  (in the complex basis) [17, 47, 73, 74]. In our case, self-interactions diagrams do not participate since they cannot generate  $\log x_{12}^2$  terms at order  $\mathcal{O}(\lambda')$ .

<sup>10</sup>For an extensive discussion of the treatment of BMN operators with vector impurities, the reader is referred to [62]. Free contractions of vector impurities are discussed in Eq. (34) of that paper, and the main results can be summarised as  $\langle \overline{D_\mu Z} D_\nu Z \rangle_{\text{free}} = 2\delta_{\mu\nu}$ , and  $\langle \overline{Z} D_\nu Z \rangle_{\text{free}} = 0$ .

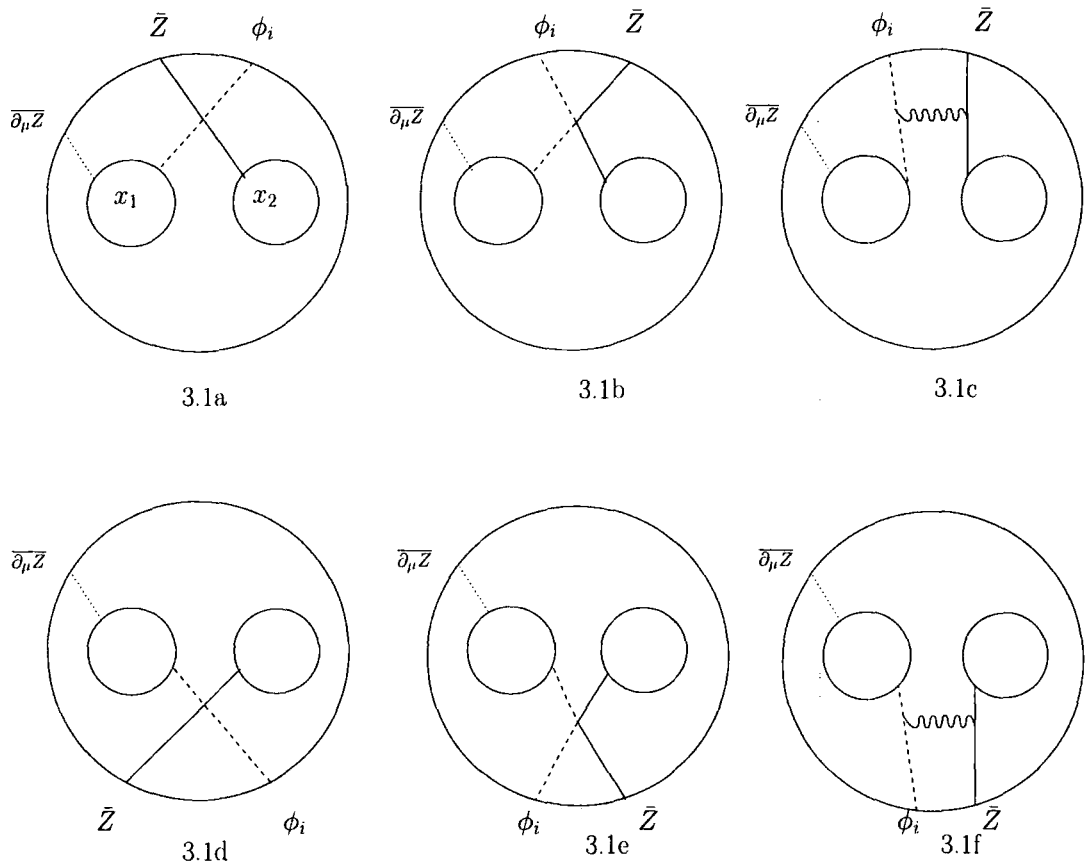
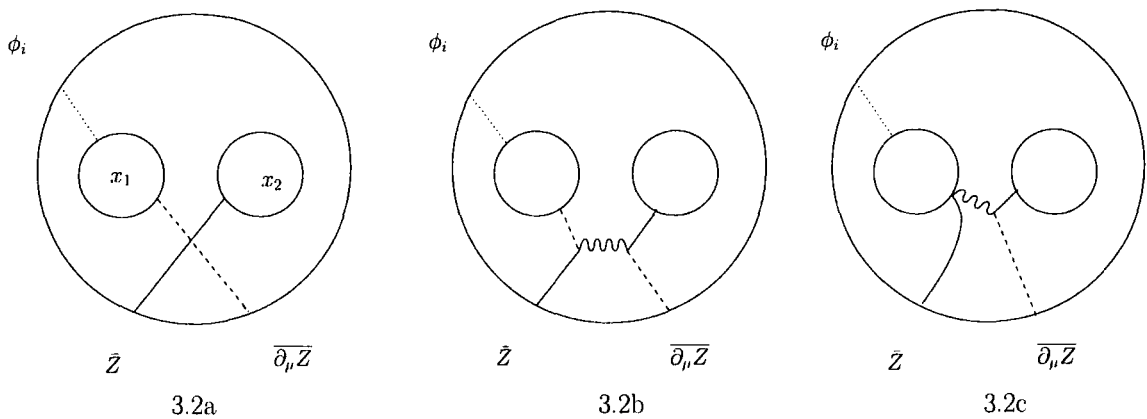


Figure 3.1: Diagrams with scalar impurity interacting. Diagrams 3.1a and 3.1d have positive signs, all the others have negative signs.

$P_I$  and  $P_{II}$  come from summing over the BMN phase factors, and their expressions are summarised in Appendix E. Mirror diagrams are associated with the complex conjugate coefficients  $\bar{P}_I$  and  $\bar{P}_{II}$ . Finally, the function  $X$  is defined in (F.2) of Appendix F.

There are additional diagrams, drawn in Figures 3.2 and 3.3, where the interaction involves now the vector impurity.

These diagrams are identical to those in Figure 5 and 6 of [62], with the only modification that the non-interacting impurity is now a scalar impurity (whereas in Figure 5 and 6 of [62] it was a vector impurity). We will not compute again these diagrams, and instead borrow the result from [62]. Their contribution turns out to be precisely the same of the contribution (3.82) from the diagrams where the scalar impurity interacts.


 Figure 3.2: Diagrams with vector impurity interacting associated to  $P_I$ .

The final result for the pure BMN diagrams is therefore:

$$\left(\frac{2}{g^2}\right) \left(\frac{g^2}{2}\right)^4 \cdot 8(P_I - P_{II} + \bar{P}_I - \bar{P}_{II}) \cdot \delta_{\mu\nu} \delta_{ij} \cdot X. \quad (3.83)$$

This quantity has still to be multiplied by the normalisations of the operators, in which we include an extra factor of  $J_2 = (1 - y) \cdot J$  coming from inequivalent Wick contractions of  $\mathcal{O}_{\text{vac}}$  with the rest,

$$\frac{1}{\sqrt{J}} \frac{\sqrt{1-y}}{\sqrt{y}} \left(\frac{1}{\sqrt{2}}\right)^2. \quad (3.84)$$

### 3.3.2 Diagrams from compensating terms

The compensating term is present in both operators at  $x_3$  and  $x_1$ , therefore there are three subclasses of diagrams: (i) diagrams with compensating term in the “external” operator at  $x_3$  and pure BMN part in the “internal” (small) operator at  $x_1$ ; (ii) diagrams where the compensating term of both operators at  $x_1$  and  $x_3$  is considered; and (iii) diagrams where the compensating term of the small operator at  $x_1$  and the pure BMN part of the operator at  $x_3$  are taken.

Each diagram in class (i) vanishes separately, since the only way to contract the impurity  $D_\nu Z$  in  $\mathcal{O}_{j\nu,n}^{y,J}(x_1)$  is with a  $\bar{Z}$  in  $\bar{\mathcal{O}}_{i\mu,m}^J(x_3)$ , and this contraction vanishes (see footnote 10). Moreover, it is not difficult to see that the total contribution of the diagrams in class (ii) vanishes. Hence we are left with diagrams in class (iii), which we now discuss.

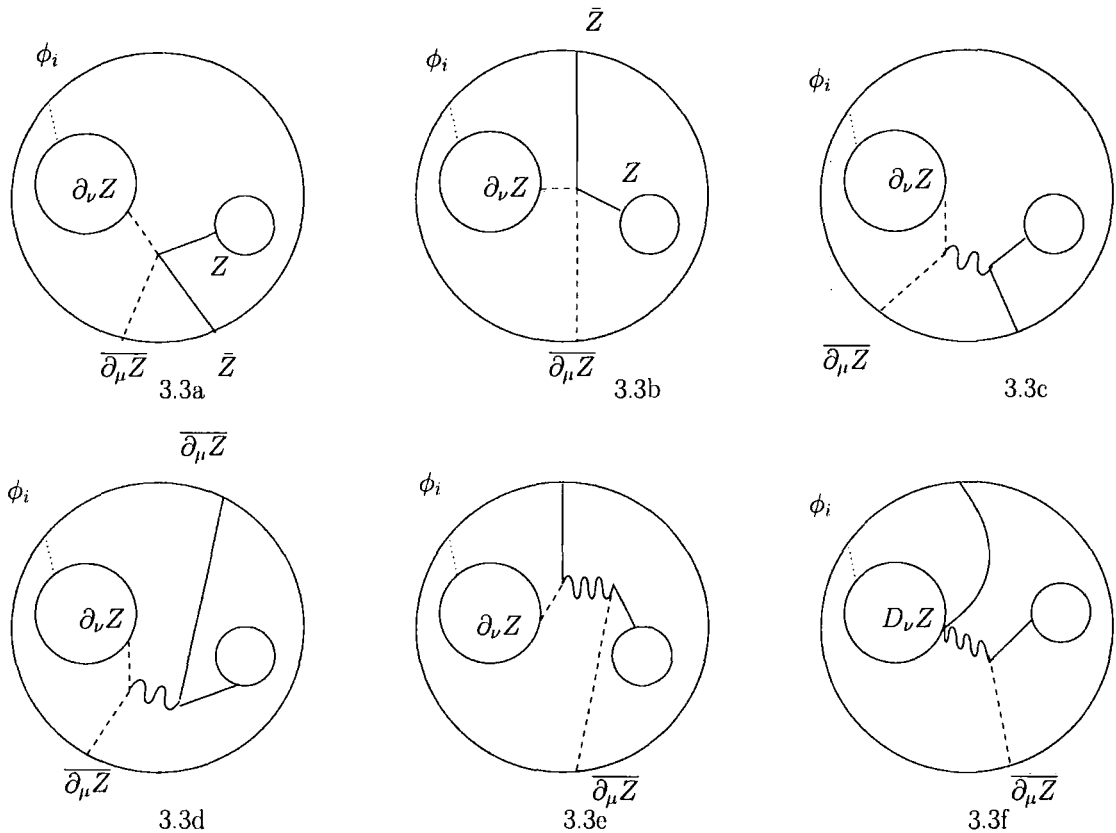


Figure 3.3: Diagrams with vector impurity interacting associated to  $P_{II}$ .

We start by considering diagrams without gluons. The first three diagrams are represented in Figure 3.4, and their contribution is

$$\left(\frac{2}{g^2}\right) \left(\frac{g^2}{2}\right)^4 \cdot (2X - X - X \cdot \bar{q}^{J_2}) \delta_{\mu\nu} \delta_{ij}, \quad (3.85)$$

where  $q = \exp(2\pi m/J)$  is the phase factor of the BMN operator at  $x_3$ . The first term in the right hand side of (3.85) comes from the first diagram in Figure 3.4. This diagram is equal to the first diagram in Figure 5 of [62], from which we borrowed the result. The factor of 2 is easily seen from the term  $\text{Tr}(2Z\phi_i\bar{Z}\phi_i)$  in  $-V_F$ , see (C.5). The opposite sign of the second term in (3.85) is also seen from the term  $-\text{Tr}(\phi_i\phi_i Z\bar{Z})$  in  $-V_F$ . The third term comes from the term  $-\text{Tr}(\phi_i\phi_i\bar{Z}Z)$  in  $-V_F$ , and carries a BMN phase factor  $\bar{q}^{J_2}$ . There are also mirror diagrams, where the interaction occurs at the bottom of the diagram (similarly to the fourth, fifth and sixth diagram in Figure 3.1). As usual, their effect is to add the complex conjugate of the previous

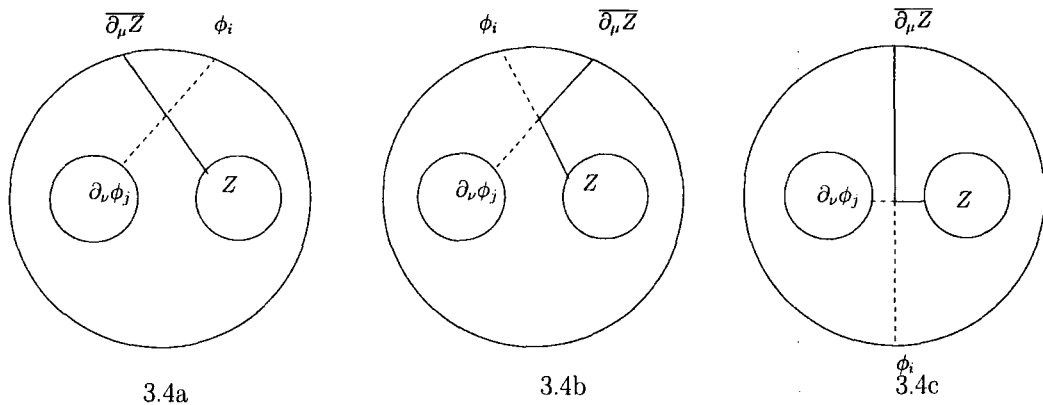


Figure 3.4: Diagrams originating from the compensating term in the ‘internal’ operator (at  $x_1$ ). In these diagrams no gluons are emitted or exchanged.

result, so that the final result for diagrams without gluons is:

$$\left(\frac{2}{g^2}\right) \left(\frac{g^2}{2}\right)^4 \cdot 2X \cdot (1 - \cos(2\pi my)) \delta_{\mu\nu} \delta_{ij} . \quad (3.86)$$

We now consider diagrams where a gluon is emitted from the covariant derivative  $D_\nu \phi_j$  at  $x_1$ . These gluon emission diagrams are represented in Figure 3.5. The total result for them is:

$$\left(\frac{2}{g^2}\right) \left(\frac{g^2}{2}\right)^4 \cdot (3X - 3X \cdot \bar{q}^{J_1}) \delta_{\mu\nu} \delta_{ij} . \quad (3.87)$$

The first term on the right hand side of (3.87) corresponds to the first diagram in Figure 3.5. This diagram was computed in [62] (it is the third diagram in Figure 5), from which we took the result. The only difference is that in the present case it is accompanied by phase factor equal to 1. The second term come from the second diagram in Figure 3.5, and carries a BMN phase factor equal to  $\bar{q}^{J_1}$ . Again, there are also mirror diagrams, where the interaction occurs at the bottom of the diagram. Their effect is to add the complex conjugate of the previous result, so that the final result for diagrams with gluon emission is:

$$\left(\frac{2}{g^2}\right) \left(\frac{g^2}{2}\right)^4 \cdot 6X \cdot (1 - \cos(2\pi my)) \delta_{\mu\nu} \delta_{ij} . \quad (3.88)$$

Finally, we have to consider gluon interaction diagrams. These are depicted in Figure 3.6 and, as before, there are also mirror diagrams, where the interaction occurs at the bottom of each diagram. However, each of the diagrams vanishes separately (this is

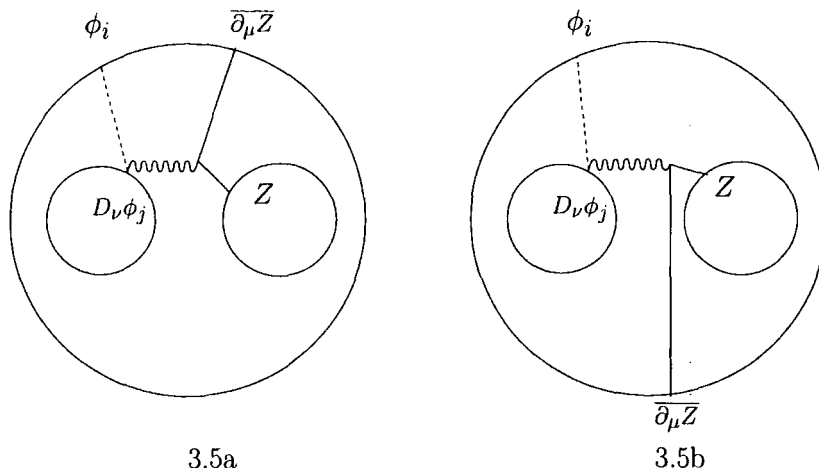


Figure 3.5: Gluon emission diagrams originating from the compensating term in the internal operator.

to be contrasted with the case of scalar interactions, where gluon interactions double up the result for the interaction from the scalar potential, as discussed in the previous subsection). This was shown again in [62] (second diagram in Figure 5 of that paper).

Adding (3.86) and (3.88) we get the total contribution of the compensating term diagrams,

$$\left(\frac{2}{g^2}\right) \left(\frac{g^2}{2}\right)^4 \cdot 16X \cdot \sin^2(\pi m y) \delta_{\mu\nu} \delta_{ij} . \tag{3.89}$$

The result (3.89) has still to be multiplied by the normalisations of the operators (3.84).

### 3.3.3 Summary: the result for mixed impurities

We add the results (3.83) and (3.89), and use (E.3) of Appendix E, to get the total result

$$\left(\frac{g^2}{2}\right)^3 \cdot (-16X) \cdot (\delta_{\mu\nu} \delta_{ij}) \cdot \frac{m + n/y}{m - n/y} \sin^2 \pi m y . \tag{3.90}$$

Multiplying this result by the normalisation (3.84), and amputating a factor of  $[(g^2/2) \Delta(x_{13})]^2$  we obtain

$$\langle \mathcal{O}_{j\nu,n}^{y \cdot J}(x_1) \mathcal{O}_{\text{vac}}^{(1-y) \cdot J}(x_2) \bar{\mathcal{O}}_{i\mu,m}^J(x_3) \rangle \Big|_{\log x_{12} \text{ term}} =$$

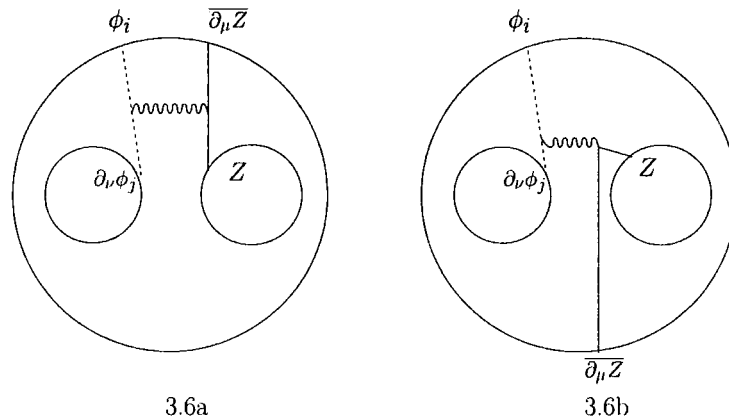


Figure 3.6: Gluon interaction diagrams, from the compensating term in the internal operator.

$$\frac{1}{\sqrt{J}} \frac{\sqrt{1-y}}{\sqrt{y}} \left( \frac{1}{\sqrt{2}} \right)^2 \left( \frac{g^2}{2} \right) \cdot \left( -16 \frac{m+n/y}{m-n/y} \sin^2 \pi m y \right) \frac{\log(x_{12}\Lambda)^{-1}}{8\pi^2} \delta_{\mu\nu} \delta_{ij} =$$

$$-\lambda' g_2 C_{m,ny} \cdot \frac{1}{2} \left( m^2 - \frac{n^2}{y^2} \right) \cdot \log(x_{12}\Lambda)^{-1} \delta_{\mu\nu} \delta_{ij} , \quad (3.91)$$

where  $C_{m,ny}$  is defined in (3.40). Equation (3.91) is the principal result of this section.

The coefficient  $[b_{m,ny}]_{\text{scalar-vector}}$  in (3.55) immediately follows by comparing (3.91) to (3.78). Finally, the three-point function coefficient (3.51) for mixed impurities is obtained from (3.55) and (3.49).

## 3.4 The correspondence for an arbitrary number of scalar impurities

In this section we shall evaluate the coefficients of three-point functions of  $\Delta$ -BMN operators with arbitrary number of scalar impurities, and use this information to derive the single- double-trace two-point function of operators with an arbitrary number of scalar impurities.

### 3.4.1 The results in field theory

Every BMN operator with an arbitrary number of impurities can be decomposed into two pieces. The pure BMN part, which contains no  $\bar{Z}$ , and the compensating part,



### 3.4. The correspondence for an arbitrary number of scalar impurities 102

which contains  $\bar{Z}$ . In order to make the structure of the general BMN operator clear, let us consider the example of an operator with three impurities. The pure BMN part consists of two terms:

$$\mathcal{O}_{\text{pure}} = \sum_{0 \leq l_2 \leq l_3} q_2^{l_2} q_3^{l_3} \text{Tr}(\phi_1 Z^{l_2} \phi_2 Z^{l_3-l_2} \phi_3 Z^{J-l_3}) + \sum_{0 \leq l_3 \leq l_2} q_2^{l_2} q_3^{l_3} \text{Tr}(\phi_1 Z^{l_3} \phi_3 Z^{l_2-l_3} \phi_2 Z^{J-l_2}). \quad (3.92)$$

In all cases  $\phi_1$  is positioned first in the trace, while we have to sum over all the different orderings of the remaining impurities. Let us denote by  $\phi_{p(i)}$  the impurity which sits in the  $i^{\text{th}}$  position of a specific ordering of the impurities, and  $l_{p(i)}$  the number of  $Z$  fields between  $\phi_1$  and  $\phi_{p(i)}$  (in the example given above  $p(2) = 2, p(3) = 3$  for the first trace while  $p(2) = 3, p(3) = 2$  for the second trace). Next we consider the compensating terms. In our example, these should be written as

$$\begin{aligned} \mathcal{O}_{\text{comp}} = & - \delta_{\phi_2 \equiv \phi_3} \sum_{0 \leq l_2} (q_2 q_3)^{l_2} \text{Tr}(\phi_1 Z^{l_2} \bar{Z} Z^{J-l_2}) - \delta_{\phi_1 \equiv \phi_2} \sum_{0 \leq l_3} q_3^{l_3} \text{Tr}(\bar{Z} Z^{l_3} \phi_3 Z^{J-l_3}) \\ & - \delta_{\phi_1 \equiv \phi_3} \sum_{0 \leq l_2} q_2^{l_2} \text{Tr}(\bar{Z} Z^{l_2} \phi_2 Z^{J-l_2}). \end{aligned} \quad (3.93)$$

In other words, whenever two impurities in  $\mathcal{O}_{\text{pure}}$  are of the same flavour, we add a compensating term where these two impurities are replaced by  $\bar{Z}$ .

With this example in mind, it is not difficult to write down the most general form of an operator with  $n$  impurities,

$$\mathcal{O}_{\{n_i\}} \equiv \frac{1}{\sqrt{J^{n-1} N^{J+n}}} \sum_{p=\text{perm}\{2, \dots, n\}} \mathcal{O}_{\{n_i\}}^{1p}, \quad (3.94)$$

where  $i = 1, \dots, n$  and

$$\mathcal{O}_{\{n_i\}^{\text{pure}}}^{1p(2)\dots p(n)} = \sum_{0 \leq l_{p(2)} \leq l_{p(3)} \dots \leq l_{p(n)}} \prod_{i=2}^n q_{p(i)}^{l_{p(i)}} \text{Tr}(\phi_1 Z^{l_{p(2)}} \phi_{p(2)} Z^{l_{p(3)}-l_{p(2)}} \phi_{p(3)} \dots \phi_{p(n)} Z^{J-l_{p(n)}}), \quad (3.95)$$

$$\begin{aligned} \mathcal{O}_{\{n_i\}^{\text{comp}}}^{1p(2)\dots p(n)} = & -\frac{1}{2} \sum_{k=2}^{n-1} \delta_{\phi_{p(k)} \equiv \phi_{p(k+1)}} \sum_{0 \leq l_{p(2)} \dots \leq l_{p(k)} \leq l_{p(k+2)} \dots \leq l_{p(n)}} \prod_{i=2, i \neq p(k+1)}^n q_{p(i)}^{l_{p(i)}} q_{p(k+1)}^{l_{p(k+1)}} \\ & \text{Tr}(\phi_1 Z^{l_{p(2)}} \phi_{p(2)} \dots Z^{l_{p(k)}-l_{p(k-1)}} \bar{Z} Z^{l_{p(k+2)}-l_{p(k)}} \phi_{p(k+2)} \dots \phi_{p(n)} Z^{J-l_{p(n)}}) \\ & - \delta_{\phi_1 \equiv \phi_{p(2)}} \sum_{0 \leq l_{p(3)} \dots \leq l_{p(n)}} \prod_{i=3}^n q_{p(i)}^{l_{p(i)}} \text{Tr}(\bar{Z} Z^{l_{p(3)}} \phi_{p(3)} \dots \phi_{p(n)} Z^{J-l_{p(n)}}) \end{aligned} \quad (3.96)$$

### 3.4. The correspondence for an arbitrary number of scalar impurities 103

The origin of the  $\frac{1}{2}$  in front of the first term of  $\mathcal{O}_{\{n_i\}\text{comp}}^{1p(2)\dots p(n)}$  is quite clear. It comes from the fact that we have counted twice the same term, since we have two orderings where  $\phi_{p(i)}$  and  $\phi_{p(i+1)}$  coincide. The one with  $\phi_{p(i)}$  coming first and  $\phi_{p(i+1)}$  following and vice versa. Finally, we note that in principle more compensating terms should be added to the right hand side of (3.96) when two or more pairs of impurities coincide. These terms are irrelevant for our purposes in the BMN limit.

In the above expression,  $\phi_{p(i)} \in \{\phi_1, \phi_2, \phi_3, \phi_4\}$ . This makes the meaning of the Kronecker  $\delta$ -symbols functions obvious. It should also be noted that the operator given above is normalised so that its two point function is one at the free theory level.<sup>11</sup>

As in section 3.2, we will need the expressions for double-trace operators,

$$\mathcal{T}_{\{n_i\}\{k_i\}}^{J,y} = : \mathcal{O}_{\{n_i\}}^{J,y} :: \mathcal{O}_{\{k_i\}}^{J,(1-y)} : . \quad (3.97)$$

On general grounds, the two-point function of the double- and single-trace BMN operators takes the form

$$\langle \mathcal{T}_{\{n_i\}\{k_i\}}^{J,y}(0) \bar{\mathcal{O}}_{\{m_i\}}^J(x) \rangle = g_2 C_{\text{free}} [1 + \lambda' (a + b + c) \log(x\Lambda)^{-2}] . \quad (3.98)$$

In (3.98) we have suppressed the indices of  $a$ ,  $b$  and  $c$ . Here  $\bar{\mathcal{O}}_{\{m_i\}}^J$  contains  $p_3$  impurities, whereas the two single-trace expressions in  $\mathcal{T}_{\{n_i\}\{k_i\}}^{J,y}$  contain  $p_1$  and  $p_2$  impurities, respectively.

Compared to (3.41), the above equation contains a new coefficient,  $c$ . This is due to the fact that the second operator on the right hand side of (3.97) is no longer just the vacuum, but instead is a generic string state. This results in an additional logarithmic part for the three-point function (3.39), i.e.  $c \cdot \log(x_{32}\Lambda)^2$ .

The next step is to calculate the matrix of classical overlaps  $S$ . To this end, we will need to compute the correlation functions of single-trace operators with double-trace operators to  $\mathcal{O}(g_2)$ . We will not need the correlation functions of two different double-trace operators, because these overlaps are of  $\mathcal{O}(g_2^2)$ . Hence, it is possible

<sup>11</sup>Strictly speaking this is true only when all the  $q$ 's which correspond to a particular  $\phi$ , say  $\phi_1$ , are different. This is the case that we are going to consider. However what follows can be applied with slight modifications to the case where two or more of the  $q$ 's are the same.

### 3.4. The correspondence for an arbitrary number of scalar impurities 104

to treat each double-trace operator independently and write the expressions (3.100), (3.104) and (3.105) as two by two matrices.

Thus the classical overlap is given by

$$S = \mathbb{1} + g_2 s , \quad (3.99)$$

where

$$s = \begin{pmatrix} 0 & C_{\text{free}} \\ C_{\text{free}} & 0 \end{pmatrix} , \quad (3.100)$$

and

$$C_{\text{free}} = \sum_{\text{perm}'} C_{\text{free}}^p , \quad (3.101)$$

where

$$C_{\text{free}}^p = \frac{(-1)^{p_2}}{\pi^{p_3} \sqrt{y^{p_1-1} (1-y)^{p_2-1}}} J \prod_{a=1}^{p_1} \frac{\sin(\pi m_{p(a)} y)}{m_{p(a)} - n_a/y} \prod_{b=1}^{p_2} \frac{\sin(\pi m_{p(b+p_1)} y)}{m_{p(b+p_1)} - k_b/(1-y)} . \quad (3.102)$$

The sum in (3.101) is over all the admissible permutations of the  $\{m_i\}$ , which label the barred BMN operator, as on the left hand side of (3.98). A permutation is admissible only when the permuted numbers belong to  $\phi$ 's of the same flavour.

Our next goal is to determine the anomalous dimension matrix  $T$ ,

$$T = d + g_2 t , \quad (3.103)$$

where the diagonal part  $d$  contains the anomalous dimensions, as in (4.47),

$$d = \lambda' \begin{pmatrix} \sum_{a=1}^{p_3} m_a^2/2 & 0 \\ 0 & \sum_{a=1}^{p_1} n_a^2/2y^2 + \sum_{a=1}^{p_2} k_a^2/2(1-y)^2 \end{pmatrix} , \quad (3.104)$$

and

$$t = \lambda' \begin{pmatrix} 0 & t_{12} \\ t_{21} & 0 \end{pmatrix} . \quad (3.105)$$

$t_{12}$  can be read from (3.98), and is given by

$$t_{12} = \sum_{\text{perm}'} C_{\text{free}}^p (a + b + c) . \quad (3.106)$$

### 3.4. The correspondence for an arbitrary number of scalar impurities 105

The coefficients  $a$  and  $c$  are given by the anomalous dimensions of the first and second operators in the definition of  $\mathcal{T}$ ,

$$a = \sum_{a=1}^{p_1} \frac{n_a^2}{2y^2}, \quad c = \sum_{a=1}^{p_2} \frac{k_a^2}{2(1-y)^2}. \quad (3.107)$$

The contributions of  $\sum_{\text{perm}'} C_{\text{free}}^p a$  and  $\sum_{\text{perm}'} C_{\text{free}}^p c$  to  $t_{12}$  in (3.106) factorise, to give

$$C_{\text{free}} a, \quad C_{\text{free}} c, \quad (3.108)$$

respectively.

The remaining contribution to  $t_{12}$  is  $\sum_{\text{perm}'} C_{\text{free}}^p b$ . It can be extracted from the coefficient of the corresponding three-point function following the same logic as in section 3.2. These three-point functions of generic BMN operators with arbitrary numbers of scalar impurities are computed in the following section. Our result is

$$\begin{aligned} \sum_{\text{perm}'} C_{\text{free}}^p b = & \sum_{\text{perm}'} C_{\text{free}}^p \frac{1}{2} \left( \sum_{a=1}^{p_1} m_{p(a)} \left( m_{p(a)} - \frac{n_a}{y} \right) + \sum_{a=1}^{p_2} m_{p(a+p_1)} \left( m_{p(a+p_1)} - \frac{k_a}{1-y} \right) \right. \\ & + \frac{1}{2} \sum_{(a,b)}^{p_1} (m_{p(a)} - n_a)(m_{p(b)} - n_b) + \frac{1}{2} \sum_{(a,b)}^{p_2} (m_{p(p_1+a)} - k_a)(m_{p(p_1+b)} - k_b) \\ & \left. + \frac{1}{2} \sum_{a=1}^{p_1} \sum_{b=1}^{p_2} (m_{p(a)} - n_a)(m_{p(p_1+b)} - k_b) \right). \end{aligned} \quad (3.109)$$

The double sum summation notation  $(a, b)$  means that we do not distinguish between the pair  $a, b$  and the pair  $b, a$  ( $a \neq b$ ).

As in section 3.2, the anomalous dimension matrix  $\Gamma$  in the isomorphic to string basis is given by

$$\Gamma = d + g_2 t', \quad t' = t - \frac{1}{2} \{s, d\}, \quad (3.110)$$

where

$$\{s, d\} = \lambda' \begin{pmatrix} 0 & C_{\text{free}}(\delta_1 + \delta_2 + \delta_3) \\ C_{\text{free}}(\delta_1 + \delta_2 + \delta_3) & 0 \end{pmatrix}, \quad (3.111)$$

### 3.4. The correspondence for an arbitrary number of scalar impurities 106

and  $\delta_i$  is the anomalous dimension of the  $i^{\text{th}}$  operator ( $i = 1, 2, 3$ ). After some algebra, we obtain the final result:

$$\begin{aligned} \Gamma_{12} = & \frac{\lambda' g_2}{4} \sum_{\text{perm}'} C_{\text{free}}^p \left( \sum_{a=1}^{p_1} \left( m_{p(a)} - \frac{n_a}{y} \right)^2 + \sum_{a=1}^{p_2} \left( m_{p(a+p_1)} - \frac{k_a}{1-y} \right)^2 \right. \\ & + \sum_{(a,b)}^{p_1} (m_{p(a)} - n_a)(m_{p(b)} - n_b) \\ & \left. + \sum_{(a,b)}^{p_2} (m_{p(p_1+a)} - k_a)(m_{p(p_1+b)} - k_b) + \sum_{a=1}^{p_1} \sum_{b=1}^{p_2} (m_{p(a)} - n_a)(m_{p(p_1+b)} - k_b) \right). \end{aligned} \quad (3.112)$$

This is our final expression for matrix elements in gauge theory. In the next section we will compute the corresponding three-string amplitude and compare it to (3.112). We will find perfect agreement.

#### 3.4.2 The results in string field theory

In this subsection we assemble the basic ingredients of the SFT calculation of the string amplitude for states with an arbitrary number of scalar impurities. The amplitude has the form [52, 53] (we refer the reader to Appendix B for more details)

$$\langle \Phi | \mathbf{P} | V_B \rangle, \quad (3.113)$$

where  $\langle \Phi |$  represents the three external string states,  $|V_B\rangle$  is the kinematic part of the bosonic vertex (D.2), and the prefactor  $\mathbf{P}$  is given by

$$\mathbf{P} = C_{\text{norm}} \sum_{r=1}^3 \sum_{-\infty}^{\infty} \frac{\omega_{rn}}{\mu \alpha_r} \alpha_n^{rI\dagger} \alpha_{-n}^{rI}. \quad (3.114)$$

$C_{\text{norm}}$  is defined in such a way that we get agreement with the field theory calculation. Its value is taken to be

$$C_{\text{norm}} = -\frac{1}{2} g_2 \frac{\sqrt{y(1-y)}}{\sqrt{J}} (-1)^{\frac{1}{2} \sum_{r=1}^3 \sum_{m=-\infty}^{+\infty} \alpha_m^{rI\dagger} \alpha_m^{rI}}. \quad (3.115)$$

The prefactor can act on the external bra-state and give a sum of  $2p_3$  terms, each of which has an external state identical to the initial  $\langle \Phi |$ , except one of the  $\alpha_n$ 's which has changed to  $\alpha_{-n}$ . Of course each of these terms is multiplied by the corresponding  $\omega_{rn}/\mu \alpha_r$ . What we are left with is the action of the exponential in  $|V_B\rangle$ . In order

### 3.4. The correspondence for an arbitrary number of scalar impurities 107

to keep the comparison to field theory as simple as possible, we choose a certain set of associations between the impurities of the third string and the impurities of the other two strings. The final result will be a sum over all possible such associations, i.e. permutations of this set.

When an external oscillator has not been changed by the prefactor, the action of  $|V_B\rangle$  gives a factor of  $\hat{N}_{n_a n'_a}^{3r}$  where  $r = 1, 2, 3$ . But if the external oscillator has been changed by the prefactor, the action of  $|V_B\rangle$  gives a factor of

$$F_{n_a - n'_a}^{3r} = \hat{N}_{-n_a n'_a}^{3r} \frac{\omega_{3n_a}}{\mu\alpha_3} + \hat{N}_{n_a - n'_a}^{3r} \frac{\omega_{rn'_a}}{\mu\alpha_r} = \hat{N}_{n_a - n'_a}^{3r} \left( \frac{\omega_{3n_a}}{\mu\alpha_3} + \frac{\omega_{rn'_a}}{\mu\alpha_r} \right). \quad (3.116)$$

One can evaluate  $F_{n_a - n'_a}^{3r}$  to get

$$\begin{aligned} F_{n_a - n'_a}^{31} &= (-1)^{n_a + n'_a} \frac{\lambda'}{2\pi\sqrt{y}} \left( n_a - \frac{n'_a}{y} \right)^2 \frac{\sin(\pi n_a y)}{n_a - n'_a/y}, \\ F_{n_a - n'_a}^{32} &= (-1)^{n_a + 1} \frac{\lambda'}{2\pi\sqrt{1-y}} (n_a - n'_a/(1-y))^2 \frac{\sin(\pi n_a y)}{n_a - n'_a/(1-y)}, \\ F_{n_a - n'_a}^{33} &= (-1)^{n_a + n'_a + 1} \frac{2 \sin(\pi n_a y) \sin(\pi n'_a y)}{\pi\mu}, \\ F_{n_a - n'_a}^{11} &= \frac{2(-1)^{n_a + n'_a}}{4\pi\mu y}, \\ F_{n_a - n'_a}^{22} &= \frac{2}{4\pi\mu(1-y)}. \end{aligned} \quad (3.117)$$

We are now in position to write down the result for a given permutation. This reads

$$\begin{aligned} &\langle \Phi | \mathcal{P} | V_B \rangle = \\ &C_{\text{norm}} \left[ \sum_a^{p_1} F_{m_a - n_a}^{31} \prod_{b \neq a}^{p_1} \hat{N}_{m_b n_b}^{31} \prod_{b=1}^{p_2} \hat{N}_{m_{b+p_1} k_b}^{32} + \sum_a^{p_2} F_{m_a - k_a}^{32} \prod_{b=1}^{p_1} \hat{N}_{m_b n_b}^{31} \prod_{b \neq a}^{p_2} \hat{N}_{m_{b+p_1} k_b}^{32} \right. \\ &\quad + \left( \sum_{(a,b)}^{p_1} F_{m_a - m_b}^{33} \hat{N}_{n_a n_b}^{11} + \sum_{(a,b)}^{p_1} F_{n_a - n_b}^{11} \hat{N}_{m_a m_b}^{33} \right) \prod_{c \neq a,b}^{p_1} \hat{N}_{m_c n_c}^{31} \prod_{c=1}^{p_2} \hat{N}_{m_{c+p_1} k_c}^{32} \\ &\quad + \left( \sum_{(a,b)}^{p_2} F_{m_{p_1+a} - m_{p_1+b}}^{33} \hat{N}_{k_a k_b}^{22} + \sum_{(a,b)}^{p_2} F_{k_a - k_b}^{22} \hat{N}_{m_{p_1+a} m_{p_1+b}}^{33} \right) \prod_{c=1}^{p_1} \hat{N}_{m_c n_c}^{31} \prod_{c \neq a,b}^{p_2} \hat{N}_{m_{c+p_1} k_c}^{32} \\ &\quad \left. + \left( \sum_{a=1}^{p_1} \sum_{b=1}^{p_2} F_{m_a - m_{p_1+b}}^{33} \hat{N}_{m_a k_b}^{12} + \sum_{a=1}^{p_1} \sum_{b=1}^{p_2} F_{n_a - k_b}^{12} \hat{N}_{m_a m_{p_1+b}}^{33} \right) \prod_{c \neq a}^{p_1} \hat{N}_{m_c n_c}^{31} \prod_{c \neq b}^{p_2} \hat{N}_{m_{c+p_1} k_c}^{32} \right]. \end{aligned} \quad (3.118)$$

As before, in the double sum over all pairs  $(a, b)$  which appears above we do not distinguish between the pair  $(a, b)$  and the pair  $(b, a)$ . Making use of the expressions

for the Neumann matrices from [98] it is now easy to obtain the final expression for the matrix element in string theory:

$$\begin{aligned}
 \langle \Phi | P | V_B \rangle = & \frac{C_{\text{free}}^p}{4} g_2 \lambda' \left( \sum_{a=1}^{p_1} \left( m_a - \frac{n_a}{y} \right)^2 + \sum_{a=1}^{p_2} \left( m_{a+p_1} - \frac{k_a}{1-y} \right)^2 \right. \\
 & + \sum_{(a,b)}^{p_1} (m_a - n_a)(m_b - n_b) + (m_b - n_a)(m_a - n_b) \\
 & + \sum_{(a,b)}^{p_2} (m_{p_1+a} - k_a)(m_{p_1+b} - k_b) + (m_{p_1+b} - k_a)(m_{p_1+a} - k_b) \\
 & \left. + \sum_{a=1}^{p_1} \sum_{b=1}^{p_2} (m_a - n_a)(m_{p_1+b} - n_b) + (m_{p_1+b} - n_a)(m_a - n_b) \right). \quad (3.119)
 \end{aligned}$$

One should note that in calculating the three string vertex we did not take into account terms where there were two contractions of oscillators belonging to the same string if the prefactor had not acted on one of these oscillators previously. This is so because these terms are of order  $(1/\mu)^4 = \lambda'^2$ , as can be easily seen.<sup>12</sup>

In order to get the final string theory result, we should not forget to sum (3.119) over all the admissible permutations, as we have done for the field theory result. This means that the first line of (3.119) should be summed over all the possible permutations, while the remaining lines should be summed over all permutations except those which exchange the  $m$ 's associated with the labels  $a$  and  $b$  (more precisely, the permutations which exchange  $m_a$  with  $m_b$ ,  $m_{p_1+a}$  with  $m_{p_1+b}$ ,  $m_a$  with  $m_{p_1+b}$  in the second, third and fourth line of (3.119), respectively). Including these permutations would result in a double-counting. Once this sums are performed, we obtain perfect agreement with the field theory result (3.112).

### 3.5 A technical aside: calculation of general scalar BMN three-point functions

This final section is devoted to the derivation of the expression (3.109).

<sup>12</sup>There is a subtlety in writing (3.119), since the  $C^p$  for each term in that equation are in fact different: to each term in (3.119) one should associate the  $C^p$  corresponding to the permutation of the indices which label  $m$ ,  $n$  and  $k$  appearing in the term considered.

Our goal is to calculate  $\langle \mathcal{O}_{\{n_i\}}^{J,y}(x_1) \mathcal{O}_{\{k_i\}}^{J,(1-y)}(x_2) \bar{\mathcal{O}}_{\{m_i\}}^J(0) \rangle$ . To simplify the notation, we will rename the operators in this Green's function as  $\mathcal{O}_1(x_1)$ ,  $\mathcal{O}_2(x_2)$  and  $\bar{\mathcal{O}}_3(0)$ . Let us assume that there are  $f_1^{(i)}$   $\phi_1$ 's,  $f_2^{(i)}$   $\phi_2$ 's,  $f_3^{(i)}$   $\phi_3$ 's and  $f_4^{(i)}$   $\phi_4$ 's in the  $i^{\text{th}}$  operator where  $i = 1, 2, 3$ . We consider the case where  $f_1^{(3)} = f_1^{(1)} + f_1^{(2)}$  with similar relations holding for the other three impurities.

There are of course many different diagrams. In order to deal efficiently with them, let us select a particular set of Wick contractions between the impurities of the barred operator and the impurities of the unbarred operators. Obviously, only impurities of the same flavour can be contracted. The full result will then be a sum over all the different permutations of such contractions.

We start by considering the diagrams where the pure BMN part is taken in each of the three operators. These are drawn in Figure 3.7. It is easy to see that there are  $f_1^{(3)}! f_2^{(3)}! f_3^{(3)}! f_4^{(3)}!$  different contributions. Let us select one of them and draw the corresponding diagrams, Figure 3.7, in which the  $i^{\text{th}}$   $\phi_1$  field of  $\bar{\mathcal{O}}_3(0)$  interacts with the  $n^{\text{th}}$   $\phi_1$  field of  $\mathcal{O}_1(x_1)$ , while all the other fields are freely contracted. The phase factor associated with these free contractions becomes, in the BMN limit:

$$\begin{aligned}
 P_2 &= \prod_{a \neq n}^{p_1} \sum_{l_a=1}^{J_1} (\bar{q}_a r_a)^{l_a} \prod_{b=1}^{p_2} \sum_{l_b=J_1+1}^J (\bar{q}_{p_1+b} p_b)^{l_b} \\
 &= \prod_{a \neq n}^{p_1} \sum_{l_a}^{J_1} e^{-2\pi i(m_a - \frac{n_a}{y}) \frac{l_a}{J}} \prod_{b=1}^{p_2} \sum_{l_b=J_1+1}^J e^{-2\pi i(m_{p_1+b} - \frac{k_b}{1-y}) \frac{l_b}{J}} \\
 &= J^{p_3-1} \prod_{a \neq n}^{p_1} \int_0^y dx e^{-2\pi i(m_a - \frac{n_a}{y})x} \prod_{b=1}^{p_2} \int_y^1 dx e^{-2\pi i(m_{p_1+b} - \frac{k_b}{y})x} \\
 &= J^{p_3-1} \prod_{a \neq n}^{p_1} e^{-\pi i m_a y} \frac{\sin \pi m_a y}{(m_a - n_a/y)\pi} \prod_{b=1}^{p_2} e^{-\pi i m_{p_1+b} y} \frac{(-1)^{p_2} \sin \pi m_{p_1+b} y}{(m_{p_1+b} - k_b/(1-y))\pi}.
 \end{aligned} \tag{3.120}$$

Recall that (3.92), (3.93) and (3.95), (3.96) do not contain  $q_1$ . In (3.120) and in what follows  $q_1$  is defined as  $q_1 = \prod_{i=2}^J \bar{q}_i$ , and  $q_i = e^{2\pi i m_i/J}$  is the phase factor of the  $i^{\text{th}}$  impurity ( $r_a$  and  $p_a$  are the phase factors of  $\mathcal{O}_1$  and  $\mathcal{O}_2$  respectively).

Note that in obtaining the above formula we have taken into account all the possible orderings of the freely contracting impurities.

We also need the phase factor associated with the fields which are involved in the

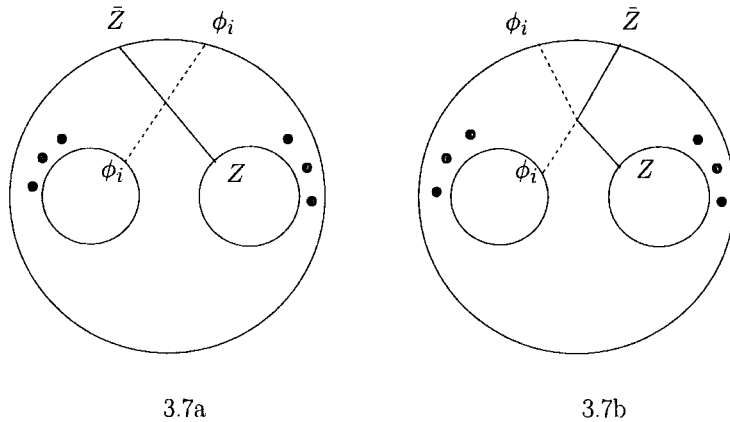


Figure 3.7: Feynman diagrams where a scalar impurity from  $\mathcal{O}_1$  interacts with a  $Z$  field. The dots stand for impurities which have free contractions. These diagrams are also accompanied by their mirror images, where the interaction occurs in the bottom part of the diagram.

interaction. This is given by

$$P_1 = (\bar{q}_i^{J_1} - 1)(\bar{q}_i - 1)g^2 = \frac{-4\pi m_i}{J} e^{-\pi i m_i y} \sin \pi m_i y . \quad (3.121)$$

The total phase factor will be  $P = P_1 P_2$ <sup>13</sup> Taking into account the normalisation of the operators, and evaluating the space-time integral associated with the vertex (see (F.1)), one gets:

$$G_3^{(1)} = \frac{J^{p_3}}{N \sqrt{J^{p_3-1} J_1^{p_1-1} J_2^{p_2-1}}} \prod_{a \neq n}^{p_1} \frac{\sin \pi m_a y}{m_a - n_a/y} \prod_{b=1}^{p_2} \frac{\sin \pi m_{p_1+b} y}{m_{p_1+b} - k_b/(1-y)} (-1)^{p_2} (-\lambda') \frac{m_i \sin \pi m_i y}{4\pi^{p_3}} \log \frac{x_1^2 x_2^2}{x_{12}^2} . \quad (3.122)$$

In the previous expression we are keeping only the  $\log x_{12}$  terms, which are relevant to determine the coefficient  $b$  in (3.98), similarly to what we did in section 3.2. We denoted by  $G_3^{(1)}$  the part of the three-point function which corresponds to the diagrams of Figure 3.7, and by  $p_3 = p_1 + p_2$  the number of the impurities of  $\mathcal{O}_3$ .

In order to make easier the comparison with the string theory result, we rewrite

<sup>13</sup>In this section the Lagrangian and Feynman rules of [74] are used.

(3.122) as

$$g_2 C_{\text{free}}^p b^{(1)} = \frac{J^{p_3}}{N \sqrt{J^{p_3-1} J_1^{p_1-1} J_2^{p_2-1}}} \prod_{a \neq n}^k \frac{\sin \pi m_a y}{m_a - n_a / y} \prod_{b=1}^{p_2} \frac{\sin \pi m_{p_1+b} y}{m_{p_1+b} - k_b / (1-y)} (-1)^{p_2} \frac{m_i \sin \pi m_i y}{2\pi^{p_3}}. \quad (3.123)$$

Equation (3.123) corresponds to the first term in the first line of (3.109). Until now we have considered only diagrams where the interacting  $\phi$  belongs to the operator  $\mathcal{O}_1$ . Of course, there are diagrams where it is an impurity in  $\mathcal{O}_2$  which interacts. These contributions produce the second term in the first line of (3.109).

Now we consider the diagrams in Figure 3.8. In these diagrams we take for

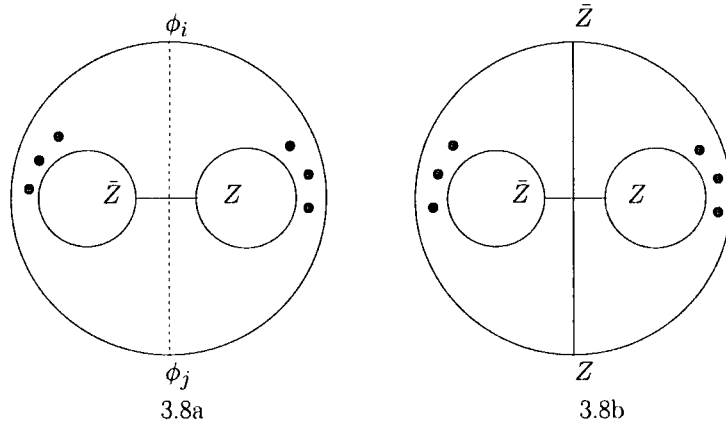


Figure 3.8: In Figure 3.8a we take the pure BMN part in the external operator, whereas in 3.8b we take the compensating term. In both cases we take the compensating term in  $\mathcal{O}_1$  and the pure BMN part in  $\mathcal{O}_2$ . Here  $i$  and  $j$  label the position of the corresponding  $\phi$  in the barred BMN operator.

$\mathcal{O}_1$  the compensating term, for  $\mathcal{O}_2$  the pure BMN part, and for  $\bar{\mathcal{O}}_3$  the pure BMN part (Figure 3.8a) or the compensating term (Figure 3.8b). In the case where two  $\phi_1$ 's interact, the number of different diagrams is  $f_1^{(3)}! f_2^{(3)}! f_3^{(3)}! f_4^{(3)}! \frac{f_1^{(1)}(f_1^{(1)}-1)}{4}$ . This number is obtained as follows. There are  $f_1^{(1)}(f_1^{(1)}-1)/2$  different ways to single out two  $\phi_1$ 's from the operator  $\mathcal{O}_1$ . This should be multiplied by the  $f_1^{(3)}(f_1^{(3)}-1)/2$  different ways in which we can choose two  $\phi_1$ 's from the barred operator  $\bar{\mathcal{O}}_3$ , times the number  $(f_1^{(3)}-2)! f_2^{(3)}! f_3^{(3)}! f_4^{(3)}!$  of independent free contractions of all the remaining impurities.

Evaluating the phase factor associated with the interacting fields we get

$$P_1 = (\bar{q}_i^{J_1} - 1)(\bar{q}_j^{J_1} - 1)g^2. \quad (3.124)$$

For the total phase factor one obtains

$$P = J^{p_1+p_2-2} \prod_{a \neq i,j}^{p_1} e^{-\pi i m_a y} \frac{\sin \pi m_a y}{(m_a - n_a/y)\pi} \prod_{b=1}^{p_2} e^{-\pi i m_{p_1+by}} \frac{\sin \pi m_{p_1+by}}{(m_{p_1+b} - k_b/(1-y))\pi} (-1)^{p_2} g^2(-4) \sin \pi m_i y \sin \pi m_j y e^{-\pi i(m_i+m_j)y}. \quad (3.125)$$

The contribution to  $G_3$  which corresponds to the diagrams of Figure 3.8 is therefore

$$G_3^{(2)} = \frac{J^{p_3}}{N \sqrt{J^{p_3-1} J_1^{p_1-1} J_2^{p_2-1}}} \prod_{a \neq i,j}^{p_1} \frac{\sin \pi m_a y}{m_a - n_a/y} \prod_{b=1}^{p_2} \frac{\sin \pi m_{p_1+by}}{m_{p_1+b} - k_b/(1-y)} (-1)^{p_2} (-\lambda') \frac{\sin \pi m_i y \sin \pi m_j y}{4\pi^{p_3}} \log \frac{x_1^2 x_2^2}{x_{12}^2}. \quad (3.126)$$

From the last equation we can extract

$$g_2 C_{\text{free}}^p b^{(2)} = \frac{J^{p_3}}{N \sqrt{J^{p_3-1} J_1^{p_1-1} J_2^{p_2-1}}} \prod_{a \neq i,j}^k \frac{\sin \pi m_a y}{m_a - n_a/y} \prod_{b=1}^{p_2} \frac{\sin \pi m_{p_1+by}}{m_{p_1+b} - k_b/(1-y)} (-1)^{p_2} \frac{\sin \pi m_i y \sin \pi m_j y}{2\pi^{p_3}}. \quad (3.127)$$

This term corresponds to the first term of the second line in (3.109). There are also diagrams where we consider the pure BMN part in  $\mathcal{O}_1$  and the compensating part in  $\mathcal{O}_2$  (rather than the opposite). These terms produce the second term in the second line of (3.109).

We now consider the last set of diagrams, which are represented in Figure 3.9. In order to draw these diagrams we have used (3.95) for the operators  $\mathcal{O}_1$ ,  $\mathcal{O}_2$ , and (3.95), (3.96) for the barred operator. In these diagrams the  $x^{\text{th}}$   $\phi_1$  belongs to  $\mathcal{O}_1$ , while the  $z^{\text{th}}$   $\phi_1$  belongs to  $\mathcal{O}_2$ .

In this case the phase factor associated with the fields which interact becomes

$$P_1 = (\bar{q}_i^{J_1} - 1)(\bar{q}_j^{J_1} - 1)(-g^2). \quad (3.128)$$

For the total phase factor one obtains

$$P = J^{p_3-2} \prod_{a \neq x}^{p_1} e^{-\pi i m_a y} \frac{\sin \pi m_a y}{m_a - n_a/y} \prod_{b \neq z}^{p_2} \exp^{-\pi i m_{p_1+by}} \frac{\sin \pi m_{p_1+by}}{m_{p_1+b} - k_b/y} (-1)^{p_2-1} \frac{(-g^2)(-4)}{\pi^{p_1-1} \pi^{p_2-1}} \sin \pi m_i y \sin \pi m_j y e^{-\pi i(m_i+m_j)y}. \quad (3.129)$$

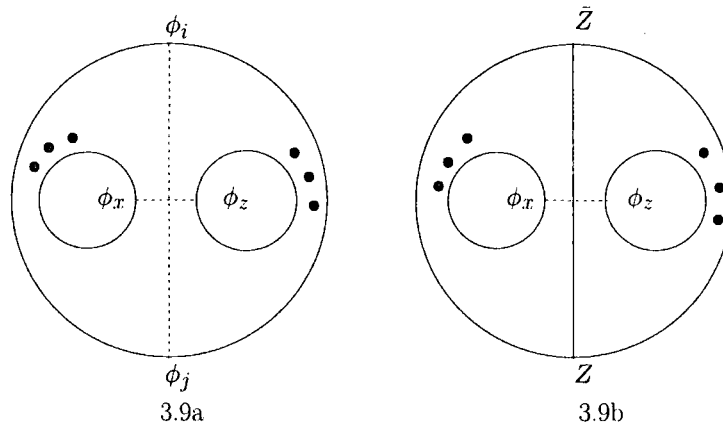


Figure 3.9: In Figure 3.9a we take the BMN part in the external operator, whereas in 3.9b we take the compensating term.

The contribution to  $G_3$  which corresponds to the diagrams of Figure 3.9 is therefore

$$G_3^{(3)} = \frac{J^{p-3}}{N \sqrt{J^{p_3-1} J_1^{p_1-1} J_2^{p_2-1}}} \prod_{a \neq x}^{p_1} \frac{\sin \pi m_a y}{m_a - n_a/y} \prod_{b \neq z}^{p_2} \frac{\sin \pi m_{p_1+b} y}{m_{p_1+b} - k_b/(1-y)} (-1)^{p_2} (-\lambda') \frac{\sin \pi m_i y \sin \pi m_j y}{4\pi^{p_3}} \log \frac{x_1^2 x_2^2}{x_{12}^2}. \quad (3.130)$$

From this equation we extract

$$g_2 C_{\text{free}}^p b^{(3)} = \frac{J^{p-3}}{N \sqrt{J^{p_3-1} J_1^{p_1-1} J_2^{p_2-1}}} \prod_{a \neq x}^{p_1} \frac{\sin \pi m_a y}{m_a - n_a/y} \prod_{b \neq z}^{p_2} \frac{\sin \pi m_{p_1+b} y}{m_{p_1+b} - k_b/(1-y)} (-1)^{p_2} \frac{\sin \pi m_i y \sin \pi m_j y}{2\pi^{p_3}}. \quad (3.131)$$

Finally, by adding (3.123), (3.127) and (3.131) (and the terms similar to (3.123) and (3.127), as discussed in the text), and summing over all permutations, it is immediate to obtain (3.109).

This chapter was devoted to a detailed study of the BMN correspondence (in the bosonic sector) as this is expressed in equation (1.137). In particular, by studying BMN operators with scalar, vector and mixed impurities we have explored and verified the correspondence for string states in all the directions of the two  $SO(4)$  groups. Among other things we have also clarified the role of the  $\mathbb{Z}_2$  symmetry of the pp-wave background and its realisation on the gauge theory side. In the next chapter we turn to the study of the fermionic sector of the BMN correspondence.

## Chapter 4

# The BMN correspondence in the fermionic sector

As discussed in the previous chapter, tests of the relation (1.137) rely on the careful comparison of string amplitudes obtained in pp-wave string field theory to the matrix elements of the dilatation operator  $\Delta$  in Yang-Mills, and have been performed, for the bosonic sector of the theory, in a variety of cases:

- a. in [48], the case of BMN operators with two scalar impurities of different flavour was studied;
- b. in [2, 49], BMN operators with an arbitrary number of scalar impurities was considered; and finally,
- c. in [2], all the  $SO(4) \times SO(4)$  representations of two scalar impurity and two vector impurity BMN operators were studied, as well as BMN operators with mixed (one scalar/one vector) impurities.

In all cases, precise agreement was found between the string amplitudes obtained using the superstring vertex and the corresponding matrix elements obtained in field theory [2, 48, 49]. In particular, the analysis of [2] clarified a puzzle concerning the realisation of the  $\mathbb{Z}_2 \subset SO(8)$  symmetry of the pp-wave background geometry.

In the previous chapter the natural emergence of the isomorphic to string basis was explained by constructing the proper overlap of states in terms of two-point function of BMN operators where the conjugated BMN operator is defined through

hermitian conjugation *plus* an inversion [62]. This procedure, which was applied in to BMN operators with scalar and/or vector impurities, will be used in section 4.2 in the case of fermion BMN operators.

Fermion BMN operators have been studied, with an emphasis on mixing issues, in [63, 64]. The aim of this chapter is to investigate the equivalence relation (1.137) in the fermionic part of the BMN sector of  $\mathcal{N} = 4$  Yang-Mills. One of the main motivations for our analysis lies in the fact that fermionic matrix elements of  $H_{\text{string}}$  have never been compared to any field theory result. Moreover, string field theory in the fermionic sector is not just a simple extension of its bosonic counterpart, and the construction of the fermionic prefactor of the string field Hamiltonian is not straightforward. Therefore, it is particularly compelling to investigate the BMN correspondence in the fermionic sector.

In this chapter we will make use of the superstring vertex in the  $SO(4) \times SO(4)$  formalism [65]. Our analysis in field theory will be performed up to and including  $\mathcal{O}(\lambda')$  in the pp-wave 't Hooft coupling and  $\mathcal{O}(g_2)$  in the genus counting parameter, and hence incorporates string interactions at the first nontrivial order.<sup>1</sup> Our result is simple: for all cases we consider, the matrix elements of the string field theory Hamiltonian derived from the superstring vertex of [52, 53, 55, 65] agree perfectly with the corresponding field theory quantities. This result allows us to confirm the validity of the conjectured duality relation (1.137) in the fermionic sector, and at the level of string interactions.

The plan of the rest of this chapter is as follows. In the next section we introduce and discuss BMN operators with two fermion impurities. In section 4.2, we describe the notion of conjugation in the case of operators with fermionic impurities. In section 4.3 we derive the desired fermionic matrix elements of the string Hamiltonian in lightcone string field theory. Sections 4.4 and 4.5 contain the calculation in field theory and the comparison to the string results previously derived.

---

<sup>1</sup>This result, as well as the results of [2, 48, 49, 67] are in contradistinction with [68], where it was argued that nonplanar effects (corresponding to string interactions in string theory) should not be incorporated into the pp-wave string theory/ $\mathcal{N} = 4$  SYM duality.

## 4.1 Fermion BMN operators

In order to study the BMN sector of  $\mathcal{N} = 4$  Super Yang-Mills, we need to pick an R-charge subgroup  $U(1)_J \subset SU(4)$ . Hence we need to decompose  $SU(4) \rightarrow SO(4) \times U(1)_J \sim SU(2) \times SU(2) \times U(1)_J$ . The branching rule for the fermion representation  $\mathbf{4}$  of  $SU(4)$ , to which the fermions  $\lambda_\alpha^A$  of the  $\mathcal{N} = 4$  theory belong, is [69]

$$\mathbf{4} \longrightarrow (\mathbf{2}, \mathbf{1})_+ + (\mathbf{1}, \mathbf{2})_- , \quad (4.1)$$

from which we have, in terms of fields,

$$\lambda_\alpha^A \longrightarrow (\lambda_{r\alpha, (1/2)}, \lambda_{\dot{r}\alpha, (-1/2)}) , \quad (4.2)$$

$$\bar{\lambda}_{A\dot{\alpha}} \longrightarrow (\bar{\lambda}_{r\dot{\alpha}, (-1/2)}, \bar{\lambda}_{\dot{r}\dot{\alpha}, (1/2)}) . \quad (4.3)$$

Here  $\alpha, \dot{\alpha} = 1, 2$  are spin indices,  $A = 1 \dots 4$ , and  $r = 3, 4$ ,  $\dot{r} = 1, 2$ . Notice that there are four fermions with positive R-charge,  $\lambda_{r\alpha, (1/2)}$  and  $\bar{\lambda}_{\dot{r}\dot{\alpha}, (1/2)}$ , and four with negative R-charge,  $\lambda_{\dot{r}\alpha, (-1/2)}$ ,  $\bar{\lambda}_{r\dot{\alpha}, (-1/2)}$ . We will refer to the former as to the BMN fermions, and to the latter as to the anti-BMN fermions. To simplify the notation, we will omit from now on the  $U(1)$  R-charge subscript in the fermion fields.

The following table summarises the field content (scalar, vector and fermion fields) of the  $\mathcal{N} = 4$  SYM theory participating in the BMN correspondence, together with their canonical dimensions, R-charge and decomposition into irreducible representations of  $SO(4) \times SO(4) \sim SU(2) \times SU(2) \times SU(2) \times SU(2)$ .

We now discuss the two-impurity fermion BMN operators. Their precise form can be obtained by acting with two supersymmetry transformations on the scalar BMN operators

$$\mathcal{O}_{ij,m}^J = \mathcal{C} \left[ \sum_{l=0}^J e^{\frac{2\pi i m l}{J}} \text{Tr} (\phi_i Z^l \phi_j Z^{J-l}) - \delta_{ij} \text{Tr} (\bar{Z} Z^{J+1}) \right] , \quad (4.4)$$

where  $i, j = 1, \dots, 4$  and we have defined

$$\mathcal{C} := \frac{1}{\sqrt{J N_0^{J+2}}} , \quad N_0 := \frac{g^2}{2} \frac{N}{4\pi^2} . \quad (4.5)$$

The normalisation of the operators is such that their two-point functions take the canonical form in the planar limit. This procedure correctly identifies the possible

field	$\Delta_0$	$J$	$\Delta_0 - J$	$SO(4) \times SO(4)$
$Z$	1	1	0	(1, 1)
$\bar{Z}$	1	-1	2	(1, 1)
$\phi^i$	1	0	1	(1, 4)
$D_\mu$	1	0	1	(4, 1)
$\lambda_{r\alpha}$	3/2	1/2	1	((2, 1), (2, 1))
$\bar{\lambda}_{\dot{r}\dot{\alpha}}$	3/2	1/2	1	((1, 2), (1, 2))
$\bar{\lambda}_{r\dot{\alpha}}$	3/2	-1/2	2	((2, 1), (1, 2))
$\lambda_{\dot{r}\alpha}$	3/2	-1/2	2	((1, 2), (2, 1))

Table 4.1: In this table we list the canonical dimension  $\Delta_0$ , R-charge  $J$  and  $SO(4) \times SO(4)$  representations for the fields of  $\mathcal{N} = 4$  Super Yang-Mills. For convenience, we also write the corresponding  $\Delta_0 - J$  for each field.

compensating terms which may be present in the expression of the operators. We would like to remind the reader that these compensating terms are crucial for a correct understanding of the dynamics of the BMN sector.

Specifically, we will be considering

$$\mathcal{O}_{\text{vac}}^J = \frac{1}{\sqrt{JN_0^J}} \text{Tr} Z^J, \quad (4.6)$$

$$\mathcal{O}_{33;m}^{\alpha\beta;J} = \frac{C}{2} \left[ \sum_{l=0}^J e^{\frac{2\pi i m l}{J}} \text{Tr}(\lambda_3^\alpha Z^l \lambda_3^\beta Z^{J-l}) \right], \quad (4.7)$$

$$\mathcal{O}_{34;m}^{\alpha\beta;J} = \frac{C}{2} \left[ \sum_{l=0}^J e^{\frac{2\pi i m l}{J}} \text{Tr}(\lambda_3^\alpha Z^l \lambda_4^\beta Z^{J-l}) - \frac{\sqrt{2}}{4} \text{Tr} \left( (F_{\mu\nu} \sigma^{\mu\nu})_\gamma^\beta \epsilon^{\alpha\gamma} Z^{J+1} \right) \right]. \quad (4.8)$$

Very similar expressions can be written for operators where  $(3, 4) \rightarrow (1, 2)$ , i.e. undotted  $SU(2)$  indices are replaced by dotted ones.

In the following, we will also make extensive use of the expressions for the double-trace operators

$$\mathcal{T}_{r\alpha,s\beta;m}^{J,y} = : \mathcal{O}_{r\alpha,s\beta;m}^{y,J} : : \mathcal{O}_{\text{vac}}^{(1-y)\cdot J} :, \quad (4.9)$$

$$\mathcal{T}_{\dot{r}\dot{\alpha},\dot{s}\dot{\beta};m}^{J,y} = : \mathcal{O}_{\dot{r}\dot{\alpha},\dot{s}\dot{\beta};m}^{y,J} : : \mathcal{O}_{\text{vac}}^{(1-y)\cdot J} :, \quad (4.10)$$

where  $y \in (0, 1)$ .

A few important comments are in order.

1. First, note the appearance on right hand side of (4.8) of an all-important compensating term which modifies the naïve expression for  $\mathcal{O}_{34;m}^{\alpha\beta;J}$ . Compensating terms are required in order for the corresponding operators to be conformal primaries in the BMN limit, and are present also in the case of scalar BMN operators [70] (as the right hand side of (4.4) for  $i = j$  shows) and vector BMN operators [71, 72].
2. Second, we would like to stress that these compensating terms play a key rôle in the evaluation of the conformal three-point functions of vector and mixed BMN operators. Indeed, had they not been taken into account, one would erroneously conclude that the three-point functions for scalar, vector and mixed BMN operators take actually all the same form. The three-point function coefficients for vector and for mixed BMN operators were computed in [62] and [2], respectively, and found to be different from that of the scalar case [73].<sup>2</sup> Of course, this is striking evidence against a direct correspondence between the conformal *three-point functions* and the superstring vertex at the nontrivial, interacting level.
3. Furthermore, the analysis of [2] showed that precisely thanks to the differences between the three-point function coefficients for scalar, vector and mixed impurity BMN operators it is possible to reproduce, from the field theory point of view, two key properties of the three-string vertex of Spradlin and Volovich, namely:
  - a. the vanishing of the three-string amplitude for string states with one vector and one scalar impurity; and
  - b. the relative minus sign in the string amplitude involving states with two vector impurities compared to that with two scalar impurities.

Once this is taken into account, perfect agreement between the string and field

---

<sup>2</sup>Their expressions are given in Eqs. (3.29)-(3.31) of [2].

theory predictions is found.

To further clarify the rôle of the compensating terms, we consider the flavour-singlet and flavour-triplet combinations:

$$\mathcal{O}_{34,\mathbf{S};m}^{\alpha\beta;J} = \frac{\mathcal{C}}{2\sqrt{2}} \left[ \sum_{l=0}^J e^{\frac{2\pi i m l}{J}} \text{Tr}(\lambda_3^\alpha Z^l \lambda_4^\beta Z^{J-l} - \lambda_4^\alpha Z^l \lambda_3^\beta Z^{J-l}) - \frac{\sqrt{2}}{2} \text{Tr}\left((F_{\mu\nu}\sigma^{\mu\nu})_\gamma^\beta \epsilon^{\alpha\gamma} Z^{J+1}\right) \right] \quad (4.11)$$

$$\mathcal{O}_{34,\mathbf{T};m}^{\alpha\beta;J} = \frac{\mathcal{C}}{2\sqrt{2}} \left[ \sum_{l=0}^J e^{\frac{2\pi i m l}{J}} \text{Tr}(\lambda_3^\alpha Z^l \lambda_4^\beta Z^{J-l} + \lambda_4^\alpha Z^l \lambda_3^\beta Z^{J-l}) \right]. \quad (4.12)$$

We can further decompose each of the two operators in (4.11) and (4.12) into singlet and triplet of the spin, that is

$$\mathcal{O}_{34,\mathbf{S};m}^{\alpha\beta;J} \longrightarrow (\mathbf{1}, \mathbf{3}^+) + (\mathbf{1}, \mathbf{1}), \quad (4.13)$$

$$\mathcal{O}_{34,\mathbf{T};m}^{\alpha\beta;J} \longrightarrow (\mathbf{3}^+, \mathbf{3}^+) + (\mathbf{3}^+, \mathbf{1}). \quad (4.14)$$

It is immediately seen that the compensating term on the right hand side of (4.11) is symmetric under the exchange of the spin indices  $\alpha$  and  $\beta$ . This means that this compensating term will affect only the  $(\mathbf{1}, \mathbf{3}^+)$  representation. This is perfectly consistent with the decomposition of the two-impurity BMN operators with *vector* impurities according to irreducible representations of  $SO(4) \times SO(4)$ . Indeed, by combining two vector impurities we can form the following representations:

$$(\mathbf{1}, \mathbf{4}) \times (\mathbf{1}, \mathbf{4}) = (\mathbf{1}, \mathbf{1}) + (\mathbf{1}, \mathbf{9}) + (\mathbf{1}, \mathbf{3}^+) + (\mathbf{1}, \mathbf{3}^-). \quad (4.15)$$

The only representation the right hand sides of (4.13) and (4.14) have in common with the right hand side of (4.15) are precisely  $(\mathbf{1}, \mathbf{3}^+)$ , which receives a compensating term, and  $(\mathbf{1}, \mathbf{1})$ , for which however no compensating term is generated as this order.<sup>3</sup>

For completeness, we mention here what are the possible irreducible representations of  $SO(4) \times SO(4) \sim SU(2) \times SU(2) \times SU(2) \times SU(2)$  that can be obtained by

---

<sup>3</sup>For a discussion along similar lines on the possible mixing of fermion BMN operators with scalar operators, see [64].

combining two fermion impurities:<sup>4</sup>

$$((\mathbf{2}, \mathbf{1}), (\mathbf{2}, \mathbf{1})) \times ((\mathbf{2}, \mathbf{1}), (\mathbf{2}, \mathbf{1})) = (\mathbf{1}, \mathbf{1}) + (\mathbf{3}^+, \mathbf{3}^+) + (\mathbf{3}^+, \mathbf{1}) + (\mathbf{1}, \mathbf{3}^+) , \quad (4.16)$$

$$((\mathbf{1}, \mathbf{2}), (\mathbf{1}, \mathbf{2})) \times ((\mathbf{1}, \mathbf{2}), (\mathbf{1}, \mathbf{2})) = (\mathbf{1}, \mathbf{1}) + (\mathbf{3}^-, \mathbf{3}^-) + (\mathbf{3}^-, \mathbf{1}) + (\mathbf{1}, \mathbf{3}^-) , \quad (4.17)$$

$$((\mathbf{2}, \mathbf{1}), (\mathbf{2}, \mathbf{1})) \times ((\mathbf{1}, \mathbf{2}), (\mathbf{1}, \mathbf{2})) = (\mathbf{4}, \mathbf{4}) . \quad (4.18)$$

## 4.2 Conjugation of scalar and fermion operators

In the previous chapter we briefly reviewed how the notion of conjugation as hermitian conjugation plus an inversion is essential in order to make scalar and vector  $\Delta$ -BMN operators orthonormalisable.

Let us now concentrate on the fermionic operators which are of direct concern for this chapter.<sup>5</sup> It is well known that, under conformal inversion, a Dirac spinor field  $\psi$  of dimension  $d$  transforms as [78]

$$\psi(x) \rightarrow \psi'(x') = \eta \frac{\hat{x}}{|x|} x^{2d} \psi(x) , \quad \eta^4 = 1 , \quad (4.19)$$

where  $\hat{x} = x_\mu \gamma^\mu$ , and  $\gamma^\mu$  are the Euclidean gamma matrices. In terms of Weyl spinors  $\lambda_\alpha, \bar{\xi}^{\dot{\alpha}}$ , (4.19) implies

$$\lambda_\alpha(x) \rightarrow \lambda'_\alpha(x') = \eta \frac{(x\bar{\xi})_\alpha}{|x|} x^{2d} , \quad (4.20)$$

$$\bar{\xi}^{\dot{\alpha}}(x) \rightarrow \bar{\xi}^{\dot{\alpha}'}(x') = \eta \frac{(\bar{x}\lambda)^{\dot{\alpha}}}{|x|} x^{2d} , \quad (4.21)$$

where we set  $x = x_\mu \sigma^\mu$ ,  $\bar{x} = x_\mu \bar{\sigma}^\mu$ . Hence, an operator of conformal dimension  $\Delta$  with  $f = p + q$  fermionic insertions transforms under inversion as:

$$\mathcal{O}_{\alpha_1 \dots \alpha_p}^{\dot{\alpha}_1 \dots \dot{\alpha}_q}(x) \rightarrow \eta^f x^{2\Delta} J_{\alpha_1 \dot{\beta}_1} \dots J_{\alpha_p \dot{\beta}_p} \dots \bar{J}^{\dot{\alpha}_1 \beta_1} \dots \bar{J}^{\dot{\alpha}_q \beta_q} \mathcal{O}_{\beta_1 \dots \beta_q}^{\dot{\beta}_1 \dots \dot{\beta}_p}(x) , \quad (4.22)$$

where

$$J_{\alpha\dot{\beta}}(x) := \frac{x_{\alpha\dot{\beta}}}{|x|} , \quad \bar{J}^{\dot{\alpha}\beta}(x) := \frac{\bar{x}^{\dot{\alpha}\beta}}{|x|} . \quad (4.23)$$

The notion of conjugation [62], as ordinary hermitian conjugation followed by an inversion, can then applied to a generic operator with conformal dimension  $\Delta$  with

<sup>4</sup>See also the discussion in section IV of [77].

<sup>5</sup>The transformation under inversion of fermionic BMN operators has also been considered in [68].

scalar, vector or fermion impurities; and the conjugated operator  $\bar{\mathcal{O}}$  can then be written (schematically) as:

$$\bar{\mathcal{O}}_{\Delta}(x) \equiv x^{2\Delta} J \cdot \mathcal{O}_{\Delta}^{\dagger}(x) , \quad (4.24)$$

where by  $J$  we mean the tensor product by the appropriate inversion operators  $J_{\mu\nu}(x)$ , for each vector index, and  $J_{\alpha\dot{\alpha}}(x)$  (or  $\bar{J}^{\dot{\alpha}\alpha}(x)$ ), for each spinor index. It was noticed in [62] that the advantage of this new conjugation resides in that the two-point function for scalar, vector and fermion  $\Delta$ -BMN operators take all the same canonical form when the  $\bar{\mathcal{O}}$  operator is employed:

$$\langle \bar{\mathcal{O}}_{\Delta_a}(x) \mathcal{O}_{\Delta_b}(0) \rangle = \delta_{ab} . \quad (4.25)$$

The right hand side of (4.25) does not depend on  $x$ , and represents the overlap of the corresponding states in conformal  $\mathcal{N} = 4$  Super Yang-Mills.<sup>6</sup>

### 4.3 Matrix elements of $H_{\text{string}}$ in string field theory

There are two equivalent ways to describe superstring interactions in string field theory, known as the  $SO(8)$  and the  $SO(4) \times SO(4)$  formalism. In the former approach, the three-string vertex in string field theory is built upon a state  $|0\rangle$  with energy equal to  $4\mu$ . This state is therefore not the ground state, but it has the advantage that, as  $\mu \rightarrow 0$ , the  $SO(8)$  construction flows smoothly to string field theory in flat space [89–92]. In the  $SO(4) \times SO(4)$  formalism, the Hilbert space of states in string field theory is built on the true vacuum  $|v\rangle$  of pp-wave string theory (see Appendix D for details). Remarkably, the two formalisms have been shown to be completely equivalent [65], hence it is only a matter of convenience which one to use. In this chapter we will make use of the  $SO(4) \times SO(4)$  vertex, since there it is more straightforward to compute string amplitudes involving fermionic oscillators.

The string amplitude has the form [52, 53]

---

<sup>6</sup>A side comment: for two-impurity fermion BMN operators, an additional minus sign should be included in the definition of the hermitian conjugation of the operators in order to get the two-point functions normalised as in (4.25).

$$\langle 1| \langle 2| H_{\text{string}} |3\rangle = \langle \Phi | \mathbf{P} | V_B \rangle | V_F \rangle , \quad (4.26)$$

where  $\langle \Phi | := \langle 1| \langle 2| \langle 3|'$  is the external three-string state, and  $|V_B\rangle$  and  $|V_F\rangle$  are the kinematical part of the bosonic and fermionic vertex, (D.2) and (D.3) respectively. Finally, the prefactor  $\mathbf{P}$  is written in (D.5).

We will be interested in external states with fermionic impurities,

$$\beta_{n(r)}^{\alpha\beta\dagger} \beta_{-n(r)}^{\alpha'\beta'\dagger} |v\rangle_r , \quad (4.27)$$

where the fermionic operators  $\beta$ 's are related to the oscillators in the string basis by [55]

$$\beta_n = \frac{1}{\sqrt{2}}(b_n + ib_{-n}) , \quad \beta_{-n} = \frac{1}{\sqrt{2}}(b_n - ib_{-n}) . \quad (4.28)$$

Specifically, we will compute matrix elements of the form

$$\mathcal{H}_{r'\alpha',s'\beta';n,J,y}^{r\alpha,s\beta;m,J} := \frac{1}{\mu} \langle \mathcal{T}_{r'\alpha',s'\beta';n}^{J,y} | H_{\text{string}} | \mathcal{O}_J^{r\alpha,s\beta;m} \rangle , \quad (4.29)$$

for all possible values of the indices. After a lengthy but straightforward algebra, we obtain:

$$\begin{aligned} \langle v | \beta_{\alpha\beta,-m(3)} \beta_{\gamma\delta,m(3)} \beta_{\alpha'\beta',n(1)} \beta_{\gamma'\delta',-n(1)} | H_3 \rangle &= C_{\text{norm}} \frac{\beta+1}{3\pi^2\mu} \sin^2 \pi m\beta \times \\ &\left[ \epsilon_{\alpha'\alpha} \epsilon_{\gamma'\gamma} (\epsilon_{\delta\beta} \epsilon_{\delta'\beta'} + \epsilon_{\delta\beta'} \epsilon_{\delta'\beta}) + \epsilon_{\gamma'\alpha} \epsilon_{\alpha'\gamma} (\epsilon_{\delta\beta} \epsilon_{\delta'\beta'} + \epsilon_{\delta\delta'} \epsilon_{\beta\beta'}) - \epsilon_{\alpha\gamma} \epsilon_{\alpha'\gamma'} (\epsilon_{\beta\beta'} \epsilon_{\delta\delta'} - \epsilon_{\delta\beta'} \epsilon_{\delta'\beta}) \right] , \end{aligned} \quad (4.30)$$

where  $C_{\text{norm}}$  is given in (D.10). An expression similar to (4.30) holds when the fermions in (4.30) have both dotted indices. Notice that from (4.30) it follows that

- the string amplitude vanishes whenever a fermion appears more than once, whereas
- it is nonvanishing when all fermions are different, and gives always the same result (up to a minus sign).

It is more illuminating to write (4.30) for a few basic cases:

$$\begin{aligned} \mathcal{H}_{11,12;n,J,y}^{12,11;m,J} &:= \mu^{-1} \langle v | \beta_{-m(3)}^{12} \beta_{m(3)}^{11} \beta_{11,n(1)} \beta_{12,-n(1)} | H_3 \rangle \\ &= -\mu^{-1} \langle v | \beta_{21,-m(3)} \beta_{22,m(3)} \beta_{11,n(1)} \beta_{12,-n(1)} | H_3 \rangle \\ &= -\lambda' C_{\text{norm}} \frac{\beta+1}{\pi^2} \sin^2 \pi m\beta , \end{aligned} \quad (4.31)$$

$$\begin{aligned} \mathcal{H}_{11,11;n,J,y}^{11,11;m,J} &:= \mu^{-1} \langle v | \beta_{-m(3)}^{11} \beta_{m(3)}^{11} \beta_{11,n(1)} \beta_{11,-n(1)} | H_3 \rangle \\ &= \mu^{-1} \langle v | \beta_{22,-m(3)} \beta_{22,m(3)} \beta_{11,n(1)} \beta_{11,-n(1)} | H_3 \rangle = 0 , \end{aligned} \quad (4.32)$$

$$\begin{aligned} \mathcal{H}_{11,22;n,J,y}^{22,11;m,J} &:= \mu^{-1} \langle v | \beta_{-m(3)}^{22} \beta_{m(3)}^{11} \beta_{11,n(1)} \beta_{22,-n(1)} | H_3 \rangle \\ &= \mu^{-1} \langle v | \beta_{11,-m(3)} \beta_{22,m(3)} \beta_{11,n(1)} \beta_{22,-n(1)} | H_3 \rangle = 0 , \end{aligned} \quad (4.33)$$

$$\mathcal{H}_{11,21;n,J,y}^{21,11;m,J} := \mu^{-1} \langle v | \beta_{-m(3)}^{21} \beta_{m(3)}^{11} \beta_{11,n(1)} \beta_{21,-n(1)} | H_3 \rangle \quad (4.34)$$

$$\begin{aligned} &= -\mu^{-1} \langle v | \beta_{12,-m(3)} \beta_{22,m(3)} \beta_{11,n(1)} \beta_{21,-n(1)} | H_3 \rangle \\ &= \lambda' C_{\text{norm}} \frac{\beta+1}{\pi^2} \sin^2 \pi m \beta . \end{aligned} \quad (4.35)$$

We can directly compare the expressions (4.31)-(4.34) to the analogous matrix elements obtained from the three-string vertex of [52, 53] for scalar and for vector and mixed (scalar-vector) BMN states:

$$\frac{1}{\mu} \langle \mathcal{T}_{ij,y}^{J,y} | H_{\text{string}} | \mathcal{O}_{ij,m}^J \rangle = -\lambda' C_{\text{norm}} \frac{\beta+1}{\pi^2} \sin^2 \pi m \beta , \quad (4.36)$$

$$\frac{1}{\mu} \langle \mathcal{T}_{i\mu,n}^{J,y} | H_{\text{string}} | \mathcal{O}_{i\mu,m}^J \rangle = 0 , \quad (4.37)$$

$$\frac{1}{\mu} \langle \mathcal{T}_{\mu\nu,n}^{J,y} | H_{\text{string}} | \mathcal{O}_{\mu\nu,m}^J \rangle = \lambda' C_{\text{norm}} \frac{\beta+1}{\pi^2} \sin^2 \pi m \beta . \quad (4.38)$$

Notice that the amplitude in (4.31) is identical to the amplitude (4.36) involving two scalars of different flavour, whereas that in (4.34) is equal to the amplitude (4.38) involving two different vectors. Similar considerations apply to the vanishing of the mixed amplitude (4.37) and (4.32), (4.33).

The equality of the string amplitude between two BMN states with scalar impurities and two BMN states with fermion impurities had already been derived, in the  $SO(8)$  formalism, in [55]. We also notice that our amplitudes, derived in the  $SO(4) \times SO(4)$  formalism, precisely coincide with those of [55].

## 4.4 Matrix elements of $\Delta$ in $\mathcal{N} = 4$ Yang-Mills

In [2], a general technique was devised for deriving the matrix of overlaps  $S$  (3.12), the matrix of anomalous dimension  $T$  (3.15), and hence the desired matrix elements of the SYM dilatation operator in the isomorphic to string basis, (3.21), from the coefficients of the *three-point* functions of BMN operators. Here we summarize the results of the analysis of [2].<sup>7</sup>

The matrices  $S$  and  $T$  have an expansion in powers of  $g_2$ , but in our analysis we will only need their expressions up to and including  $\mathcal{O}(g_2)$  terms. We will also work at one loop in the effective 't Hooft coupling  $\lambda'$ . Notice that the matrix  $T$  is of  $\mathcal{O}(\lambda')$ , whereas  $S$  is of  $\mathcal{O}(1)$ . In this case, (3.14) is simply

$$\langle \mathcal{O}_\alpha(0) \bar{\mathcal{O}}_\beta(x) \rangle = S_{\alpha\beta} + T_{\alpha\beta} \log(x\Lambda)^{-2}. \quad (4.39)$$

Let us focus on the following *three-point* correlators,

$$G(x_1, x_2, x_3) = \langle \mathcal{O}_{AB,n}^{y,J}(x_1) \mathcal{O}_{\text{vac}}^{(1-y),J}(x_2) \bar{\mathcal{O}}_{AB,m}^J(x_3) \rangle, \quad (4.40)$$

where  $A$  can be a scalar, vector or fermion index, and  $A \neq B$ . On general grounds, these three-point function take the form [47, 73–76]

$$G(x_1, x_2, x_3) = g_2 C_{m,ny} \left[ 1 - \lambda' (a_{m,ny} \log(x_{31}\Lambda)^2 + b_{m,ny} \log(x_{32}x_{31}\Lambda/x_{12})) \right], \quad (4.41)$$

where  $g_2 C_{m,ny}$  is the tree-level contribution, with

$$C_{m,ny} := \frac{\sqrt{(1-y)/y} \sin^2(\pi my)}{\sqrt{J} \pi^2 (m - n/y)^2}, \quad (4.42)$$

and the coefficients  $a_{m,ny}$  and  $b_{m,ny}$  must be calculated in perturbation theory at  $\mathcal{O}(\lambda')$ . The *two-point* function  $\langle \mathcal{T}_{AB,n}^{J,y}(0) \bar{\mathcal{O}}_{AB,m}^J(x) \rangle$  can easily be derived from (5.5) by simply setting  $x_{13} = x_{23} = x$  and  $x_{12} = \Lambda^{-1}$  [76],

$$\langle \mathcal{T}_{AB,n}^{J,y}(0) \bar{\mathcal{O}}_{AB,m}^J(x) \rangle = g_2 C_{m,ny} \left[ 1 + \lambda' (a_{m,ny} + b_{m,ny}) \log(x\Lambda)^{-2} \right]. \quad (4.43)$$

The analysis of section 3 of [2] then showed that the matrices  $S$  and  $T$  are then given,

---

<sup>7</sup>Our notation and conventions in Yang-Mills are reviewed in Appendix C.

up to  $\mathcal{O}(g_2)$ , by the following expressions:

$$S = \begin{pmatrix} \delta_{mn} & g_2 C_{m,qz} \\ g_2 C_{py,n} & \delta_{pq} \end{pmatrix} + \mathcal{O}(g_2^2) = \mathbf{1} + g_2 s + \mathcal{O}(g_2^2), \quad (4.44)$$

(4.45)

$$T = \lambda' \begin{pmatrix} m^2 \delta_{mn} & g_2 C_{m,ny} (a+b)_{m,qz} \\ g_2 C_{py,n} (a+b)_{py,n} & (p^2/y^2) \delta_{pq} \delta_{yz} \end{pmatrix} + \mathcal{O}(g_2^2) \quad (4.46)$$

$$\equiv d + g_2 t + \mathcal{O}(g_2^2),$$

with

$$d = \lambda' \begin{pmatrix} m^2 \delta_{mn} & 0 \\ 0 & (p^2/y^2) \delta_{pq} \delta_{yz} \end{pmatrix}, \quad (4.47)$$

$$t = \lambda' \begin{pmatrix} 0 & C_{m,ny} (a+b)_{m,qz} \\ C_{py,n} (a+b)_{py,n} & 0 \end{pmatrix}. \quad (4.48)$$

It then follows that

$$S^{-1/2} = \mathbf{1} - g_2 (s/2) + \mathcal{O}(g_2^2) \quad (4.49)$$

diagonalises  $S$  at  $\mathcal{O}(g_2)$ , and hence one obtains

$$\Gamma = d + g_2 \left[ t - \frac{1}{2} \{s, d\} \right]. \quad (4.50)$$

We now need to compute the explicit expressions for  $a_{mn}^y$  and  $b_{mn}^y$  for the fermion case. First, it was observed in [2] that, at  $\mathcal{O}(\lambda')$  in planar perturbation theory, the coefficient  $a_{mn}^y$  is simply given by the  $\mathcal{O}(\lambda')$  anomalous dimension of the “small” BMN operator at  $x_1$ . In accordance with supersymmetry, it turns out that the  $\mathcal{O}(\lambda')$  anomalous dimension of BMN operators with two arbitrary impurities is given by

$$a_{m,ny} = \frac{n^2}{y^2}, \quad (4.51)$$

independently of the type of impurity considered. This result was first obtained for the case of two scalar impurities in [41], for one scalar and one vector impurity in [71],

for two vector impurities in [94]. We have also explicitly derived (4.51) in the fermion case with a perturbative calculation in Yang-Mills.

We now move on to consider  $b_{m,ny}$ . From (4.41), we see that  $b_{m,ny}$  is the coefficient which multiplies the  $\log x_{12}$  contribution in the three-point function  $G(x_1, x_2, x_3)$  in (5.5), where the “large” (“small”) BMN operator  $\bar{\mathcal{O}}_{AB,m}^J$  ( $\mathcal{O}_{AB,n}^{y,J}$ ) is inserted at  $x_3$  ( $x_1$ ), and the vacuum operator  $\mathcal{O}_{\text{vac}}$  at point  $x_2$ . Hence, the tactic we will follow in the next section will consist in computing the  $\log x_{12}$  term of the three-point function  $G(x_1, x_2, x_3)$ .

Let us quote here the result for  $b_{m,ny}$  in the case of scalar, mixed, or vector BMN operators in (5.5) [2]:

$$[b_{m,ny}]_{\text{scalar}} = m^2 - \frac{mn}{y}, \quad (4.52)$$

$$[b_{m,ny}]_{\text{scalar-vector}} = \frac{1}{2} \left( m^2 - \frac{n^2}{y^2} \right), \quad (4.53)$$

$$[b_{m,ny}]_{\text{vector}} = -\frac{n^2}{y^2} + \frac{mn}{y}. \quad (4.54)$$

We conclude this section with one important comment, which anticipates our results for the fermions to be derived in the next section: we will show that, for fermion BMN operators, the coefficients  $b_{m,ny}$  for the various representations precisely take one of the three expressions (4.52)-(4.54).

#### 4.4.1 The three-point function of fermion BMN operators

In the previous section we explained how to obtain the matrix elements of the SYM dilatation operator in any arbitrary basis of SYM operators, and specifically in the isomorphic to string basis. Here we present the field theory computation of the coefficients  $b_{m,ny}$  appearing in (4.41), from which the coefficient of the conformal three-point function of two-impurity fermion BMN operators can also be derived. The matrix elements (4.50) of the SYM dilatation operators in the natural string basis will then be obtained using the expressions for  $b_{m,ny}$  and (4.44)-(4.48) and (4.51).

Let us consider the three-point function of the operators in (4.8), i.e.

$$\langle \mathcal{O}_{3\alpha,4\beta;n}^{y,J}(x_1) \mathcal{O}_{\text{vac}}^{(1-y)\cdot J}(x_2) \bar{\mathcal{O}}_{3\dot{\alpha},4\dot{\beta};m}^J(x_3) \rangle. \quad (4.55)$$

We start off by evaluating the Feynman diagrams which originate from the pure BMN parts of both the barred and unbarred operators. These diagrams are represented in Figure 4.1, where we draw only the diagrams where the impurities  $\lambda_{4\alpha}$  and  $\bar{\lambda}_{4\beta}$  participate in the interactions, and the other impurity propagates freely. In diagram 4.1a (type I), the interacting impurity goes across, while in 4.1b the interacting impurity goes straight (type II). The latter diagram has a minus sign relative to the former from the Yukawa vertex (see (C.3)). The result for the type I diagram is,

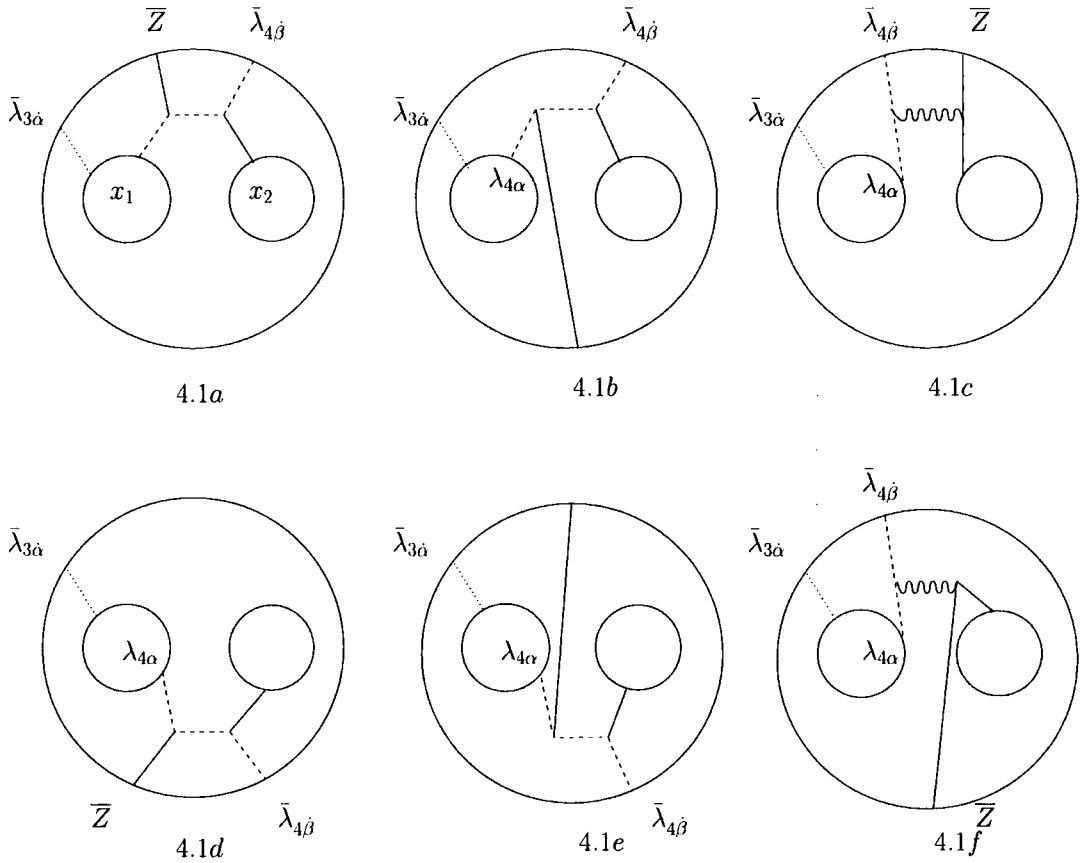


Figure 4.1: Feynman diagrams from the pure BMN parts: of type I (in 4.1a and 4.1d) and type II (4.1b and 4.1e). Diagrams 4.1d, 4.1e, are the mirrors of 4.1a, 4.1b. Diagrams 4.1d and 4.1e have phase factors which are the complex conjugate of those of 4.1a and 4.1b. The gluon interaction diagrams in 4.1c and 4.1f have the same BMN factor and cancel each other.

concentrating on the interacting part:

$$J_{\alpha\dot{\beta}}^I = (\partial_\nu^1 \sigma_{\alpha\dot{\alpha}}^\nu) (-\sqrt{2}i\epsilon^{\psi\dot{\alpha}}) \sigma_{\chi\dot{\psi}}^\rho (-\sqrt{2}i\epsilon^{\beta\dot{\chi}}) (-\partial_\mu^3 \sigma_{\beta\dot{\beta}}^\mu) H_{\rho 1423} , \quad (4.56)$$

where

$$\begin{aligned} H_{\rho 1423} &= \int d^4x d^4y \Delta(x_1 - x) \Delta(x_4 - x) [-\partial_\rho^x \Delta(x - y)] \Delta(x_3 - y) \Delta(x_4 - y) \\ &= -(\partial_\rho^1 + \partial_\rho^4) H_{1432} . \end{aligned} \quad (4.57)$$

Notice that in order to be able to perform the inversion in the conjugated operator, we momentarily split the insertion points of the fermion and the  $Z$  impurity, respectively  $x_3$  and  $x_4$ . The last equality is obtained after integrating by parts with respect to  $x$  and then converting the  $x$  derivative acting on  $\Delta(x_1 - x)$  and  $\Delta(x_4 - x)$  to derivatives with respect to  $x_1$  and  $x_4$ , respectively. The partial derivatives in (4.56) come from the fermion propagator  $S_{\alpha\dot{\alpha}}(x) = -\partial_{\alpha\dot{\alpha}} \Delta(x)$ , where  $\partial_{\alpha\dot{\alpha}} := \partial_\mu \sigma_{\alpha\dot{\alpha}}^\mu$ .

Using now (C.12) and ignoring the  $\epsilon$  term which eventually does not contribute to the  $\log x_{12}^2$  term, one obtains:

$$J_{\alpha\dot{\beta}}^I = 2[\partial_{\alpha\dot{\beta}}^3 J_A + \partial_{\alpha\dot{\beta}}^1 J_B + (\partial^1 + \partial^4)_{\alpha\dot{\beta}} J_C] , \quad (4.58)$$

where

$$J_A = \partial^1 \cdot (\partial^1 + \partial^4) H_{1423} , \quad (4.59)$$

$$J_B = \partial^3 \cdot (\partial^1 + \partial^4) H_{1423} , \quad (4.60)$$

$$J_C = -\partial^3 \cdot \partial^1 H_{1423} . \quad (4.61)$$

The explicit expressions for  $J_A$ ,  $J_B$  and  $J_C$  are worked out in (G.8)-(G.10). After some algebra, one realises that the only non-zero contribution to  $J_{\alpha\dot{\beta}}^I$  comes from the term involving  $J_A$ . Keeping track of the relevant to us terms which contain  $\log x_{12}^2$ , we get:

$$J_{\alpha\dot{\beta}}^I = \frac{1}{2^3 \pi^2} \log x_{12}^2 \Delta(x_4 - x_1) [\partial_{\alpha\dot{\beta}}^4 \Delta(x_4 - x_1)] . \quad (4.62)$$

We note that (4.62) is precisely of the form of (a first-order correction to) two freely propagating fields, one  $Z$  boson and one fermion, as it is expected. In order to make the comparison with the string amplitude, we should now apply the inversion on the conjugated operator, that is on the scalar  $Z$  field and the interacting fermion. For the scalar field this is rather trivial: according to (3.8), one has to multiply  $J_{\alpha\dot{\beta}}^I$  by  $x_4^2$ .

For the fermion, (4.20) instructs us to multiply by  $\eta x_4^2 \bar{\sigma}_\mu^{\dot{\beta}\beta} x_4^\mu$ . Taking into account the identity  $(\sigma_\mu)_{\alpha\dot{\beta}} \bar{\sigma}_\nu^{\dot{\beta}\beta} x^\mu x^\nu = \delta_\alpha^\beta x^2$  one obtains:

$$-4 \left( \frac{g^2}{2} \right)^3 P_I \frac{\log x_{12}^2}{2^8 \pi^6} \eta^2 \delta_\alpha^\beta. \quad (4.63)$$

The overall factor  $(g^2/2)^3$  comes from the insertion of two vertices, which give  $(2/g^2)^2$ , and five propagators, which give  $(g^2/2)^5$ .  $P_I$  is the phase factor associated with the diagrams of type I, and is explicitly calculated in (E.2). In order to obtain the final result for the type I diagrams, we have still to multiply (4.63) by a factor of 2 from the free contraction of the non-interacting impurity, and by a factor of 1/4 from the normalisation of the two fermion BMN operators. Doing so, and setting  $\eta^2 = 1$  we get:

$$\text{type I - fermions :} \quad -2 \left( \frac{g^2}{2} \right)^3 P_I \frac{\log x_{12}^2}{2^8 \pi^6} \delta_\alpha^\beta. \quad (4.64)$$

Notice that this result is precisely the same as the result for the case of two different scalar impurities. Similarly, one gets, for the type II diagrams:

$$\text{type II - fermions :} \quad 2 \left( \frac{g^2}{2} \right)^3 P_{II} \frac{\log x_{12}^2}{2^8 \pi^6} \delta_\alpha^\beta. \quad (4.65)$$

To the type II diagrams is associated the phase factor  $P_{II}$  of (E.2). Moreover, in order to get the final expression for the coefficient  $b_{m,ny}$ , one should also include the diagrams where the other impurity,  $\lambda_3$ , participates in the interaction.

If this was the whole story, we would conclude that three-point functions of fermions take the same form as the three-point functions for scalars. But the correct expressions for BMN operators often contain compensating terms, and so is the case for the operator in (4.8). Importantly, these compensating terms do contribute to the three-point functions and must be taken into account. In our case, the compensating terms affect the fermion operators that have a projection in the  $(\mathbf{1}, \mathbf{3}^+)$  representation (see the discussion after (4.14)), and the corresponding contribution is important and we will now compute it.

In Figure 4.2 we draw the Feynman diagrams obtained by taking the compensating term on the right hand side of (4.8) for the operator sitting at  $x_1$ . To the diagrams 4.2a and 4.2c a BMN phase factor equal to 1 is associated. From the first diagram

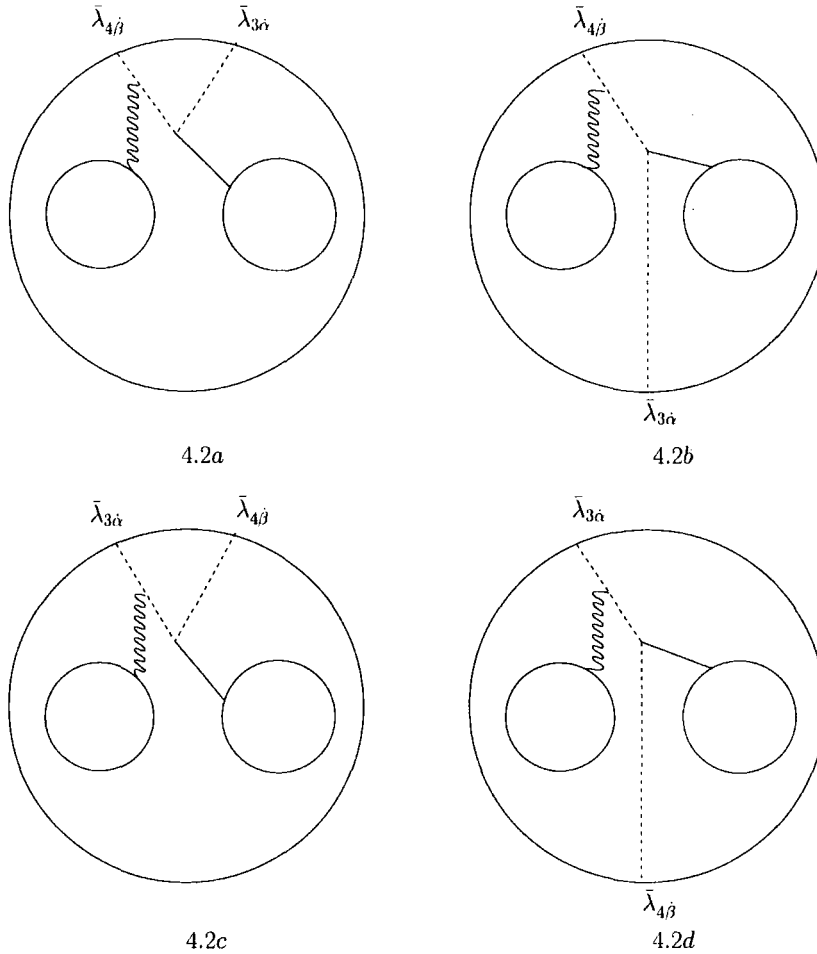


Figure 4.2: Gluon emission diagrams originating from the compensating term in the internal operator. The gluon is absorbed by the fermion field. There are also mirror diagrams, not drawn in this figure.

in Figure 4.2 we get:<sup>8</sup>

$$I_{\dot{\alpha}\dot{\gamma},\dot{\alpha}\dot{\beta}} = -2 \cdot (-1)^3 \partial_\mu^4 \sigma_{\beta\dot{\beta}}^\mu \partial_\nu^3 \sigma_{\alpha\dot{\alpha}}^\nu (-i\bar{\sigma}_\rho^{\dot{\gamma}\beta}) \sigma_{\dot{\gamma}\gamma}^\tau (-\sqrt{2}i\epsilon^{\gamma\alpha}) \partial_\delta^1 (\sigma_{\delta\rho})_{\dot{\gamma}}^{\dot{\beta}} \epsilon_{\dot{\alpha}\dot{\beta}} (-H_{\tau 1432}) . \quad (4.66)$$

The factor of  $(-1)^3$  comes from three propagators, while the factor of 2 arises from the two terms in the field strength  $F_{\rho\delta}$ . The  $\sigma_{\rho\delta}$  is related to the compensating term of the operator at  $x_1$  while the  $\bar{\sigma}_\rho$  matrix comes from the gluon-fermion interaction vertex. Finally, the minus sign in front of (4.66) comes from Wick contracting fermions.

<sup>8</sup>As in [2], the diagrams where the compensating term is taken in the external operator, or both in the external and internal operator, do not contribute.

We can now elaborate (4.66) using the completeness relation (C.11), to obtain:

$$I_{\hat{\alpha}\hat{\gamma},\hat{\alpha}\hat{\beta}} = 2\sqrt{2}[(\sigma^\delta\bar{\sigma}^\tau\sigma^\nu)_{\hat{\gamma}\hat{\alpha}}\sigma_{\hat{\alpha}\hat{\beta}}^\mu + (\sigma^\delta\bar{\sigma}^\tau\sigma^\nu)_{\hat{\alpha}\hat{\alpha}}\sigma_{\hat{\gamma}\hat{\beta}}^\mu] \partial_\mu^4 \partial_\nu^3 \partial_\delta^1 (-H_{\tau,1432}) . \quad (4.67)$$

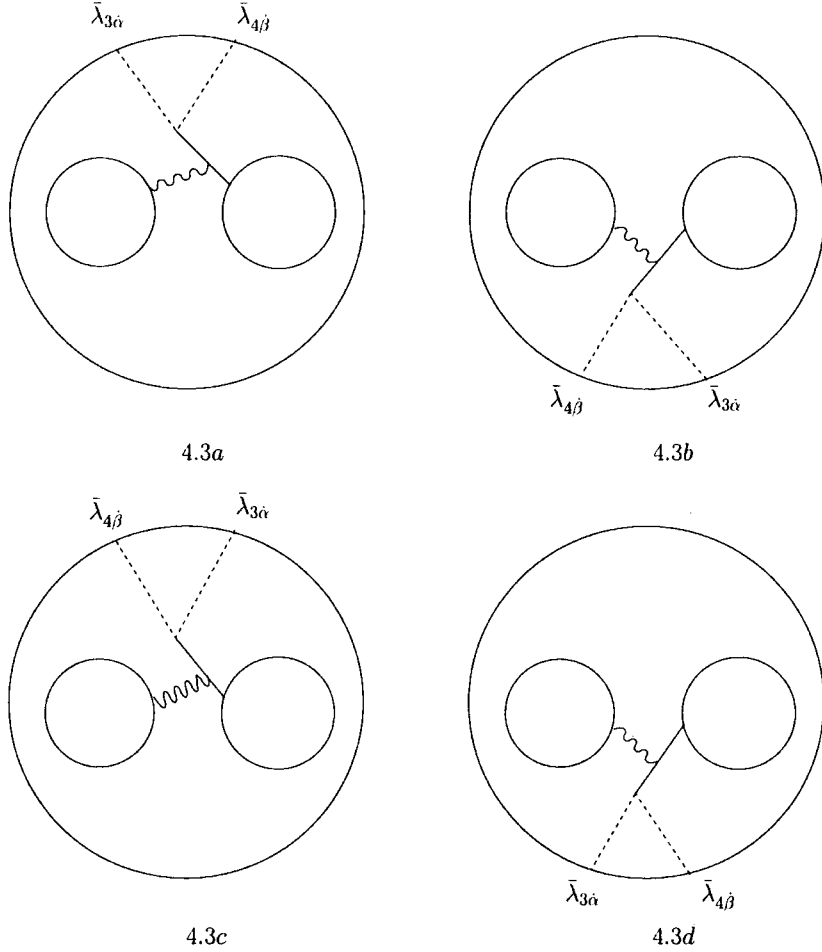


Figure 4.3: Gluon emission diagrams originating from the compensating term in the internal operator. The gluon is absorbed by the  $Z$  field.

Using (C.12), and discarding the irrelevant  $\epsilon$ -terms as before, we get:

$$I_{\hat{\alpha}\hat{\gamma},\hat{\alpha}\hat{\beta}} = 2\sqrt{2}\partial_{\hat{\alpha}\hat{\beta}}^4 (\partial_{\hat{\gamma}\hat{\alpha}}^3 J_A + \partial_{\hat{\gamma}\hat{\alpha}}^1 J_B + (\partial^1 + \partial^4)_{\hat{\gamma}\hat{\alpha}} J_C) + \hat{\alpha} \longleftrightarrow \hat{\gamma} . \quad (4.68)$$

Similarly to the diagrams in Figure 4.1, the  $\log x_{12}^2$  contributions from  $J_B$  and  $J_C$  cancel out, and we are left with:

$$I_{\hat{\alpha}\hat{\gamma},\hat{\alpha}\hat{\beta}} = 8\sqrt{2} \frac{1}{28\pi^6} \log x_{12}^2 (\sigma_{\hat{\alpha}\hat{\beta}}^\mu \sigma_{\hat{\gamma}\hat{\alpha}}^\nu + \sigma_{\hat{\gamma}\hat{\beta}}^\mu \sigma_{\hat{\alpha}\hat{\alpha}}^\nu) \frac{x_3^\mu x_3^\nu}{(x_3^2)^4} . \quad (4.69)$$

Now we perform the inversion for the fermions, thus arriving at:

$$I_{\hat{\alpha}\hat{\gamma}}^{\alpha\beta} = 8\sqrt{2}\frac{1}{28\pi^6} \log x_{12}^2 (\delta_{\hat{\alpha}}^{\alpha}\delta_{\hat{\gamma}}^{\beta} + \delta_{\hat{\gamma}}^{\alpha}\delta_{\hat{\alpha}}^{\beta}). \quad (4.70)$$

The calculation for the diagram in Figure 4.2c (where the other fermion absorbs the gluon) proceeds in a similar fashion to that of Figure 4.2a, giving the same result as in (4.70) but with  $\alpha$  and  $\beta$  swapped. Since the expression for  $I_{\hat{\alpha}\hat{\gamma}}^{\alpha\beta}$  is symmetric under this exchange, the result is the same as for the diagram in Figure 4.2a. We should also not forget to multiply our result by  $1/4$  due to the normalisation of the operators ( $1/2$  for each operator), and by a factor of  $-\sqrt{2}/4$  coming from the compensating term on the right hand side of (4.8). Taking also account the powers of  $g^2/2$  associated with vertices and propagators, we finally get the result for the sum of diagrams 4.2a and 4.2c:

$$-2 \left(\frac{g^2}{2}\right)^3 \frac{1}{28\pi^6} \log x_{12}^2 (\delta_{\hat{\alpha}}^{\alpha}\delta_{\hat{\gamma}}^{\beta} + \delta_{\hat{\gamma}}^{\alpha}\delta_{\hat{\alpha}}^{\beta}). \quad (4.71)$$

The diagrams in Figure 4.2b and 4.2d can be computed in a similar way. Notice that they have a relative minus sign compared to 4.2a and 4.2c, and a different BMN factor  $\bar{q}^{J_1+1}$ .

For  $\alpha \neq \beta$ , the result of (4.71) is exactly the same as the result obtained from the compensating diagrams for the case of BMN operators with *mixed* impurities (one vector and one scalar impurity). We addressed this case in section 4 of [2]. Furthermore, for  $\alpha = \beta$  we get the same result as that of the compensating diagrams of BMN operators with *vector* impurities, i.e. twice that of the mixed case (see [2,62]). From (4.52)-(4.54), one can easily work out the contributions of the compensating terms alone for the mixed and vector case,

$$[b_{m,ny}]_{\text{mixed}}^{\text{c.t.}} = [b_{m,ny}]_{\text{mixed}} - [b_{m,ny}]_{\text{scalar}} = -\frac{1}{2} \left(m - \frac{n}{y}\right)^2, \quad (4.72)$$

$$\begin{aligned} [b_{m,ny}]_{\text{vector}}^{\text{c.t.}} &= [b_{m,ny}]_{\text{vector}} - [b_{m,ny}]_{\text{scalar}} = -\left(m - \frac{n}{y}\right)^2 \\ &= 2 [b_{m,ny}]_{\text{mixed}}^{\text{c.t.}}. \end{aligned} \quad (4.73)$$

Finally, let us note that at the order we are working, the diagrams of Figure 4.3 are also present. However, the diagram in 4.3a cancels against that in 4.3b because of the relative minus sign associated with the vertex where the gluon is absorbed; and,

similarly, 4.3c cancels against 4.3d. Therefore the net contribution of the diagrams in Figure 4.3 is zero.

We conclude by summarising the results of this section.

- a. The contribution of the pure BMN part of the operators involved in the three-point function (4.55) is precisely the same obtained for *scalar* BMN operators. Hence the corresponding coefficient  $b_{m,ny}$  is given by (4.52).
- b. The previous remark also implies that, when no compensating term is present in the expression for the BMN operator considered, the result (4.52) gives the full answer.
- c. When a compensating term appears, it contributes precisely as the compensating term of the mixed (scalar-vector) case when  $\alpha \neq \beta$ , of the vector case for  $\alpha = \beta$ . The corresponding expressions for  $b_{m,ny}$  are then (4.53) and (4.54), respectively.

## 4.5 Testing the BMN correspondence in the fermion sector

We can now apply the results derived in the previous section to test the pp-wave/SYM correspondence in the fermionic sector. In particular, we will reproduce in the gauge theory the three-string amplitudes for the following flavour-conserving processes:

$$(\lambda_{31} \dots \lambda_{32})_m \longrightarrow (\lambda_{31} \dots \lambda_{32})_n + \text{vac.} , \quad (4.74)$$

$$(\lambda_{31} \dots \lambda_{31})_m \longrightarrow (\lambda_{31} \dots \lambda_{31})_n + \text{vac.} , \quad (4.75)$$

$$(\lambda_{31} \dots \lambda_{42})_m \longrightarrow (\lambda_{31} \dots \lambda_{42})_n + \text{vac.} , \quad (4.76)$$

$$(\lambda_{31} \dots \lambda_{41})_m \longrightarrow (\lambda_{31} \dots \lambda_{41})_n + \text{vac.} . \quad (4.77)$$

A few comments are in order.

1. First, it does not take long to realise that these cases actually cover all the irreducible representations of the two-impurity fermion BMN operators, where the two impurities are Weyl spinor of the same chirality (see (4.16) and (4.17)).
2. The case where the two impurities have opposite chirality,  $\lambda_{r\alpha}$  and  $\bar{\lambda}_{\dot{r}\dot{\beta}}$  (see (4.18)), can of course be treated with a similar technique. Notice that, in that

case, a compensating term containing  $(D_\mu \phi^i) \sigma_{\alpha\beta}^\mu$  will always be present in the precise expression of the BMN operator containing the  $\lambda_{r\alpha}$ ,  $\bar{\lambda}_{\dot{r}\beta}$  impurities, in agreement with the fact that the right hand side of (4.18) contains only one irreducible representation.

3. Finally, notice that the operators taking part in the first two processes (4.74) and (4.75) do not have compensating terms, i.e. they do not have a projection onto the  $(\mathbf{1}, \mathbf{3}^+)$  representation of  $SO(4) \times SO(4)$ , in contradistinction with the operators taking part in the remaining last two, (4.76) and (4.77).

Let us write down the string amplitudes corresponding to the processes of (4.74)-(4.77), taking into account that in the three-string vertex of [52, 53, 55, 65] all the external states are written as ket states:

$$\begin{aligned} \mu^{-1} \langle v | \beta_{-m(3)}^{12} \beta_{m(3)}^{11} \beta_{11,n(1)} \beta_{12,-n(1)} | H_3 \rangle &\equiv A_1 , \\ \mu^{-1} \langle v | \beta_{-m(3)}^{11} \beta_{m(3)}^{11} \beta_{11,n(1)} \beta_{11,-n(1)} | H_3 \rangle &\equiv A_2 , \\ \mu^{-1} \langle v | \beta_{-m(3)}^{22} \beta_{m(3)}^{11} \beta_{11,n(1)} \beta_{22,-n(1)} | H_3 \rangle &\equiv A_3 , \\ \mu^{-1} \langle v | \beta_{-m(3)}^{21} \beta_{m(3)}^{11} \beta_{11,n(1)} \beta_{21,-n(1)} | H_3 \rangle &\equiv A_4 . \end{aligned} \quad (4.78)$$

We have already computed the string amplitudes in (4.78) in (4.31)-(4.34), finding

$$A_1 = -\lambda' C_{\text{norm}} \frac{\beta+1}{\pi^2} \sin^2 \pi m \beta , \quad (4.79)$$

$$A_2 = 0 , \quad (4.80)$$

$$A_3 = 0 , \quad (4.81)$$

$$A_4 = \lambda' C_{\text{norm}} \frac{\beta+1}{\pi^2} \sin^2 \pi m \beta . \quad (4.82)$$

We start our analysis from the first process (4.74). For this case, we have found in the previous section that the corresponding coefficient  $b_{m,ny}$  of the field theory three-point function is exactly the same as that obtained in the case of BMN operators with two scalar impurities of different flavours. This is due to the absence of compensating terms in the operators participating in the process (4.74), so that only the diagrams of Figure 4.1 contribute (with  $\lambda_4$  replaced by the second  $\lambda_3$ ). As explained in (4.51), supersymmetry guarantees that the anomalous dimension of the two fermion BMN operators is the same as that of two scalars; therefore, the coefficient  $a_{m,ny}$  for the

fermions is identical to that of two different scalars. The consequence of this is that the gauge theory prediction for the string amplitude of (4.74) is exactly the same as the prediction obtained in the case of BMN operators with two different scalar impurities; and it was shown in [2] that there is precise agreement between the field theory and string theory prediction in the case of two scalar impurities of different flavours. The result obtained in string field theory for the process (4.74) is given in (4.79). Indeed, this result (4.79) precisely coincides with the string amplitude for the case of two scalar impurities, Eq. (4.36). This is our first test.

Two identical fermions, both in the unbarred and barred operators, take part in the process in (4.75). The corresponding gauge theory calculation is therefore slightly more complicated, since there are twice as many contractions as in the previous case, and thus twice as many Feynman diagrams. Taking these diagrams into account, the  $S$  and  $T$  matrices take the following form:

$$S = \begin{pmatrix} \delta_{mn} & g_2 (C_{m,qz} - C_{m,-qz}) \\ g_2 (C_{py,n} - C_{-py,n}) & \delta_{pq} \end{pmatrix} + \mathcal{O}(g_2^2) \quad (4.83)$$

$$= \mathbb{1} + g_2 s + \mathcal{O}(g_2^2),$$

$$T = \lambda' \begin{pmatrix} m^2 \delta_{mn} & g_2 [C_{m,qz} (a+b)_{m,qz} \\ -C_{m,-qz} (a+b)_{m,-qz}] \\ g_2 [C_{py,n} (a+b)_{py,n} & (p^2/y^2) \delta_{pq} \delta_{yz} \\ -C_{-py,n} (a+b)_{-py,n}] \end{pmatrix} + \mathcal{O}(g_2^2) \quad (4.84)$$

$$= d + g_2 t + \mathcal{O}(g_2^2).$$

In (4.84) the coefficient  $a_{m,ny}$  is as in (4.51), and  $b_{m,ny}$  is given in (4.52), as explained in section 4.4. We should note the crucial minus sign between the two terms appearing in the non-diagonal matrix elements of  $T$ . This comes from the anticommuting nature

of the fermion impurities. We can now work out the expression for the matrix  $\Gamma$  of the SYM dilatation operator in the field theory basis which is isomorphic to the natural string basis. Using (4.50), we get immediately

$$\Gamma = d + g_2 \left[ t - (1/2) \{s, d\} \right] = \lambda' \begin{pmatrix} m^2 \delta_{mn} & 0 \\ 0 & (p^2/y^2) \delta_{pq} \delta_{yz} \end{pmatrix}. \quad (4.85)$$

Thus, we conclude that the field theory prediction for the second process (4.75) is 0. This is in agreement with the vanishing of the corresponding string amplitude of (4.80).

Next, we consider the third process, (4.76). In this case the compensating diagrams of Figure 4.2 should be taken into account. As we have noticed in the previous section (see the discussion after (4.71)), the contribution of the compensating term is the same as that arising from compensating terms of BMN operators with mixed (one scalar-one vector) impurities. Furthermore, the contribution of the diagrams where only the pure BMN parts of the operators is taken into account, is the same for all the cases (i.e. scalar, mixed, vector and fermion impurities). Therefore, we conclude that the coefficient  $b_{m,ny}$  appearing in the the three-point function, and thus the whole calculation, are identical to the mixed case studied in [2].<sup>9</sup> It was found in [2] that the matrix elements of the dilatation operator in the isomorphic to string basis for the case of BMN operators with mixed impurities is given by

$$\Gamma_{\text{mixed}} = d + g_2 \left[ t_{\text{mixed}} - (1/2) \{s, d\} \right] = \lambda' \begin{pmatrix} m^2 \delta_{mn} & 0 \\ 0 & (p^2/y^2) \delta_{pq} \delta_{yz} \end{pmatrix}. \quad (4.86)$$

Therefore, the previous result (4.86) precisely reproduces, in the gauge theory, the vanishing three-string amplitude of (4.81).

Finally, we focus on the last process of (4.77). We noticed in section 4.4 that the diagrams from the compensating terms contribute, in this case, exactly as the diagrams from the compensating term for two vector operators. Following similar

---

<sup>9</sup>As before, in order to reach this conclusion we also used the fact that the anomalous dimension of all two-impurity operators, i.e. is the  $a_{m,ny}$  coefficient, is the same for any kind of impurity.

arguments as before, we conclude that the field theory prediction for this process is the same as that for the vector case. The result for the vector case was found in [2] to be equal to the negative of the result for the process for the scalars, which in turns is equal to the result for (4.74). This is again in perfect agreement with the string amplitude obtained in (4.82). This is our last test.

We close this section with a comment about how the  $\mathbb{Z}_2$  symmetry of the pp-wave background is realised in the string amplitudes of (4.78). It is known that under the  $\mathbb{Z}_2$  symmetry the two indices of a fermion creation or annihilation operator are exchanged,

$$\mathbb{Z}_2 : \quad \beta_{\alpha\beta} \longrightarrow \beta_{\beta\alpha} . \quad (4.87)$$

However, whereas the string vertex  $|H_3\rangle$  is invariant under  $\mathbb{Z}_2$ , the true vacuum  $|v\rangle$  corresponds to a combination of the trace of the metric and the five-form field on one of the  $\mathbb{R}_4$ 's [96], and thus one has to assign negative  $\mathbb{Z}_2$  parity to it [59, 65]. The correctness of this assignment was also verified from the field theory perspective in [2] (see also the discussion in the Introduction). If we apply (4.87) to the string amplitudes in (4.78) we obtain:

$$\begin{aligned} \hat{\mathbb{Z}}_2 A_1 &\equiv -A_4 = A_1 , \\ \hat{\mathbb{Z}}_2 A_2 &\equiv -A_2 = A_2 , \\ \hat{\mathbb{Z}}_2 A_3 &\equiv -A_3 = A_3 , \\ \hat{\mathbb{Z}}_2 A_4 &\equiv -A_1 = A_4 . \end{aligned} \quad (4.88)$$

Therefore, we conclude that the  $\mathbb{Z}_2$  symmetry leaves the value of the string amplitudes of (4.74)-(4.77) invariant.

In this chapter, we have investigated the fermionic sector of the pp-wave/SYM duality to find perfect agreement between field theory and string theory providing, thus, solid evidence in favour of the duality.

Recently, another type of weak-to-weak duality which relates  $\mathcal{N} = 4$  SYM to a topological string theory in twistor space was proposed in [107]. This duality is particularly interesting from both the theoretical and the phenomenological point of view since it has inspired a completely new diagrammatic approach for calculating

scattering amplitudes in gauge theory. We discuss this approach and some of its generalisations in the next two chapters.

# Chapter 5

## Tree Amplitudes in Gauge Theory as Scalar MHV Diagrams

In a recent paper [107] Witten proposed that tree level amplitudes of  $\mathcal{N} = 4$  SYM can be reproduced by integrating over the moduli space of certain D-instantons in the open string topological B-model whose target space is the super-twistor space  $CP^{3|4}$ . This gives rise to a new duality between weakly coupled  $\mathcal{N} = 4$  SYM and a weakly coupled, topological string theory in twistor space.

Inspired by this correspondence, a novel diagrammatic method for calculating all gluon scattering amplitudes at tree level was proposed by Cachazo, Svrcek and Witten [106].

In this approach tree amplitudes in a pure gauge theory are found by summing tree-level scalar Feynman diagrams with new vertices. The building blocks of this formalism are scalar propagators  $1/p^2$ , and tree-level maximal helicity violating (MHV) amplitudes, which are interpreted as new scalar vertices. Using multi-particle amplitudes as effective vertices enables one to save dramatically on a number of permutations in usual Feynman diagrams.

The new perturbation theory involves scalar diagrams since MHV vertices are scalar quantities. They are linked together by scalar propagators at tree-level, and the internal lines are continued off-shell in a particular fashion. The final result for

any particular amplitude can be shown to be Lorentz-covariant and is independent of a particular choice for the off-shell continuation. The authors of [106] derived new expressions for a class of tree amplitudes with three negative helicities and any number of positive ones. It has been verified in [106] and [108] that the new scalar graph approach agrees with a number of known conventional results for scattering amplitudes in pure gauge theory.

The aim of this chapter is to apply the new diagrammatic approach of [106] to tree amplitudes which involve fermion fields as well as gluons. As we proceed we will also describe the details of the CSW proposal. In the presence of fermions there are two new classes of MHV vertices, which involve one and two quark-antiquark lines. This is in addition to the the single class of purely gluonic MHV vertices considered in [106]. All three classes of vertices can in principle be connected to one another via propagators at tree level. This leads to new diagrams and provides us with useful tests of the method. Confirmation of the new diagrammatic approach of [106] in more general settings is important for two reasons. First, as mentioned earlier, this approach offers a much simpler alternative to the usual Feynman diagrams in gauge theory and can be used for deriving a variety of new closed-form expressions for multi-parton tree amplitudes. Of course, in practice, in deriving multi-parton amplitudes there is no need to calculate Feynman diagrams directly as there are other powerful techniques based on the recursion relations [102,123]. We also note that scalar graphs as a powerful method for calculating amplitudes in field theories with gauge fields and fermions was introduced already in [103].<sup>1</sup>

Our second reason for studying and generalising this approach is its relation to string theory in twistor space. On the string side, the SYM amplitude is interpreted in [107] as coming from a D-instanton of charge  $d$ , where  $d$  is equal to the number of negative helicity particles minus 1 plus the number of loops. The new scalar graph method of [106] is interpreted on the string side as the contribution coming entirely from  $d$  single instantons. On the other hand, in an interesting recent paper [104] it

---

<sup>1</sup>In the approach of [103] one also works in the helicity basis and uses scalar propagators and scalar vertices. However the scalar vertices utilized in [103] are not the MHV vertices used in [106] and here.

is argued that the SYM amplitude is fully determined by the opposite extreme case – a single  $d$ -instanton. In principle, there are also contributions from a mixed set of connected and disconnected instantons of total degree  $d$ .

From the gauge theory perspective, there are two questions we can ask:

(1) does the scalar formalism of [106] correctly incorporate gluinos in a generic supersymmetric theory, and

(2) does it work for diagrams with fundamental quarks in a non-supersymmetric  $SU(N)$  theory, i.e. in QCD?

It is often stated in the literature that any gauge theory is supersymmetric at tree level. This is because at tree level superpartners cannot propagate in loops. This observation, on its own, does not answer the question of how to relate amplitudes with quarks to amplitudes with gluinos. The colour structure of these amplitudes is clearly different.<sup>2</sup> However, we will see that the purely kinematic parts of these amplitudes are the same at tree level.

In the next section we briefly recall well-known results about decomposition of full amplitudes into the colour factor  $T_n$  and the purely kinematic partial amplitude  $A_n$ . A key point in the approach of [106] and also in [104, 107] is that only the kinematic amplitude  $A_n$  is evaluated directly. Since  $A_n$  does not contain colour factors, it is the same for tree amplitudes involving quarks and for those with gluinos. There is an important point we should stress here. A priori, when comparing kinematic amplitudes in a non-supersymmetric and in a supersymmetric theory, we should make sure that both theories have a similar field content. In particular, when comparing kinematic amplitudes in QCD and in SYM, (at least initially) we need to restrict to the SYM theory with vectors, fermions and no scalars. Scalars are potentially dangerous, since they can propagate in the internal lines and spoil the agreement between the amplitudes. Hence, while the kinematic tree-level amplitudes in massless QCD agree with those in  $\mathcal{N} = 1$  pure SYM, one might worry that the agreement will be lost when comparing QCD with  $\mathcal{N} = 4$  (and  $\mathcal{N} = 2$ ) theories. Fortunately,

---

<sup>2</sup>Also, amplitudes with gluons and gluinos are automatically planar at tree level. This is not the case for tree diagrams with quarks, as they do contain  $1/N$ -suppressed terms in  $SU(N)$  gauge theory.

this is not the case, the agreement between amplitudes in QCD and amplitudes in SYM theories does not depend on  $\mathcal{N}$ . The main point here is that in  $\mathcal{N} = 2$  and  $\mathcal{N} = 4$  theories, the scalars  $\phi$  couple to gluinos  $\Lambda^A$  and  $\Lambda^B$  from different  $\mathcal{N} = 1$  supermultiplets,

$$S_{\text{Yukawa}} = g_{\text{YM}} \text{tr} \Lambda_A^- [\phi^{AB}, \Lambda_B^-] + g_{\text{YM}} \text{tr} \Lambda^{A+} [\bar{\phi}_{AB}, \Lambda^{B+}], \quad (5.1)$$

where  $A, B = 1, \dots, \mathcal{N}$ , and  $\phi^{AB} = -\phi^{BA}$ , hence  $A \neq B$ . At the same time, in the kinematic amplitudes quarks are identified with gluinos of the same fixed  $A$ , i.e.

$$q \leftrightarrow \Lambda^{A=1+}, \bar{q} \leftrightarrow \Lambda_{A=1}^-.$$

QCD-amplitudes with  $m$  quarks,  $m$  antiquarks and  $l$  gluons in external lines correspond to SYM-amplitudes with  $m$  gluinos  $\Lambda^{1+}$ ,  $m$  anti-gluinos  $\Lambda_1^-$ , and  $l$  gluons. Since all external (anti)-gluinos are from the same  $\mathcal{N} = 1$  supermultiplet, they cannot produce scalars in the internal lines of tree diagrams. These diagrams are the same for all  $\mathcal{N} = 0, \dots, 4$ . Of course, in  $\mathcal{N} = 4$  and  $\mathcal{N} = 2$  theories there are other classes of diagrams with gluinos from different  $\mathcal{N} = 1$  supermultiplets, and also with scalars in external lines. Applications of the scalar graph approach to these more general classes of tree amplitudes in  $\mathcal{N} = 2, 4$  are presented in [105].

We conclude that, if the new formalism gives correct results for partial amplitudes  $A_n$  in a supersymmetric theory, it will also work in a nonsupersymmetric case, and for a finite number of colours. Full amplitudes are then determined uniquely from the kinematic part  $A_n$ , and the known expressions for  $T_n$ , given in (5.4), (5.6) below. This means that for tree amplitudes questions (1) and (2) are essentially the same.

In section 5.2 we explain how the diagrammatic approach of [106] works for calculating scattering amplitudes of gluons and fermions at tree level. This method leads to explicit and relatively simple expressions for many amplitudes. As a first example, using the scalar graph approach, we derive an expression for non-MHV  $---+ \dots +$  amplitudes  $A_n$  with two fermions and  $n - 2$  gluons. We furthermore derive a non-MHV  $n$ -point amplitude which involves four fermions. These new results are checked successfully against some previously known expressions for  $n = 4, 5$ .

## 5.1 Tree Amplitudes

We concentrate on tree-level amplitudes in a gauge theory with an arbitrary finite number of colours. For definiteness we take the gauge group to be  $SU(N)$  and consider tree-level scattering amplitudes with arbitrary numbers of external gluons and fermions (it is also straightforward to include scalar fields, but we leave them out from most of what follows for simplicity).  $SU(N)$  is unbroken and all fields are taken to be massless, we refer to them generically as gluons, gluinos and quarks, though the gauge theory is not necessarily assumed to be supersymmetric.

### 5.1.1 Colour decomposition

It is well-known that a full  $n$ -point amplitude  $\mathcal{M}_n$  can be represented as a sum of products of colour factors  $T_n$  and purely kinematic partial amplitudes  $A_n$ ,

$$\mathcal{M}_n(\{k_i, h_i, c_i\}) = \sum_{\sigma} T_n(\{c_{\sigma(i)}\}) A_n(\{k_{\sigma(i)}, h_{\sigma(i)}\}). \quad (5.2)$$

Here  $\{c_i\}$  are colour labels of external legs  $i = 1 \dots n$ , and the kinematic variables  $\{k_i, h_i\}$  are on-shell external momenta and helicities: all  $k_i^2 = 0$ , and  $h_i = \pm 1$  for gluons,  $h_i = \pm \frac{1}{2}$  for fermions. The sum in (5.2) is over appropriate simultaneous permutations  $\sigma$  of colour labels  $\{c_{\sigma(i)}\}$  and kinematic variables  $\{k_{\sigma(i)}, h_{\sigma(i)}\}$ . The colour factors  $T_n$  are easy to determine, and the non-trivial information about the full amplitude  $\mathcal{M}_n$  is contained in the purely kinematic part  $A_n$ . If the partial amplitudes  $A_n(\{k_i, h_i\})$  are known for all permutations  $\sigma$  of the kinematic variables, the full amplitude  $\mathcal{M}_n$  can be determined from (5.2).

We first consider tree amplitudes with arbitrary numbers of gluons and gluinos (and with no quarks). The colour variables  $\{c_i\}$  correspond to the adjoint representation indices,  $\{c_i\} = \{a_i\}$ , and the colour factor  $T_n$  is a single trace of generators,

$$\mathcal{M}_n^{\text{tree}}(\{k_i, h_i, a_i\}) = \sum_{\sigma} \text{tr}(T^{a_{\sigma(1)}} \dots T^{a_{\sigma(n)}}) A_n^{\text{tree}}(k_{\sigma(1)}, h_{\sigma(1)}, \dots, k_{\sigma(n)}, h_{\sigma(n)}). \quad (5.3)$$

Here the sum is over  $(n-1)!$  noncyclic inequivalent permutations of  $n$  external particles. The single-trace structure in (5.3),

$$T_n = \text{tr}(T^{a_1} \dots T^{a_n}), \quad (5.4)$$

implies that all tree level amplitudes of particles transforming in the adjoint representation of  $SU(N)$  are planar. This is not the case neither for loop amplitudes, nor for tree amplitudes involving fundamental quarks.

Fields in the fundamental representation couple to the trace  $U(1)$  factor of the  $U(N)$  gauge group. In passing to the  $SU(N)$  case this introduces power-suppressed  $1/N^p$  terms. However, there is a remarkable simplification for tree diagrams involving fundamental quarks: the factorisation property (5.2) still holds. More precisely, for a fixed colour ordering  $\sigma$ , the amplitude with  $m$  quark-antiquark pairs and  $l$  gluons (and gluinos) is still a perfect product,

$$T_{l+2m}(\{c_{\sigma(i)}\}) A_{l+2m}(\{k_{\sigma(i)}, h_{\sigma(i)}\}), \quad (5.5)$$

and all  $1/N^p$  corrections to the amplitude are contained in the first term. For tree amplitudes the exact colour factor in (5.5) is [125]

$$T_{l+2m} = \frac{(-1)^p}{N^p} (T^{a_1} \dots T^{a_{l_1}})_{i_1 \alpha_1} (T^{a_{l_1+1}} \dots T^{a_{l_2}})_{i_2 \alpha_2} \dots (T^{a_{l_{m-1}+1}} \dots T^{a_l})_{i_m \alpha_m}. \quad (5.6)$$

Here  $l_1, \dots, l_m$  correspond to an arbitrary partition of an arbitrary permutation of the  $l$  gluon indices;  $i_1, \dots, i_m$  are colour indices of quarks, and  $\alpha_1, \dots, \alpha_m$  – of the antiquarks. In perturbation theory each external quark is connected by a fermion line to an external antiquark (all particles are counted as incoming). When quark  $i_k$  is connected by a fermion line to antiquark  $\alpha_k$ , we set  $\alpha_k = \bar{i}_k$ . Thus, the set of  $\alpha_1, \dots, \alpha_m$  is a permutation of the set  $\bar{i}_1, \dots, \bar{i}_m$ . Finally, the power  $p$  is equal to the number of times  $\alpha_k = \bar{i}_k$  minus 1. When there is only one quark-antiquark pair,  $m=1$  and  $p=0$ . For a general  $m$ , the power  $p$  in (5.6) varies from 0 to  $m-1$ .

The kinematic amplitudes  $A_{l+2m}$  in (5.5) have the colour information stripped off and hence do not distinguish between fundamental quarks and adjoint gluinos. Thus,

$$A_{l+2m}(q, \dots, \bar{q}, \dots, g^+, \dots, g^-, \dots) = A_{l+2m}(\Lambda^+, \dots, \Lambda^-, \dots, g^+, \dots, g^-, \dots), \quad (5.7)$$

where  $q, \bar{q}, g^\pm, \Lambda^\pm$  denote quarks, antiquarks, gluons and gluinos of  $\pm$  helicity.

In section 5.2 we will use the scalar graph formalism of [106] to evaluate the kinematic amplitudes  $A_n$  in (5.7). Full amplitudes can then be determined uniquely from the kinematic part  $A_n$ , and the known expressions for  $T_n$  in (5.4) and (5.6) by summing over the inequivalent colour orderings in (5.2).

From now on we concentrate on the purely kinematic part of the amplitude,  $A_n$ .

### 5.1.2 Helicity amplitudes

We will be studying tree level partial amplitudes  $A_n = A_{l+2m}$  with  $l$  gluons and  $2m$  fermions in the helicity basis. All external lines are defined to be incoming, and a fermion of helicity  $+\frac{1}{2}$  is always connected by a fermion propagator to a helicity  $-\frac{1}{2}$  fermion,<sup>3</sup> hence the number of fermions  $2m$  is always even.

A tree amplitude  $A_n$  with  $n$  or  $n - 1$  particles of positive helicity vanishes identically. The same is true for  $A_n$  with  $n$  or  $n - 1$  particles of negative helicity. First nonvanishing amplitudes contain  $n - 2$  particles with helicities of the same sign and are called maximal helicity violating (MHV) amplitudes.

The spinor helicity formalism<sup>4</sup> is defined in terms of two commuting spinors of positive and negative chirality,  $\lambda_a$  and  $\tilde{\lambda}_{\dot{a}}$ . Using these spinors, any on-shell momentum of a massless particle,  $p_\mu p^\mu = 0$ , can be written as

$$p_{a\dot{a}} = p_\mu \sigma^\mu = \lambda_a \tilde{\lambda}_{\dot{a}} . \quad (5.8)$$

Spinor inner products are introduced as

$$\langle \lambda, \lambda' \rangle = \epsilon_{ab} \lambda^a \lambda'^b , \quad [\tilde{\lambda}, \tilde{\lambda}'] = \epsilon_{\dot{a}\dot{b}} \tilde{\lambda}^{\dot{a}} \tilde{\lambda}'^{\dot{b}} . \quad (5.9)$$

Then a scalar product of two null vectors,  $p_{a\dot{a}} = \lambda_a \tilde{\lambda}_{\dot{a}}$  and  $q_{a\dot{a}} = \lambda'_a \tilde{\lambda}'_{\dot{a}}$ , is

$$p_\mu q^\mu = \frac{1}{2} \langle \lambda, \lambda' \rangle [\tilde{\lambda}, \tilde{\lambda}'] . \quad (5.10)$$

Momentum conservation in an  $n$ -point amplitude provides another useful identity

$$\sum_{i=1}^n \langle \lambda_r, \lambda_i \rangle [\tilde{\lambda}_i, \tilde{\lambda}_s] = 0 , \quad (5.11)$$

for arbitrary  $1 \leq r, s \leq n$ .

---

<sup>3</sup>This is generally correct only in theories without scalar fields. In the  $\mathcal{N} = 4$  theory, a pair of positive helicity fermions,  $\Lambda^{1+}$ ,  $\Lambda^{2+}$ , can be connected to another pair of positive helicity fermions,  $\Lambda^{3+}$ ,  $\Lambda^{4+}$ , by a scalar propagator. As already mentioned in the introduction, for all amplitudes considered in this chapter we will take external fermions from the same  $\mathcal{N} = 1$  supermultiplet, i.e.  $A = 1$ , and this will rule out contributions of scalar fields even in the  $\mathcal{N} = 4$  theory.

<sup>4</sup>This formalism was used for calculating scattering amplitudes first in [122–124]. We follow conventions of [107] and refer the reader also to comprehensive reviews [125, 126] where more detail and references can be found. Our helicity spinor conventions are summarised in the Appendix H

In the usual perturbative evaluation of amplitudes, external on-shell lines in Feynman diagrams are multiplied by wave-function factors: a polarization vector  $\varepsilon_{\pm}^{\mu}$  for each external gluon  $A_{\mu}$ , and spinors  $u_{\pm}$  and  $\bar{u}_{\pm}$  for external quarks and antiquarks. The resulting amplitude is a Lorentz scalar. The spinors  $\lambda$  and  $\tilde{\lambda}$  are precisely the wave-functions of fermions and corresponding antifermions (see Appendix H for more detail)

$$u_{+}(k_i)_a = \lambda_{ia}, \quad \overline{u_{+}(k_i)}_{\dot{a}} = \tilde{\lambda}_{i\dot{a}}, \quad (5.12)$$

and the polarization vectors  $\varepsilon_{\pm}^{\mu}$  are also defined in a natural way in terms of  $\lambda$ ,  $\tilde{\lambda}$  (and a ‘reference’ spinor), as in [107].

$A_n(g_1^+, \dots, g_{r-1}^+, g_r^-, g_{r+1}^+, \dots, g_{s-1}^+, g_s^-, g_{s+1}^+, \dots, g_n^+)$  is the ‘mostly plus’ purely gluonic MHV amplitude with  $n - 2$  gluons of positive helicity and 2 gluons of negative helicity in positions  $r$  and  $s$ . To simplify notation, from now on we will not indicate the positive helicity gluons in the mostly plus amplitudes and the negative helicity gluons in the mostly minus amplitudes. Also, the mostly plus maximal helicity violating amplitudes will be referred to simply as the MHV amplitudes, and the mostly minus maximal helicity violating amplitudes will be called the  $\overline{\text{MHV}}$ . Finally, in all the amplitudes  $A_n$  we will suppress the common momentum conservation factor of

$$i g_{\text{YM}}^{n-2} (2\pi)^4 \delta^{(4)} \left( \sum_{i=1}^n \lambda_{ia} \tilde{\lambda}_{i\dot{a}} \right) \quad (5.13)$$

Using these conventions, the MHV gluonic amplitude is

$$A_n(g_r^-, g_s^-) = \frac{\langle \lambda_r, \lambda_s \rangle^4}{\prod_{i=1}^n \langle \lambda_i, \lambda_{i+1} \rangle} \equiv \frac{\langle r s \rangle^4}{\prod_{i=1}^n \langle i i+1 \rangle}, \quad (5.14)$$

where  $\lambda_{n+1} \equiv \lambda_1$ . The corresponding  $\overline{\text{MHV}}$  amplitude with positive helicity gluons in positions  $r$  and  $s$  is

$$A_n(g_r^+, g_s^+) = \frac{[\tilde{\lambda}_r, \tilde{\lambda}_s]^4}{\prod_{i=1}^n [\tilde{\lambda}_i, \tilde{\lambda}_{i+1}]} \equiv \frac{[r s]^4}{\prod_{i=1}^n [i i+1]}. \quad (5.15)$$

The closed-form expressions (5.14), (5.15) were derived in [122, 123]. These and other results in the helicity formalism are reviewed in [125, 126].

An MHV amplitude  $A_n = A_{l+2m}$  with  $l$  gluons and  $2m$  fermions (from the same  $\mathcal{N} = 1$  supermultiplet) exists only for  $m = 0, 1, 2$ . This is because it must have precisely  $n - 2$  particles with positive and 2 with negative helicities, and our fermions

always come in pairs with helicities  $\pm\frac{1}{2}$ . Hence, including (5.14), there are three types of MHV tree amplitudes,

$$A_n(g_r^-, g_s^-), \quad A_n(g_t^-, \Lambda_r^-, \Lambda_s^+), \quad A_n(\Lambda_t^-, \Lambda_s^+, \Lambda_r^-, \Lambda_q^+). \quad (5.16)$$

Expressions for all three MHV amplitudes in (5.16) can be simply read off the  $\mathcal{N} = 4$  supersymmetric formula of Nair [120]:

$$A_n^{\mathcal{N}=4} = \delta^{(8)} \left( \sum_{i=1}^n \lambda_{ia} \eta_i^A \right) \frac{1}{\prod_{i=1}^n \langle i \ i+1 \rangle}, \quad (5.17)$$

where  $\eta_i^A$ ,  $A = 1, 2, 3, 4$  is the  $\mathcal{N} = 4$  Grassmann coordinate. Taylor expanding (5.17) in powers of  $\eta_i$ , one can identify each term in the expansion with a particular tree-level MHV amplitude in the  $\mathcal{N} = 4$  theory.  $(\eta_i)^k$  for  $k = 0, \dots, 4$  is interpreted as the  $i^{\text{th}}$  particle with helicity  $h_i = 1 - \frac{k}{2}$ . Hence,  $h_i = \{1, \frac{1}{2}, 0, -\frac{1}{2}, -1\}$ , where zero is the helicity of a scalar field. It is straightforward to write down a general rule for associating a power of  $\eta$  with all component fields in  $\mathcal{N} = 4$ ,

$$\begin{aligned} g_i^- &\leftarrow \eta_i^1 \eta_i^2 \eta_i^3 \eta_i^4, & \phi^{AB} &\leftarrow \eta_i^A \eta_i^B, & \Lambda^{A+} &\leftarrow \eta_i^A, & g_i^+ &\leftarrow 1, \\ \Lambda_1^- &\leftarrow -\eta_i^2 \eta_i^3 \eta_i^4, & \Lambda_2^- &\leftarrow -\eta_i^1 \eta_i^3 \eta_i^4, & \Lambda_3^- &\leftarrow -\eta_i^1 \eta_i^2 \eta_i^4, & \Lambda_4^- &\leftarrow -\eta_i^1 \eta_i^2 \eta_i^3. \end{aligned} \quad (5.18)$$

The amplitude (5.14) can be obtained from (5.17), (5.18) by selecting the  $(\eta_r)^4 (\eta_s)^4$  term; the second amplitude in (5.16) follows an appropriate  $(\eta_t)^4 (\eta_r)^3 (\eta_s)^1$  term in (5.17); and the third amplitude in (5.16) is an  $(\eta_r)^3 (\eta_s)^1 (\eta_p)^3 (\eta_q)^1$  term. For our calculations in addition to (5.14) we will need expressions for MHV amplitudes with  $m = 1$  and  $m = 2$  pairs of fermions (with the same  $A$ ). The MHV amplitude with two external fermions and  $n - 2$  gluons is

$$A_n(g_t^-, \Lambda_r^-, \Lambda_s^+) = \frac{\langle t \ r \rangle^3 \langle t \ s \rangle}{\prod_{i=1}^n \langle i \ i+1 \rangle}, \quad A_n(g_t^-, \Lambda_s^+, \Lambda_r^-) = -\frac{\langle t \ r \rangle^3 \langle t \ s \rangle}{\prod_{i=1}^n \langle i \ i+1 \rangle}, \quad (5.19)$$

where the first expression corresponds to  $r < s$  and the second to  $s < r$  (and  $t$  is arbitrary). The MHV amplitudes with four fermions and  $n - 4$  gluons on external lines are

$$A_n(\Lambda_t^-, \Lambda_s^+, \Lambda_r^-, \Lambda_q^+) = \frac{\langle t \ r \rangle^3 \langle s \ q \rangle}{\prod_{i=1}^n \langle i \ i+1 \rangle}, \quad A_n(\Lambda_t^-, \Lambda_r^-, \Lambda_s^+, \Lambda_q^+) = -\frac{\langle t \ r \rangle^3 \langle s \ q \rangle}{\prod_{i=1}^n \langle i \ i+1 \rangle} \quad (5.20)$$

The first expression in (5.20) corresponds to  $t < s < r < q$ , the second – to  $t < r < s < q$ , and there are other similar expressions, obtained by further permutations of fermions, with the overall sign determined by the ordering.

The  $\overline{\text{MHV}}$  amplitude can be obtained, as always, by exchanging helicities  $+ \leftrightarrow -$  and  $\langle i j \rangle \leftrightarrow [i j]$ . Expressions (5.19), (5.20) can also be derived from  $\mathcal{N} = 1$  supersymmetric Ward identities, as in [125, 126].

All amplitudes following from Nair's general expression (5.17) are analytic in the sense that they depend only on  $\langle \lambda_i \lambda_j \rangle$  spinor products, and not on  $[\tilde{\lambda}_i \tilde{\lambda}_j]$ . These include amplitudes in (5.14), (5.19), (5.20), as well as more complicated classes of amplitudes, i.e. with external gluinos  $\Lambda^A, \Lambda^{B \neq A}$ , etc, and with external scalar fields.

## 5.2 Calculating Amplitudes Using Scalar Graphs

The formalism of [106] represents all non-MHV tree amplitudes (including  $\overline{\text{MHV}}$ ) as sums of tree diagrams in an effective scalar perturbation theory. The vertices in this theory are the MHV amplitudes (5.16), continued off-shell as described below, and connected by scalar bosonic propagators  $1/p^2$ .

An obvious question one might ask is why one should use the  $1/p^2$  propagator when connecting fermion lines in MHV vertices (5.16). To answer this, recall that the vertices (5.16) already contain the wave-function factors for all external lines, including fermions (5.12). An incoming fermion in one MHV vertex, connected by  $1/p^2$  to an incoming antifermion of another MHV vertex, corresponds to a factor of

$$u_+(p)_a \frac{1}{p^2} \overline{u_+(p)}_{\dot{a}} = \frac{\not{p}_{a\dot{a}}}{p^2}, \quad (5.21)$$

for an internal line in the usual Feynman diagram, which is just the right answer. There is a subtlety with choosing the ordering of fermions in each vertex which is explained in Appendix H in equations (H.5) and (H.7).

When one leg of an MHV vertex is connected by a propagator to a leg of another MHV vertex, both of these legs become internal to the diagram and have to be continued off-shell. Off-shell continuation is defined as follows [106]: we pick an arbitrary spinor  $\eta^{\dot{a}}$  and define  $\lambda_a$  for any internal line carrying momentum  $p_{a\dot{a}}$  by

$$\lambda_a = p_{a\dot{a}} \eta^{\dot{a}}. \quad (5.22)$$

The same  $\eta$  is used for all the off-shell lines in all diagrams contributing to a given amplitude. In practice it will be convenient to choose  $\eta^{\dot{a}}$  to be equal to  $\tilde{\lambda}^{\dot{a}}$  of one of the external legs of negative helicity. External lines in a diagram remain on-shell, and for them  $\lambda$  is defined in the usual way.

Since in each MHV vertex (5.16) there are precisely two lines with negative helicities, and since a propagator always connects lines with opposite helicities, there is a simple relation between the number of negative helicity particles in a given amplitude and the number of MHV vertices needed to construct it,

$$q_{(-1)} + q_{(-\frac{1}{2})} = \sum v - 1 . \quad (5.23)$$

Here  $q_{(-1)}$  is the number of negative helicity gluons,  $q_{(-\frac{1}{2})}$  is the number of negative helicity fermions, and  $\sum v$  is the total number of all MHV vertices (5.16) needed to construct this amplitude.

This formalism leads to explicit and relatively simple expressions for many amplitudes.  $n$ -point amplitudes with three particles of negative helicity is the next case beyond simple MHV amplitudes.

### 5.2.1 Calculating $---+++ \dots ++$ amplitudes with 2 fermions

To illustrate the power of the method in pure gauge theory, the authors of [106] have calculated  $n$  gluon amplitudes with three consecutive gluons of negative helicity  $---+++ \dots ++$ . In order to see precisely what is new when fermions are present, and to provide another useful application of the method, in this section we will calculate a similar amplitude with three negative helicities which are now carried by a fermion and two gluons.

We consider an  $n$ -point amplitude,

$$A_n(\Lambda_1^-, g_2^-, g_3^-, \Lambda_k^+) , \quad (5.24)$$

with one fermion and two gluons of negative helicities consecutive to each other, and a positive-helicity fermion in arbitrary position  $k$ , such that  $3 < k \leq n$ . As in the case considered in [106], this amplitude comes from scalar diagrams with two vertices and one propagator, but in our case there is more than one type of vertex in (5.16). There

are three classes of scalar diagrams which contribute to  $A_n(\Lambda_1^-, g_2^-, g_3^-, \Lambda_k^+)$ , they are depicted in Figure 5.1. First two classes of diagrams involve the first and the second vertex in (5.16), and the third class involves two second vertices in (5.16).

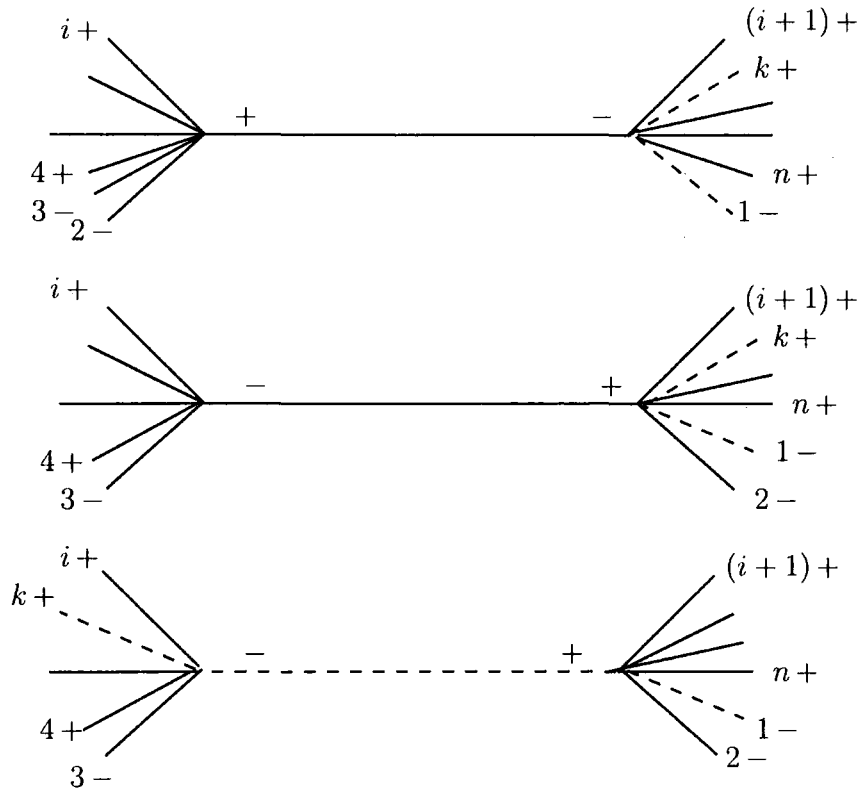


Figure 5.1: Tree diagrams with MHV vertices contributing to the  $---++++\dots++$  amplitude with 2 fermions and  $n - 2$  gluons in Eq. (5.24). Fermions are represented by dashed lines and gluons – by solid lines.

First two diagrams in Figure 5.1 involve a gluon exchange. The third diagram involves a fermion exchange, and can be schematically represented as

$$A(\Lambda_1^-, g_2^-, \underline{\Lambda}_I^+) \frac{1}{q_I^2} A(g_3^-, \Lambda_k^+, \underline{\Lambda}_{-I}^-). \quad (5.25)$$

Here  $\underline{\Lambda}_I^+$  and  $\underline{\Lambda}_{-I}^-$  denote internal off-shell fermions, which are Wick-contracted via the scalar propagator  $1/q_I^2$ . The order in which these internal fermion appear in (5.25) is according to the  $\text{ket}^+ \text{ket}^-$  prescription discussed in the Appendix H.

The three diagrams in Figure 5.1 give

$$\begin{aligned}
A_n &= \sum_{i=3}^{k-1} \frac{\langle 1 (2, i) \rangle^2 \langle k (2, i) \rangle}{\langle (2, i) i+1 \rangle \langle i+1 i+2 \rangle \dots \langle n 1 \rangle} \frac{1}{q_{2i}^2} \frac{\langle 2 3 \rangle^3}{\langle (2, i) 2 \rangle \langle 3 4 \rangle \dots \langle i (2, i) \rangle} \\
&+ \sum_{i=4}^{k-1} \frac{\langle 1 2 \rangle^2 \langle k 2 \rangle}{\langle 2 (3, i) \rangle \langle (3, i) i+1 \rangle \dots \langle n 1 \rangle} \frac{1}{q_{3i}^2} \frac{\langle (3, i) 3 \rangle^3}{\langle 3 4 \rangle \dots \langle i-1 i \rangle \langle i (3, i) \rangle} \\
&+ \sum_{i=k}^n \frac{-\langle 1 2 \rangle^2}{\langle (3, i) i+1 \rangle \langle i+1 i+2 \rangle \dots \langle n 1 \rangle} \frac{1}{q_{3i}^2} \frac{\langle (3, i) 3 \rangle^2 \langle k 3 \rangle}{\langle 3 4 \rangle \dots \langle i-1 i \rangle \langle i (3, i) \rangle}.
\end{aligned} \tag{5.26}$$

Following notations of [106] we have introduced  $q_{ij} = p_i + p_{i+1} + \dots + p_j$ . The corresponding off-shell spinor  $\lambda_{ij a}$  is defined as in (6.1),  $\lambda_{ij a} = q_{ij a \dot{a}} \eta^{\dot{a}}$ . All other spinors  $\lambda_i$  are on-shell and  $\langle i (j, k) \rangle$  is an abbreviation for a spinor product  $\langle \lambda_i, \lambda_{jk} \rangle$ .

As in [106] we choose  $\eta^{\dot{a}} = \tilde{\lambda}_2^{\dot{a}}$ , and evaluate the amplitude (5.26) as a function of the on-shell kinematic variables,  $\lambda_i$  and  $\tilde{\lambda}_1, \tilde{\lambda}_2, \tilde{\lambda}_3$ . The final expression for the amplitude can be written as the sum of three terms:

$$A_n = \frac{1}{\prod_{l=3}^n \langle l l+1 \rangle} [A_n^{(1)} + A_n^{(2)} + A_n^{(3)}]. \tag{5.27}$$

We have to treat the  $i = 3$  term in the first sum in (5.26) and the  $i = n$  term in the last sum in (5.26) separately, as individually they are singular for our choice of  $\eta^{\dot{a}} = \tilde{\lambda}_2^{\dot{a}}$ . These two terms are assembled into  $A_n^{(3)}$ .

For  $i \neq 3$  the first and the second lines in (5.26) give

$$\begin{aligned}
A_n^{(1)} &= \sum_{i=4}^{k-1} \frac{\langle i i+1 \rangle}{\langle i^- | \not{q}_{2,i} | 2^- \rangle \langle (i+1)^- | \not{q}_{i+1,2} | 2^- \rangle \langle 2^- | \not{q}_{2,i} | 2^- \rangle} \\
&\cdot \left( \frac{\langle 3 2 \rangle^3 \langle 1^- | \not{q}_{2,i} | 2^- \rangle^2 \langle k^- | \not{q}_{2,i} | 2^- \rangle}{q_{2,i}^2} + \frac{\langle 1 2 \rangle^2 \langle k 2 \rangle \langle 3^- | \not{q}_{i+1,2} | 2^- \rangle^3}{q_{i+1,2}^2} \right).
\end{aligned} \tag{5.28}$$

In evaluating (5.28) we used the Lorentz-invariant combination  $\langle i^- | \not{p} | j^- \rangle = i^\alpha p_{a \dot{a}} j^{\dot{a}}$ , see Eq. (H.3) in the Appendix H. We also used momentum conservation to set  $q_{3,i} = -q_{i+1,2}$ , and the anticommuting nature of spinor products to simplify the formula.

The second term in (5.27) is the contribution of the third line in (5.26) for  $i \neq n$ . We find

$$A_n^{(2)} = \sum_{i=k}^{n-1} \langle i i+1 \rangle \frac{1}{q_{i+1,2}^2} \frac{\langle 1 2 \rangle^2 \langle k 3 \rangle \langle 3^- | \not{q}_{i+1,2} | 2^- \rangle^2}{\langle i^- | \not{q}_{i+1,2} | 2^- \rangle \langle (i+1)^- | \not{q}_{i+1,2} | 2^- \rangle}. \tag{5.29}$$

The remaining terms – the  $i = 3$  term in the first sum in (5.26) and the  $i = n$  term in the last sum in (5.26) – both contain a factor  $[2 \eta]$  in the denominator and are singular

for  $|\eta^-\rangle = |2^-\rangle$ . For the method to work, the singularity has to cancel between the two terms. This is indeed the case, and rather nontrivially the cancellation occurs between the diagrams of different types – the first and the last in Figure 5.1 – with different MHV vertices. After the singularity cancels, the remaining finite contribution from these two terms is derived by setting  $|\eta^-\rangle = |2^-\rangle + |\epsilon^-\rangle$ , bringing two terms to a common denominator and using Schouten’s identity,  $[\alpha \beta][\gamma \delta] + [\alpha \gamma][\delta \beta] + [\alpha \delta][\beta \gamma] = 0$ . In the end  $|\epsilon^-\rangle$  is set to zero. The result is

$$A_n^{(3)} = \langle 3 \ 1 \rangle \langle 3 \ k \rangle \left( \frac{s_{13} + 2(s_{12} + s_{23})}{[1 \ 2][2 \ 3]} + \frac{\langle 3 \ 1 \rangle \langle 2 \ n \rangle}{[1 \ 2] \langle 1 \ n \rangle} + \frac{\langle 3 \ 1 \rangle \langle 2 \ 4 \rangle}{[2 \ 3] \langle 3 \ 4 \rangle} - \frac{\langle 3 \ 1 \rangle \langle 2 \ k \rangle}{[2 \ 3] \langle 3 \ k \rangle} \right) \quad (5.30)$$

where  $s_{km} = (p_k + p_m)^2 = \langle k \ m \rangle [k \ m]$ .

### 5.2.2 Tests of the amplitude (5.27)–(5.30)

We will now test our result for an  $n$ -point  $- - - + + + \dots + +$  amplitude with 2 fermions, against some known simple cases with  $n = 4, 5$ .

We first consider a 4-point amplitude with three negative helicities,  $A_4(\Lambda_1^-, g_2^-, g_3^-, \Lambda_4^+)$  and check if this amplitude vanishes. Hence, we set  $n = 4 = k$  and find that

$$A_n^{(1)} = 0, \quad A_n^{(2)} = 0, \quad (5.31)$$

since both expressions, (5.28) and (5.29), are proportional to  $\sum_{i=4}^3 \dots \equiv 0$ . The remaining contribution  $A_n^{(3)}$  in (5.30) gives

$$A_n^{(3)} = \langle 3 \ 1 \rangle \langle 3 \ k \rangle \left( -\frac{\langle 1 \ 3 \rangle [1 \ 3]}{[1 \ 2][2 \ 3]} + \frac{\langle 3 \ 1 \rangle \langle 2 \ 4 \rangle}{[1 \ 2] \langle 1 \ 4 \rangle} \right) = 0. \quad (5.32)$$

Here we first used that for  $n = 4$  case  $s_{12} + s_{23} + s_{13} = 0$ , and a momentum conservation identity,  $\langle 4 \ 1 \rangle [1 \ 3] + \langle 4 \ 2 \rangle [2 \ 3] = 0$ .

The next test involves a 5-point amplitude with three negative helicities,  $A_5(\Lambda_1^-, g_2^-, g_3^-, \Lambda_4^+, g_5^+)$ . This is necessarily an  $\overline{\text{MHV}}$  amplitude, or a mostly minus MHV amplitude which is (cf second equation in (5.19))

$$A_5(\Lambda_1^-, g_2^-, g_3^-, \Lambda_4^+, g_5^+) = -\frac{[5 \ 4]^3 [5 \ 1]}{\prod_{i=1}^5 [i \ i + 1]} = \frac{[4 \ 5]^2}{[1 \ 2][2 \ 3][3 \ 4]}. \quad (5.33)$$

We set  $n = 5$ ,  $k = 4$  and evaluate expressions in (5.28)-(5.30). First, we notice again that

$$A_n^{(1)} = 0, \quad (5.34)$$

since  $\sum_{i=4}^3 \equiv 0$ . However,  $A_n^{(2)}$  and  $A_n^{(3)}$  are both non-zero,

$$\frac{A_n^{(2)}}{\prod_{l=3}^5 \langle l l+1 \rangle} = \frac{[4 2]^2 \langle 1 2 \rangle^2}{\langle 1 5 \rangle^2} \frac{1}{[1 2][2 3][3 4]}, \quad (5.35)$$

$$\frac{A_n^{(3)}}{\prod_{l=3}^5 \langle l l+1 \rangle} = \frac{\langle 3 1 \rangle}{\langle 4 5 \rangle \langle 5 1 \rangle} \left( 2 \frac{\langle 4 5 \rangle [4 5]}{[1 2][2 3]} - \frac{\langle 1 3 \rangle [1 3]}{[1 2][2 3]} + \frac{\langle 3 1 \rangle \langle 2 5 \rangle}{[1 2] \langle 1 5 \rangle} \right) \quad (5.36)$$

We further use a momentum conservation identity to re-write the first factor in (5.35) as

$$\frac{[4 2]^2 \langle 1 2 \rangle^2}{\langle 1 5 \rangle^2} = \left( [4 5] - \frac{\langle 1 3 \rangle [3 4]}{\langle 1 5 \rangle} \right)^2 = [4 5]^2 + \frac{\langle 1 3 \rangle^2 [3 4]^2}{\langle 1 5 \rangle^2} - 2 \frac{\langle 1 3 \rangle [3 4] [4 5]}{\langle 1 5 \rangle} \quad (5.37)$$

Now, the last term on the right hand side of (5.37) cancels the first term in brackets in (5.35) and the second term in (5.37) cancels the last two terms in (5.35) via an identity

$$[3 4] \langle 4 5 \rangle + [3 1] \langle 1 5 \rangle + [3 2] \langle 2 5 \rangle = 0. \quad (5.38)$$

The remaining  $[4 5]^2$  term on the right hand side of (5.35) leads to the final answer for the amplitude,

$$\frac{[4 5]^2}{[1 2][2 3][3 4]}. \quad (5.39)$$

We expect that other, more involved tests of the amplitude at the 6-point level and beyond will also be successful.

### 5.2.3 Calculating $---+++ \dots ++$ amplitudes with 4 fermions

Since the scalar graph method gives correct results for non-MHV amplitudes with 2 external fermions, the next step is to apply this method to 4-fermion amplitudes. In this section we will calculate an  $n$ -point amplitude with 4 fermions for three negative helicities consecutive to each other,

$$A_n(g_1^-, \Lambda_2^-, \Lambda_3^-, \Lambda_p^+, \Lambda_q^+), \quad (5.40)$$

where  $3 < p < q \leq n$ . As always, positive-helicity gluons in amplitudes will not be indicated explicitly, unless they appear in internal lines.

There are four scalar diagrams which contribute to this process. They are drawn in Figure 5.2. The first diagram in Figure 5.2 is a gluon exchange between two 2-fermion MHV-vertices. This diagram has a schematic form,

$$A(g_1^-, \Lambda_2^-, \underline{g}_I^+, \Lambda_q^+) \frac{1}{q_I^2} A(\Lambda_3^-, \Lambda_p^+, \underline{g}_{-I}^-). \quad (5.41)$$

Here  $\underline{g}_I^+$  and  $\underline{g}_{-I}^-$  are off-shell (internal) gluons which are Wick-contracted via a scalar propagator, and  $I = (3, i)$ .

The second diagram involves a gluon exchange between a 0-fermion and a 4-fermion MHV vertex,

$$A(g_1^-, \underline{g}_I^-) \frac{1}{q_I^2} A(\Lambda_2^-, \Lambda_3^-, \Lambda_p^+, \Lambda_q^+, \underline{g}_{-I}^+), \quad (5.42)$$

with external index  $I = (2, i)$ . Note that this diagram exists only for  $n > 5$ , i.e. there must be at least one  $g^+$  in the first vertex, otherwise it is a 2-point vertex which does not exist.

The third and the fourth diagrams in Figure 5.2 involve a fermion exchange between a 2-fermion and a 4-fermion MHV vertices. They are given, respectively by

$$A(\Lambda_2^-, \Lambda_3^-, \Lambda_p^+, \underline{\Lambda}_{-I}^+) \frac{1}{q_I^2} A(\Lambda_q^+, g_1^-, \underline{\Lambda}_I^-), \quad (5.43)$$

with  $I = (2, i)$ , and

$$A(g_1^-, \Lambda_2^-, \underline{\Lambda}_I^+) \frac{1}{q_I^2} A(\Lambda_3^-, \Lambda_p^+, \Lambda_q^+, \underline{\Lambda}_{-I}^-), \quad (5.44)$$

with  $I = (3, i)$ . Both expressions, (5.43) and (5.44), are written in the form which is in agreement with our ordering prescription for internal fermions,  $\text{ket}^+ \text{ket}^-$ .

We will continue using the same off-shell prescription  $\eta^{\dot{a}} = \tilde{\lambda}_2^{\dot{a}}$  as in the section 5.2.1. But there is an important simplification in the present case compared to 5.2.1 – there will be no singular terms appearing in individual diagrams. This is because the reference spinor  $\eta^{\dot{a}} = \tilde{\lambda}_2^{\dot{a}}$  now corresponds to a gluino, rather than a gluon  $g^-$ . The reason for singularities encountered in section 5.2.1 and in Ref. [106] was simply the singular collinear limit of the 3-gluon vertex where all gluons went on-shell. We

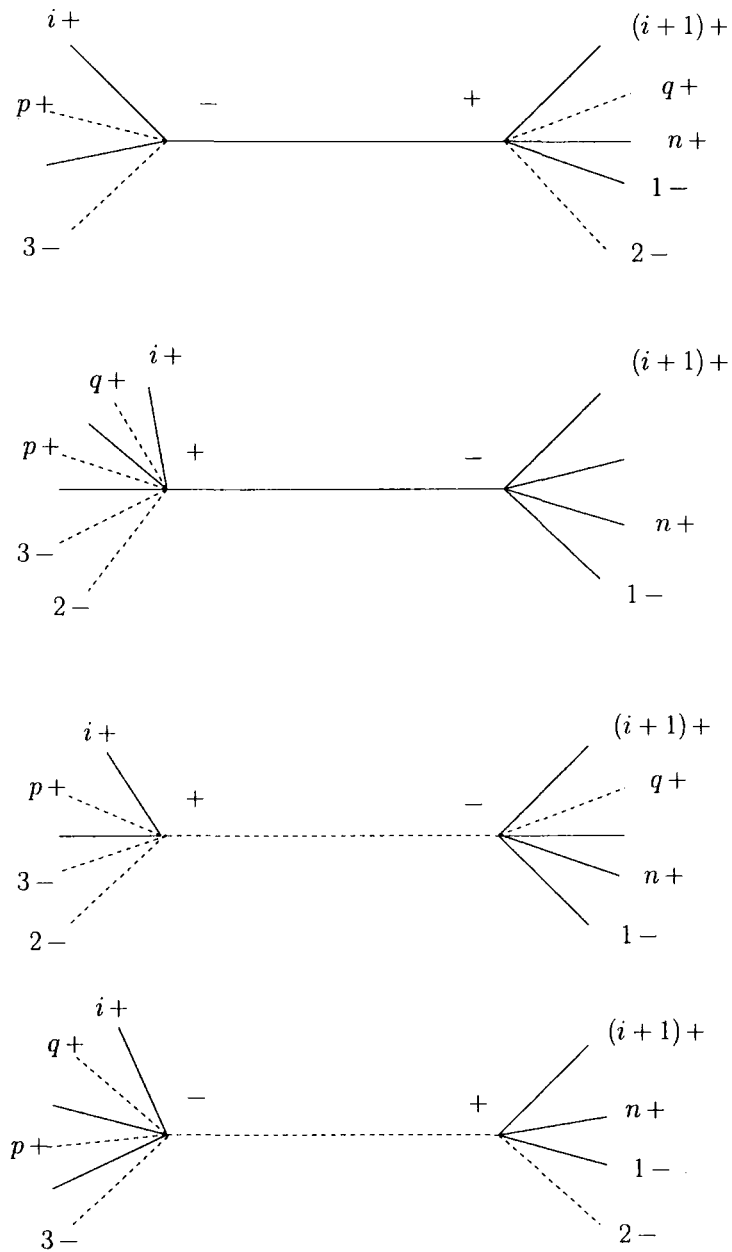


Figure 5.2: Diagrams contributing to the 4-fermion  $n$ -point amplitude (5.40)

will see that these singularities would not occur in the present case, and not having to cancel them will save us some work.<sup>5</sup>

For extra clarity we will first present a simpler version of the evaluation of (5.40) for the case  $n = 5$ . This result will then be generalized to all values of  $n$ . For  $n = 5$ , we set  $p = 4$  and  $q = 5$  in (5.40), and the calculation is straightforward.

1. The first diagram in Figure 5.2, Eq. (5.41), is

$$\begin{aligned} & \frac{-\langle 1\ 2 \rangle^2}{(\langle 2\ 3 \rangle[2\ 3] + \langle 2\ 4 \rangle[2\ 4])\langle 5\ 1 \rangle[2\ 1]} \cdot \frac{1}{\langle 3\ 4 \rangle[3\ 4]} \cdot \langle 4\ 3 \rangle[2\ 4]^2 \\ &= \frac{[2\ 4]^2 \langle 1\ 2 \rangle^2}{[3\ 4](\langle 2\ 3 \rangle[2\ 3] + \langle 2\ 4 \rangle[2\ 4])\langle 5\ 1 \rangle[2\ 1]} \end{aligned} \quad (5.45)$$

2. The second diagram is zero.

3. The third diagram, Eq. (5.43), is

$$\begin{aligned} & \frac{-\langle 2\ 3 \rangle^2}{(\langle 2\ 3 \rangle[2\ 3] + \langle 2\ 4 \rangle[2\ 4])\langle 3\ 4 \rangle} \cdot \frac{1}{\langle 5\ 1 \rangle[5\ 1]} \cdot \frac{\langle 5\ 1 \rangle[2\ 5]^2}{[2\ 1]} \\ &= \frac{-[2\ 5]^2 \langle 2\ 3 \rangle^2}{[2\ 1][5\ 1](\langle 2\ 3 \rangle[2\ 3] + \langle 2\ 4 \rangle[2\ 4])\langle 3\ 4 \rangle} \end{aligned} \quad (5.46)$$

4. The fourth diagram, Eq. (5.44):

$$\frac{\langle 2\ 1 \rangle}{[2\ 1]} \cdot \frac{1}{\langle 1\ 2 \rangle[1\ 2]} \cdot \frac{\langle 3\ 1 \rangle^2 [2\ 1]}{\langle 3\ 4 \rangle \langle 5\ 1 \rangle} = \frac{\langle 3\ 1 \rangle^2}{[2\ 1] \langle 3\ 4 \rangle \langle 5\ 1 \rangle} \quad (5.47)$$

Now, we need to add up the three contributions. We first combine the expressions in (5.45) and (5.46) into

$$\frac{[4\ 5]^2}{[2\ 1][3\ 4][5\ 1]} - \frac{\langle 3\ 1 \rangle^2}{[2\ 1] \langle 3\ 4 \rangle \langle 5\ 1 \rangle} \quad (5.48)$$

using momentum conservation identities, and the fact that  $\langle 2\ 3 \rangle[2\ 3] + \langle 2\ 4 \rangle[2\ 4] = -\langle 3\ 4 \rangle[3\ 4] + \langle 5\ 1 \rangle[5\ 1]$ . Then, adding the remaining contribution (5.47) we obtain the final result for the amplitude,

$$A_5(g_1^-, \Lambda_2^-, \Lambda_3^-, \Lambda_4^+, \Lambda_5^+) = \frac{-[4\ 5]^3 [2\ 3]}{[1\ 2][2\ 3][3\ 4][4\ 5][5\ 1]} \quad (5.49)$$

which is the precisely right answer for the MHV-bar 5-point ‘mostly minus’ diagram!

<sup>5</sup>In view of this, the calculation in section 5.2.1 could have been made simpler, if we had chosen the reference spinor to be the spinor of the negative-helicity gluino  $\Lambda_1^-$ .

We now present the general expression for the amplitude with  $n$  external legs. Using the same prescription for the vertices as above the first diagram of Figure 5.2 gives

$$\begin{aligned}
 A_n^{(1)} &= \sum_{i=p}^{q-1} \frac{\langle 1 2 \rangle^2 \langle 1 q \rangle}{\langle 2 (3, i) \rangle \langle (3, i) i+1 \rangle \langle i+1 i+2 \rangle \dots \langle n 1 \rangle} \frac{1}{q_{3i}^2} \frac{\langle 3 - (3, i) \rangle^3 \langle p - (3, i) \rangle}{\langle 3 4 \rangle \dots \langle i - (3, i) \rangle \langle -(3, i) 3 \rangle} \\
 &= -\frac{1}{\prod_{l=3}^n \langle l l+1 \rangle} \sum_{i=p}^{q-1} \frac{\langle 1 2 \rangle^2 \langle 1 q \rangle \langle i i+1 \rangle \langle 3^- | \not{d}_{i+1,2} | 2^- \rangle^2 \langle p^- | \not{d}_{2,i} | 2^- \rangle}{q_{i+1,2}^2 \langle i^- | \not{d}_{2,i} | 2^- \rangle \langle (i+1)^- | \not{d}_{i+1,2} | 2^- \rangle \langle 2^- | \not{d}_{2,i} | 2^- \rangle}.
 \end{aligned} \tag{5.50}$$

For the second diagram of Figure 5.2 one obtains

$$\begin{aligned}
 A_n^{(2)} &= \sum_{i=q}^{n-1} \frac{\langle 1 (2, i) \rangle^3}{\langle (2, i) i+1 \rangle \langle i+1 i+2 \rangle \dots \langle n 1 \rangle} \frac{1}{q_{2,i}^2} \frac{-\langle 2 3 \rangle^2 \langle p q \rangle}{\langle 3 4 \rangle \dots \langle i - (2, i) \rangle \langle -(2, i) 2 \rangle} \\
 &= \frac{1}{\prod_{l=3}^n \langle l l+1 \rangle} \sum_{i=q}^{n-1} \frac{\langle 2 3 \rangle^2 \langle p q \rangle \langle i i+1 \rangle \langle 1^- | \not{d}_{2,i} | 2^- \rangle^3}{q_{2,i}^2 \langle i^- | \not{d}_{2,i} | 2^- \rangle \langle (i+1)^- | \not{d}_{i+1,2} | 2^- \rangle \langle 2^- | \not{d}_{2,i} | 2^- \rangle}.
 \end{aligned} \tag{5.51}$$

The contribution of the third diagram of Figure 5.2 is

$$\begin{aligned}
 A_n^{(3)} &= \sum_{i=p}^{q-1} \frac{\langle 1 (2, i) \rangle^2 \langle 1 q \rangle}{\langle (2, i) i+1 \rangle \langle i+1 i+2 \rangle \dots \langle n 1 \rangle} \frac{1}{q_{2,i}^2} \frac{-\langle 2 3 \rangle^2 \langle p - (2, i) \rangle}{\langle 3 4 \rangle \dots \langle i - (2, i) \rangle \langle -(2, i) 2 \rangle} \\
 &= \frac{1}{\prod_{l=3}^n \langle l l+1 \rangle} \sum_{i=p}^{q-1} \frac{\langle 2 3 \rangle^2 \langle 1 q \rangle \langle i i+1 \rangle \langle p^- | \not{d}_{2,i} | 2^- \rangle \langle 1^- | \not{d}_{2,i} | 2^- \rangle^2}{q_{2,i}^2 \langle i^- | \not{d}_{2,i} | 2^- \rangle \langle (i+1)^- | \not{d}_{i+1,2} | 2^- \rangle \langle 2^- | \not{d}_{2,i} | 2^- \rangle}.
 \end{aligned} \tag{5.52}$$

Finally, from the fourth diagram of Figure 5.2 we get

$$\begin{aligned}
 A_n^{(4)} &= \sum_{i=q}^n \frac{\langle 1 2 \rangle^2 \langle 1 (3, i) \rangle}{\langle 2 (3, i) \rangle \langle (3, i) i+1 \rangle \langle i+1 i+2 \rangle \dots \langle n 1 \rangle} \frac{1}{q_{3i}^2} \frac{-\langle 3 - (3, i) \rangle^3 \langle p q \rangle}{\langle 3 4 \rangle \dots \langle i - (3, i) \rangle \langle -(3, i) 3 \rangle} \\
 &= -\frac{1}{\prod_{l=3}^n \langle l l+1 \rangle} \sum_{i=q}^n \frac{\langle 1 2 \rangle^2 \langle p q \rangle \langle i i+1 \rangle \langle 3^- | \not{d}_{i+1,2} | 2^- \rangle^2 \langle 1^- | \not{d}_{2,i} | 2^- \rangle}{q_{i+1,2}^2 \langle i^- | \not{d}_{2,i} | 2^- \rangle \langle (i+1)^- | \not{d}_{i+1,2} | 2^- \rangle \langle 2^- | \not{d}_{2,i} | 2^- \rangle}.
 \end{aligned} \tag{5.53}$$

One can combine the result for the first and the third diagram to get:

$$A_n^{(1,3)} = \frac{1}{\prod_{l=3}^n \langle l l+1 \rangle} \sum_{i=p}^{q-1} \frac{\langle 1 q \rangle \langle i i+1 \rangle \langle p^- | \not{d}_{2,i} | 2^- \rangle}{\langle i^- | \not{d}_{2,i} | 2^- \rangle \langle (i+1)^- | \not{d}_{i+1,2} | 2^- \rangle \langle 2^- | \not{d}_{2,i} | 2^- \rangle} \tag{5.54}$$

$$\cdot \left( -\frac{\langle 1 2 \rangle^2 \langle 3^- | \not{d}_{i+1,2} | 2^- \rangle^2}{q_{i+1,2}^2} + \frac{\langle 2 3 \rangle^2 \langle 1^- | \not{d}_{2,i} | 2^- \rangle^2}{q_{2,i}^2} \right). \tag{5.55}$$

The final result for the  $n$ -point amplitude is with 4 fermions

$$A_n(g_1^-, \Lambda_2^-, \Lambda_3^-, \Lambda_p^+, \Lambda_q^+) = A_n^{(1,3)} + A_n^{(2)} + A_n^{(4)}. \quad (5.56)$$

All the individual terms are regular, and the equation above is the final result of this section.

In this chapter, we saw how the CSW method, initially used for gluonic amplitudes in  $\mathcal{N} = 4$  SYM, can be naturally extended to include fermions in theories with any degree of supersymmetry  $\mathcal{N} = 4, 2, 1, 0$ . This method appears to be much more efficient than the usual Feynman diagrammatic method especially when the number of external particles increases. In the next chapter, we shall see how the application of the CSW method to amplitudes involving fermions leads to expressions free of unphysical singularities related to the choice of the reference spinor. The purely gluonic amplitudes can then be straightforwardly obtained by employing supersymmetric Ward identities to express them in terms of amplitudes with gluons and fermions.

# Chapter 6

## Non-MHV tree amplitudes in gauge theory

In the previous chapter, we explained, in some detail, how the CSW method can be used to calculate gauge theory amplitudes in theories with any degree of supersymmetry and any number of colours.

In the present chapter we show how non-MHV (NMHV) tree-level amplitudes in  $0 \leq \mathcal{N} \leq 4$  gauge theories can be obtained directly from the scalar graph approach. One of the main points we want to make is that after the ‘Feynman rules’ for scalar diagrams are used, together with the off-shell continuation of helicity spinors on internal lines, expressions for all relevant individual diagrams are automatically free of unphysical singularities at generic phase space points, and amplitudes are manifestly Lorentz- (and gauge-) invariant. Hence, no further helicity-spinor algebra is required to convert the results into an immediately usable form.

To illustrate the method, we will derive expressions for  $n$ -point amplitudes with three negative helicities carried by fermions and/or gluons. We will also write down a supersymmetric expression which gives rise to all such amplitudes in  $0 \leq \mathcal{N} \leq 4$  gauge theories. This complements a very recent calculation of Kosower [110] of such amplitudes in the purely gluonic case.

As in [4], we will consider tree-level amplitudes in a generic  $SU(N)$  gauge theory with an arbitrary finite number of colours.  $SU(N)$  is unbroken and all fields are taken to be massless, we refer to them generically as gluons, fermions and scalars.

The gauge theory is not necessarily assumed to be supersymmetric, i.e. the number of supercharges is  $4\mathcal{N}$ , where  $0 \leq \mathcal{N} \leq 4$ .

This chapter is organised as follows. In section 6.2 we will use supersymmetric Ward identities to express NMHV purely gluonic amplitudes in terms of NMHV amplitudes with gluons and two fermions<sup>1</sup>. Then, using the CSW scalar graph method for gluons [106] and fermions [4], in sections 6.3 and 6.4 we will derive expressions for the NMHV amplitudes with three negative helicities involving gluons and fermions.

Section 6.5 of this chapter considers the scalar graph method with the single analytic supervertex of Nair [120]. We provide a single formula which gives rise to all tree-level NMHV amplitudes with three negative helicities in  $0 \leq \mathcal{N} \leq 4$  supersymmetric gauge theories, involving all possible configurations of gauge fields, fermions and scalars. There is also no principal obstacle to continue with further iterations of the analytic supervertex and derive formal expressions for tree amplitudes with an arbitrary number of negative helicities. Depending on the topology of the iteration, these expressions would correspond to different skeleton diagrams of [109] in  $0 \leq \mathcal{N} \leq 4$  supersymmetric gauge theories.

## 6.1 Amplitudes in the spinor helicity formalism

We will first consider theories with  $\mathcal{N} \leq 1$  supersymmetry. Gauge theories with extended supersymmetry have a more intricate behaviour of their amplitudes in the helicity basis and their study will be postponed until section 6.5. Theories with  $\mathcal{N} = 4$  (or  $\mathcal{N} = 2$ ) supersymmetry have  $\mathcal{N}$  different species of gluinos and 6 (or 4) scalar fields. This leads to a large number of elementary MHV-like vertices in the scalar graph formalism. This proliferation of elementary vertices asks for a super-graph generalization of the CSW scalar graph method, which will be outlined in section 6.5.

---

<sup>1</sup>It may be worthwhile to note that while a gluonic non-MHV amplitude can be determined in terms of amplitudes with fermions and gluons, the converse of this statement is not true. Individual non-MHV amplitudes involving fermions cannot be deduced with susy Ward identities from amplitudes with gluons only.

Now we concentrate on tree level partial amplitudes  $A_n = A_{l+2m}$  with  $l$  gluons and  $2m$  fermions in the helicity basis, and all external lines are defined to be incoming. The three types of MHV tree amplitudes in  $\mathcal{N} \leq 1$  theories are given by (5.14), (5.19) and (5.20).

## 6.2 Gluonic NMHV amplitudes and the CSW method

The formalism of CSW was developed in [106] for calculating purely gluonic amplitudes at tree level. In this approach all non-MHV  $n$ -gluon amplitudes (including  $\overline{\text{MHV}}$ ) are expressed as sums of tree diagrams in an effective scalar perturbation theory. The vertices in this theory are the MHV amplitudes (5.14), continued off-shell as described below, and connected by scalar propagators  $1/q^2$ .

Based on [4], it was shown in the previous chapter that the same idea continues to work in theories with fermions and gluons. Scattering amplitudes are determined from scalar diagrams with three types of MHV vertices, (5.14), (5.19) and (5.20), which are connected to each other with scalar propagators  $1/q^2$ . Also, at tree level, supersymmetry is irrelevant and the method applies to supersymmetric and non-supersymmetric theories [4].

When one leg of an MHV vertex is connected by a propagator to a leg of another MHV vertex, both legs become internal to the diagram and have to be continued off-shell. Off-shell continuation is defined as follows [106]: we pick an arbitrary spinor  $\xi_{\text{Ref}}^{\dot{a}}$  and define  $\lambda_a$  for any internal line carrying momentum  $q_{a\dot{a}}$  by

$$\lambda_a = q_{a\dot{a}} \xi_{\text{Ref}}^{\dot{a}}. \tag{6.1}$$

External lines in a diagram remain on-shell, and for them  $\lambda$  is defined in the usual way. For the off-shell lines, the same  $\xi_{\text{Ref}}$  is used in all diagrams contributing to a given amplitude.

For practical applications the authors of [106] have chosen  $\xi_{\text{Ref}}^{\dot{a}}$  in (6.1) to be equal to  $\tilde{\lambda}_1^{\dot{a}}$  of one of the external legs of negative helicity, e.g. the first one,

$$\xi_{\text{Ref}} = \tilde{\lambda}_1^{\dot{a}}. \tag{6.2}$$

This corresponds to identifying the reference spinor with one of the kinematic variables of the theory. The explicit dependence on the reference spinor  $\xi_{\text{Ref}}^{\dot{a}}$  disappears and the resulting expressions for all scalar diagrams in the CSW approach are the functions only of the kinematic variables  $\lambda_{i_a}$  and  $\tilde{\lambda}_i^{\dot{a}}$ . This means that the expressions for all individual diagrams automatically appear to be Lorentz-invariant (in the sense that they do not depend on an external spinor  $\xi_{\text{Ref}}^{\dot{a}}$ ) and also gauge-invariant (since the reference spinor corresponds to the axial gauge fixing  $n_{\mu}A^{\mu} = 0$ , where  $n_{a\dot{a}} = \xi_{\text{Ref } a}\xi_{\text{Ref } \dot{a}}$ ).

There is a price to pay for this invariance of the individual diagrams. Equations (6.1),(6.2) lead to unphysical singularities<sup>2</sup> which occur for the whole of phase space and which have to be cancelled between the individual diagrams. The result for the total amplitude is, of course, free of these unphysical singularities, but their cancellation and the retention of the finite part requires some work, see [106] and section 3.1 of [4].

It will be important for the purposes of this chapter to note that these unphysical singularities are specific to the three-gluon MHV vertices and, importantly, they do not occur in any of the MHV vertices involving a fermion field [4]. To see how these singularities arise in gluon vertices, consider a 3-point MHV vertex,

$$A_3(g_1^-, g_2^-, g_3^+) = \frac{\langle 1 2 \rangle^4}{\langle 1 2 \rangle \langle 2 3 \rangle \langle 3 1 \rangle} = \frac{\langle 1 2 \rangle^3}{\langle 2 3 \rangle \langle 3 1 \rangle}. \quad (6.3)$$

This vertex exists only when one of the legs is off-shell. Take it to be the  $g_3^+$  leg. Then Eqs. (6.1), (6.2) give

$$\lambda_{3_a} = (p_1 + p_2) \tilde{\lambda}_1^{\dot{a}} = -\lambda_{1_a} [1 1] - \lambda_{2_a} [2 1] = -\lambda_{2_a} [2 1]. \quad (6.4)$$

This implies that  $\langle 2 3 \rangle = -\langle 2 2 \rangle [2 1] = 0$ , and the denominator of (6.3) vanishes. This is precisely the singularity we are after. If instead of the  $g_3^+$  leg, one takes the  $g_2^-$  leg go off-shell, then,  $\langle 2 3 \rangle = -\langle 3 3 \rangle [3 1] = 0$  again.

Now consider a three-point MHV vertex involving two fermions and a gluon,

$$A_3(\Lambda_1^-, g_2^-, \Lambda_3^+) = \frac{\langle 2 1 \rangle^3 \langle 2 3 \rangle}{\langle 1 2 \rangle \langle 2 3 \rangle \langle 3 1 \rangle} = -\frac{\langle 2 1 \rangle^2}{\langle 3 1 \rangle}. \quad (6.5)$$

---

<sup>2</sup>Unphysical means that these singularities are not the standard IR soft and collinear divergences in the amplitudes.

Choose the reference spinor to be as before,  $\tilde{\lambda}_1^a$ , and take the second or the third leg off-shell. This again makes  $\langle 2\ 3 \rangle = 0$ , but now the factor of  $\langle 2\ 3 \rangle$  is cancelled on the right hand side of (6.5). Hence, the vertex (6.5) is regular, and there are no unphysical singularities in the amplitudes involving at least one negative helicity fermion when it's helicity is chosen to be the reference spinor [4]. One concludes that the difficulties with singularities at intermediate stages of the calculation occur only in purely gluonic amplitudes. One way to avoid these intermediate singularities is to choose an off-shell continuation different from the CSW prescription (6.1),(6.2).

Kosower [110] used an off-shell continuation by projection of the off-shell momentum with respect to an on-shell reference momentum  $q_{\text{Ref}}^\mu$ , to derive, for the first time, an expression for a general NMHV amplitude with three negative helicity gluons. The amplitude in [110] was from the start free of unphysical divergences, however it required a certain amount of spinor algebra to bring it into the form independent of the reference momentum.

Here we will propose another simple method for finding all purely gluonic NMHV amplitudes. Using  $\mathcal{N} = 1$  supersymmetric Ward identities one can relate purely gluonic amplitudes to a linear combination of amplitudes with one fermion–antifermion pair. As explained above, the latter are free of singularities and are manifestly Lorentz-invariant. These fermionic amplitudes will be calculated in the following section using the CSW scalar graph approach with fermions [4].

To derive supersymmetric Ward identities [121] we use the fact that, supercharges  $Q$  annihilate the vacuum, and consider the following equation,

$$\langle [Q, \Lambda_k^+ \dots g_{r_1}^- \dots g_{r_2}^- \dots g_{r_3}^- \dots] \rangle = 0, \quad (6.6)$$

where dots indicate positive helicity gluons. In order to make anticommuting spinor  $Q$  to be a singlet entering a commutative (rather than anticommutative) algebra with all the fields we contract it with a commuting spinor  $\eta$  and multiply it by a Grassmann number  $\theta$ . This defines a commuting singlet operator  $Q(\eta)$ . Following [126] we can write down the following susy algebra relations,

$$\begin{aligned} [Q(\eta), \Lambda^+(k)] &= -\theta \langle \eta k \rangle g^+(k), & [Q(\eta), \Lambda^-(k)] &= +\theta [\eta k] g^-(k), \\ [Q(\eta), g^-(k)] &= +\theta \langle \eta k \rangle \Lambda^-(k), & [Q(\eta), g^+(k)] &= -\theta [\eta k] \Lambda^+(k). \end{aligned} \quad (6.7)$$

In what follows, the anticommuting parameter  $\theta$  will cancel from the relevant expressions for the amplitudes. The arbitrary spinors  $\eta_a, \eta_{\dot{a}}$ , will be fixed below. It then follows from (6.7) that

$$\begin{aligned} \langle \eta k \rangle A_n(g_{r_1}^-, g_{r_2}^-, g_{r_3}^-) &= \langle \eta r_1 \rangle A_n(\Lambda_k^+, \Lambda_{r_1}^-, g_{r_2}^-, g_{r_3}^-) + \langle \eta r_2 \rangle A_n(\Lambda_k^+, g_{r_1}^-, \Lambda_{r_2}^-, g_{r_3}^-) \\ &\quad + \langle \eta r_3 \rangle A_n(\Lambda_k^+, g_{r_1}^-, g_{r_2}^-, \Lambda_{r_3}^-) . \end{aligned} \quad (6.8)$$

After choosing  $\eta$  to be one of the three  $r_j$  we find from (6.8) that the purely gluonic amplitude with three negative helicities is given by a sum of two fermion-antifermion-gluon-gluon amplitudes. Note that in the expressions above and in what follows, in  $n$ -point amplitudes we show only the relevant particles, and suppress all the positive helicity gluons  $g^+$ .

Remarkably, this approach works for any number of negative helicities, and the NMHV amplitude with  $h$  negative gluons is expressed via a simple linear combination of  $h - 1$  NMHV amplitudes with one fermion-antifermion pair.

In sections 6.3 and 6.4 we will evaluate NMHV amplitudes with fermions. In particular, in section 6.3 we will calculate the following three amplitudes,

$$A_n(\Lambda_{m_1}^-, g_{m_2}^-, g_{m_3}^-, \Lambda_k^+) , \quad A_n(\Lambda_{m_1}^-, g_{m_2}^-, \Lambda_k^+, g_{m_3}^-) , \quad A_n(\Lambda_{m_1}^-, \Lambda_k^+, g_{m_2}^-, g_{m_3}^-) . \quad (6.9)$$

In terms of these, the purely gluonic amplitude of (6.8) reads

$$\begin{aligned} A_n(g_{r_1}^-, g_{r_2}^-, g_{r_3}^-) &= -\frac{\langle \eta r_1 \rangle}{\langle \eta k \rangle} A_n(\Lambda_{m_1}^-, g_{m_2}^-, g_{m_3}^-, \Lambda_k^+) |_{m_1=r_1, m_2=r_2, m_3=r_3} \\ &\quad - \frac{\langle \eta r_2 \rangle}{\langle \eta k \rangle} A_n(\Lambda_{m_1}^-, g_{m_2}^-, \Lambda_k^+, g_{m_3}^-) |_{m_1=r_2, m_2=r_3, m_3=r_1} \\ &\quad - \frac{\langle \eta r_3 \rangle}{\langle \eta k \rangle} A_n(\Lambda_{m_1}^-, \Lambda_k^+, g_{m_2}^-, g_{m_3}^-) |_{m_1=r_3, m_2=r_1, m_3=r_2} , \end{aligned} \quad (6.10)$$

and  $\eta$  can be chosen to be one of the three  $m_j$  to further simplify this formula.

## 6.3 NMHV (- - -) Amplitudes with Two Fermions

We start with the case of one fermion-antifermion pair,  $\Lambda^-, \Lambda^+$ , and an arbitrary number of gluons,  $g$ . The amplitude has a schematic form,  $A_n(\Lambda_{m_1}^-, g_{m_2}^-, g_{m_3}^-, \Lambda_k^+)$ , and without loss of generality we can have  $m_1 < m_2 < m_3$ . With these conventions,

there are three different classes of amplitudes depending on the position of the  $\Lambda_k^+$  fermion relative to  $m_1, m_2, m_3$ :

$$A_n(\Lambda_{m_1}^-, g_{m_2}^-, g_{m_3}^-, \Lambda_k^+) , \quad (6.11a)$$

$$A_n(\Lambda_{m_1}^-, g_{m_2}^-, \Lambda_k^+, g_{m_3}^-) , \quad (6.11b)$$

$$A_n(\Lambda_{m_1}^-, \Lambda_k^+, g_{m_2}^-, g_{m_3}^-) . \quad (6.11c)$$

Each of these three amplitudes receives contributions from different types of scalar diagrams in the CSW approach. In all of these scalar diagrams there are precisely two MHV vertices connected to each other by a single scalar propagator [106]. We will always arrange these diagrams in such a way that the MHV vertex on the left has a positive helicity on the internal line, and the right vertex has a negative helicity. Then, there are three choices one can make [110] for the pair of negative helicity particles to enter external lines of the left vertex,  $(m_1, m_2)$ ,  $(m_2, m_3)$ , or  $(m_3, m_1)$ . In addition to this, each diagram in  $\mathcal{N} \leq 1$  theory corresponds to either a gluon exchange, or a fermion exchange.

The diagrams contributing to the first process (6.11a) are drawn in Figure 6.1. There are three gluon exchange diagrams for all three partitions  $(m_2, m_3)$ ,  $(m_1, m_2)$ ,  $(m_3, m_1)$ , and there is one fermion exchange diagram for the partition  $(m_1, m_2)$ .

It is now straightforward, using the expressions for the MHV vertices (5.14),(5.19), to write down an analytic expression for the first diagram of Figure 6.1:

$$A_n^{(1)} = \frac{1}{\prod_{l=1}^n \langle l \ l+1 \rangle} \sum_{i=m_1}^{m_2-1} \sum_{j=m_3}^{k-1} \frac{-\langle (i+1, j) \ m_1 \rangle^3 \langle (i+1, j) \ k \rangle \langle i \ i+1 \rangle \langle j \ j+1 \rangle}{\langle i \ (i+1, j) \rangle \langle (i+1, j) \ j+1 \rangle} \frac{q_{i+1, j}^2}{q_{i+1, j}^2} \times \frac{\langle m_2 \ m_3 \rangle^4}{\langle (j+1, i) \ i+1 \rangle \langle j \ (j+1, i) \rangle} . \quad (6.12)$$

This expression is a direct rendering of the ‘Feynman rules’ for the scalar graph method [4, 106], followed by factoring out the overall factor of  $(\prod_{l=1}^n \langle l \ l+1 \rangle)^{-1}$ . The objects  $(i+1, j)$  and  $(j+1, i)$  appearing on the right hand side of (6.12) denote the spinors  $\lambda_{i+1, j}$  and  $\lambda_{j+1, i}$  corresponding to the off-shell momentum  $q_{i+1, j}$

$$q_{i+1, j} \equiv p_{i+1} + p_{i+2} + \dots + p_j , \quad q_{j+1, i} \equiv p_{j+1} + p_{j+2} + \dots + p_i , \quad q_{i+1, j} + q_{j+1, i} = 0 \quad (6.13)$$

$$\lambda_{i+1, j a} \equiv q_{i+1, j a \dot{a}} \xi_{\text{Ref}}^{\dot{a}} = -\lambda_{j+1, i a} , \quad (6.14)$$

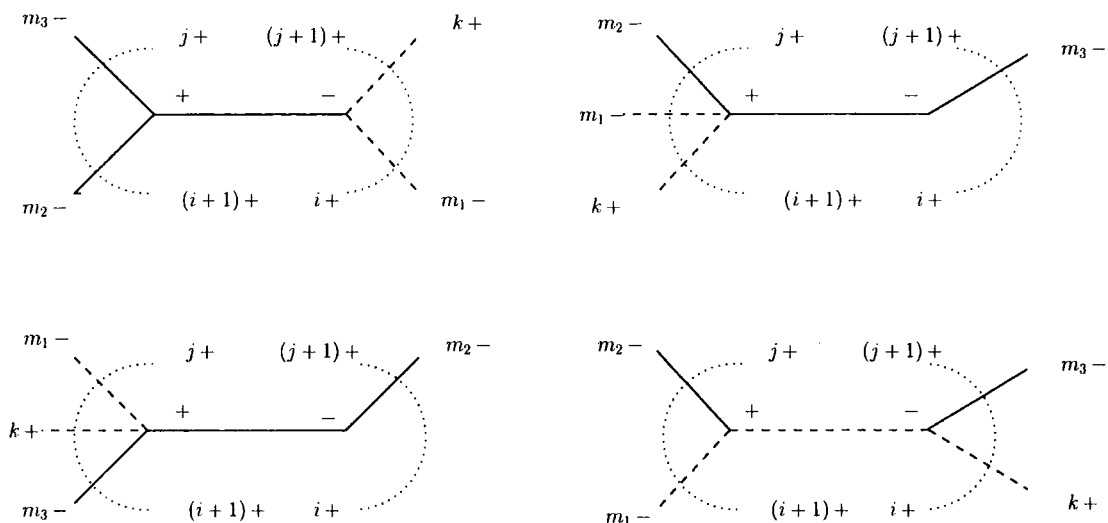


Figure 6.1: Tree diagrams with MHV vertices contributing to the amplitude  $A_n(\Lambda_{m_1}^-, g_{m_2}^-, g_{m_3}^-, \Lambda_k^+)$ . Fermions,  $\Lambda^+$  and  $\Lambda^-$ , are represented by dashed lines and negative helicity gluons,  $g^-$ , by solid lines. Positive helicity gluons  $g^+$  emitted from each vertex are indicated by dotted semicircles with labels showing the bounding  $g^+$  lines in each MHV vertex.

where  $\xi_{\text{Ref}}^{\dot{a}}$  is the reference (dotted) spinor [106] as in Eq. (6.1). All other spinors  $\lambda_i$  are on-shell and  $\langle i(j, k) \rangle$  is an abbreviation for a spinor product  $\langle \lambda_i, \lambda_{jk} \rangle$ .

Having the freedom to choose any reference spinor we will always choose it to be the spinor of the fermion  $\Lambda^-$ . In this section, this is the spinor of  $\Lambda_{m_1}^-$ ,

$$\xi_{\text{Ref}} = \tilde{\lambda}_{m_1}^{\dot{a}}. \quad (6.15)$$

We can now re-write

$$\begin{aligned} & \langle i(i+1, j) \rangle \langle (i+1, j) j+1 \rangle \langle (j+1, i) i+1 \rangle \langle j(j+1, i) \rangle \\ &= \langle i^- | \not{p}_{i+1, j} | m_1^- \rangle \langle j+1^- | \not{p}_{i+1, j} | m_1^- \rangle \langle i+1^- | \not{p}_{i+1, j} | m_1^- \rangle \langle j^- | \not{p}_{i+1, j} | m_1^- \rangle, \end{aligned} \quad (6.16)$$

and define a universal combination,

$$D = \langle i^- | \not{p}_{i+1, j} | m_1^- \rangle \langle j+1^- | \not{p}_{i+1, j} | m_1^- \rangle \langle i+1^- | \not{p}_{i+1, j} | m_1^- \rangle \langle j^- | \not{p}_{i+1, j} | m_1^- \rangle \frac{q_{i+1, j}^2}{\langle i i+1 \rangle \langle j j+1 \rangle} \quad (6.17)$$

Note that Here we introduced the standard Lorentz-invariant matrix element

$\langle i^- | \not{p}_k | j^- \rangle = i^a p_{k a \dot{a}} j^{\dot{a}}$ , which in terms of the spinor products is

$$\langle i^- | \not{p}_k | j^- \rangle = \langle i^- |^a | k^+ \rangle_a \langle k^+ |_{\dot{a}} | j^- \rangle^{\dot{a}} = -\langle i k \rangle [k j] = \langle i k \rangle [j k]. \quad (6.18)$$

The expression for  $A_n^{(1)}$  now becomes:

$$A_n^{(1)} = \frac{-1}{\prod_{l=1}^n \langle l \ l + 1 \rangle} \sum_{i=m_1}^{m_2-1} \sum_{j=m_3}^{k-1} \frac{\langle m_1^- | \not{q}_{i+1,j} | m_1^- \rangle^3 \langle k^- | \not{q}_{i+1,j} | m_1^- \rangle \langle m_2 \ m_3 \rangle^4}{D} . \quad (6.19)$$

For the second diagram of Figure 6.1, we have

$$A_n^{(2)} = \frac{-1}{\prod_{l=1}^n \langle l \ l + 1 \rangle} \sum_{i=m_3}^{k-1} \sum_{j=m_2}^{m_3-1} \frac{\langle m_3^- | \not{q}_{i+1,j} | m_1^- \rangle^4 \langle m_2 \ m_1 \rangle^3 \langle m_2 \ k \rangle}{D} . \quad (6.20)$$

The MHV vertex on the right in the second diagram in Figure 6.1 can collapse to a 2-leg vertex. This occurs when  $i = m_3$  and  $j + 1 = m_3$ . This vertex is identically zero, since  $q_{j+1,i} = p_{m_3} = -q_{i+1,j}$ , and  $\langle m_3 \ m_3 \rangle = 0$ . Similar considerations apply in (6.21), (6.25), (6.27), (6.30), (6.31), (6.36) and (6.44).

Expressions corresponding to the third and fourth diagrams in Figure 6.1 are

$$A_n^{(3)} = \frac{-1}{\prod_{l=1}^n \langle l \ l + 1 \rangle} \sum_{i=m_2}^{m_3-1} \sum_{j=m_1}^{m_2-1} \frac{\langle m_2^- | \not{q}_{i+1,j} | m_1^- \rangle^4 \langle m_3 \ m_1 \rangle^3 \langle m_3 \ k \rangle}{D} , \quad (6.21)$$

$$A_n^{(4)} = \frac{-1}{\prod_{l=1}^n \langle l \ l + 1 \rangle} \sum_{i=k}^{n+m_1-1} \sum_{j=m_2}^{m_3-1} \frac{\langle m_3^- | \not{q}_{i+1,j} | m_1^- \rangle^3 \langle m_2^- | \not{q}_{i+1,j} | m_1^- \rangle \langle m_2 \ m_1 \rangle^3 \langle m_3 \ k \rangle}{D} . \quad (6.22)$$

Note that the first sum in (6.22),  $\sum_{i=k}^{n+m_1-1}$ , is understood to run in cyclic order, for example  $\sum_{i=4}^3 = \sum_{i=4,\dots,n,1,2,3}$ . The same comment will also apply to similar sums in Eqs. (6.24), (6.27), (6.29), (6.30) below.

The total amplitude is the sum of (6.19), (6.20), (6.21) and (6.22),

$$A_n(\Lambda_{m_1}^-, g_{m_2}^-, g_{m_3}^-, \Lambda_k^+) = \sum_{i=1}^4 A_n^{(i)} . \quad (6.23)$$

There are three sources of zeroes in the denominator combination  $D$  defined in (6.17). First, there are genuine zeroes in, for example,  $\langle i^- | \not{q}_{i+1,j} | m_1^- \rangle$  when  $q_{i+1,j}$  is proportional to  $p_i$ . This occurs when  $j = i - 1$ . Such terms are always associated with two-leg vertices as discussed above and produce zeroes in the numerator. In fact, the number of zeroes in the numerator always exceeds the number of zeroes in the denominator and this contribution vanishes. Second, there are zeroes associated with three-point vertices when, for example,  $i = m_2$  and  $q_{i+1,j} = p_{m_2} + p_{m_1}$  so that  $\langle m_2^- | \not{q}_{i+1,j} | m_1^- \rangle = 0$ . As discussed in Sec. 2, there is always a compensating

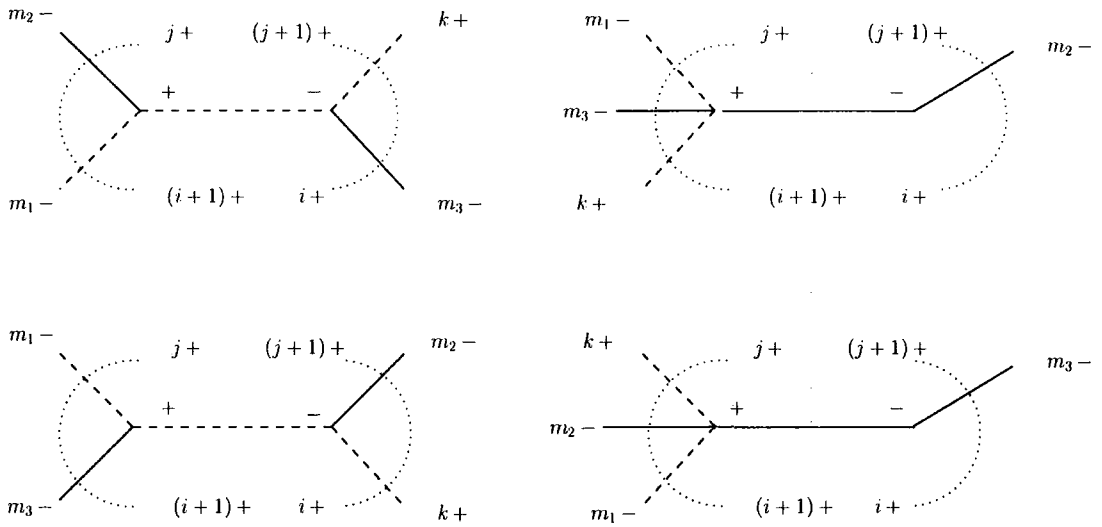


Figure 6.2: Tree diagrams with MHV vertices contributing to the amplitude  $A_n(\Lambda_{m_1}^-, g_{m_2}^-, \Lambda_k^+, g_{m_3}^-)$ .

factor in the numerator. Such terms give a finite contribution (see (6.5)). Third, there are accidental zeroes when  $q_{i+1,j}$  happens to be a linear combination of  $p_i$  and  $p_{m_1}$ . For general phase space points this is not the case. However, at certain phase space points, the Gram determinant of  $p_i, p_{m_1}$  and  $q_{i+1,j}$  does vanish. This produces an apparent singularity in individual terms in (6.19)–(6.22) which cancels when all contributions are taken into account. This cancellation can be achieved numerically or straightforwardly eliminated using standard spinor techniques [110].

For the special case of coincident negative helicities,  $m_1 = 1, m_2 = 2, m_3 = 3$ , the double sums in Eqs. (6.19)–(6.22) collapse to single sums. Furthermore, we see that the contribution from (6.21) vanishes due to momentum conservation,  $q_{2,1} = 0$ . The remaining three terms agree with the result presented in Eq. (3.6) of Ref. [4].

We now consider the second amplitude, Eq. (6.11b). The scalar graph diagrams are shown in Figure 6.2. There is a fermion exchange and a gluon exchange diagram for two of the line assignments,  $(m_1, m_2)$ , and  $(m_3, m_1)$ , and none for the remaining assignment  $(m_2, m_3)$ .

These four diagrams result in:

$$A_n^{(1)'} = \frac{1}{\prod_{l=1}^n \langle l \ l + 1 \rangle} \sum_{i=m_3}^{n+m_1-1} \sum_{j=m_2}^{k-1} \frac{\langle m_3^- | \not{d}_{i+1,j} | m_1^- \rangle^3 \langle m_2^- | \not{d}_{i+1,j} | m_1^- \rangle \langle m_2 \ m_1 \rangle^3 \langle m_3 \ k \rangle}{D} \quad (6.24)$$

$$A_n^{(2)'} = \frac{1}{\prod_{l=1}^n \langle l \ l + 1 \rangle} \sum_{i=m_2}^{k-1} \sum_{j=m_1}^{m_2-1} \frac{\langle m_2^- | \not{d}_{i+1,j} | m_1^- \rangle^4 \langle m_3 \ m_1 \rangle^3 \langle m_3 \ k \rangle}{D} , \quad (6.25)$$

$$A_n^{(3)'} = \frac{1}{\prod_{l=1}^n \langle l \ l + 1 \rangle} \sum_{i=k}^{m_3-1} \sum_{j=m_1}^{m_2-1} \frac{\langle m_2^- | \not{d}_{i+1,j} | m_1^- \rangle^3 \langle m_3^- | \not{d}_{i+1,j} | m_1^- \rangle \langle m_3 \ m_1 \rangle^3 \langle m_2 \ k \rangle}{D} , \quad (6.26)$$

$$A_n^{(4)'} = \frac{-1}{\prod_{l=1}^n \langle l \ l + 1 \rangle} \sum_{i=m_3}^{n+m_1-1} \sum_{j=k}^{m_3-1} \frac{\langle m_3^- | \not{d}_{i+1,j} | m_1^- \rangle^4 \langle m_2 \ m_1 \rangle^3 \langle m_2 \ k \rangle}{D} , \quad (6.27)$$

and the final answer for (6.11b) is,

$$A_n(\Lambda_{m_1}^-, g_{m_2}^-, \Lambda_k^+, g_{m_3}^-) = \sum_{i=1}^4 A_n^{(i)'} . \quad (6.28)$$

Finally, we give the result for (6.11c). The corresponding diagrams are drawn in Figure 6.3. We find

$$A_n^{(1)''} = \frac{1}{\prod_{l=1}^n \langle l \ l + 1 \rangle} \sum_{i=k}^{m_2-1} \sum_{j=m_3}^{n+m_1-1} \frac{\langle m_1^- | \not{d}_{i+1,j} | m_1^- \rangle^3 \langle k^- | \not{d}_{i+1,j} | m_1^- \rangle \langle m_2 \ m_3 \rangle^4}{D} \quad (6.29)$$

$$A_n^{(2)''} = \frac{1}{\prod_{l=1}^n \langle l \ l + 1 \rangle} \sum_{i=m_3}^{n+m_1-1} \sum_{j=m_2}^{m_3-1} \frac{\langle m_3^- | \not{d}_{i+1,j} | m_1^- \rangle^4 \langle m_2 \ m_1 \rangle^3 \langle m_2 \ k \rangle}{D} \quad (6.30)$$

$$A_n^{(3)''} = \frac{1}{\prod_{l=1}^n \langle l \ l + 1 \rangle} \sum_{i=m_2}^{m_3-1} \sum_{j=k}^{m_2-1} \frac{\langle m_2^- | \not{d}_{i+1,j} | m_1^- \rangle^4 \langle m_3 \ m_1 \rangle^3 \langle m_3 \ k \rangle}{D} \quad (6.31)$$

$$A_n^{(4)''} = \frac{-1}{\prod_{l=1}^n \langle l \ l + 1 \rangle} \sum_{i=m_2}^{m_3-1} \sum_{j=m_1}^{k-1} \frac{\langle m_2^- | \not{d}_{i+1,j} | m_1^- \rangle^3 \langle m_3^- | \not{d}_{i+1,j} | m_1^- \rangle \langle m_3 \ m_1 \rangle^3 \langle m_2 \ k \rangle}{D} . \quad (6.32)$$

As before, the full amplitude is given by the sum of contributions,

$$A_n(\Lambda_{m_1}^-, \Lambda_k^+, g_{m_2}^-, g_{m_3}^-) = \sum_{i=1}^4 A_n^{(i)''} . \quad (6.33)$$

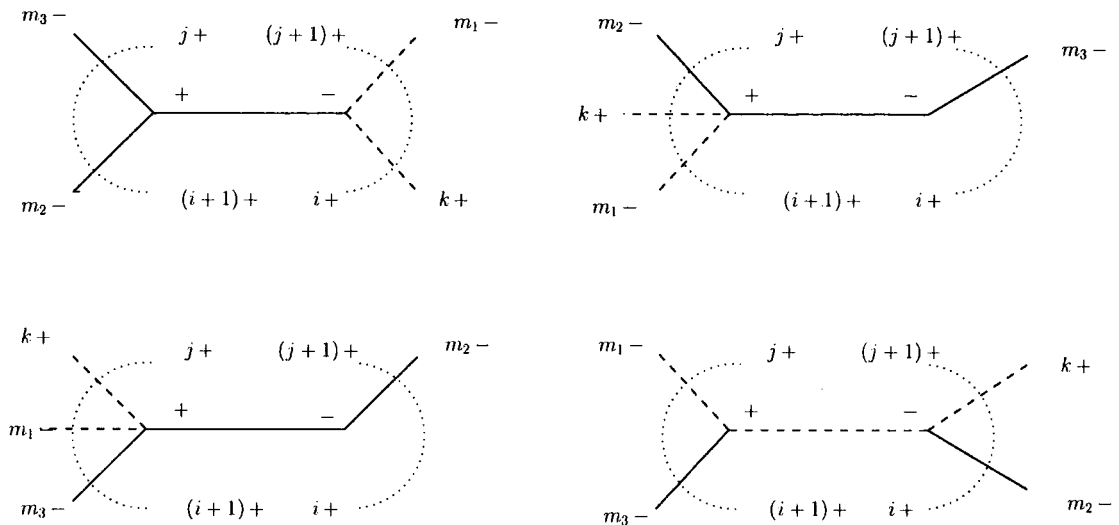


Figure 6.3: Tree diagrams with MHV vertices contributing to the amplitude  $A_n(\Lambda_{m_1}^-, \Lambda_k^+, g_{m_2}^-, g_{m_3}^-)$ .

## 6.4 NMHV ( - - - ) Amplitudes with Four Fermions

We now consider the amplitudes with 2 fermion-antifermion lines. In what follows, without loss of generality we will choose the negative helicity gluon to be the first particle. With this convention, we can write the six inequivalent amplitudes as:

$$A_n(g_1^-, \Lambda_{m_2}^-, \Lambda_{m_3}^-, \Lambda_{m_p}^+, \Lambda_{m_q}^+), \quad (6.34a)$$

$$A_n(g_1^-, \Lambda_{m_2}^-, \Lambda_{m_p}^+, \Lambda_{m_3}^-, \Lambda_{m_q}^+), \quad (6.34b)$$

$$A_n(g_1^-, \Lambda_{m_2}^-, \Lambda_{m_p}^+, \Lambda_{m_q}^+, \Lambda_{m_3}^-), \quad (6.34c)$$

$$A_n(g_1^-, \Lambda_{m_p}^+, \Lambda_{m_2}^-, \Lambda_{m_3}^-, \Lambda_{m_q}^+), \quad (6.34d)$$

$$A_n(g_1^-, \Lambda_{m_p}^+, \Lambda_{m_2}^-, \Lambda_{m_q}^+, \Lambda_{m_3}^-), \quad (6.34e)$$

$$A_n(g_1^-, \Lambda_{m_p}^+, \Lambda_{m_q}^+, \Lambda_{m_2}^-, \Lambda_{m_3}^-). \quad (6.34f)$$

The calculation of the amplitudes of (6.34a)-(6.34f) is straightforward. The diagrams contributing to the first process are shown in Figure 6.4. It should be noted that not all the amplitudes in (6.34a)-(6.34f) receive contributions from the same number of diagrams. For example, there are four diagrams for the process of (6.34a) while there are six for that of (6.34b). In order to avoid vanishing denominators, one

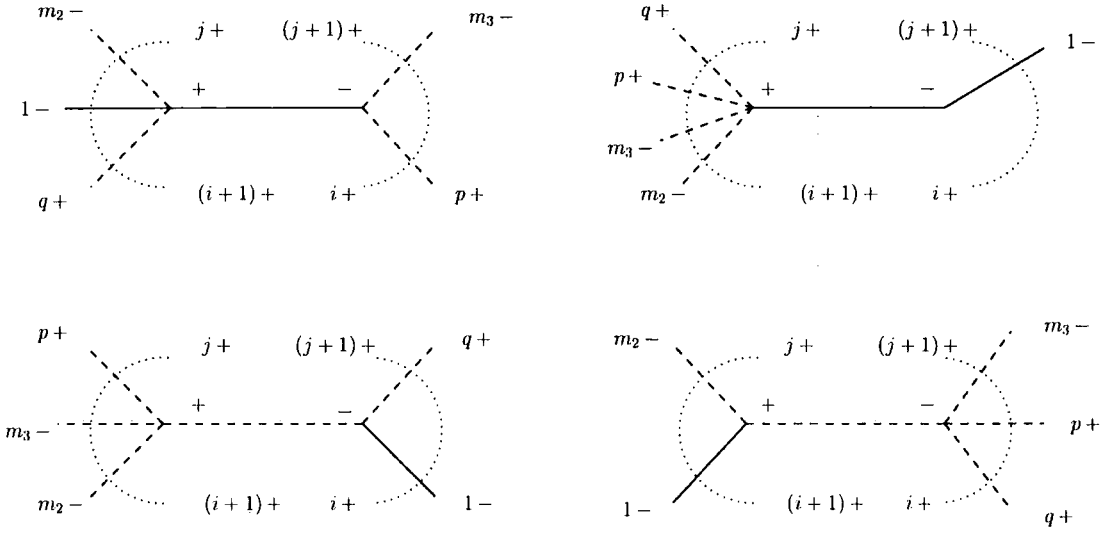


Figure 6.4: Tree diagrams with MHV vertices contributing to the four fermion amplitude  $A_n(g_1^-, \Lambda_{m_2}^-, \Lambda_{m_3}^-, \Lambda_{m_p}^+, \Lambda_{m_q}^+)$ .

can choose the reference spinor to be  $\tilde{\eta} = \tilde{\lambda}_{m_2}$ . With this choice the result can be written as:

$$\tilde{A}_n^{(1)} = \frac{1}{\prod_{l=1}^n \langle l l+1 \rangle} \sum_{i=p}^{q-1} \sum_{j=m_2}^{m_3-1} \frac{\langle m_3^- | \not{d}_{i+1,j} | m_2^- \rangle^3 \langle p^- | \not{d}_{i+1,j} | m_2^- \rangle \langle 1 m_2 \rangle^3 \langle 1 q \rangle}{D}, \quad (6.35)$$

$$\tilde{A}_n^{(2)} = \frac{-1}{\prod_{l=1}^n \langle l l+1 \rangle} \sum_{i=1}^{m_2-1} \sum_{j=q}^n \frac{\langle 1^- | \not{d}_{i+1,j} | m_2^- \rangle^4 \langle m_2 m_3 \rangle^3 \langle p q \rangle}{D}, \quad (6.36)$$

$$\tilde{A}_n^{(3)} = \frac{1}{\prod_{l=1}^n \langle l l+1 \rangle} \sum_{i=1}^{m_2-1} \sum_{j=p}^{q-1} \frac{\langle 1^- | \not{d}_{i+1,j} | m_2^- \rangle^3 \langle p^- | \not{d}_{i+1,j} | m_2^- \rangle \langle m_2 m_3 \rangle^3 \langle 1 q \rangle}{D}, \quad (6.37)$$

$$\tilde{A}_n^{(4)} = \frac{-1}{\prod_{l=1}^n \langle l l+1 \rangle} \sum_{i=q}^n \sum_{j=m_2}^{m_3-1} \frac{\langle m_3^- | \not{d}_{i+1,j} | m_2^- \rangle^3 \langle 1^- | \not{d}_{i+1,j} | m_2^- \rangle \langle 1 m_2 \rangle^3 \langle p q \rangle}{D}. \quad (6.38)$$

As before the final result is the sum of Eq. (6.35)-(6.38).

$$A_n(g_1^-, \Lambda_{m_2}^-, \Lambda_{m_3}^-, \Lambda_{m_p}^+, \Lambda_{m_q}^+) = \sum_{i=1}^4 \tilde{A}_n^{(i)}. \quad (6.39)$$

Once again, for the case of coincident negative helicities,  $m_2 = 2$ ,  $m_3 = 3$ , the double sums collapse to single summations and we recover the results given in Ref. [4].

As a last example we write down the expression for the amplitude of (6.34b). The corresponding diagrams are shown in Figure 6.5. We find,

$$\tilde{A}_n^{(1)'} = \frac{-1}{\prod_{l=1}^n \langle l l+1 \rangle} \sum_{i=m_3}^{q-1} \sum_{j=m_2}^{p-1} \frac{\langle m_3^- | \not{d}_{i+1,j} | m_2^- \rangle^3 \langle p^- | \not{d}_{i+1,j} | m_2^- \rangle \langle 1 m_2 \rangle^3 \langle 1 q \rangle}{D}, \quad (6.40)$$

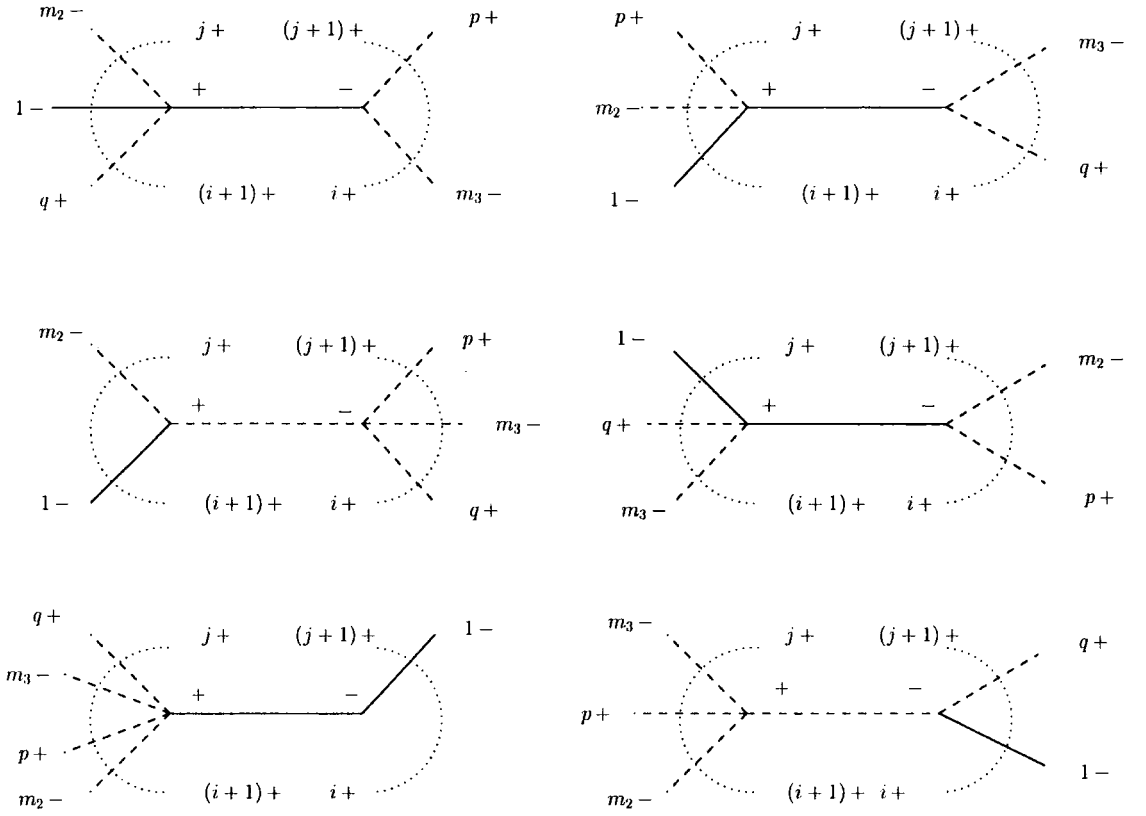


Figure 6.5: Tree diagrams with MHV vertices contributing to the four fermion amplitude  $A_n(g_1^-, \Lambda_{m_2}^-, \Lambda_{m_p}^+, \Lambda_{m_3}^-, \Lambda_{m_q}^+)$ .

$$\tilde{A}_n^{(2)'} = \frac{1}{\prod_{l=1}^n \langle l \ l+1 \rangle} \sum_{i=q}^n \sum_{j=p}^{m_3-1} \frac{\langle m_3^- | \not{q}_{i+1,j} | m_2^- \rangle^3 \langle q^- | \not{q}_{i+1,j} | m_2^- \rangle \langle 1 \ m_2 \rangle^3 \langle 1 \ p \rangle}{D}, \quad (6.41)$$

$$\tilde{A}_n^{(3)'} = \frac{1}{\prod_{l=1}^n \langle l \ l+1 \rangle} \sum_{i=q}^n \sum_{j=m_2}^{p-1} \frac{\langle m_3^- | \not{q}_{i+1,j} | m_2^- \rangle^3 \langle 1^- | \not{q}_{i+1,j} | m_2^- \rangle \langle 1 \ m_2 \rangle^3 \langle p \ q \rangle}{D}, \quad (6.42)$$

$$\tilde{A}_n^{(4)'} = \frac{1}{\prod_{l=1}^n \langle l \ l+1 \rangle} \sum_{i=p}^{m_3-1} \sum_{j=1}^{m_2-1} \frac{\langle m_2^- | \not{q}_{i+1,j} | m_2^- \rangle^3 \langle p^- | \not{q}_{i+1,j} | m_2^- \rangle \langle 1 \ m_3 \rangle^3 \langle 1 \ q \rangle}{D}, \quad (6.43)$$

$$\tilde{A}_n^{(5)'} = \frac{1}{\prod_{l=1}^n \langle l \ l+1 \rangle} \sum_{i=1}^{m_2-1} \sum_{j=q}^n \frac{\langle 1^- | \not{q}_{i+1,j} | m_2^- \rangle^4 \langle m_2 \ m_3 \rangle^3 \langle p \ q \rangle}{D}, \quad (6.44)$$

$$\tilde{A}_n^{(6)'} = \frac{-1}{\prod_{l=1}^n \langle l \ l+1 \rangle} \sum_{i=1}^{m_2-1} \sum_{j=m_3}^{q-1} \frac{\langle 1^- | \not{q}_{i+1,j} | m_2^- \rangle^3 \langle p^- | \not{q}_{i+1,j} | m_2^- \rangle \langle m_2 \ m_3 \rangle^3 \langle 1 \ q \rangle}{D}. \quad (6.45)$$

The full amplitude is the sum of Eq. (6.35)-(6.38).

$$A_n(g_1^-, \Lambda_{m_2}^-, \Lambda_{m_p}^+, \Lambda_{m_3}^-, \Lambda_{m_q}^+) = \sum_{i=1}^6 \tilde{A}_n^{(i)'} . \quad (6.46)$$

We close this section by listing the inequivalent NMHV amplitudes with three fermion-antifermion pairs. There are ten such amplitudes since choosing the first particle to be a negative helicity fermion we are left with five fermions (two of which have negative helicity and three positive) which should be distributed in all possible ways among themselves, and, in addition there are  $(n - 6)$  positive helicity gluons. Thus the number of different possible ways is  $5!$ . However, the order of the particles of the same helicity is immaterial (since one can always choose  $m_2 \leq m_3$  and  $m_p \leq m_q \leq m_r$ ). This means that we have to divide  $5!$  by  $3!$  (for the positive helicity fermions) and by  $2!$  (for the negative helicity fermions.) Thus there are ten different fermion amplitudes. These are listed below:

$$\begin{aligned} & A_n(\Lambda_1^-, \Lambda_{m_2}^-, \Lambda_{m_3}^-, \Lambda_{m_p}^+, \Lambda_{m_q}^+, \Lambda_{m_r}^+) , & A_n(\Lambda_1^-, \Lambda_{m_2}^-, \Lambda_{m_p}^+, \Lambda_{m_3}^-, \Lambda_{m_q}^+, \Lambda_{m_r}^+) , \\ & A_n(\Lambda_1^-, \Lambda_{m_2}^-, \Lambda_{m_p}^+, \Lambda_{m_q}^+, \Lambda_{m_3}^-, \Lambda_{m_r}^+) , & A_n(\Lambda_1^-, \Lambda_{m_p}^+, \Lambda_{m_2}^-, \Lambda_{m_3}^-, \Lambda_{m_q}^+, \Lambda_{m_r}^+) , \\ & A_n(\Lambda_1^-, \Lambda_{m_p}^+, \Lambda_{m_2}^-, \Lambda_{m_q}^+, \Lambda_{m_3}^-, \Lambda_{m_r}^+) , & A_n(\Lambda_1^-, \Lambda_{m_p}^+, \Lambda_{m_q}^+, \Lambda_{m_2}^-, \Lambda_{m_3}^-, \Lambda_{m_r}^+) , \\ & A_n(\Lambda_1^-, \Lambda_{m_p}^+, \Lambda_{m_q}^+, \Lambda_{m_r}^+, \Lambda_{m_2}^-, \Lambda_{m_3}^-) , & A_n(\Lambda_1^-, \Lambda_{m_p}^+, \Lambda_{m_q}^+, \Lambda_{m_2}^-, \Lambda_{m_r}^+, \Lambda_{m_3}^-) , \\ & A_n(\Lambda_1^-, \Lambda_{m_p}^+, \Lambda_{m_2}^-, \Lambda_{m_q}^+, \Lambda_{m_r}^+, \Lambda_{m_3}^-) , & A_n(\Lambda_1^-, \Lambda_{m_2}^-, \Lambda_{m_p}^+, \Lambda_{m_q}^+, \Lambda_{m_r}^+, \Lambda_{m_3}^-) . \end{aligned} \quad (6.47)$$

These amplitudes also present no difficulty, and they can be evaluated in the same manner as before.

## 6.5 Iterations of the Analytic Supervertex

### 6.5.1 Analytic Supervertex

So far we have encountered three types of MHV amplitudes (5.14), (5.19) and (5.20). The key feature which distinguishes these amplitudes is the fact that they depend only on  $\langle \lambda_i \lambda_j \rangle$  spinor products, and not on  $[\tilde{\lambda}_i \tilde{\lambda}_i]$ .

All amplitudes following from (5.17) are analytic in the sense that they depend only on  $\langle \lambda_i \lambda_j \rangle$  spinor products, and not on  $[\tilde{\lambda}_i \tilde{\lambda}_i]$ . There is a large number of such component amplitudes for an extended susy Yang-Mills, and what is remarkable,

not all of these amplitudes are MHV. The analytic amplitudes of the  $\mathcal{N} = 4$  SYM obtained from (5.17), (5.18) are

$$\begin{aligned}
& A_n(g^-, g^-), \quad A_n(g^-, \Lambda_A^-, \Lambda^{A+}), \quad A_n(\Lambda_A^-, \Lambda_B^-, \Lambda^{A+}, \Lambda^{B+}), \\
& A_n(g^-, \Lambda^{1+}, \Lambda^{2+}, \Lambda^{3+}, \Lambda^{4+}), \quad A_n(\Lambda_A^-, \Lambda^{A+}, \Lambda^{1+}, \Lambda^{2+}, \Lambda^{3+}, \Lambda^{4+}), \\
& A_n(\Lambda^{1+}, \Lambda^{2+}, \Lambda^{3+}, \Lambda^{4+}, \Lambda^{1+}, \Lambda^{2+}, \Lambda^{3+}, \Lambda^{4+}), \quad A_n(\bar{\phi}_{AB}, \Lambda^{A+}, \Lambda^{B+}, \Lambda^{1+}, \Lambda^{2+}, \Lambda^{3+}, \Lambda^{4+}), \\
& A_n(g^-, \bar{\phi}_{AB}, \phi^{AB}), \quad A_n(g^-, \bar{\phi}_{AB}, \Lambda^{A+}, \Lambda^{B+}), \quad A_n(\Lambda_A^-, \Lambda_B^-, \phi^{AB}), \\
& A_n(\Lambda_A^-, \phi^{AB}, \bar{\phi}_{BC}, \Lambda^{C+}), \quad A_n(\Lambda_A^-, \bar{\phi}_{AB}, \Lambda^{A+}, \Lambda^{B+}, \Lambda^{C+}), \\
& A_n(\bar{\phi}, \phi, \bar{\phi}, \phi), \quad A_n(\bar{\phi}, \phi, \bar{\phi}, \Lambda^+, \Lambda^+), \quad A_n(\bar{\phi}, \bar{\phi}, \Lambda^+, \Lambda^+, \Lambda^+, \Lambda^+),
\end{aligned} \tag{6.48}$$

where it is understood that  $\bar{\phi}_{AB} = \frac{1}{2}\epsilon_{ABCD}\phi^{CD}$ . In Eqs. (6.48) we do not distinguish between the different particle orderings in the amplitudes. The labels refer to supersymmetry multiplets,  $A, B = 1, \dots, 4$ . Analytic amplitudes in (6.48) include the familiar MHV amplitudes, (5.14), (5.19), (5.20), as well as more complicated classes of amplitudes with external gluinos  $\Lambda^A, \Lambda^{B \neq A}$ , etc, and with external scalar fields  $\phi^{AB}$ .

The second and third lines in (6.48) are not even MHV amplitudes, they have less than two negative helicities, and nevertheless, these amplitudes are non-vanishing in  $\mathcal{N} = 4$  SYM.

All the analytic amplitudes listed in (6.48) can be calculated directly from (5.17), (5.18). There is a simple algorithm for doing this.

1. For each amplitude in (6.48) substitute the fields by their  $\eta$ -expressions (5.18). There are precisely eight  $\eta$ 's for each analytic amplitude.
2. Keeping track of the overall sign, rearrange the anticommuting  $\eta$ 's into a product of four pairs:  $(\text{sign}) \times \eta_i^1 \eta_j^1 \eta_k^2 \eta_l^2 \eta_m^3 \eta_n^3 \eta_r^4 \eta_s^4$ .
3. The amplitude is obtained by replacing each pair  $\eta_i^A \eta_j^A$  by the spinor product  $\langle i j \rangle$  and dividing by the usual denominator,

$$A_n = (\text{sign}) \times \frac{\langle i j \rangle \langle k l \rangle \langle m n \rangle \langle r s \rangle}{\prod_{l=1}^n \langle l l+1 \rangle}. \tag{6.49}$$

### 6.5.2 Scalar graphs with analytic vertices

The conclusion we draw from the previous section is that in the scalar graph formalism in  $\mathcal{N} \leq 4$  SYM, the amplitudes are characterised not by a number of negative helicities, but rather by the total number of  $\eta$ 's associated to each amplitude via the rules (5.18).

The vertices of the scalar graph method are the analytic vertices (6.48) which are all of degree-8 in  $\eta$ . These vertices are analytic (they depend only on  $\langle i j \rangle$  spinor products) and not necessarily MHV. These are component vertices of a single analytic supervertex<sup>3</sup> (5.17). The analytic amplitudes are of degree-8 and they are the elementary blocks of the scalar graph approach. The next-to-minimal case are the amplitudes of degree-12 in  $\eta$ , and they are obtained by connecting two analytic vertices [120] with a scalar propagator  $1/q^2$ . Each analytic vertex contributes 8  $\eta$ 's and a propagator removes 4. Scalar diagrams with three degree-8 vertices give the degree-12 amplitude, etc. In general, all  $n$ -point amplitudes are characterised by a degree 8, 12, 16,  $\dots$ ,  $(4n-8)$  which are obtained from scalar diagrams with 1, 2, 3,  $\dots$  analytic vertices.<sup>4</sup> In the next section we derive a simple expression for the first iteration of the degree-8 vertex. This iterative process can be continued straightforwardly to higher orders.

### 6.5.3 Two analytic supervertices

We now consider a diagram with two analytic supervertices (5.17) connected to one another by a single scalar propagator. The diagram is depicted in Figure 6.6. We follow the same conventions as in the previous sections, and the left vertex has a positive helicity on the internal line  $\bar{I}$ , while the right vertex has a negative helicity on the internal line  $I$ . The labelling of the external lines in Figure 6.6 is also consistent with our conventions. The right vertex has  $n_1$  lines, and the left one has  $n_2$  lines in

<sup>3</sup>The list of component vertices (6.48) is obtained by writing down all partitions of 8 into groups of 4, 3, 2 and 1. For example,  $A_n(g^-, \bar{\phi}_{AB}, \Lambda^{A+}, \Lambda^{B+})$  follows from  $8 = 4 + 2 + 1 + 1$ .

<sup>4</sup>In practice, one needs to know only the first half of these amplitudes, since degree- $(4n-8)$  amplitudes are anti-analytic (formerly known as googly  $\overline{\text{MHV}}$  and they are simply given by degree- $8^*$  amplitudes, similarly degree- $(4n-12)$  are given by degree- $12^*$ , etc.

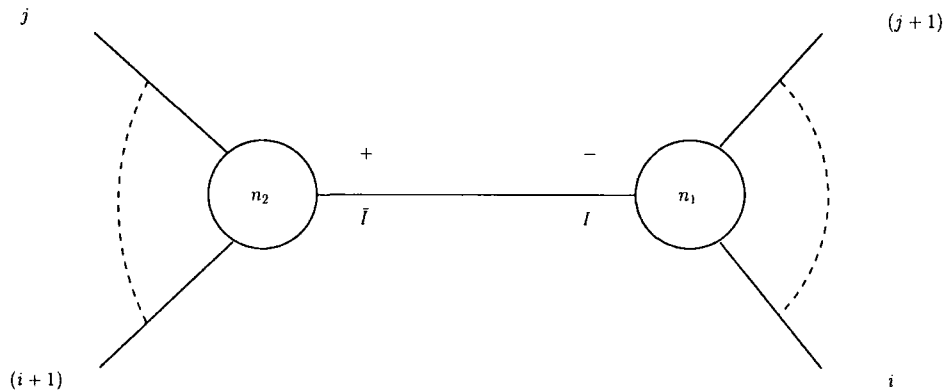


Figure 6.6: Tree diagrams with MHV vertices contributing to the first amplitude of Eq. (6.34b).

total, such that resulting amplitude  $A_n$  has  $n = n_1 + n_2 - 2$  external lines. Suppressing summations over the distribution of  $n_1$  and  $n_2$  between the two vertices, we can write down an expression for the corresponding amplitude which follows immediately from (5.17) and Figure 6.6:

$$A_n = \frac{1}{\prod_{l=1}^{n_2} \langle l \ l+1 \rangle} \frac{1}{q_I^2} \frac{\langle j \ j+1 \rangle \langle i \ i+1 \rangle}{\langle j \ \bar{I} \rangle \langle \bar{I} \ i+1 \rangle \langle i \ I \rangle \langle I \ j+1 \rangle} \times \int \prod_{A=1}^4 d\eta_I^A \delta^{(8)} \left( \lambda_{\bar{I}a} \eta_I^A + \sum_{l_2 \neq \bar{I}}^{n_2} \lambda_{l_2 a} \eta_{l_2}^A \right) \delta^{(8)} \left( \lambda_{Ia} \eta_I^A + \sum_{l_1 \neq I}^{n_1} \lambda_{l_1 a} \eta_{l_1}^A \right). \quad (6.50)$$

The two delta-functions in (6.50) come from the two vertices (5.17). The summations in the delta-functions arguments run over the  $n_1 - 1$  external lines for right vertex, and  $n_2 - 1$  external lines for the left one. The integration over  $d^4 \eta_I$  arises in (6.50) for the following reason. Two separate (unconnected) vertices in Figure 6.6 would have  $n_1 + n_2$  lines and, hence,  $n_1 + n_2$  different  $\eta$ 's (and  $\lambda$ 's). However the  $I$  and the  $\bar{I}$  lines are connected by the propagator, and there must be only  $n = n_1 + n_2 - 2$   $\eta$ -variables left. This is achieved in (6.50) by setting

$$\eta_{\bar{I}}^A = \eta_I^A, \quad (6.51)$$

and integrating over  $d^4 \eta_I$ . The off-shell continuation of the internal spinors is defined as before,

$$\lambda_{Ia} = \sum_{l_1 \neq I}^{n_1} p_{l_1 a \dot{a}} \xi_{\text{Ref}}^{\dot{a}} = -\lambda_{\bar{I}a}. \quad (6.52)$$

We now integrate out four  $\eta_I$ 's which is made simple by rearranging the arguments of the delta-functions via  $\int \delta(f_2)\delta(f_1) = \int \delta(f_1 + f_2)\delta(f_1)$ , and noticing that the sum of two arguments,  $f_1 + f_2$ , does not depend on  $\eta_I$ .

The final result is

$$A_n = \frac{1}{\prod_{l=1}^n \langle l \ l + 1 \rangle} \delta^{(8)} \left( \sum_{i=1}^n \lambda_{ia} \eta_i^A \right) \prod_{A=1}^4 \left( \sum_{l_1 \neq I}^{n_1} \langle I \ l_1 \rangle \eta_{l_1}^A \right) \frac{1}{D}, \quad (6.53)$$

and  $D$  is the same as (6.17) used in sections 6.3 and 6.4,

$$\frac{1}{D} = \frac{1}{q_I^2} \frac{\langle j \ j + 1 \rangle \langle i \ i + 1 \rangle}{\langle j \ I \rangle \langle I \ i + 1 \rangle \langle i \ I \rangle \langle I \ j + 1 \rangle}. \quad (6.54)$$

There are 12  $\eta$ 's in the superamplitude (6.53), and the coefficients of the Taylor expansion in  $\eta$ 's give all the component amplitudes of degree-12.

We have, thus, seen that all the results obtained in the last two chapters can in principle be recovered from Nair's  $\mathcal{N} = 4$  supervertex. This analytic vertex generates all possible interactions which, strictly speaking, are not MHV (they do not necessarily contain two negative helicity particles). In the next chapter, we'll summarise the findings obtained from the study of the BMN correspondence and from the study of the CSW method performed in chapters 2-4 and 5-6 respectively.

# Chapter 7

## Conclusions

In this final chapter, we close the thesis by drawing our conclusions.

In chapter 2, we provided evidence for a vertex-correlator type duality in the pp-wave background. This kind of correspondence relates the coefficients of 3-point correlators of  $\Delta$ -BMN operators in gauge theory to 3-string amplitudes in light-cone string field theory in the pp-wave background. By using field theoretical data, that is by calculating the 3-point function coefficients of correlators involving operators with three scalar impurities <sup>1</sup>, we determined the form the prefactor P of the 3-string vertex should have so that a vertex-correlator type duality like that of Eq. (2.4) to be valid.

This kind of duality was questioned for a long time, since none of the 3-string vertices discussed in chapter 1 has a prefactor resembling the one proposed in chapter 2 <sup>2</sup>. Nevertheless, recently Dobashi and Yoneya [32] derived an explicit holographic

---

<sup>1</sup>In order to calculate the 3-point function coefficient of  $\Delta$ -BMN operators at order  $g_2\lambda'$  the mixing of single trace with double trace operators should be taken into account, otherwise the resulting operators will not have well defined scaling dimensions. This fact makes the calculation of 3-point correlators really involved. However, a simple observation can save us a lot of work. Namely, at the desired order, these mixing effects do not give any contribution to the coefficient of the  $\log x_1^2$  part of the correlator. Then, by assuming that the 3-point function takes the canonical form dictated by conformal symmetry, one can determine the 3-point function coefficient without having to compute the exact expression for the  $\Delta$ -BMN operators (only the single trace part is needed).

<sup>2</sup>The second proposal of [68] is supporting a vertex-correlator type duality but only at the non-

duality map for the supergravity sector of the pp-wave string theory by taking the semiclassical limit of the GKP-Witten relation in AdS/CFT. Then they argued that correct full string theory vertex is half the Spradlin-Volovich vertex plus half the vertex proposed in [68], since this linear combination, when restricted to the supergravity sector, reduces to the supergravity vertex which they explicitly found. Using the expressions for the 3-point function coefficients obtained in [2,3] they tested their holographic vertex beyond the supergravity sector. The same authors checked the validity of their proposal for the impurity non-preserving 3-point correlators with bosonic excitations [33]. What is interesting is that when the holographic vertex is restricted to the bosonic (scalar) sector it gives the effective vertex of chapter 2. This can be easily seen by just inspecting the scalar part of the prefactor of their holographic vertex appearing in equation (4.7) of [32] and comparing to the prefactor given in chapter 2. Let us, now, comment on the compatibility of the extended BMN duality discussed in chapters 3 and 4 and the holographic proposal of [32]. In what follows we keep the discussion general and denote by  $\delta_i$  the  $\lambda'$  correction to the anomalous dimension of the operator  $\mathcal{O}_i(x_i)$  and by  $C_{123}^{(0)}$  the coefficient of the free three point function of the operators  $\mathcal{O}_i(x_i), i = 1, 2, 3$ . Then the matrices  $s, d$  and  $t$  defined in chapter 3 take the form:

$$s = \begin{pmatrix} 0 & C_{123}^{(0)} \\ C_{123}^{(0)} & 0 \end{pmatrix} \quad (7.1)$$

$$d = \lambda' \begin{pmatrix} \delta_1 & 0 \\ 0 & \delta_2 + \delta_3 \end{pmatrix} \quad (7.2)$$

$$t = \lambda' \begin{pmatrix} 0 & (\delta_2 + \delta_3 + b_{123})C_{123}^{(0)} \\ (\delta_2 + \delta_3 + b_{123})C_{123}^{(0)} & 0 \end{pmatrix} \quad (7.3)$$

---

interacting level in gauge theory. In particular, the 3-point function coefficient compared to the 3-string amplitude was the free coefficient  $C_{123}^{(0)}$ . No mixing with double trace operators, whatsoever, had been taken into account. This duality relation ceased to hold at  $\lambda'$  order providing us with a rather trivial version of the vertex-correlator type duality.

It is now straightforward to calculate the off-diagonal matrix elements of the  $\Gamma$ -matrix also defined in chapter 3. They are given by

$$\Gamma_{\text{o.d.}} = g_2 \frac{1}{2} (-\Delta_1 + \Delta_2 + \Delta_3) C_{123}^{(0)} + g_2 \lambda' b_{123} C_{123}^{(0)}. \quad (7.4)$$

When the vertex-correlator type duality described in chapter 2 but with the holographic string field theory vertex of [32] is combined with the expression for the correct CFT coefficient

$$C_{123} = \frac{\lambda' b_{123} C_{123}^{(0)}}{\Delta_1 - \Delta_2 - \Delta_3}. \quad (7.5)$$

it leads directly to

$$\frac{\sqrt{J_1 J_2 J_3}}{N} \langle 1, 2, 3 | \left( \frac{1}{2\mu} |\hat{H}_3\rangle_D + \frac{1}{2\mu} |\hat{H}_3\rangle_{SV} \right) = -g_2 \lambda' b_{123} C_{123}^{(0)}. \quad (7.6)$$

On the other hand, the result of [68] indicates that

$$\frac{\sqrt{J_1 J_2 J_3}}{N} \frac{1}{\mu} \langle 1, 2, 3 | \hat{H}_3\rangle_D = g_2 (-\Delta_1 + \Delta_2 + \Delta_3) C_{123}^{(0)}. \quad (7.7)$$

Using the equations (7.5), (7.6) and (7.7), we finally find

$$\Gamma_{\text{o.d.}} = -\frac{\sqrt{J_1 J_2 J_3}}{N} \frac{1}{2\mu} \langle 1, 2, 3 | \hat{H}_3\rangle_{SV}. \quad (7.8)$$

This is nothing but the relation describing the extended BMN duality discussed in chapters 3 and 4, except for the overall factor  $-1/2$ . This factor can be understood from the different normalization adopted in [32] compared to the one adopted in the rest of the literature.

Two final remarks are in order. First notice that the relation employed in chapters 3 and 4 is restricted to the processes where the numbers of impurities are conserved. For this particular class of processes, one can interpret the part  $|\hat{H}_3\rangle_D$  as describing the ‘bare’ part of the interaction of BMN operators, while the part  $|\hat{H}_3\rangle_{SV}$  as describing the mixing between them [32]. Our second remark is related to the factor of  $(-1)^p$  appearing in equation (2.9), where  $2p$  is the total number of impurities (string excitations) participating in the interaction. What this factor does is to fix the normalisation of the string vertex so that agreement with the 3-point function coefficient calculated in field theory can be obtained. The same factor appears also in [49]

where the string states with  $n$  impurities are given by  $|(d_i, N_i)\rangle = i^n \delta_{\sum_i n_i, 0} \prod_i a_{n_i}^{d_i \dagger} |v\rangle$ . There, the arbitrary phase of the state,  $i^n$ , is determined by comparison with gauge theory. This arbitrary phase has exactly the same effect as our  $(-1)^p$  factor. Thus, we see that this factor can be absorbed in the definition of the string state which is dual to a specific gauge operator  $\mathcal{O}$ . In particular, the dictionary of the duality can be stated as follows  $\mathcal{O}_{n_1, n_2, \dots} \longleftrightarrow i^n \delta_{\sum_i n_i, 0} \prod_i a_{n_i}^{d_i \dagger} |v\rangle$ .

In chapter 3 we explained how the correspondence between the natural string basis and the isomorphic to it gauge theory basis is realised so that one can compare matrix elements and not just the eigenvalues of the operators  $H_{\text{string}}$  and  $\Delta - J$ .

In particular, we extended the construction of [48] for the case of two scalar impurities to incorporate BMN operators with vector and mixed impurities. This enables us to verify from the gauge theory perspective two key properties of the three-string interaction vertex of Spradlin and Volovich:

(1) the vanishing of the three-string amplitude for string states with one vector and one scalar impurity; and (2) the relative minus sign in the string amplitude involving states with two vector impurities compared to that with two scalar impurities. This implies a spontaneous breaking of the  $\mathbb{Z}_2$  symmetry of the string field theory in the pp-wave background. Furthermore, we calculated the matrix elements of  $\Delta - J$  and  $H_{\text{string}}$  for states with an arbitrary number of scalar impurities. In all cases we found perfect agreement with the corresponding string amplitudes derived from the three-string vertex. We, thus, explored and verified the extended BMN correspondence in all directions of the two  $SO(4)$  groups.

Let us, now, briefly comment on the role of  $\mathbb{Z}_2$  symmetry.  $\mathbb{Z}_2$  symmetry is apparent for the pp-wave background since both the metric and the five-form field  $F_5$  are invariant under the exchange  $x^i \longleftrightarrow y^i$ . It is also apparent for the string theory side at the non-interacting level since the free string Hamiltonian is invariant under the action of the  $\mathbb{Z}_2$  symmetry. This means that the mass of a string state does not change if one converts an excitation along the first  $SO(4)$  subgroup to one along the second  $SO(4)$  subgroup, i.e.  $\alpha^{i \dagger} \longleftrightarrow \alpha^{i' \dagger}$ ,  $i = 1, \dots, 4$ ,  $i' = 5, \dots, 8$ . However at the interacting level things appear to be more complicated. In particular, the behaviour of the 3-string vertex under the action of  $\mathbb{Z}_2$  depends on what  $\mathbb{Z}_2$  parity

is assigned to the pp-wave ground state  $|v\rangle$ . As discussed in chapter 2 the Spradlin-Volovich vertex was originally built not on the ground state  $|v\rangle$  but on the state  $|0\rangle = \beta_{011}^\dagger \beta_{012}^\dagger \beta_{021}^\dagger \beta_{022}^\dagger |v\rangle$  which has energy  $4\mu$ . It was explained in [58] that these two states,  $|v\rangle$  and  $|0\rangle$  have opposite  $\mathbb{Z}_2$  parity. As a result, one has two choices:

$$1) \mathbb{Z}_2 : |v\rangle \longrightarrow -|v\rangle, |0\rangle \longrightarrow |0\rangle$$

$$2) \mathbb{Z}_2 : |v\rangle \longrightarrow |v\rangle, |0\rangle \longrightarrow -|0\rangle.$$

In our opinion, the first choice is more natural although it assigns a negative  $\mathbb{Z}_2$  parity to the real vacuum of the theory. In [96] the correspondence between the lowest lying string states and the fluctuation modes of supergravity on the pp-wave was examined. In particular, the state  $|0\rangle$  corresponds to the complex scalar arising from the dilaton-axion fields. As dilaton and axion are scalars under  $SO(8)$  and  $\mathbb{Z}_2$  is just a particular  $SO(8)$  transformation, we conclude that the assignment of positive  $\mathbb{Z}_2$  to the state  $|0\rangle$  appears to be the correct choice. With this parity assignment the Spradlin-Volovich vertex is invariant under  $\mathbb{Z}_2$  while the proposal of [68] is not (has negative  $\mathbb{Z}_2$  parity).

On the gauge theory side, the  $\mathbb{Z}_2$  parity is not apparent since the exchange of  $\phi^i$  with  $D_i Z$ ,  $i = 1, \dots, 4$  in the Lagrangian makes no sense. On the other hand, one expects that the anomalous dimension of a  $\Delta$ -BMN operator involving two scalar impurities, for example, is the same with the anomalous dimension of an operator involving two vector impurities, or one scalar and one vector impurity due to the fact that the supersymmetries that convert one species of operators to the other commute with the dilatation operator of  $\mathcal{N} = 4$  SYM<sup>3</sup>. This fact seems to be in contradiction with the vanishing of the 3-string amplitude in the case of mixed impurities, and the relative minus sign the 3-string amplitude with two scalar impurities has compared to that with two vector impurities. Thus, it turns out that, although the Spradlin-Volovich vertex is  $\mathbb{Z}_2$  invariant, the string amplitudes themselves are not. In chapter

---

<sup>3</sup>The one loop mass correction calculations for the string states with scalar, vector and mixed impurities were performed in [49–51] to obtain the same correction for all three cases in accordance with the fact that the three corresponding BMN operators have the same anomalous dimension. However, for the calculations to be feasible, one has to restrict himself to the case where the intermediate virtual string states belong to the impurity preserving subsector of all possible states.

3, we verified these properties of the 3-string vertex (and hence the spontaneous breaking of the  $\mathbb{Z}_2$  symmetry) with an independent gauge theory calculation.

In chapter 4 we studied the BMN correspondence in the fermionic sector. On the field theory side, we computed matrix elements of the dilatation operator in  $\mathcal{N} = 4$  Super Yang-Mills for BMN operators containing two fermion impurities. Our calculations were performed up to and including  $\mathcal{O}(\lambda')$  in the 't Hooft coupling and  $\mathcal{O}(g_2)$  in the Yang-Mills genus counting parameter. On the string theory side, we computed the corresponding matrix elements of the interacting string Hamiltonian in string field theory, using the three-string interaction vertex constructed by Spradlin and Volovich (and subsequently elaborated by Pankiewicz and Stefanski). In string theory we used the natural string basis, and in field theory the basis which is isomorphic to it. We found that the matrix elements computed in field theory and the corresponding string amplitudes derived from the three-string vertex are in perfect agreement for all the representations of two-impurity BMN operators with both fermions having the same chirality (both fermions having their  $SO(4) \otimes SO(4)$  indices dotted or undotted).

On the string theory side, we saw that the string amplitude vanishes whenever a fermion appears more than once, whereas it gives the same result (up to a minus sign) when all fermions are different. On the field theory side, we verified the crucial role played by the compensating terms of the BMN operators. Had these terms not been taken into account one would erroneously conclude that the 3-point functions of all operators with two impurities (scalar, vector, mixed and fermion) take the same form spoiling, thus, the BMN correspondence. Finally, we examined the action of the  $\mathbb{Z}_2$  symmetry on the string amplitudes involving two fermionic impurities to conclude that it leaves the value of the string amplitudes invariant.

As discussed in section 1.6 the pp-wave/SYM correspondence, studied in the first four chapters, can be viewed as a weak to weak duality. The weak to weak dualities are particularly interesting because it is easier to check whether they hold or not since perturbative calculations can be made on both sides of the duality.

Another, recently proposed, weak to weak duality is between tree level perturbative  $N = 4$  SYM and the open string topological B-model in supertwistor space  $CP^{3|4}$ . Inspired by this correspondence, a novel diagrammatic method for calculating

all gluon scattering amplitude at tree level was proposed by Cachazo, Svrcek, and Witten. This method was based on the fact that after Fourier transforming these amplitudes from the helicity basis to twistor space they acquire a surprisingly simple geometric structure, namely they are supported on certain configuration of curves in twistor space. This method uses maximally helicity violating amplitudes as effective vertices continued off-shell in a particular fashion and connected by scalar propagators. In chapter 5 we explored and extended this proposal. We applied this approach for calculating tree amplitudes of gauge fields and fermions (gluinos and quarks) to find agreement with known results. One of the main features of the formalism is that it amounts to an effective scalar perturbation theory (the MHV diagrams are scalar quantities and the propagator is  $1/(p^2 + i\epsilon)$  even when the virtual particle is a fermion) which offers a much simpler alternative to the usual Feynman diagrams in gauge theory and can be used for deriving new simple expressions for tree amplitudes. We have also, concluded that at tree level the formalism works in a generic gauge theory, with or without supersymmetry, and for a finite number of colours.

In chapter 6 we have continued the study of this novel diagrammatic approach. In particular, we have shown how all non-MHV tree-level amplitudes in  $0 \leq \mathcal{N} \leq 4$  gauge theories can be obtained directly from the known MHV amplitudes using the scalar graph approach of Cachazo, Svrcek and Witten. As a specific example, we have focussed on amplitudes which are next-to-MHV, i.e. contain three negative helicity particles and an arbitrary number of positive helicity particles. By starting with amplitudes containing fermions, the reference spinor for the negative helicity gluons can be chosen to be that of the negative helicity fermion. As a consequence, the amplitudes are free of unphysical singularities for generic phase space points and no further helicity-spinor algebra is required to convert the results into a numerically usable form. The gluons only amplitudes can then be simply obtained as sums of fermionic amplitudes using the supersymmetric Ward identity. These amplitudes are therefore also immediately free of unphysical poles. We have provided expressions for  $(-, -, -)$  amplitudes with a two and four fermions and shown how to construct the amplitudes for six fermions. The extension to amplitudes with four or more negative helicity particles is straightforward. In principle one could use the results presented

here to write a numerical program for evaluating generic processes involving fermions and bosons [127, 128].

All of these results can be recovered from Nair's  $\mathcal{N} = 4$  supervertex. This analytic vertex generates all possible interactions that depend only on products of  $\langle \lambda_i \lambda_j \rangle$ . Interestingly, all of the allowed vertices are not MHV. For example,  $A_n(g^-, \Lambda^{1+}, \Lambda^{2+}, \Lambda^{3+}, \Lambda^{4+})$ . This implies that the scalar graph approach is not primarily based on MHV amplitudes.

Subsequently, it was shown [130] that the method works for the one-loop MHV diagrams in  $\mathcal{N} = 4, 1$  theories and that it can reproduce the constructible part of the one-loop MHV diagrams in non-supersymmetric theories. This fact was rather unexpected since it is quite clear by now that the multi-loop amplitudes can not be calculated using the same string theory used for the tree level amplitudes. This is because in twistor string theories conformal supergravity does not decouple from the gauge theory resulting to supergravity fields propagating in the loops. Nevertheless, there is growing evidence that higher loop amplitudes might be computed by some sort of string theory in twistor space. It would be a nice thing to identify this string theory, principally because it may give us insights into the most efficient ways to calculate multi-loop scattering amplitudes in gauge theory.

More recent, Britto, Cachazo and Feng wrote down a new set of tree level recursion relations [132]. Recursion relations have long been in QCD, and are an elegant and efficient means for computing tree level amplitudes. The new recursion relations differ in that they employ only on-shell amplitudes at complex values of the external momenta, however. These relations were inspired by the compact forms of seven and higher point tree amplitudes [134] that emerged from studying infrared consistency equations for one-loop amplitudes. A simple and elegant proof of the relation using special complex continuation of the external momenta has been given by Britto, Cachazo, Feng and Witten [133]. Its application yields compact expressions for tree amplitudes in gravity as well as gauge theory [135]. These tree level recursion relations naturally extend to incorporate massive particles [136]. Amplitudes calculated by employing these relations can be used as building blocks in the computation of one-loop amplitudes using unitarity based methods, as discussed below.

The date that LHC will start operating is approaching fast, demanding new versatile tools for calculating multiparticle loop-level scattering amplitudes in the component gauge theories of the Standard Model. Computing these amplitudes is important in order to subtract the QCD background from possible new physics. Unfortunately, unlike the case of massless supersymmetric theories, QCD one-loop amplitudes are not cut-constructible. This means that the knowledge of the cuts is not enough to fully determine the amplitude. This is so because the amplitudes contain also a rational part which is absent in the case of supersymmetric theories [130]. There are, essentially, two ways to proceed. The first way is based on the unitarity method [129] and its generalised version of quadruple cuts developed in [131]. This method was used in the past in order to calculate the one-loop amplitudes in supersymmetric theories [129]. It can also be used to determine complete amplitudes, including rational pieces [137–140] by applying full  $D$ -dimensional unitarity, where  $D = 4 - 2\epsilon$  is the parameter of dimensional regularisation. This approach requires the computation of tree amplitudes where at least two of the momenta are in  $D$  dimensions. For one-loop amplitudes containing only external gluons, these tree amplitudes can be interpreted as four dimensional amplitudes but with massive scalars. Recent work has used on-shell recursive techniques [132, 133] to extend the number of known massive scalar amplitudes [136]. At present, the  $D$ -dimensional unitarity approach has been applied to all  $n$  gluon amplitudes with  $n = 4$  and to special helicity configurations with  $n$  up to 6 [138, 140]. This method of calculating the full one-loop non-supersymmetric amplitude although adequate in principle is somewhat involved and tedious.

An alternative approach for obtaining the rational parts of the amplitudes is based on constructing one-loop on-shell recursion relations [141–143]. This method uses the proof of tree level on-shell recursion relations given in [133] as a starting point. There are, however, a number of issues and subtleties that arise, which are not present at the tree level. Among them is the fact that the tree level proof relies on the amplitudes having only simple poles and no branch cuts; loop amplitudes in general contain branch cuts and spurious poles which would interfere with a naive recursion on the rational terms. The way of how to overcome these difficulties is shown in [143].

It would be particularly interesting to see if these ideas and techniques which

have appeared to be so fruitful for the tree level and one-loop amplitudes can also be applied to higher loop amplitudes of supersymmetric and/or non-supersymmetric theories. One attempt towards this direction is the conjecture for the all-orders MHV amplitudes in  $\mathcal{N}=4$  SYM proposed in [144]. The authors of [144] based on the calculation of the four-point MHV amplitude at three loops and the exponentiation of infrared singularities, gave an exponentiated ansatz for the maximally helicity-violating n-point amplitudes to all loop orders. The  $1/\epsilon^2$  pole in the four-point amplitude determines the soft, or cusp, anomalous dimension at three loops in  $\mathcal{N}=4$  supersymmetric Yang-Mills theory. The value for this soft anomalous dimension is exactly the same as the one obtained by Staudacher [145] by using the spin chain approach and assuming integrability of  $\mathcal{N}=4$  SYM. The agreement of these two completely different calculations strongly suggest that  $\mathcal{N}=4$  SYM is, indeed, an integrable system. We feel that these assumptions deserve further investigation especially in connection with the AdS/CFT correspondence.

# Appendix A

## Expressions for Neumann matrices

Here we outline the pp-wave string field theory conventions used in the text. The combination  $\alpha'p^+$  for the  $r$ -th string is denoted  $\alpha_r$  and  $\sum_{r=1}^3 \alpha_r = 0$ . As is standard in the literature, we will choose a frame in which  $\alpha_3 = -1$

$$\alpha_r = \alpha'p_{(r)}^+ : \quad \alpha_3 = -1, \quad \alpha_1 = y, \quad \alpha_2 = 1 - y. \quad (\text{A.1})$$

In terms of the  $U(1)$  R-charges of the BMN operators in the three-point function,  $\langle \mathcal{O}_1^{J_1} \mathcal{O}_2^{J_2} \bar{\mathcal{O}}_3^J \rangle$ , where  $J = J_1 + J_2$ , we have

$$y = \frac{J_1}{J}, \quad 1 - y = \frac{J_2}{J}, \quad 0 < y < 1. \quad (\text{A.2})$$

The effective SYM coupling constant  $\lambda'$  in the frame (A.1) takes a simple form

$$\lambda' = \frac{1}{(\mu p^+ \alpha')^2} \equiv \frac{1}{(\mu \alpha_3)^2} = \frac{1}{\mu^2}. \quad (\text{A.3})$$

Here  $\mu$  is the mass parameter which appears in the pp-wave metric, in the chosen frame it is dimensionless<sup>1</sup> and the expansion in powers of  $1/\mu^2$  is equivalent to the perturbative expansion in  $\lambda'$ . Finally the frequencies are defined via,

$$\omega_{rm} = \sqrt{m^2 + (\mu \alpha_r)^2}. \quad (\text{A.4})$$

The infinite-dimensional Neumann matrices,  $N_{mn}^{rs}$  are usually specified in the original  $a$ -oscillator basis of the string field theory. In this basis the bosonic overlap factor

---

<sup>1</sup>It is  $p^+ \mu$  which is invariant under longitudinal boosts and is frame-independent.

$|V_B\rangle$  of the 3-strings vertex is given by

$$|V_B\rangle = \exp\left(\frac{1}{2} \sum_{r,s=1}^3 \sum_{m,n=-\infty}^{\infty} a_m^{rI^\dagger} N_{mn}^{rs} a_n^{sI^\dagger}\right) |0\rangle. \quad (\text{A.5})$$

However, for the purposes of the pp-wave/SYM correspondence it is more convenient to use another, the so-called BMN or  $\alpha$ -basis of string oscillators, which is in direct correspondence with the BMN operators in gauge theory. The two bases are related as follows:

$$\alpha_n = \frac{1}{\sqrt{2}}(a_{|n|} - i \text{sign}(n)a_{-|n|}), \quad \alpha_0 = a_0, \quad (\text{A.6})$$

and satisfy the same oscillator algebra

$$[\alpha_m, \alpha_n^\dagger] = \delta_{mn}. \quad (\text{A.7})$$

In this basis, the bosonic overlap factor (A.5) in the vertex reads

$$|V_B\rangle = \exp\left(\frac{1}{2} \sum_{r,s=1}^3 \sum_{m,n=-\infty}^{\infty} \alpha_m^{rI^\dagger} \hat{N}_{mn}^{rs} \alpha_n^{sI^\dagger}\right), \quad (\text{A.8})$$

where  $\hat{N}$  are the Neumann matrices in the  $\alpha$ -basis and are related to the  $N$ 's via (here  $m, n > 0$ ):

$$\hat{N}_{mn}^{rs} = \hat{N}_{-m-n}^{rs} := \frac{1}{2}(N_{mn}^{rs} - N_{-m-n}^{rs}), \quad (\text{A.9})$$

$$\hat{N}_{m-n}^{rs} = \hat{N}_{-mn}^{rs} := \frac{1}{2}(N_{mn}^{rs} + N_{-m-n}^{rs}), \quad (\text{A.10})$$

$$\hat{N}_{m0}^{rs} = \hat{N}_{-m0}^{rs} := \frac{1}{\sqrt{2}}N_{m0}^{rs} = \hat{N}_{0m}^{rs} = \hat{N}_{0-m}^{rs}, \quad (\text{A.11})$$

$$\hat{N}_{00}^{rs} := N_{00}^{rs}. \quad (\text{A.12})$$

We now copy the explicit expressions for the Neumann matrices [98] in the  $\alpha$ -basis from the Appendix of [101]. These expressions are needed for our calculations

in Section 5.

$$N_{mn}^{31} = \frac{2(-1)^{m+n+1}}{\pi} \frac{m \sin(\pi my)}{\sqrt{y}(m^2 - n^2/y^2)} + \mathcal{O}\left(\frac{1}{\mu^2}\right), \quad (\text{A.13})$$

$$N_{mn}^{32} = \frac{2(-1)^m}{\pi} \frac{m \sin(\pi my)}{\sqrt{1-y}(m^2 - n^2/(1-y)^2)} + \mathcal{O}\left(\frac{1}{\mu^2}\right), \quad (\text{A.14})$$

$$N_{mn}^{21} = \frac{1}{\mu} \frac{(-1)^{n+1}}{2\pi} \frac{1}{\sqrt{y(1-y)}} + \mathcal{O}\left(\frac{1}{\mu^3}\right), \quad (\text{A.15})$$

$$N_{mn}^{33} = \mathcal{O}\left(\frac{1}{\mu^3}\right), \quad (\text{A.16})$$

$$N_{mn}^{11} = \frac{1}{\mu} \frac{(-1)^{m+n}}{2\pi} \frac{1}{y} + \mathcal{O}\left(\frac{1}{\mu^3}\right), \quad (\text{A.17})$$

$$N_{mn}^{22} = \frac{1}{\mu} \frac{1}{2\pi} \frac{1}{1-y} + \mathcal{O}\left(\frac{1}{\mu^3}\right). \quad (\text{A.18})$$

$$N_{-m-n}^{31} = \frac{2(-1)^{m+n}}{\pi} \frac{n \sin(\pi my)}{y^{3/2}(m^2 - n^2/y^2)} + \mathcal{O}\left(\frac{1}{\mu^2}\right), \quad (\text{A.19})$$

$$N_{-m-n}^{32} = \frac{2(-1)^{m+1}}{\pi} \frac{n \sin(\pi my)}{(1-y)^{3/2}(m^2 - n^2/(1-y)^2)} + \mathcal{O}\left(\frac{1}{\mu^2}\right), \quad (\text{A.20})$$

$$N_{-m-n}^{21} = \mathcal{O}\left(\frac{1}{\mu^3}\right), \quad (\text{A.21})$$

$$N_{-m-n}^{33} = \frac{1}{\mu} \frac{2(-1)^{m+n}}{\pi} \sin(\pi my) \sin(\pi ny) + \mathcal{O}\left(\frac{1}{\mu^3}\right), \quad (\text{A.22})$$

$$N_{-m-n}^{11} = \mathcal{O}\left(\frac{1}{\mu^3}\right), \quad (\text{A.23})$$

$$N_{-m-n}^{22} = \mathcal{O}\left(\frac{1}{\mu^3}\right). \quad (\text{A.24})$$

$$N_{00}^{33} = 0, \quad N_{00}^{31} = -\sqrt{y}, \quad N_{00}^{32} = -\sqrt{1-y}, \quad (\text{A.25})$$

$$N_{00}^{12} = \frac{1}{\mu} \frac{(-1)}{4\pi} \frac{1}{\sqrt{y(1-y)}} = N_{00}^{21}, \quad (\text{A.26})$$

$$N_{00}^{11} = \frac{1}{\mu} \frac{1}{4\pi} \frac{1}{y}, \quad (\text{A.27})$$

$$N_{00}^{22} = \frac{1}{\mu} \frac{1}{4\pi} \frac{1}{1-y}. \quad (\text{A.28})$$

For the zero-positive Neumann matrices below we have

$$N_{0n}^{31} = 0, \quad N_{0n}^{32} = 0, \quad N_{0n}^{33} = 0. \quad (\text{A.29})$$

$$N_{0n}^{13} = \frac{\sqrt{2}(-1)^{n+1} \sin(\pi ny)}{\pi n\sqrt{y}} + \mathcal{O}\left(\frac{1}{\mu^2}\right), \quad (\text{A.30})$$

$$N_{0n}^{23} = \frac{\sqrt{2}(-1)^n \sin(\pi ny)}{\pi n\sqrt{1-y}} + \mathcal{O}\left(\frac{1}{\mu^2}\right), \quad (\text{A.31})$$

$$N_{0n}^{21} = \frac{1}{\mu} \frac{\sqrt{2}(-1)^{n+1}}{4\pi} \frac{1}{\sqrt{y(1-y)}} + \mathcal{O}\left(\frac{1}{\mu^3}\right), \quad (\text{A.32})$$

$$N_{0n}^{12} = -\frac{1}{\mu} \frac{\sqrt{2}}{4\pi} \frac{1}{\sqrt{y(1-y)}} + \mathcal{O}\left(\frac{1}{\mu^3}\right), \quad (\text{A.33})$$

$$N_{0n}^{11} = \frac{1}{\mu} \frac{\sqrt{2}(-1)^n}{4\pi} \frac{1}{y} + \mathcal{O}\left(\frac{1}{\mu^3}\right), \quad (\text{A.34})$$

$$N_{0n}^{22} = \frac{1}{\mu} \frac{\sqrt{2}}{4\pi} \frac{1}{1-y} + \mathcal{O}\left(\frac{1}{\mu^3}\right). \quad (\text{A.35})$$

# Appendix B

## The bosonic part of the three-string vertex

The three-string vertex  $|H_3\rangle$  can be represented as a ket-state in the tensor product of three string Fock spaces. It has the form [52, 53]

$$\frac{1}{\mu} |H_3\rangle = \mathsf{P} |V_F\rangle |V_B\rangle \delta\left(\sum_{r=1}^3 \alpha_r\right), \quad (\text{B.1})$$

where the kets  $|V_B\rangle$  and  $|V_F\rangle$  are constructed to satisfy the bosonic and fermionic kinematic symmetries, and  $\alpha_r$  are defined in (A.1). The bosonic factor  $|V_B\rangle$  is given by

$$|V_B\rangle = \exp\left(\frac{1}{2} \sum_{r,s=1}^3 \sum_{m,n=-\infty}^{\infty} \sum_{I=1}^8 \alpha_m^{rI\dagger} \hat{N}_{mn}^{rs} \alpha_n^{sI\dagger}\right) |0\rangle|0\rangle|0\rangle, \quad (\text{B.2})$$

where the  $\hat{N}_{mn}^{rs}$  are the Neumann matrices in the BMN-basis of string oscillators. The complete perturbative expansion of the Neumann matrices in the pp-wave background in the vicinity of  $\mu = \infty$ , was constructed in [98]<sup>1</sup>. The fermionic factor  $|V_F\rangle$  is not going to be relevant for the present chapter, where only external bosonic string states are considered.

The prefactor  $\mathsf{P}$  is a polynomial in the bosonic and fermionic oscillators, and is determined from imposing the remaining symmetries of the pp-wave background.

---

<sup>1</sup>We refer the reader to the Appendix of Ref. [101] for some useful properties of the perturbative Neumann matrices and relations between different string-oscillator bases.

The relevant for us bosonic part of the prefactor, as determined by Spradlin and Volovich in [53], reads

$$P = C_{\text{norm}} \sum_{r=1}^3 \sum_{-\infty}^{\infty} \frac{\omega_{rn}}{\mu \alpha_r} \alpha_n^{rI\dagger} \alpha_{-n}^{rJ} v_{IJ} , \quad (\text{B.3})$$

where  $v_{IJ} = \text{diag}(\mathbf{1}_4, -\mathbf{1}_4)$ , and the overall normalisation  $C_{\text{norm}}$  is left undetermined. Notice that it is the expression for  $v_{IJ}$  which leads to the relative minus sign between the string amplitudes involving states with excitations along the two different  $SO(4)$ 's as e.g. in (4.36) and (4.38).

# Appendix C

## Notation and conventions in gauge theory

We write the Euclidean  $\mathcal{N} = 4$  Lagrangian as

$$\mathcal{L} = \mathcal{L}_B + \mathcal{L}_F , \quad (\text{C.1})$$

where

$$\begin{aligned} \mathcal{L}_B &= \frac{2}{g^2} \text{Tr} \left( \frac{1}{4} F_{\mu\nu} F_{\mu\nu} + (D^\mu \bar{Z}^i)(D_\mu Z_i) - [Z_i, Z_j][\bar{Z}^i, \bar{Z}^j] + \frac{1}{2} [Z_i, \bar{Z}^i][Z_j, \bar{Z}^j] \right) \\ &= \frac{2}{g^2} \text{Tr} \left( \frac{1}{4} F_{\mu\nu} F_{\mu\nu} + \frac{1}{2} (D_\mu \phi_i)(D_\mu \phi_i) - \frac{1}{4} [\phi_i, \phi_j][\phi_i, \phi_j] \right) , \end{aligned} \quad (\text{C.2})$$

and

$$\begin{aligned} \mathcal{L}_F &= \frac{2}{g^2} \times \\ &\text{Tr} \left( \lambda_A \sigma^\mu D_\mu \bar{\lambda}^A - \sqrt{2}i([\lambda_4, \lambda_i]\bar{Z}^i + [\bar{\lambda}^4, \bar{\lambda}^i]Z_i) + \frac{i}{\sqrt{2}}(\epsilon^{ijk}[\lambda_i, \lambda_j]Z_k + \epsilon_{ijk}[\bar{\lambda}^i, \bar{\lambda}^j]\bar{Z}^k) \right) . \end{aligned} \quad (\text{C.3})$$

The bosonic part of the  $\mathcal{N} = 4$  Lagrangian can be re-expressed as

$$\mathcal{L} = \frac{2}{g^2} \text{Tr} \left( \frac{1}{4} F_{\mu\nu} F_{\mu\nu} + \overline{(D^\mu Z)}(D_\mu Z) + \frac{1}{2} (D^\mu \phi^i)(D_\mu \phi^i) \right) + V_F + V_D , \quad (\text{C.4})$$

where the F-term and D-term potential are

$$V_F = -\frac{2}{g^2} \text{Tr} \left( 2 Z \phi_i \bar{Z} \phi_i - \phi_i \phi_i (Z \bar{Z} + \bar{Z} Z) + \dots \right) , \quad (\text{C.5})$$

$$V_D = -\frac{2}{g^2} \text{Tr} \left( Z Z \bar{Z} \bar{Z} - Z \bar{Z} Z \bar{Z} + \dots \right) , \quad (\text{C.6})$$

are the F-term and D-term of the scalar potential respectively. In the last equalities the dots stand for impurity flavour changing terms, which mutually cancel between the F- and the D-term. In the above equations  $A = 1, \dots, 4$  and  $i, j, k = 1, \dots, 3$ .  $Z_i$  are the the three complex scalars defined by

$$Z_1 = \frac{\phi_1 + i\phi_2}{\sqrt{2}}, \quad Z_2 = \frac{\phi_3 + i\phi_4}{\sqrt{2}}, \quad Z_3 = \frac{\phi_5 + i\phi_6}{\sqrt{2}}, \quad (\text{C.7})$$

where  $\phi_i$ ,  $i = 1, \dots, 6$  are the real scalar fields transforming under the  $SO(6)$  R-symmetry group. We will also set  $Z_3 := Z$ .

We define the covariant derivative is  $D_\mu \phi_i = \partial_\mu \phi_i - i[A_\mu, \phi_i]$ , where  $A_\mu = A_\mu^a T^a$ , and  $F_{\mu\nu} = \partial_\mu A_\nu - \partial_\nu A_\mu - i[A_\mu, A_\nu]$ .

Our  $SU(N)$  generators are normalised as

$$\text{Tr}(T^a T^b) = \delta^{ab}, \quad (\text{C.8})$$

so that, for example,

$$\langle Z_j^i(x) \bar{Z}_m^l(0) \rangle = \frac{g^2}{2} \delta_m^i \delta_j^l \Delta(x), \quad \Delta(x) = \frac{1}{4\pi^2 x^2}. \quad (\text{C.9})$$

Our Euclidean sigma matrices satisfy

$$\sigma_\mu \bar{\sigma}_\nu + \sigma_\nu \bar{\sigma}_\mu = 2\delta_{\mu\nu}, \quad \bar{\sigma}_\mu \sigma_\nu + \bar{\sigma}_\nu \sigma_\mu = 2\delta_{\mu\nu}. \quad (\text{C.10})$$

The completeness relation reads:

$$\sigma_{\alpha\beta}^\mu \bar{\sigma}_\mu^{\dot{\gamma}\delta} = 2\delta_\alpha^\delta \delta_\beta^{\dot{\gamma}}. \quad (\text{C.11})$$

Another useful identity is:

$$\sigma_\nu \bar{\sigma}_\rho \sigma_\mu = \delta_{\nu\rho} \sigma_\mu + \delta_{\mu\rho} \sigma_\nu - \delta_{\mu\nu} \sigma_\rho + \epsilon_{\nu\rho\mu\tau} \sigma_\tau \quad (\text{C.12})$$

We also define  $\sigma_{\mu\nu}$  and  $\bar{\sigma}_{\mu\nu}$  by:

$$\sigma_{\mu\nu} = \frac{1}{2}(\sigma_\mu \bar{\sigma}_\nu - \sigma_\nu \bar{\sigma}_\mu) = i\eta_{\mu\nu}^a \sigma^a, \quad (\text{C.13})$$

$$\bar{\sigma}_{\mu\nu} = \frac{1}{2}(\bar{\sigma}_\mu \sigma_\nu - \bar{\sigma}_\nu \sigma_\mu) = i\bar{\eta}_{\mu\nu}^a \sigma^a, \quad (\text{C.14})$$

where  $\eta_{\mu\nu}^a$  ( $\bar{\eta}_{\mu\nu}^a$ ) are the (anti-)self-dual 't Hooft symbols [97].

Finally, we will use the definitions  $J := J_1 + J_2$  and  $J_1 = y \cdot J$ , where  $y \in (0, 1)$ .

# Appendix D

## The three-string vertex

In this appendix we summarise the form of the three-string vertex when built on the real vacuum  $|v\rangle$  of the theory, whose construction we sketched in chapter 1.

This is [55]

$$\frac{1}{\mu} |H_3\rangle = \mathbf{P} |V_F\rangle |V_B\rangle \delta\left(\sum_{r=1}^3 \alpha_r\right), \quad (\text{D.1})$$

where the kets  $|V_B\rangle$  and  $|V_F\rangle$  are constructed by requiring they satisfy the bosonic and fermionic kinematical symmetries, and  $\alpha_r$  are defined in (A.1).  $|V_B\rangle$  is given by

$$|V_B\rangle = \exp\left(\frac{1}{2} \sum_{r,s=1}^3 \sum_{m,n=-\infty}^{\infty} \sum_{I=1}^8 a_m^{(r)I\dagger} \overline{N}_{mn}^{(rs)} a_n^{(s)I\dagger}\right) |v\rangle_1 |v\rangle_2 |v\rangle_3, \quad (\text{D.2})$$

where the  $\overline{N}_{mn}^{(rs)}$  are the Neumann matrices in the number operator basis. The fermionic ket state  $|V_F\rangle$ , which is relevant for this chapter, is given in the  $SO(4) \times SO(4)$  formalism by [65, 99]

$$|V_F\rangle = \exp\left(\sum_{r,s=1}^3 \sum_{m,n \geq 0} (b_{-m(r)}^{\alpha\beta\dagger} b_{n(s)}^{\dagger\alpha\beta} + b_{m(r)}^{\dot{\alpha}\dot{\beta}\dagger} b_{-n(s)}^{\dagger\dot{\alpha}\dot{\beta}}) \overline{Q}_{mn}^{(rs)}\right) |v\rangle_1 |v\rangle_2 |v\rangle_3, \quad (\text{D.3})$$

where  $\overline{Q}_{mn}^{(rs)}$  are the fermionic Neumann matrices. The complete perturbative expansion of the Neumann matrices in the pp-wave background in the vicinity of  $\mu = \infty$ , was constructed in [98]<sup>1</sup>. The vacuum state  $|v\rangle \equiv |v\rangle_1 |v\rangle_2 |v\rangle_3$  is defined as the state which is annihilated by all  $a$ 's and  $b$ 's,

$$a_{n(r)} |v\rangle_r = 0, \quad b_{n(r)} |v\rangle_r = 0, \quad \forall n. \quad (\text{D.4})$$

<sup>1</sup>See also [100], and Appendix of [101] for some useful properties of the Neumann matrices.

The prefactor  $P$  is determined by imposing the dynamical symmetries of the pp-wave superalgebra, and was derived in [65]. Its expressions reads:

$$\begin{aligned}
 P = & \left[ \left( \mathcal{K}^i \tilde{\mathcal{K}}^j + \frac{\mu\beta(\beta+1)}{2} \alpha_3^3 \delta^{ij} \right) V_{ij} - \left( \mathcal{K}^a \tilde{\mathcal{K}}^b + \frac{\mu\beta(\beta+1)}{2} \alpha_3^3 \delta^{ab} \right) V_{ab} \right. \\
 & \left. - \mathcal{K}_1^{\dot{\alpha}\alpha} \tilde{\mathcal{K}}_2^{\dot{\beta}\beta} S_{\alpha\beta}^+(Y) S_{\dot{\alpha}\dot{\beta}}^-(Z) - \tilde{\mathcal{K}}_1^{\dot{\alpha}\alpha} \mathcal{K}_2^{\dot{\beta}\beta} S_{\alpha\beta}^-(Y) S_{\dot{\alpha}\dot{\beta}}^+(Z) \right] C_{\text{norm}} , \quad (\text{D.5})
 \end{aligned}$$

where  $i = 1 \dots 4$  and  $a = 1 \dots 4$  label the first and second group of four bosonic directions of the pp-wave geometry, respectively. Full details about the expressions appearing in (D.5) can be found in the original paper [65] or, for instance, in the review [77]. We will only need the following expressions:

$$\begin{aligned}
 V_{ij} = & \delta_{ij} \left[ 1 + \frac{1}{12} (Y^4 + Z^4) + \frac{1}{144} Y^4 Z^4 \right] - \frac{i}{2} \left[ Y_{ij}^2 \left( 1 + \frac{1}{12} Z^4 \right) - Z_{ij}^2 \left( 1 + \frac{1}{12} Y^4 \right) \right] \\
 & + \frac{1}{4} (Y^2 Z^2)_{ij} , \quad (\text{D.6})
 \end{aligned}$$

$$\begin{aligned}
 V_{ab} = & \delta_{ab} \left[ 1 - \frac{1}{12} (Y^4 + Z^4) + \frac{1}{144} Y^4 Z^4 \right] - \frac{i}{2} \left[ Y_{ab}^2 \left( 1 - \frac{1}{12} Z^4 \right) - Z_{ab}^2 \left( 1 - \frac{1}{12} Y^4 \right) \right] \\
 & + \frac{1}{4} (Y^2 Z^2)_{ab} , \quad (\text{D.7})
 \end{aligned}$$

where

$$Y^{\alpha\beta} = \sum_{r=1}^3 \sum_{n \geq 0} \bar{G}_{n(r)} b_{n(r)}^{\dagger\alpha\beta} , \quad Z^{\dot{\alpha}\dot{\beta}} = \sum_{r=1}^3 \sum_{n \geq 0} \bar{G}_{n(r)} b_{-n(r)}^{\dagger\dot{\alpha}\dot{\beta}} , \quad (\text{D.8})$$

$$Y_{\alpha\beta}^2 := Y_{\alpha\gamma} Y_{\beta}^{\gamma} , \quad Y^4 := Y_{\alpha\beta}^2 (Y^2)^{\alpha\beta} . \quad (\text{D.9})$$

Similar expressions hold for the  $Z$ 's. The matrices  $\bar{G}_{n(r)}$  are given in (3.12) of [65]. Finally, the overall normalisation  $C_{\text{norm}}$  cannot be fixed by imposing the dynamical constraints, and is determined (once and for all) by requiring agreement with a single field theory calculation. Its value will be taken to be:

$$C_{\text{norm}} = -\frac{g_2}{2} \frac{1}{\sqrt{J}} \frac{1}{\sqrt{y(1-y)}} . \quad (\text{D.10})$$

# Appendix E

## Summing over the BMN phase factors

We report here the expressions for the coefficients  $P_I$  and  $P_{II}$  which arise after summing over the BMN phase factors in the interacting diagrams derived in section 4.4.1.

Defining

$$q = e^{2\pi im/J} , \quad q_1 = e^{2\pi in/J_1} , \quad (\text{E.1})$$

the expressions for  $P_I$  and  $P_{II}$  are given by

$$P_I = \sum_{l=0}^{J_1} (\bar{q}q_1)^l \bar{q} , \quad P_{II} = \sum_{l=0}^{J_1} (\bar{q}q_1)^l . \quad (\text{E.2})$$

We also need to evaluate the quantity  $2(P_I + \bar{P}_I) - 2(P_{II} + \bar{P}_{II})$ , which in the BMN limit is

$$2(P_I + \bar{P}_I) - 2(P_{II} + \bar{P}_{II}) = -\frac{8m}{m - n/y} \sin^2 \pi m y . \quad (\text{E.3})$$

# Appendix F

## The functions $X$ , $Y$ and $H$

The expressions for three-point functions of BMN operators with scalar, vector, mixed or fermion impurities involve the integral

$$X_{1234} = \int d^4 z \Delta(x_1 - z) \Delta(x_2 - z) \Delta(x_3 - z) \Delta(x_4 - z) . \quad (\text{F.1})$$

$X_{1234}$  develops a  $\log x_{12}^2$  term  $X$  as  $x_1$  approaches  $x_2$ , which repeatedly appears in section 4.4.1. The expression for  $X$  is [62]

$$X := X_{1234}|_{x_3=x_4} = \frac{\log(x_{12}\Lambda)^{-1}}{8\pi^2(4\pi^2 x_{31}^2)^2} . \quad (\text{F.2})$$

Another important function ubiquitously appearing in the calculations is

$$Y_{123} = \int d^4 z \Delta(x_1 - z) \Delta(x_2 - z) \Delta(x_3 - z) . \quad (\text{F.3})$$

It is easy to realise that, as  $x_{12} \rightarrow 0$ , the function  $Y_{123}$  contains a logarithmic term given by

$$Y_{123}|_{x_{12} \rightarrow 0} = -\frac{1}{2^4 \pi^2} \Delta(x_{13}) \log x_{12}^2 . \quad (\text{F.4})$$

One also needs the following expression for the  $\log x_{12}^2$  term in the first derivative of  $Y$ :

$$(\partial_{1\alpha} Y_{123})_{x_{12} \rightarrow 0} = \frac{1}{2^5 \pi^2} \log x_{12}^2 \partial_{3\alpha} \Delta(x_{13}) . \quad (\text{F.5})$$

Notice that (F.5) should be derived directly from (F.3) rather than by differentiating (F.4).

In the calculation, we also encounter the function  $H$  defined by

$$H_{14,23} = (\partial_\mu^{x_1} - \partial_\mu^{x_4})(\partial_\mu^{x_2} - \partial_\mu^{x_3}) \int d^4 z d^4 t \Delta(x_1 - z) \Delta(x_4 - z) \Delta(x_2 - t) \Delta(x_3 - t) \Delta(z - t) , \quad (\text{F.6})$$

which can be evaluated with the useful relation proved in [73]

$$\frac{H_{14,23}}{\Delta_{14}\Delta_{23}} = X_{1234} \left( \frac{1}{\Delta_{12}\Delta_{43}} - \frac{1}{\Delta_{13}\Delta_{24}} \right) + G_{1,23} - G_{4,23} + G_{2,14} - G_{3,14} \quad , \quad (\text{F.7})$$

where  $\Delta_{ij} = \Delta(x_i - x_j)$  and

$$G_{i,jk} = Y_{ijk} \left( \frac{1}{\Delta_{ik}} - \frac{1}{\Delta_{ij}} \right) \quad . \quad (\text{F.8})$$

We can recast (F.7) as

$$\begin{aligned} H_{14,23} &= -X_{1234} \frac{\Delta_{14}\Delta_{23}}{\Delta_{13}\Delta_{24}} + \left( \frac{Y_{123}}{\Delta_{13}} + \frac{Y_{124}}{\Delta_{24}} \right) \Delta_{14}\Delta_{23} + \dots \\ &= H_I + H_{II} + \dots \quad , \end{aligned} \quad (\text{F.9})$$

where the dots stand for terms which either vanish or do not contain the  $\log x_{12}^2$ .

# Appendix G

## More detailed calculations for the evaluation of the Feynman diagrams

The three-point functions with fermion BMN operators discussed in chapter 4 are expressed in terms of  $J_A$ ,  $J_B$  and  $J_C$  defined in (4.59)-(4.61). Here we sketch the calculation of the  $\log(x_{12}^2)$  parts of these quantities. Let us start by calculating the following integral:

$$\begin{aligned}
 A &= \partial_k^1 \partial_k^4 H_{1432} = \int d^4 z d^4 t \partial_k^z \Delta_{1z} \partial_k^z \Delta_{4z} \Delta_{zt} \Delta_{2t} \Delta_{3t} = \\
 &\quad - \int d^4 z d^4 t \Delta_{1z} \square_z \Delta_{4z} \Delta_{zt} \Delta_{2t} \Delta_{3t} - \int d^4 z d^4 t \Delta_{1z} \partial_k^z \Delta_{4z} \partial_k^z \Delta_{zt} \Delta_{2t} \Delta_{3t} .
 \end{aligned} \tag{G.1}$$

The box acting on the propagator gives a delta function which eliminates the  $z$  integration, giving a result proportional to  $Y_{234}$ .  $Y_{234}$ , however, does not contain any  $\log x_{12}^2$  term so for our purposes this term can safely be ignored. Therefore we are left with:

$$\begin{aligned}
 A &= \int d^4 z d^4 t \partial_k^z \Delta_{1z} \Delta_{4z} \partial_k^z \Delta_{zt} \Delta_{2t} \Delta_{3t} + \int d^4 z d^4 t \Delta_{1z} \Delta_{4z} \square_z \Delta_{zt} \Delta_{2t} \Delta_{3t} \\
 &= - \int d^4 z d^4 t \square_z \Delta_{1z} \Delta_{4z} \Delta_{zt} \Delta_{2t} \Delta_{3t} - \int d^4 z d^4 t \partial_k^z \Delta_{1z} \partial_k^z \Delta_{4z} \Delta_{zt} \Delta_{2t} \Delta_{3t} - X_{1234} \\
 &= \Delta_{14} Y_{123} - A - X_{1234} .
 \end{aligned} \tag{G.2}$$

From the last expression one can obtain  $A$ :

$$A = \frac{1}{2} (-X_{1234} + \Delta_{14} Y_{123}) . \tag{G.3}$$

In the above derivation, we have integrated by parts with respect to  $z$  several times, and we used  $\square_x \Delta(x) = -\delta(x)$ . Since the  $\log x_{12}$  terms of  $X_{1234}$  and  $Y_{123}$  are well known (see Appendix F), the same is also true for  $A$ .

Upon using the useful identity  $(\partial_\mu^1 + \partial_\mu^2 + \partial_\mu^3 + \partial_\mu^4)H_{1423} = 0$ , and the expression for  $A$  derived above, one can evaluate  $(\partial^3 \cdot \partial^4 + \partial^2 \cdot \partial^4)H_{1423}$ :

$$(\partial^2 + \partial^3) \cdot \partial^4 H_{1423} = -(\partial^1 + \partial^4) \cdot \partial^4 H_{1423} = -A - \square_4 H_{1423} \rightarrow = -A, \quad (\text{G.4})$$

since again  $\square_4$  acting on  $H_{1423}$  does not give rise to a  $\log x_{12}^2$  term. One can also evaluate the difference  $(\partial^3 \cdot \partial^4 - \partial^2 \cdot \partial^4)H_{1423}$  using

$$\partial^i \cdot \partial^j H_{1423} = \frac{1}{2}(\square_k + \square_l - \square_i - \square_j)H_{1423} + \partial^k \cdot \partial^l H_{1423}, \quad (\text{G.5})$$

where (G.5) holds for  $i \neq j \neq k \neq l$ .

Starting from

$$H_{14,23} = (\partial^1 - \partial^4) \cdot (\partial^2 - \partial^3)H_{1423}, \quad (\text{G.6})$$

substituting for  $\partial^1 \cdot \partial^2$  and  $\partial^1 \cdot \partial^3$  the corresponding expressions from (G.5), and solving for  $(\partial^3 \cdot \partial^4 - \partial^2 \cdot \partial^4)H_{1423}$ , we obtain:

$$(\partial^3 \cdot \partial^4 - \partial^2 \cdot \partial^4)H_{1423} = \frac{1}{2} \left[ H_{14,23} + (\square_2 - \square_3)H_{1423} \right]. \quad (\text{G.7})$$

Now, since the divergences of the right hand side of (G.7) are known [2], the divergence of  $(\partial^3 \cdot \partial^4 - \partial^2 \cdot \partial^4)H_{1423}$  is also known. In conclusion, we have computed the  $\log x_{12}^2$  parts of (G.7) and (G.4). That means we can evaluate the  $\log x_{12}^2$  parts of  $\partial^3 \cdot \partial^4 H_{1423}$  and  $\partial^2 \cdot \partial^4 H_{1423}$  separately.

We are now in position to write down the expressions for the  $J$ 's as functions of  $X_{1234}$ ,  $Y_{123}$  and  $Y_{124}$ . These are the following:

$$J_A = -\frac{1}{2}(X_{1234} + \Delta_{41}Y_{123}) + \dots, \quad (\text{G.8})$$

$$J_B = -\frac{1}{2}(-X_{1234} + \Delta_{23}Y_{124}) + \dots, \quad (\text{G.9})$$

$$J_C = \frac{1}{4}(-\Delta_{41}Y_{123} - X_{1234} + \Delta_{23}Y_{124} + H_{14,23}) + \dots, \quad (\text{G.10})$$

where the dots stand for terms which do not contain the  $\log x_{12}^2$ .  $H_{14,23}$  is given in (F.7). In the evaluation of the diagrams involving the compensating term, we also

made use of the following relations:

$$\partial_\nu^4 \partial_\mu^3 X_{1234} \Big|_{x_3 = x_4, x_{12} \rightarrow 0} = -\frac{1}{(4\pi^2)^3} \frac{x_{3\mu} x_{3\nu}}{(x_3^2)^4} \log x_{12}^2, \quad (\text{G.11})$$

$$\begin{aligned} \partial_\nu^4 \partial_\mu^4 X_{1234} \Big|_{x_3 = x_4, x_{12} \rightarrow 0} &= \Delta_{23} \partial_\nu^4 \partial_\mu^4 Y_{124} \Big|_{x_3 = x_4, x_{12} \rightarrow 0} \quad (\text{G.12}) \\ &= \frac{\log x_{12}^2}{2(4\pi^2)^3 (x_3^2)^3} \left( \delta_{\mu\nu} - 4 \frac{x_{3\mu} x_{3\nu}}{x_3^2} \right), \end{aligned}$$

$$\partial_\nu^1 Y_{123} \Big|_{x_3 = x_4, x_{12} \rightarrow 0} = \frac{-x_{3\nu}}{2^6 \pi^4 (x_3^2)^2} \log x_{12}^2, \quad (\text{G.13})$$

$$\partial_\nu^3 Y_{123} \Big|_{x_3 = x_4, x_{12} \rightarrow 0} = \frac{x_{3\nu}}{2^5 \pi^4 (x_3^2)^2} \log x_{12}^2. \quad (\text{G.14})$$

# Appendix H

## Note on Spinor Conventions

Spinor products are defined as

$$\langle i j \rangle \equiv \langle i^- | j^+ \rangle = \lambda_i^a \lambda_{j a} , \quad [i j] \equiv \langle i^+ | j^- \rangle = \tilde{\lambda}_i^{\dot{a}} \tilde{\lambda}_{j \dot{a}} . \quad (\text{H.1})$$

Here spinor indices are raised and lowered with  $\epsilon$ -symbols, and we follow the sign conventions of [106, 107]. It should be noted, that slightly different sign conventions from (H.1) have been used in earlier literature for  $[i j]$ . For example, in [126] the dotted spinor product,  $[i j]$ , is defined as  $\tilde{\lambda}_i^{\dot{a}} \tilde{\lambda}_{j \dot{a}} = -\tilde{\lambda}_i^{\dot{a}} \tilde{\lambda}_{j \dot{a}}$ . In conventions of [126], equation (5.10) would have a minus sign on the right hand side.

An on-shell momentum of a massless particle,  $p_k^\mu$  can be written as

$$p_{k a \dot{a}} = p_{k\mu} \sigma^\mu = \lambda_{k a} \tilde{\lambda}_{k \dot{a}} . \quad (\text{H.2})$$

In section 3 we use a Lorentz-invariant combination  $\langle i^- | \not{p}_k | j^- \rangle = i^a p_{k a \dot{a}} j^{\dot{a}}$ , which in terms of the spinor products (H.1) is

$$\langle i^- | \not{p}_k | j^- \rangle = \langle i^- |^a \langle k^+ \rangle_a \langle k^+ |_{\dot{a}} | j^- \rangle^{\dot{a}} = -\langle i k \rangle [k j] = \langle i k \rangle [j k] . \quad (\text{H.3})$$

The spinors  $\lambda$  and  $\tilde{\lambda}$  appearing in the helicity formalism are precisely the wavefunctions of fermions of positive and negative helicities,

$$\begin{aligned} \langle i^- |^a &= \lambda_i^a = \bar{u}_-(k_i)^a , & |i^+ \rangle_a &= \lambda_{i a} = u_+(k_i)_a , \\ \langle i^+ |^{\dot{a}} &= \tilde{\lambda}_i^{\dot{a}} = \bar{u}_+(k_i)^{\dot{a}} , & |i^- \rangle_{\dot{a}} &= \tilde{\lambda}_{i \dot{a}} = u_-(k_i)_{\dot{a}} . \end{aligned} \quad (\text{H.4})$$

In our conventions for MHV vertices we treat all fermions and antifermions as incoming and the fermion propagator connects two incoming fermions with opposite

helicities. Thus, the completeness relation relevant for us and with a correct index structure gives

$$\frac{|i^+\rangle_a |i^-\rangle_{\dot{a}}}{k_i^2} = \frac{\lambda_{i a} \tilde{\lambda}_{i \dot{a}}}{k_i^2} = \frac{k_{i a\dot{a}}}{k_i^2}, \quad (\text{H.5})$$

which is, of course, the correct fermion propagator in usual Feynman perturbation theory.

Scalars have no wave-functions, and their propagator remains  $1/k^2$ , and vectors give (in Feynman gauge)

$$\frac{\varepsilon_+^\mu \varepsilon_-^\nu}{k^2} = \frac{-g^{\mu\nu}}{k^2}, \quad (\text{H.6})$$

which is the correct form of the massless vector boson propagator.

An important consequence of (H.5) is the ordering prescription of fermions in MHV vertices. This concerns only the case of scalar diagrams with internal fermion lines, such as the third diagram in Figure 27. In this case, in order to get the ket<sup>+</sup> ket<sup>-</sup> structure  $|i^+\rangle_a |i^-\rangle_{\dot{a}}$  the two fermions which are to be connected by a propagator should be both on the right of each vertex (rather than adjacent to each other). This means that, for example, the third diagram in Figure 27 comes from

$$A(\Lambda_1^-, g_2^-, \underline{\Lambda_{(3i)}^+}) A(g_3^-, \Lambda_k^+, \underline{\Lambda_{-(3i)}^-}). \quad (\text{H.7})$$

If the contracted fermion factors,  $\underline{\Lambda_{(3i)}^+}$  and  $\underline{\Lambda_{-(3i)}^-}$  were, instead, chosen to be next to each other, the overall contribution would change sign, since fermions anticommute with each other.

# Bibliography

- [1] G. Georgiou and V. V. Khoze, “*BMN operators with three scalar impurities and the vertex-correlator duality in pp-wave*,” JHEP **0304** (2003) 015, hep-th/0302064.
- [2] G. Georgiou, V. V. Khoze and G. Travaglini, “*New tests of the pp-wave correspondence*,” JHEP **0310** (2003) 049, hep-th/0306234.
- [3] G. Georgiou, and G. Travaglini, “*Fermion BMN operators, the dilatation operator of  $N=4$  SYM, and pp-wave string interactions*,” JHEP **0404** (2004) 001, hep-th/0403188.
- [4] G. Georgiou and V. V. Khoze, “*Tree amplitudes in gauge theory as scalar MHV diagrams*,” JHEP **0405** (2004) 070, hep-th/0404072.
- [5] G. Georgiou, E. W. N. Glover, and V. V. Khoze, “*Non-MHV Tree Amplitudes in Gauge Theory*,” JHEP **0407**, 048 (2004), hep-th/0407027.
- [6] G. 't Hooft, “*A planar digram theory for strong interactions*,” Nucl. Phys. B **72** (1974) 461.
- [7] “*The large  $N$  limit of superconformal field theories and supergravity*,” Adv. Theor. Math. Phys. **2** (1998) 231, hep-th/9711200.
- [8] A. V. Manohar, “*Large  $N$  QCD*,” hep-ph/9802419.
- [9] D. J. Gross, “*Two-dimensional QCD as a string theory*,” Nucl. Phys. B **400** (1993) 161, hep-th/9212149.

- [10] D. J. Gross and W. Taylor, “*Two-dimensional QCD is a string theory*,” Nucl. Phys. B **400** (1993) 181, hep-th/9301068.
- [11] E. D’Hoker, D. Z. Freedman “*Supersymmetric Gauge Theories and the AdS/CFT Correspondence*,” hep-th/0201253.
- [12] M. B. Green, J. H. Schwarz and E. Witten “*Introduction*,” Cambridge Univ. Pr. (1987).
- [13] M. B. Green, J. H. Schwarz and E. Witten “*Superstring theory: 2 Loop amplitudes, anomalies and phenomenology*,” Cambridge Univ. Pr. (1987).
- [14] O. Aharony, S. S. Gubser, J. Maldacena, H. Ooguri, Y. Oz “*Large N Field Theories, String Theory and Gravity*,” Phys. Rept. **323** (2000) 183, hep-th/9905111.
- [15] J. Polchinski “*Dirichlet Branes and Ramond-Ramond charges*,” Phys. Rev. Lett. **75** (1995) 4724, hep-th/9510017.
- [16] M. Cvetič, H. Lu, C. N. Pope, H. Ooguri, and T. A. Tran “*Exact absorption probability in the extremal six-dimensional dyonic string background*,” hep-th/9901002.
- [17] E. D’Hoker, D. Z. Freedman and W. Skiba, “*Field theory tests for correlators in the AdS/CFT correspondence*,” Phys. Rev. D **59**, 045008 (1999), hep-th/9807098.
- [18] W. Skiba, “*Correlators of short multi-trace operators in  $N = 4$  supersymmetric Yang-Mills*,” Phys. Rev. D **60**, 105038 (1999), tt hep-th/9907088; F. Gonzalez-Rey, B. Kulik and I. Y. Park, “*Non-renormalization of two point and three point correlators of  $N = 4$  SYM in  $N = 1$  superspace*,” Phys. Lett. B **455**, 164 (1999), hep-th/9903094.
- [19] S. Penati, A. Santambrogio and D. Zanon, “*Two-point functions of chiral operators in  $N = 4$  SYM at order  $g^4$* ,” JHEP **9912**, 006 (1999), hep-th/9910197;

- S. Penati, A. Santambrogio and D. Zanon, “More on correlators and contact terms in  $N = 4$  SYM at order  $g^4$ ,” Nucl. Phys. B **593**, 651 (2001), hep-th/0005223.
- [20] K. Intriligator, “Bonus symmetries of  $N = 4$  super-Yang-Mills correlation functions via AdS duality,” Nucl. Phys. B **551**, 575 (1999) hep-th/9811047; K. Intriligator and W. Skiba, “Bonus symmetry and the operator product expansion of  $N = 4$  super-Yang-Mills,” Nucl. Phys. B **559**, 165 (1999) hep-th/9905020.
- [21] P. Howe and P. West, “Superconformal invariants and extended supersymmetry,” Phys. Lett. B **400** (1997) 307, hep-th/9611075; P. S. Howe, E. Sokatchev and P. C. West, “3-point functions in  $N = 4$  Yang-Mills,” Phys. Lett. B **444**, 341 (1998), hep-th/9808162; B. Eden, P. S. Howe and P. C. West, “Nilpotent invariants in  $N = 4$  SYM,” Phys. Lett. B **463**, 19 (1999) hep-th/9905085; P. S. Howe, C. Schubert, E. Sokatchev and P. C. West, “Explicit construction of nilpotent covariants in  $N = 4$  SYM,” Nucl. Phys. B **571**, 71 (2000) hep-th/9910011.
- [22] P. J. Heslop and P. S. Howe, “OPEs and 3-point correlators of protected operators in  $N = 4$  SYM,” hep-th/0107212; E. D’Hoker and A.V. Ryzhov, “Three Point Functions of Quarter BPS Operators in  $N=4$  SYM,” hep-th/0109065; L. Hoffmann, L. Mesref, A. Meziane and W. Ruhl, “Multi-trace quasi-primary fields of  $N = 4$  SYM(4) from AdS  $n$ -point functions,” hep-th/0112191.
- [23] B. Eden, P. S. Howe, C. Schubert, E. Sokatchev and P. C. West, “Extremal correlators in four-dimensional SCFT,” Phys. Lett. B **472**, 323 (2000), hep-th/9910150.
- [24] B. U. Eden, P. S. Howe, E. Sokatchev and P. C. West, “Extremal and next-to-extremal  $n$ -point correlators in four-dimensional SCFT,” Phys. Lett. B **494**, 141 (2000), hep-th/0004102.
- [25] D. Sadri, and M. M. Sheikh-Jabbari, “The plane-wave/Super Yang-Mills duality,” hep-th/0310119.

- [26] D. Amati, and C. Klimcik, Phys. Lett. B **210**, 92 (1988).
- [27] G. T. Horowitz, and A. R. Steif, Phys. Rev. Lett. **64**, 260 (1990).
- [28] I. Bena, and R. Roiban, Phys. Rev. D **67**, 125014 (2003).
- [29] J. Polchinski “*String theory. Vol.1 and 2,*” Cambridge Univ. Pr. (1998).
- [30] M. Kaku, and K. Kikkawa, “*Field theory of relativistic strings. I. Trees,*” Phys. Rev. D **10**, 1110 (1974).
- [31] M. Kaku, and K. Kikkawa, “*Field theory of relativistic strings. II. Loops and pomerons,*” Phys. Rev. D **10**, 1823 (1974).
- [32] S. Dobashi, and T. Yoneya, “*Resolving the Holography in the Plane-Wave Limit of AdS/CFT Correspondence,*” hep-th/0406225.
- [33] S. Dobashi, and T. Yoneya, “*Impurity non-preserving 3-point correlators of BMN operators from pp-wave holography: bosonic excitations ,*” hep-th/0409058.
- [34] D. J. Gross, A. Mikhailov and R. Roiban, “*Operators with large R charge in  $N = 4$  Yang-Mills theory,*” hep-th/0205066.
- [35] E. Witten, “*Anti-de Sitter space and holography,*” Adv. Theor. Math. Phys. **2** (1998) 253, hep-th/9802150.
- [36] S. S. Gubser, I. R. Klebanov and A. M. Polyakov, “*Gauge theory correlators from non-critical string theory,*” Phys. Lett. B **428** (1998) 105, hep-th/9802109.
- [37] M. X. Huang, “*Three point functions of  $N=4$  Super Yang Mills from light cone string field theory in pp-wave,*” hep-th/0205311.
- [38] G. Arutyunov and E. Sokatchev, “*Conformal fields in the pp-wave limit,*” JHEP **0208** (2002) 014, hep-th/0205270.
- [39] M. Bianchi, B. Eden, G. Rossi and Y. S. Stanev, “*On operator mixing in  $N = 4$  SYM,*” Nucl. Phys. B **646** (2002) 69, hep-th/0205321.

- [40] C. S. Chu, M. Petrini, R. Russo and A. Tanzini, “*String interactions and discrete symmetries of the pp-wave background,*” hep-th/0211188.
- [41] D. Berenstein, J. M. Maldacena and H. Nastase, “*Strings in flat space and pp waves from  $N = 4$  super Yang Mills,*” JHEP **0204** (2002) 013, hep-th/0202021.
- [42] R. R. Metsaev, “*Type IIB Green-Schwarz superstring in plane wave Ramond-Ramond background,*” Nucl. Phys. B **625** (2002) 70, hep-th/0112044.
- [43] A. Santambrogio and D. Zanon, “*Exact anomalous dimensions of  $N=4$  Yang-Mills operators with large  $R$  charge,*” Phys. Lett. B **545** (2002) 425, hep-th/0206079.
- [44] H. Verlinde, “*Bits, matrices and  $1/N$ ,*” JHEP **0312** (2003) 052, hep-th/0206059.
- [45] D. J. Gross, A. Mikhailov and R. Roiban, “*A calculation of the plane wave string Hamiltonian from  $N = 4$  super-Yang-Mills theory,*” JHEP **0305** (2003) 025, hep-th/0208231.
- [46] C. Kristjansen, J. Plefka, G. W. Semenoff and M. Staudacher, “*A new double-scaling limit of  $N = 4$  super Yang-Mills theory and PP-wave strings,*” Nucl. Phys. B **643** (2002) 3, hep-th/0205033.
- [47] N. R. Constable, D. Z. Freedman, M. Headrick, S. Minwalla, L. Motl, A. Postnikov and W. Skiba, “*PP-wave string interactions from perturbative Yang-Mills theory,*” JHEP **0207** (2002) 017, hep-th/0205089.
- [48] J. Gomis, S. Moriyama and J. w. Park, “*SYM description of SFT Hamiltonian in a pp-wave background,*” Nucl. Phys. B **659** (2003) 179, hep-th/0210153.
- [49] J. Gomis, S. Moriyama and J. w. Park, “*SYM description of pp-wave string interactions: Singlet sector and arbitrary impurities,*” Nucl. Phys. B **665** (2003) 49, hep-th/0301250.
- [50] A. Pankiewicz, “*Strings in plane wave backgrounds,*” hep-th/0307027.

- [51] R. Roiban, M. Spradlin and A. Volovich, “*On light-cone SFT contact terms in a plane wave,*” hep-th/0211220.
- [52] M. Spradlin and A. Volovich, “*Superstring interactions in a pp-wave background,*” Phys. Rev. D **66** (2002) 086004, hep-th/0204146.
- [53] M. Spradlin and A. Volovich, “*Superstring interactions in a pp-wave background. II,*” JHEP **0301** (2003) 036, hep-th/0206073.
- [54] A. Pankiewicz, “*More comments on superstring interactions in the pp-wave background,*” JHEP **0209** (2002) 056, hep-th/0208209.
- [55] A. Pankiewicz and B. Stefanski, “*pp-wave light-cone superstring field theory,*” Nucl. Phys. B **657** (2003) 79, hep-th/0210246.
- [56] Y. j. Kiem, Y. b. Kim, S. m. Lee and J. m. Park, “*pp-wave / Yang-Mills correspondence: An explicit check,*” Nucl. Phys. B **642** (2002) 389, hep-th/0205279.
- [57] P. Lee, S. Moriyama and J. w. Park, “*Cubic interactions in pp-wave light cone string field theory,*” Phys. Rev. D **66** (2002) 085021, hep-th/0206065.
- [58] C. S. Chu, V. V. Khoze, M. Petrini, R. Russo and A. Tanzini, “*A note on string interaction on the pp-wave background,*” hep-th/0208148.
- [59] Y. j. Kiem, Y. b. Kim, J. Park and C. Ryou, “*Chiral primary cubic interactions from pp-wave supergravity,*” JHEP **0301** (2003) 026, hep-th/0211217.
- [60] D. Vaman, and H. Verlinde, “*Bit strings from  $N=4$  gauge theory,*” hep-th/0209215.
- [61] J. Pearson, M. Spradlin, D. Vaman, H. Verlinde and A. Volovich, “*Tracing the string: BMN correspondence at finite  $J^2/N,$ ” JHEP **0305** (2003) 022, hep-th/0210102.*
- [62] C. S. Chu, V. V. Khoze and G. Travaglini, “*BMN operators with vector impurities,  $\mathbb{Z}_2$  symmetry and pp-waves,*” JHEP **0306** (2003) 050, hep-th/0303107.

- [63] B. Eden, “*On two fermion BMN operators,*” Nucl. Phys. B **681** (2004) 195, hep-th/0307081.
- [64] M. Bianchi, G. Rossi and Y. S. Stanev, “*Surprises from the resolution of operator mixing in  $N = 4$  SYM,*” hep-th/0312228.
- [65] A. Pankiewicz, “*An alternative formulation of light-cone string field theory on the plane wave,*” JHEP **0306** (2003) 047, hep-th/0304232.
- [66] A. Pankiewicz and B. J. Stefanski, “*On the uniqueness of plane-wave string field theory,*” hep-th/0308062.
- [67] J. Gomis, S. Moriyama and J. w. Park, “*Open + closed string field theory from gauge fields,*”, Nucl. Phys. B **678** (2004) 101, hep-th/0305264.
- [68] P. Di Vecchia, J. L. Petersen, M. Petrini, R. Russo and A. Tanzini, “*The 3-string vertex and the AdS/CFT duality in the pp-wave limit,*” hep-th/0304025.
- [69] R. Slansky, “*Group Theory For Unified Model Building,*” Phys. Rept. **79** (1981) 1.
- [70] A. Parnachev and A. V. Ryzhov, “*Strings in the near plane wave background and AdS/CFT,*” JHEP **0210** (2002) 066, hep-th/0208010.
- [71] U. Gursoy, “*Vector operators in the BMN correspondence,*” JHEP **0307** (2003) 048, hep-th/0208041.
- [72] N. Beisert, “*BMN operators and superconformal symmetry,*” Nucl. Phys. B **659** (2003) 79, hep-th/0211032.
- [73] N. Beisert, C. Kristjansen, J. Plefka, G. W. Semenoff and M. Staudacher, “*BMN correlators and operator mixing in  $N = 4$  super Yang-Mills theory,*” Nucl. Phys. B **650** (2003) 125, hep-th/0208178.
- [74] C. S. Chu, V. V. Khoze and G. Travaglini, “*Three-point functions in  $N = 4$  Yang-Mills theory and pp-waves,*” JHEP **0206** (2002) 011, hep-th/0206005.

- [75] C. S. Chu, V. V. Khoze and G. Travaglini, “*pp-wave string interactions from  $n$ -point correlators of BMN operators*,” JHEP **0209** (2002) 054, hep-th/0206167.
- [76] N. R. Constable, D. Z. Freedman, M. Headrick and S. Minwalla, “*Operator mixing and the BMN correspondence*,” JHEP **0210** (2002) 068, hep-th/0209002.
- [77] D. Sadri and M. M. Sheikh-Jabbari, “*The plane-wave / super Yang-Mills duality*,” hep-th/0310119.
- [78] E. S. Fradkin and M. Y. Palchik, “*Conformal Quantum Field Theory In D-Dimensions*,” Mathematics and its applications, **376**, Kluwer, Dordrecht 1996.
- [79] R. A. Janik, “*BMN operators and string field theory*,” Phys. Lett. B **549** (2002) 237, hep-th/0209263.
- [80] J. A. Minahan and K. Zarembo, “*The Bethe-ansatz for  $N = 4$  super Yang-Mills*,” JHEP **0303** (2003) 013, hep-th/0212208.
- [81] N. Beisert, C. Kristjansen, J. Plefka and M. Staudacher, “*BMN gauge theory as a quantum mechanical system*,” Phys. Lett. B **558** (2003) 229, hep-th/0212269.
- [82] M. Spradlin and A. Volovich, “*Note on plane wave quantum mechanics*,” Phys. Lett. B **565** (2003) 253, hep-th/0303220.
- [83] N. Beisert, C. Kristjansen and M. Staudacher, “*The dilatation operator of  $N = 4$  super Yang-Mills theory*,” hep-th/0303060.
- [84] N. Beisert, “*The complete one-loop dilatation operator of  $N = 4$  super Yang-Mills theory*,” Nucl. Phys. B **676** (2004) 3, hep-th/0307015.
- [85] N. Beisert and M. Staudacher, “*The  $N = 4$  SYM integrable super spin chain*,” Nucl. Phys. B **670** (2003) 439, hep-th/0307042.
- [86] N. Beisert, “*The  $su(2|3)$  dynamic spin chain*,” hep-th/0310252.
- [87] C. Kristjansen, “*Three-spin strings on  $AdS(5) \times S^5$  from  $N = 4$  SYM*,” hep-th/0402033.

- [88] G. Arutyunov and M. Staudacher, “*Two-loop commuting charges and the string / gauge duality*,” hep-th/0403077.
- [89] S. Mandelstam, “*Interacting String Picture Of The Neveu-Schwarz-Ramond Model*,” Nucl. Phys. B **69** (1974) 77.
- [90] M. B. Green and J. H. Schwarz, “*Superstring Interactions*,” Nucl. Phys. B **218** (1983) 43.
- [91] M. B. Green, J. H. Schwarz and L. Brink, “*Superfield Theory Of Type Ii Superstrings*,” Nucl. Phys. B **219** (1983) 437.
- [92] M. B. Green and J. H. Schwarz, “*Superstring Field Theory*,” Nucl. Phys. B **243** (1984) 475.
- [93] U. Gursoy, “*Predictions for pp-wave string amplitudes from perturbative SYM*,” JHEP **0310** (2003) 027, hep-th/0212118.
- [94] T. Klose, “*Conformal dimensions of two-derivative BMN operators*,” JHEP **0303** (2003) 012, hep-th/0301150.
- [95] M. Bianchi, B. Eden, G. Rossi and Y. S. Stanev, “*On operator mixing in  $N = 4$  SYM*,” Nucl. Phys. B **646** (2002) 69, hep-th/0205321.
- [96] R. R. Metsaev and A. A. Tseytlin, “*Exactly solvable model of superstring in plane wave Ramond-Ramond background*,” Phys. Rev. D **65** (2002) 126004, hep-th/0202109.
- [97] G. 't Hooft, “*Computation Of The Quantum Effects Due To A Four-Dimensional Pseudoparticle*,” Phys. Rev. D **14** (1976) 3432 [Erratum-ibid. D **18** (1978) 2199].
- [98] Y. H. He, J. H. Schwarz, M. Spradlin and A. Volovich, “*Explicit formulas for Neumann coefficients in the plane-wave geometry*,” Phys. Rev. D **67** (2003) 086005, hep-th/0211198.

- [99] C. S. Chu, M. Petrini, R. Russo and A. Tanzini, “*String interactions and discrete symmetries of the pp-wave background,*” *Class. Quant. Grav.* **20** (2003) S457, hep-th/0211188.
- [100] J. Lucietti, S. Schafer-Nameki and A. Sinha, “*On the plane-wave cubic vertex,*” hep-th/0402185.
- [101] C. S. Chu and V. V. Khoze, “*Correspondence between the 3-point BMN correlators and the 3-string vertex on the pp-wave,*” *JHEP* **0304** (2003) 014, hep-th/0301036.
- [102] D. A. Kosower, “*Light Cone Recurrence Relations For QCD Amplitudes,*” *Nucl. Phys. B* **335** (1990) 23.
- [103] G. Chalmers and W. Siegel, “*Simplifying algebra in Feynman graphs. II: Spinor helicity from the spacecone,*” *Phys. Rev. D* **59** (1999) 045013, hep-ph/9801220; W. Siegel, “*Fields,*” hep-th/9912205.
- [104] R. Roiban, M. Spradlin and A. Volovich, “*A googly amplitude from the B-model in twistor space,*” hep-th/0402016;  
R. Roiban and A. Volovich, “*All googly amplitudes from the B-model in twistor space,*” hep-th/0402121;  
R. Roiban, M. Spradlin and A. Volovich, “*On the tree-level S-matrix of Yang-Mills theory,*” hep-th/0403190.
- [105] V. V. Khoze, “*Gauge Theory Amplitudes, Scalar Graphs and Twistor Space,*” hep-th/0408233.
- [106] F. Cachazo, P. Svrcek and E. Witten, “*MHV vertices and tree amplitudes in gauge theory,*” hep-th/0403047.
- [107] E. Witten, “*Perturbative gauge theory as a string theory in twistor space,*” hep-th/0312171.
- [108] C. J. Zhu, “*The googly amplitudes in gauge theory,*” *JHEP* **0404** (2004) 032 hep-th/0403115;

- J. B. Wu and C. J. Zhu, “*MHV vertices and scattering amplitudes in gauge theory*,” hep-th/0406085.
- [109] I. Bena, Z. Bern and D. A. Kosower, “*Twistor-space recursive formulation of gauge theory amplitudes*,” hep-th/0406133.
- [110] D. A. Kosower, “*Next-to-maximal helicity violating amplitudes in gauge theory*,” hep-th/0406175.
- [111] F. Cachazo, P. Svrcek and E. Witten, “*Twistor space structure of one-loop amplitudes in gauge theory*,” hep-th/0406177.
- [112] N. Berkovits, “*An alternative string theory in twistor space for  $N = 4$  super-Yang-Mills*,” hep-th/0402045.  
N. Berkovits and L. Motl, “*Cubic twistorial string field theory*,” JHEP **0404** (2004) 056 hep-th/0403187.
- [113] A. Neitzke and C. Vafa, “ *$N = 2$  strings and the twistorial Calabi-Yau*,” hep-th/0402128.  
N. Nekrasov, H. Ooguri and C. Vafa, “*S-duality and topological strings*,” hep-th/0403167.
- [114] E. Witten, “*Parity invariance for strings in twistor space*,” hep-th/0403199.
- [115] S. Gukov, L. Motl and A. Neitzke, “*Equivalence of twistor prescriptions for super Yang-Mills*,” hep-th/0404085.
- [116] W. Siegel, “*Untwisting the twistor superstring*,” hep-th/0404255.
- [117] S. Giombi, R. Ricci, D. Robles-Llana and D. Trancanelli, “*A note on twistor gravity amplitudes*,” hep-th/0405086.
- [118] A. D. Popov and C. Saemann, “*On supertwistors, the Penrose-Ward transform and  $N = 4$  super Yang-Mills theory*,” hep-th/0405123.
- [119] N. Berkovits and E. Witten, “*Conformal supergravity in twistor-string theory*,” hep-th/0406051.

- [120] V. P. Nair, "A Current Algebra For Some Gauge Theory Amplitudes," Phys. Lett. B **214** (1988) 215.
- [121] M. T. Grisaru, H. N. Pendleton and P. van Nieuwenhuizen, "Supergravity And The S Matrix," Phys. Rev. D **15** (1977) 996;  
M. T. Grisaru and H. N. Pendleton, "Some Properties Of Scattering Amplitudes In Supersymmetric Theories," Nucl. Phys. B **124** (1977) 81.
- [122] S. J. Parke and T. R. Taylor, "An Amplitude For N Gluon Scattering," Phys. Rev. Lett. **56** (1986) 2459.
- [123] F. A. Berends and W. T. Giele, "Recursive Calculations For Processes With N Gluons," Nucl. Phys. B **306** (1988) 759.
- [124] F. A. Berends, R. Kleiss, P. De Causmaecker, R. Gastmans and T. T. Wu, Phys. Lett. B **103** (1981) 124;  
P. De Causmaecker, R. Gastmans, W. Troost and T. T. Wu, Nucl. Phys. B **206** (1982) 53;  
R. Kleiss and W. J. Stirling, Nucl. Phys. B **262** (1985) 235;  
J. F. Gunion and Z. Kunszt, Phys. Lett. B **161** (1985) 333.
- [125] M. L. Mangano and S. J. Parke, "Multiparton Amplitudes In Gauge Theories," Phys. Rept. **200** (1991) 301.
- [126] L. J. Dixon, "Calculating scattering amplitudes efficiently," hep-ph/9601359.
- [127] F. A. Berends, W. T. Giele and H. Kuijf, Phys. Lett. B **232**, 266 (1989);  
F. A. Berends, H. Kuijf, B. Tausk and W. T. Giele, Nucl. Phys. B **357**, 32 (1991);  
F. Caravaglios and M. Moretti, Phys. Lett. B **358**, 332 (1995) hep-ph/9507237;  
P. Draggiotis, R. H. Kleiss and C. G. Papadopoulos, Phys. Lett. B **439**, 157 (1998) hep-ph/9807207;  
P. D. Draggiotis, R. H. Kleiss and C. G. Papadopoulos, Eur. Phys. J. C **24**, 447 (2002) hep-ph/0202201;  
M. L. Mangano, M. Moretti, F. Piccinini, R. Pittau and A. D. Polosa, JHEP **0307**, 001 (2003) hep-ph/0206293.

- [128] T. Stelzer and W. F. Long, *Comput. Phys. Commun.* **81**, 357 (1994) hep-ph/9401258;  
A. Pukhov *et al.*, hep-ph/9908288;  
F. Yuasa *et al.*, *Prog. Theor. Phys. Suppl.* **138**, 18 (2000) hep-ph/0007053;  
F. Krauss, R. Kuhn and G. Soff, *JHEP* **0202**, 044 (2002) hep-ph/0109036;  
F. Maltoni and T. Stelzer, *JHEP* **0302** (2003) 027 hep-ph/0208156.
- [129] Z. Bern, L. J. Dixon, D. C. Dunbar and D. A. Kosower, “*Fusing gauge theory tree amplitudes into loop amplitudes*,” *Nucl. Phys. B* **435**:59 (1995) hep-ph/9409265;  
Z. Bern, L. J. Dixon and D. A. Kosower, “*Unitarity-based techniques for one-loop calculations in QCD*,” *Nucl. Phys. Proc. Suppl.* **51C**:243 (1996) hep-ph/9606378.
- [130] A. Brandhuber, B. Spence, and G. Travaglini “*One-Loop Gauge Theory Amplitudes in  $N=4$  Super Yang-Mills from MHV Vertices*,” *Nucl. Phys B* **706**, 150 (2005), hep-th/0407214;  
J. Bedford, A. Brandhuber, B. Spence, and G. Travaglini “*A Twistor Approach to One-Loop Amplitudes in  $N=1$  Supersymmetric Yang-Mills Theory*,” *Nucl. Phys B* **706**, 100 (2005), hep-th/0410280;  
J. Bedford, A. Brandhuber, B. Spence, and G. Travaglini “*Non-Supersymmetric Loop Amplitudes and MHV Vertices*,” *Nucl. Phys B* **712**, 59 (2005), hep-th/0412108.
- [131] R. Britto, F. Cachazo, and B. Feng, “*Generalized Unitarity and One-Loop Amplitudes in  $N=4$  Super-Yang-Mills*,” hep-th/0412103.
- [132] R. Britto, F. Cachazo, and B. Feng, “*New Recursion Relations for Tree Amplitudes of Gluons*,” hep-th/0412308.
- [133] R. Britto, F. Cachazo, B. Feng, and E. Witten “*Direct Proof Of Tree-Level Recursion Relation In Yang-Mills Theory*,” hep-th/0501052.
- [134] R. Roiban, M. Spradlin and A. Volovich, “*Dissolving  $N = 4$  loop amplitudes into QCD tree amplitudes*,” *Phys. Rev. Lett.* **94**:102002 (2005), hep-th/0412265.

- [135] M. Luo and C. Wen, “*Recursion relations for tree amplitudes in super gauge theories*,” JHEP 0503:004 (2005), hep-th/0501121; Phys. Rev. D71:091501 (2005), hep-th/0502009;  
J. Bedford, A. Brandhuber, B. Spence and G. Travaglini, “*A recursion relation for gravity amplitudes*,” Nucl. Phys. B721:98 (2005), hep-th/0502146;  
F. Cachazo and P. Svrček, “*Tree level recursion relations in general relativity*,” hep-th/0502160;  
R. Britto, B. Feng, R. Roiban, M. Spradlin and A. Volovich, “*All split helicity tree-level gluon amplitudes*,” Phys. Rev. D71:105017 (2005), hep-th/0503198.
- [136] S. D. Badger, E. W. N. Glover, V. V. Khoze and P. Svrček, “*Recursion Relations for Gauge Theory Amplitudes with Massive Particles*,” JHEP 0507:025 (2005), hep-th/0504159;  
D. Forde and D. A. Kosower, “*All-multiplicity amplitudes with massive scalars*,” hep-th/0507292.
- [137] Z. Bern and A. G. Morgan, “*Massive Loop Amplitudes from Unitarity*,” Nucl. Phys. B467:479 (1996), hep-ph/9511336.
- [138] Z. Bern, L. J. Dixon, D. C. Dunbar and D. A. Kosower, “*One-loop self-dual and  $N = 4$  superYang-Mills*,” Phys. Lett. B394:105 (1997), hep-th/9611127.
- [139] Z. Bern, L. J. Dixon and D. A. Kosower, “*A two-loop four-gluon helicity amplitude in QCD*,” JHEP 0001:027 (2000), hep-ph/0001001;  
Z. Bern, A. De Freitas and L. J. Dixon, “*Two-loop amplitudes for gluon fusion into two photons*,” JHEP 0109:037 (2001), hep-ph/0109078;  
Z. Bern, A. De Freitas and L. J. Dixon, “*Two-loop helicity amplitudes for gluon gluon scattering in QCD and supersymmetric Yang-Mills theory*,” JHEP 0203:018 (2002), hep-ph/0201161.
- [140] A. Brandhuber, S. McNamara, B. Spence and G. Travaglini, “*Loop Amplitudes in Pure Yang-Mills from Generalised Unitarity*,” JHEP 0510:011 (2005), hep-th/0506068.

- [141] Z. Bern, L. J. Dixon and D. A. Kosower, “*On-shell recurrence relations for one-loop QCD amplitudes*,” Phys. Rev. D71:105013 (2005), hep-th/0501240.
- [142] Z. Bern, L. J. Dixon and D. A. Kosower, “*The last of the finite loop amplitudes in QCD*,” Phys. Rev. D72:125003 (2005), hep-ph/0505055.
- [143] Z. Bern, L. J. Dixon and D. A. Kosower, “*Bootstrapping multi-parton loop amplitudes in QCD*,” hep-ph/0507005.
- [144] Z. Bern, L. J. Dixon and V. A. Smirnov, “*Iteration of Planar Amplitudes in Maximally Supersymmetric Yang-Mills Theory at Three Loops and Beyond*,” Phys. Rev. D72:085001 (2005), hep-th/0505205.
- [145] M. Staudacher, “*The Factorized S-Matrix of CFT/AdS*,” JHEP 0505 (2005) 054, hep-th/0412188.

